



AUBURN UNIVERSITY

SAMUEL GINN
COLLEGE OF ENGINEERING

Research Report No. 1 for ALDOT Project 930-832

**IMPROVING CAMBER PREDICTIONS FOR
PRESTRESSED CONCRETE GIRDERS:
PART 1 OF 2**

Submitted to

The Alabama Department of Transportation

Prepared by

David M. Mante, Robert W. Barnes, Anton K. Schindler

Andric Hofrichter, Levent Isbiliroglu

October 2019

Highway Research Center

Harbert Engineering Center
Auburn, Alabama 36849

www.eng.auburn.edu/research/centers/hrc.html

1. Report No. ALDOT 930-832-1		2. Government Accession No.		3. Recipient Catalog No.	
4 Title and Subtitle Improving Camber Predictions for Prestressed Girders: Part 1 of 2				5 Report Date October 2019	
				6 Performing Organization Code	
7. Author(s) David M. Mante, Robert W. Barnes, Anton K. Schindler Andric Hofrichter, Levent Isbiloglu				8 Performing Organization Report No. ALDOT 930-832-1	
9 Performing Organization Name and Address Highway Research Center Department of Civil Engineering 238 Harbert Engineering Center Auburn, AL 36849				10 Work Unit No. (TRAIS)	
				11 Contract or Grant No.	
12 Sponsoring Agency Name and Address Alabama Department of Transportation 1409 Coliseum Boulevard Montgomery, Alabama 36130-3050				13 Type of Report and Period Covered Technical Report	
				14 Sponsoring Agency Code	
15 Supplementary Notes Research performed in cooperation with the Alabama Department of Transportation					
16 Abstract <p>In precast, prestressed concrete construction, the eccentricity of the prestressing force typically results in a net upward girder deflection known as camber. Camber is first observed at the time of prestress transfer and tends to increase thereafter as a function of time-dependent material properties. While accurately predicted levels of camber are desirable to concrete bridge construction, inaccuracies in design camber estimates can result in construction difficulties and the need to modify bridge designs to ensure proper girder fit. In order to mitigate such troublesome issues, the Alabama Department of Transportation (ALDOT) sponsored this investigation to develop a suggested procedure for use during girder design to more accurately predict pre-erection camber in precast, prestressed concrete bridge girders. In support of this objective, various laboratory and field studies were conducted exploring relevant regionally-variable concrete material properties (e.g. concrete compressive strength, concrete unit stiffness, and creep and shrinkage behavior) as well as the effect of transient environmental conditions on girder camber. Relying on the conclusions of these laboratory and field studies, a revised camber prediction procedure was developed, implemented in a user-friendly computer software (<i>ALCAMBER v1.0</i>) and validated by comparison to multiple design and production cycles of ALDOT precast, prestressed concrete bridge girders.</p>					
17 Key Words Bridge, deflection, camber, overstrength, elastic modulus, time-dependent, creep and shrinkage, thermal effects			18 Distribution Statement No restrictions. This document is available to the public through the National Technical Information Service, Springfield, Virginia 22161		
19 Security Classification (of this report) Unclassified		20 Security Classification (of this report) Unclassified		21 No. of pages 243	22 Price

DISCLAIMERS

The contents of this report reflect the views of the authors, who are responsible for the facts and the accuracy of the data presented herein. The contents do not necessarily reflect the official views or policies of Auburn University or the Federal Highway Administration. This report does not constitute a standard, specification, or regulation.

NOT INTENDED FOR CONSTRUCTION, BIDDING, OR PERMIT PURPOSES

Robert W. Barnes, Ph.D., P.E.

Anton K. Schindler, Ph.D., P.E.

Research Supervisors

ACKNOWLEDGEMENTS

Material contained herein was obtained in connection with a research project ALDOT 930-601, conducted by the Auburn University Highway Research Center. Funding for the project was provided by the Alabama Department of Transportation (ALDOT) with donations received from BASF Corporation, Holcim Inc., Elkem Materials, and CEMEX. The funding, cooperation, and assistance of many individuals from each of these organizations are gratefully acknowledged. The authors would like to acknowledge the various contributions of the following individuals:

Tim Colquitt, ALDOT, State Bridge Engineer
Buddy Black, ALDOT, State Bridge Engineer (*Retired*)
Drew Waldrop, ALDOT, Concrete/Cement Engineer
Keith Hegler, ALDOT, Field Inspection Team
Nathan Emmerich, Forterra
Frankie Smith, Forterra, Plant Manager
Dwayne Hamby, Forterra, Engineering Manager
Don Theobald, Gulf Coast Prestress, Engineering Manager
Larry Nicely, Gulf Coast Prestress, Plant Manager

ABSTRACT

In precast, prestressed concrete construction, the eccentricity of the prestressing force typically results in a net upward girder deflection known as camber. Camber is first observed at the time of prestress transfer and tends to increase thereafter as a function of time-dependent material properties. While accurately predicted levels of camber are desirable to concrete bridge construction, inaccuracies in design camber estimates can result in construction difficulties and the need to modify bridge designs to ensure proper girder fit. In order to mitigate such troublesome issues, the Alabama Department of Transportation (ALDOT) sponsored this investigation to develop a suggested procedure for use during girder design to more accurately predict pre-erection camber in precast, prestressed concrete bridge girders. In support of this objective, various laboratory and field studies were conducted exploring relevant regionally-variable concrete material properties (e.g. concrete compressive strength, concrete unit stiffness, and creep and shrinkage behavior) as well as the effect of transient environmental conditions on girder camber. Relying on the conclusions of these laboratory and field studies, a revised camber prediction procedure was developed, implemented in a user-friendly computer software (*ALCAMBER v1.0*) and validated by comparison to multiple design and production cycles of ALDOT precast, prestressed concrete bridge girders.

TABLE OF CONTENTS

LIST OF TABLES	ix
LIST OF FIGURES	xi
Chapter 1: Introduction	1
1.1 Background on Camber in Precast, Prestressed Concrete Girders.....	1
1.2 Justification for Research	2
1.3 Research Objectives.....	3
1.4 Research Approach	3
1.5 Report Organization and Outline	5
Chapter 2: Background	6
2.1 Introduction	6
2.2 Variability and Limitations of Deflection Predictions	6
2.3 Deflections in One-Way Prestressed Flexural Members.....	10
2.4 Primary Factors Influencing Flexural Deflection Predictions	11
2.4.1 Geometric Properties	12
2.4.2 Concrete Density	14
2.4.3 Concrete Compressive Strength	14
2.4.4 Concrete Stiffness	14
2.4.5 Concrete Creep	15
2.4.6 Concrete Shrinkage.....	15
2.4.7 Steel Relaxation	15
2.4.8 Prestress Losses	16
2.5 Techniques For Computing Short-Term Deflections	18
2.5.1 Elastic Camber Computation by Moment-Area Theorem	18
2.5.2 Elastic Camber Computation by Tabulated Equation	22
2.5.3 Elastic Camber Computation by Energy Method	25
2.6 Techniques to Compute Long-Term Deflections	25
2.6.1 PCI Multiplier Method	25
2.6.2 Incremental Time-Steps Method	28
2.6.3 Approximate Time-Steps Method.....	29
2.6.4 Prestress Loss Method.....	29
Chapter 3: Previous Camber Studies.....	30
3.1 Introduction	30
3.2 Previous Camber Literature.....	30
3.2.1 Buettner and Libby (1979).....	31
3.2.2 Tadros, Ghali, and Meyer (1985)	31
3.2.3 Kelly, Bradberry, and Breen (1987).....	32
3.2.4 Brown (1998).....	32
3.2.5 Wyffels, French, and Shield (2000).....	33
3.2.6 Stallings, Barnes, and Eskildsen (2003)	34
3.2.7 Cook and Bloomquist (2005).....	35

3.2.8	Barr, Stanton, and Eberhard (2005)	35
3.2.9	Hinkle (2006)	36
3.2.10	Rosa, Stanton, and Eberhard (2007)	36
3.2.11	Jayaseelan and Russell (2007)	37
3.2.12	Omar, Pui Lai, Poh Huat, and Omar (2008)	37
3.2.13	Barr and Angomas (2010)	38
3.2.14	Lee (2010)	38
3.2.15	Tadros, Fawzy, and Hanna (2011)	39
3.2.16	French and O'Neill (2012)	39
3.2.17	Schrantz (2012)	40
3.2.18	Johnson (2012)	40
3.2.19	Precast/Prestressed Concrete Institute Committee on Bridges (2012)	41
3.2.20	Storm, Rizkalla, and Zia (2013)	42
3.2.21	Mahmood (2013)	43
3.2.22	He (2013)	43
3.2.23	Nervig (2014)	44
3.2.24	Keske (2014)	44
3.2.25	Hofrichter (2014)	44
3.2.26	Isbiliroglu (2014)	45
3.2.27	Davison (2014)	45
3.3	Comments on Previous Camber Studies	45
Chapter 4: Current Design and Construction Practices for ALDOT Precast, Prestressed Concrete Bridge Girders		
47		
4.1	Introduction	47
4.2	Background	47
4.2.1	Prevalence of Precast, Prestressed Concrete Bridges in Alabama	48
4.2.2	Regional Precast, Prestressed Concrete Producers	48
4.2.3	Distribution of ALDOT Girder Types	50
4.3	Design of Precast, Prestressed Concrete Bridge Girders in Alabama	51
4.3.1	Preliminary Girder Design by ALDOT	52
4.3.2	Design Review and Shop Drawing Submittal by Producer	58
4.4	Concrete Mixtures for Precast, Prestressed Bridge Girders in Alabama	59
4.4.1	ALDOT Mixture Design and Approval Procedures	59
4.4.2	ALDOT Requirements for Concrete in Precast, Prestressed Bridge Girders	60
4.4.3	ALDOT-Approved Concrete Mixture Proportions	61
4.4.4	Prestressed Concrete Fresh Properties	63
4.5	Construction Practices Relevant to Camber	64
4.5.1	Production Camber Measurements and Permissible Tolerances	65
4.5.2	Chronological Time to Prestress Release	66
4.5.3	Maturity at Prestress Release	69
4.5.4	Girder Handling and Storage Conditions	70
4.6	Required Girder Production Documentation and Data Reporting Formats	71
4.7	Summary	71
4.8	Recommendations	72
Chapter 5: Accurately Predicting Expected Concrete Compressive Strength		
73		
5.1	Introduction	73
5.1.1	Chapter Objectives	74

5.1.2	Chapter Outline	74
5.2	Background.....	75
5.2.1	Concrete Compressive Strength	75
5.2.2	Concrete Compressive Strength Nomenclature and Definitions.....	77
5.2.3	Concrete Compressive Strength Growth Provisions.....	79
5.3	Current Overstrength Provisions in the Concrete Industry.....	84
5.3.1	General Concept	84
5.3.2	Measures of Variability	89
5.3.3	Relevant Design Code Provisions.....	93
5.3.4	Regional Use of Overstrength in Serviceability Computation	99
5.4	Overstrength in the Precast, Prestressed Concrete Industry	102
5.4.1	Overstrength at Prestress Release	102
5.4.2	Overstrength at 28 Days	105
5.4.3	Applicability of Existing Overstrength Provisions to Precast, Prestressed Industry.....	108
5.5	Historical Data Set.....	109
5.5.1	Historical Strength Data Set Description.....	109
5.5.2	Normalizing for Air Content	113
5.6	Predicting Expected Concrete Compressive Strength at Prestress Release.....	116
5.6.1	Analytical Approach.....	116
5.6.2	Concept of Minimum Preferred Cementitious Materials Content (MPCMC).....	118
5.6.3	Simple Fully Empirical Models	120
5.6.4	Piecewise Fully Empirical Models	122
5.6.5	Semi-Empirical Piecewise Data Fit with MPCMC Concept.....	123
5.6.6	ACI 214-Based Model (Constant s).....	125
5.6.7	ACI 214-Based Model (Constant s and MPCMC Concept)	129
5.6.8	ACI 214-Based Model (Variable s and MPCMC Concept)	130
5.6.9	Comparison of Trial Models	134
5.6.10	Final Recommendations	141
5.7	Predicting Expected Concrete Compressive Strength at 28 Days.....	142
5.7.1	Fully Empirical Models	143
5.7.2	ACI 214-Based Empirical Models.....	144
5.7.3	Theoretically-Derived Strength Growth Model	146
5.7.4	Comparison of Proposed Models	152
5.7.5	Final Recommendations.....	153
5.8	Summary and Conclusions.....	153
5.8.1	Summary	153
5.8.2	Conclusions and Recommendations.....	154
Chapter 6: Concrete Modulus of Elasticity Relationships.....		157
6.1	Introduction	157
6.1.1	Chapter Objectives	157
6.1.2	Chapter Outline	158
6.2	Background.....	158
6.2.1	Modulus of Elasticity Definition.....	158
6.2.2	Primary Factors Affecting Concrete Modulus of Elasticity	160
6.2.2.1	Concrete Compressive Strength	160
6.2.2.2	Unit Weight	162
6.2.2.3	Aggregate Stiffness	164
6.2.2.4	Use of Supplementary Cementing Materials	165

6.2.3	Available Prediction Equations.....	165
6.2.3.1	Pauw (1960) / ACI 318-14 / ACI 209 Method.....	166
6.2.3.2	AASHTO LRFD (2014) / NCHRP Report 496 Method.....	167
6.2.3.3	Carrasquillo et al. (1981) / ACI 363 Method.....	168
6.2.3.4	fib Model Code 2010 Method.....	168
6.2.3.5	Noguchi et al. (2009) Method.....	170
6.3	Experimental Program.....	170
6.3.1	Laboratory Study.....	171
6.3.1.1	Summary of Work.....	171
6.3.1.2	Concrete Mixtures and Raw Materials.....	172
6.3.1.3	Mixture Preparation.....	176
6.3.1.4	Sampling and Curing Procedures.....	177
6.3.1.5	Fresh and Hardened Concrete Properties Testing Plan.....	178
6.3.1.6	Ungrouped Laboratory Data Set.....	180
6.3.2	Field Data Collection.....	182
6.3.2.1	Summary of Work.....	182
6.3.2.2	Mixtures and Raw Materials.....	183
6.3.2.3	Sampling and Curing Procedures.....	185
6.3.2.4	Fresh and Hardened Concrete Properties Testing Plan.....	185
6.3.2.5	Field Data Set.....	186
6.3.3	Additional Data Sources.....	187
6.3.3.1	Keske (2014).....	187
6.3.3.2	Boehm et al. (2010).....	188
6.3.4	Complete Compiled Data Set For Stiffness-Strength Analysis.....	188
6.4	Presentation and Analysis of Results.....	189
6.4.1	Preliminary Analysis and Data Groupings.....	190
6.4.2	Concrete Stiffness at Prestress Release.....	194
6.4.2.1	Calibration of AASHTO LRFD Equation.....	195
6.4.2.2	Calibration of fib Model Code 2010 Equation.....	197
6.4.2.3	Calibration of Noguchi et al. (2009) Equation.....	197
6.4.2.4	Comparison of Available Prediction Equations.....	198
6.4.2.5	Preliminary Recommendations for Designers.....	204
6.4.3	Concrete Stiffness at 28 Days.....	204
6.4.3.1	Calibration of AASHTO LRFD Equation.....	205
6.4.3.2	Calibration of fib Model Code 2010 Equation.....	205
6.4.3.3	Calibration of Noguchi et al. (2009) Equation.....	206
6.4.3.4	Comparison of Available Prediction Equations.....	207
6.4.3.5	Preliminary Recommendations for Designers.....	211
6.4.4	Time-Dependence of Aggregate Stiffness Effect.....	212
6.4.5	Reduced Stiffness of Crushed Granite Concrete Laboratory Mixtures.....	217
6.5	Summary and Conclusions.....	221
6.5.1	Summary.....	221
6.5.2	Conclusions and Recommendations.....	221
References	223

LIST OF TABLES

Table 2-1: Long-Term Deflection Multipliers (Adapted from Martin 1977).....	28
Table 4-1: Prevalence of Prestressed Concrete Bridges in Alabama (Baughn 2014).....	48
Table 4-2: Typical Mixture Proportions for Alabama Precast, Prestressed Concrete	62
Table 4-3: Statistical Summary of Chronological Age to Release by Subgroup.....	69
Table 5-1: Recalibrated Constants for Strength Prediction Equations (Hofrichter 2014)	84
Table 5-2: Principal Sources of Strength Variation Adapted from ACI 224R-11 (ACI Committee 214 2011)	86
Table 5-3: Required Average Compressive Strength, f_{cr} , with Historical Data (Adapted from ACI 301-10)	94
Table 5-4: Standards of Concrete Control for General Construction (Adapted from ACI 214-R11).....	95
Table 5-5: Required Average Compressive Strength, f_{cr} , without Historical Data (Adapted from ACI 301-10)	96
Table 5-6: Format of Condensed Raw Strength Data Set	110
Table 5-7: Approximate Correlation between w/cm , Cementitious Materials Content, and Expected 28-Day Strength for Typical Concrete Mixtures (Adapted from ACI 211.4R-08 Table 6.5).....	119
Table 5-8: Simple Fully Empirical Model Description	121
Table 5-9: Piecewise Fully Empirical Model Description	122
Table 5-10: Semi-Empirical Piecewise Model Description	124
Table 5-11: Required Average Compressive Strength, f_{cr} , with Historical Data (Adapted from ACI 301-10)	125
Table 5-12: Standard Deviation of the Difference Statistic Distribution by Producer	128
Table 5-13: Results of Statistical Analysis of Variances of the Difference Statistic among Plants	128
Table 5-14: Preliminary ACI 214-Based Model (Constant $s = 1,050$ psi).....	129
Table 5-15: Analysis of Standard Deviation by Specified Release Strength Subsets.....	131
Table 5-16: Trial Prediction Equations for Prestress Transfer.....	135
Table 5-17: Goodness-of-Fit for Trial Prediction Equations at Prestress Release	137
Table 5-18: Findings of Previous Researchers for Overstrength at Prestress Transfer.....	139
Table 5-19: Comparison of Trial Prediction Equations at Prestress Release Suggested by Previous Researchers to Experimental Data	140
Table 5-20: Fully Empirical Model Description.....	143
Table 5-21: ACI 214-Based Empirical Model Description.....	145
Table 5-22: Expected Overstrength Factor at 28 Days as a Function of Specified Release Strength and Specified 28-Day Strength	151

Table 5-23: Goodness-of-Fit for Trial Prediction Equations at 28 Days	152
Table 6-1: Laboratory Phase Concrete Mixture Proportions	174
Table 6-2: Experimental Matrix of Laboratory Mixtures	176
Table 6-3: Mixture Proportions for On-site Production Cycles.....	184
Table 6-4: Effect of Coarse Aggregate Type on Elastic Modulus	192
Table 6-5: Effect of Time of Measurement on Elastic Modulus	192
Table 6-6: Effect of Curing Conditions on Elastic Modulus.....	193
Table 6-7: Effect of Supplementary Cementing Material (SCM) on Elastic Modulus	194
Table 6-8: Candidate Modulus Prediction Equations Calibrated for Prestress Release	200
Table 6-9: Standard Error of the Estimate, <i>SEE</i> for Calibrated Modulus Prediction Equations at Prestress Release	202
Table 6-10: Candidate Modulus Prediction Equations Calibrated for 28 Days.....	208
Table 6-11: Standard Error of the Estimate, <i>SEE</i> , for Calibrated Modulus Prediction Equations at 28 Days	209

LIST OF FIGURES

Figure 1-1: Exaggerated Girder Deformation and Midspan Camber	1
Figure 2-1: Random Variability of a Measured Length	7
Figure 2-2: Systematic Error of a Random Variable	9
Figure 2-3: Net Instantaneous Deflections at Prestress Transfer in Prestressed Girders (adapted from Isbilloglu 2014).....	11
Figure 2-4: Primary Factors Influencing Deflections in Prestressed Concrete Girders	12
Figure 2-5: Standard Dimensions of PCI Bulb-Tee Cross-Sections (Adapted from PCI 2011).....	13
Figure 2-6: Detailed Section Properties of PCI Bulb-Tee Shapes (Adapted from PCI 2011).....	13
Figure 2-7: Graphical Representation of Prestress Loss Contributions (Adapted from Tadros et al. 2003)	17
Figure 2-8: Engineering Beam Theory in a Flat-Strand Prestressed Girder (Adapted from Hibbeler 2006)	19
Figure 2-9: Application of Moment-Area Theorem to Calculate Elastic Camber in Flat-Strand Prestressed Girder	20
Figure 2-10: Application of Moment-Area Theorem to Calculate Elastic Camber in Simple Harped-Strand Prestressed Girder	21
Figure 2-11: Camber and Rotational Coefficients for Prestress Force and Loads (Precast/Prestressed Concrete Institute 2011).....	24
Figure 3-1: Effect of Pre-Release Cracking on Elastic Camber Magnitude (Adapted from Wyffels et al. 2000)	34
Figure 3-2: Proposed PCI Camber Tolerance Limit Revisions (Adapted from PCI Committee on Bridges 2012)	42
Figure 4-1: PCI-Qualified Prestressed Concrete Plants in Alabama and Neighboring States	49
Figure 4-2: ALDOT Qualified Precast, Prestressed Concrete Producers in 2012.....	50
Figure 4-3: Frequency of ALDOT Girder Types from 2007-2013	51
Figure 4-4: LEAP CONSPAN Material Input GUI	55
Figure 4-5: <i>PSBEAM</i> Material Input GUI	55
Figure 4-6: Long-term Deflection Multipliers in <i>CONSPAN</i> (left) and <i>PSBEAM</i> (right).	56
Figure 4-7: Typical Camber Diagram on ALDOT Contract Drawings	57
Figure 4-8: Historical Data for Select Fresh Concrete Properties: Slump (left) and Air Content (right).	64
Figure 4-9: Permissible Camber Production Tolerances (Adapted from ALDOT 367 2015).....	66
Figure 4-10: Frequency Histogram for Chronological Age at Release.	67
Figure 4-11: Cumulative Percent Occurrence for Chronological Age at Release.	68
Figure 4-12: Frequency Histogram for Equivalent Age at Prestress Release.	70

Figure 5-1: Relationship between water to cement ratio, w/c , and compressive strength as expressed by D. Abrams (1927).....	76
Figure 5-2: ACI 209R-92 Strength Growth Equation with Various Constants	81
Figure 5-3: MC 2010 Concrete Strength Growth Provisions with Varying Constants	82
Figure 5-4: Gaussian Distribution of Sampled Concrete Compressive Strength.....	87
Figure 5-5: Relationship between Standard Deviation and Expected Data Spread	87
Figure 5-6: Concept of Probability of Failure	89
Figure 5-7: Relationship between Standard Deviation and Coefficient of Variation for Various Target Strength Levels	91
Figure 5-8: Concept of Preservation of Standard Deviation	92
Figure 5-9: Implicit Standard Deviations for No Historical Data ACI Overstrength Provisions.....	97
Figure 5-10: Comparison of Current ACI Overstrength Parameters.....	98
Figure 5-11: Percent Error in Square Root of Compressive Strengths	101
Figure 5-12: Concept of 28-Day Overstrength Derivation	107
Figure 5-13: Comparison of Specified vs. Measured Release Strength for Historical Data Set	110
Figure 5-14: Comparison of Specified vs. Measured 28-Day Strength for Historical Data Set.....	111
Figure 5-15: Overstrength Values at Prestress Release for the Historical Data Set.....	112
Figure 5-16: Overstrength Values at 28 Days for the Historical Data Set	112
Figure 5-17: Comparison of Specified vs. Air Content Adjusted Measured Release Strength for Historical Data Set.	114
Figure 5-18: Comparison of Specified vs. Air Content Adjusted Measured 28-Day Strength for Historical Data Set.	115
Figure 5-19: Analytical Approach of Release Strength Prediction Equation Development	117
Figure 5-20: Correlation between MPCMC and Expected Concrete Compressive Strength at Prestress Release	120
Figure 5-21: Calibrated Simple Fully Empirical Release Strength Prediction Models.....	121
Figure 5-22: Calibrated Piecewise Fully Empirical Release Strength Prediction Models.....	123
Figure 5-23: Calibrated Piecewise Semi-Empirical Release Strength Prediction Models.....	124
Figure 5-24: Frequency Histogram of Measured Release Strengths in Historical Data Set	126
Figure 5-25: Frequency Histogram of Difference Statistic at Prestress Release in Historical Data Set...	127
Figure 5-26: Preliminary ACI 214-Based Prediction Model (Constant $s = 1,050$ psi).....	129
Figure 5-27: ACI 214-Based Prediction Model with MPCMC (Constant $s = 1,050$ psi).....	130
Figure 5-28: Standard Deviation of Difference Statistic by Subgroup	132
Figure 5-29: Linear Regression of Standard Deviation of Difference Statistic	133
Figure 5-30: ACI 214-Based Model (Variable s with MPCMC).....	134
Figure 5-31: Trial Prediction Models for Expected Concrete Release Strength at Prestress Release	136
Figure 5-32: Comparison of ACI 214-Based Prediction Equation with Previous Findings by Others	140
Figure 5-33: Analytical Approach of 28-Day Prediction Equation Development	142
Figure 5-34: Calibrated Fully Empirical 28-Day Strength Prediction Models.....	144

Figure 5-35: ACI 214-Based Empirical Models for 28-Day Concrete Strength	145
Figure 5-36: Comparison of Expected 28-Day Strength Based on Measured Release Strength and Measured 28-Day Strength.....	147
Figure 5-37: Comparison of Expected 28-Day Strength Based on Expected Release Strength and Measured 28-Day Strength.....	148
Figure 5-38: Theoretical Strength Growth Model Predictions for 28-Day Concrete Strength Compared with Measured Values of Historical Data Set.	149
Figure 6-1: Stress-Strain Curve and Elastic Modulus Depictions (Adapted from Naaman 2004)	159
Figure 6-2: Experimental Results of Noguchi et al. (2009).....	162
Figure 6-3: Historic Data Set Compiled by Pauw (1960).....	166
Figure 6-4: <i>SURECURE</i> Jacket for Accelerated Curing	178
Figure 6-5: Cylinder Prepared for Elastic Modulus Testing	180
Figure 6-6: Ungrouped Stiffness-Strength Data from Laboratory Study Neglecting Effect of Unit Weight	181
Figure 6-7: Raw Stiffness-Strength Data from Laboratory Study Including Effect of Unit Weight.....	182
Figure 6-8: Stiffness-Strength Data from Field Study Neglecting Effect of Unit Weight.....	186
Figure 6-9: Stiffness-Strength Data from Field Study Including Effect of Unit Weight	187
Figure 6-10: Stiffness-Strength Data Neglecting Effect of Unit Weight	188
Figure 6-11: Stiffness-Strength Data Including Effect of Unit Weight.....	189
Figure 6-12: Analytical Procedure for Stiffness-Strength Data Set.....	195
Figure 6-13: Calibration of AASHTO LRFD Equation for Prestress Release	196
Figure 6-14: Calibration of <i>fib</i> Model Code 2010 for Prestress Release	197
Figure 6-15: Calibration of Noguchi et al. (2009) for Prestress Release.....	198
Figure 6-16: Relative Fit of Calibrated Modulus Prediction Equations for Prestress Release Data for Dolomitic Limestones with Assumed Unit Weight of 150 pcf.....	203
Figure 6-17: Calibration of AASHTO LRFD Equation for 28 Days	205
Figure 6-18: Calibration of <i>fib</i> Model Code 2010 for 28 Days.....	206
Figure 6-19: Calibration of Noguchi et al. (2009) for 28 Days	207
Figure 6-20: Relative Fit of Calibrated Modulus Prediction Equations for 28-Day Data for Dolomitic Limestones with Assumed Unit Weight of 150 pcf.....	211
Figure 6-21: Early-Age Disproportionality of Concrete Compressive Strength and Elastic Modulus at Two Producers (French and O'Neill 2012)	214
Figure 6-22: Crushed Granite (#67) Aggregate Sample.....	218
Figure 6-23: Cracking in the Vicinity of Schist Aggregate Particles at Failure.....	220

Chapter 1: Introduction

1.1 Background on Camber in Precast, Prestressed Concrete Girders

Camber can be defined as a deflection intentionally built into a structural element or form to improve appearance or to compensate for the deflection of the element under the effects of loads, shrinkage, and creep (ACI 2013). Within the precast, prestressed concrete community, camber is more precisely regarded as the net *upward* deflection due to the eccentricity of the prestressing force (Buettner and Libby 1979), as shown in Figure 1-1.

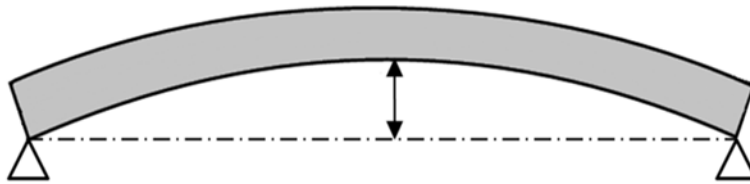


Figure 1-1: Exaggerated Girder Deformation and Midspan Camber

When properly predicted during the design phase, an appropriate amount of camber is desirable to avoid the perception of sagging under applied loads and to ensure proper alignment of adjacent bridge components.

Initial camber, or elastic camber, is the camber induced upon transfer of the prestressing force during fabrication of a bridge girder and is heavily dependent on the geometric properties of the girder, the stiffness of the constitutive materials, and the magnitude of the prestressing force (PCI 2011). The term camber growth refers to the tendency of the initial camber to experience a net time-dependent increase as a result of various interrelated factors including maturing concrete properties, time-dependent deformations of concrete (creep and shrinkage), relaxation of the prestressing steel, and varying girder curing and storage conditions. Midspan camber in precast, prestressed bridge girders is widely regarded as the beam deformation of greatest interest to bridge designers (PCI 2011) and thus, is the deflection most essential to accurately predict during the girder design phase.

1.2 Justification for Research

During the design of a bridge which relies on precast, prestressed concrete girders as the primary flexural elements, it is essential for engineers to accurately predict the midspan camber to ensure proper fit of girders during installation. Predictions of camber during the design phase are based heavily on assumptions—namely, those of future material properties used in constructing the element, and therefore are regarded as estimates at best (ACI Committee 435 2003). Design engineers are frequently cautioned against placing a high degree of confidence in the accuracy of predicted camber values to avoid constructability problems and related litigation exposure (Tadros, Fawzy, and Hanna 2011; Buettner and Libby 1979).

With the recent widespread implementation of high-strength concrete and self-consolidating concrete (SCC) for use in producing prestressed bridge girders, the accuracy of traditional camber prediction methods has been called into question by researchers and industry alike. Specifically, PCI bulb-tee shaped girders seem to exhibit some of the greatest disparities between predicted and observed camber, with design camber estimates most commonly tending to over-predict the actual observed field camber (Stallings, Barnes, and Eskildsen 2003; Rosa, Stanton and Eberhard 2007; PCI Committee on Bridges 2012). That is, the camber magnitude observed in the field is significantly less than that predicted during the girder design phase. Overestimation of camber can lead to construction difficulties and the need for placement of more deck concrete than originally estimated, as well as the unforeseen dead load that accompanies this additional concrete. In extreme cases, overestimations of camber during the design phase can even result in a bridge that ultimately sags under superimposed dead loads. Consequences of inaccurate camber predictions negatively affect multiple parties involved in the bridge construction industry, and thus, there has been a rising industry research effort to address this problem.

In recent years, the Alabama Department of Transportation (ALDOT) has experienced many cases where less-than-expected field camber values have resulted in construction difficulties and contentious relations between contractor, girder producers, and ALDOT. Although each involved entity has hypothesized various reasons for the disparity between the predicted and observed values, little has been done to date to alleviate the problem. Accordingly, this research study aims to explore the primary causes of inaccurate camber predictions in precast, prestressed concrete girders in the study region and

provide recommendations to those parties involved in the design and production of bridge girders to mitigate this troublesome issue in the future.

1.3 Research Objectives

The primary objective of this work is to advance the understanding of various factors that collectively influence the accuracy with which the magnitude of the observed camber can be predicted during the girder design phase. The scope of this investigation includes those factors influencing both the initial elastic camber, as well as the camber growth occurring prior to deck placement. A primary goal of this study is to develop and recommend a procedure resulting in more accurate predictions of camber in precast, prestressed girders during the design phase. Areas of particular focus include the following key topics:

- The disparity between the concrete compressive strength as specified by the design engineer and the strength achieved during girder production (hereafter termed overstrength);
- The relationships between modulus of elasticity and concrete compressive strength for regionally specific concrete mixtures utilizing varying constitutive materials;
- The time-dependent behavior (creep and shrinkage) of regionally specific concrete mixtures composed of varying constitutive materials;
- The effects of transient temperature gradients on the deformations of precast, prestressed girders; and
- The extent that camber predictions can be improved by implementing the cumulative recommendations resulting from the aforementioned focus areas.

1.4 Research Approach

A variety of research approaches are employed in this study to ensure that solutions practical, relevant, agreeable, and useful to all interested parties can be reached. This research represents a close collaborative effort among Auburn University Highway Research Center (AUHRC) researchers, ALDOT design and construction personnel, and various regional precast, prestressed concrete producers. The results of three major research approaches are documented in this report: (1) a historical review of available field production records, (2) a laboratory investigation aimed at characterizing various concrete

material properties relevant to camber prediction, and (3) a series of field-monitoring studies during and after the production of ALDOT prestressed bridge girders.

The historical review of available girder production records was primarily aimed at exploring the standard practices of the precast, prestressed concrete industry in the region and quantifying the difference between the concrete compressive strength as specified by the design engineer and the strength observed in the field during girder production. This effort included visits to four regional precast, prestressed concrete producers and the compilation of available production records for various ALDOT bridge girder projects produced in the preceding seven-year period. From these historical data, various valuable trends were captured regarding the practices of the precast, prestressed concrete industry in the region, and recommendations were derived to help design engineers estimate the overstrength expected in a bridge girder.

The laboratory phase of this project was designed to explore the effect of varying regional prestressed concrete compositions on those concrete material properties most relevant to camber predictions. Most importantly, the laboratory effort sought to capture the effect of varying coarse aggregate sources and supplementary cementing materials (SCMs) on concrete modulus of elasticity as well as creep and shrinkage behavior. By systematically varying the composition of the concrete mixtures included in this study, valuable information regarding the material properties of concretes used in the precast, prestressed industry was discovered.

The field monitoring phase of this project was performed to validate and expand the findings of the previous phases, while also capturing the in-place structural and deformational behavior of ALDOT bridge girders during construction. In an attempt to provide a view of various in-situ camber-relevant factors uninfluenced by research efforts, a deliberate effort was made by researchers to minimize disruptions to the girder production process. The field monitoring phase included (1) on-site concrete testing, (2) measurement of beam deformations and temperatures during production, (3) extended field monitoring covering the early life of selected girders, and (4) targeted field studies to quantify the influence of temperature on girder camber behavior. Using this approach, researchers were able to document the observed field camber and camber growth of various production girders in order to compare to the results of analytic camber prediction techniques.

1.5 Report Organization and Outline

This report is divided into eleven chapters representing three distinct sections. Chapters 1-4 acquaint the reader with the research topic, provide a general background of previous work in the area, and document the current design and girder production practices in the region. The literature review of Chapter 3 serves as an introduction to, and a general summary of, previous camber studies. Chapters 5-8 each address a specific research objective and incorporate a synthesized literature review of each topic. Then, the experimental efforts, analytical work, and conclusions are presented for each topic. Chapters 9-10 detail (1) the implementation of the cumulative recommendations proposed in Chapters 5-8 to generate predictions of camber for the projects observed during field monitoring studies and (2) comparisons between the predicted cambers and the observed field cambers as used to evaluate the adequacy of the recommendations to improve camber predictions in precast, prestressed concrete girders.

Chapter 2: Background

2.1 Introduction

This chapter is intended as a brief background discussion of deflections in one-way prestressed flexural elements and various intrinsically related topics. Explicit design code provisions or specific recommendations by previous researchers are withheld until later chapters, where presented by topic. A brief discussion on the variability and expected degree of accuracy of deflection calculations is first offered, followed by a general introduction to deflections of one-way prestressed flexural elements and a review of the primary factors affecting these deflections. Finally, various common methods for computing both short-term deflections (e.g. instantaneous elastic camber) and long-term deflections (e.g. camber growth) are reviewed.

2.2 Variability and Limitations of Deflection Predictions

A logical first question in a study aimed at improving predictions of deflections is how accurately can an engineer expect to predict deflections during the design phase? This section aims to provide a discussion of this topic, as well as to address other related questions including (1) when are deflection predictions accurate enough, and (2) to what extent is effort spent attempting to improve the accuracy of deflection predictions justified in the precast, prestressed concrete industry?

Control of Deflection in Concrete Structures (ACI Committee 435 2003), representing the consensus of ACI Committee 435, is a logical starting point for those seeking clarification on the anticipated accuracy of deflection calculations. ACI Committee 435 (2003) notes that deflection calculations are based on various randomly distributed variables (e.g. concrete strength, concrete stiffness, and creep and shrinkage behavior) and that the distributions of these constitutive variables cannot be established with great precision. An example showing the random variability (as represented by the mean, μ , and standard deviation, σ) in a simple parameter such as a measured length (or quantity derived thereof) is shown in Figure 2-1.

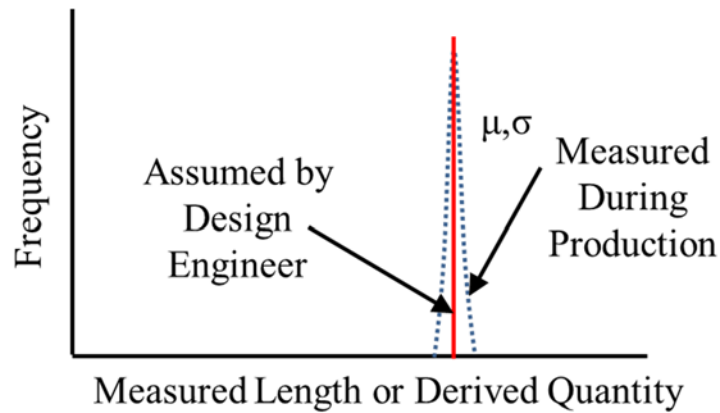


Figure 2-1: Random Variability of a Measured Length

The vertical solid line might represent an exact value for the specified length of a girder (i.e. 1,000 in.). Here, it is assumed that the contractor producing beams targets the specified length as precisely as possible given available measurement techniques (i.e. a length measurement tool with precision of 1/16 in.). The dashed curve represents a sampling of the random variable girder length for all similar girders produced. This dashed curve is normally distributed by virtue of it being derived from a manufacturing process with discrete limits to the precision of available tools. In this case, the mean, μ , of the sampled distribution coincides with the targeted value and the sampling distribution indicates excellent agreement between the girder length specified by design engineer and the average girder length observed during construction. While the distribution for the variable girder length is rather narrow (as evidenced by a small standard deviation, σ), the distribution of other random variables necessary for design computations (i.e. concrete strength, concrete stiffness, and internal force effects) exhibit much greater variability. By virtue of the compounded effect of those random variables used in deflection calculations, an intrinsic level of variability is unavoidable in these computations. Accordingly, deflection calculations should be regarded only as reasonable estimates of the anticipated deflection response of a structure. Buettner and Libby (1979); Tadros, Fawzy, and Hanna (2011); and the PCI Bridge Design Manual (2011) share this cautionary sentiment, advising design engineers against heavy reliance on the accuracy of design deflection predictions.

Another logical question is how accurate is accurate enough when predicting deflections during the girder design phase? At first thought, the answer appears to be simple—when deflections are predicted accurately enough, constructability issues do not ensue during production or erection of the

element. While partially true, it is important to note that the avoidance of constructability issues may not be wholly due to an overly accurate *estimate* of deflections, but instead due to a forgiving level of tolerance in design or construction. In fact, various parties have suggested that the solution to camber prediction inaccuracies lies not in improving camber prediction methods, but instead in increasing design and construction tolerances to avert constructability issues (PCI 2012; Tadros et al. 2011). A complex relationship exists between these parameters and is perhaps best stated as follows: for a given level of design and construction tolerance, a deflection prediction is accurate enough when constructability problems (of the nature capable of being avoided by progressively more accurate predictions) do not ensue during production or erection of the element. More simply put, the degree of accuracy in camber predictions needed to avert constructability problems in a bridge detailed with relatively low levels of design tolerance (i.e. minimal thickness girder haunch¹) is much higher than the degree of accuracy needed to avert constructability problems in a bridge detailed increased levels of design tolerance (i.e. more substantial haunch).

An additional factor also further complicates the issue of pinpointing an acceptable level of accuracy for deflection predictions for girders designed with varying cambers. Suppose a certain procedure used by a design engineer for computing deflections yields up to a 25 percent error when compared to the constructed element. Those girders with a relatively small camber may still fall within prescribed tolerance allowances, while girders with larger cambers may exceed tolerance allowances and experience constructability problems. For instance, a 50 percent error on a predicted camber of 1 in. is unlikely to be significant, but a 50 percent error on a girder with a more extreme design camber of 5 in. may well cause constructability problems. The relevance of the concept (relative error versus absolute error) was first discussed by Buettner and Libby (1979) in the context of camber prediction accuracy, but remains equally relevant today.

A final discussion is now offered exploring (1) the extent to which effort spent attempting to improve deflection *estimates* is justified and (2) the most logical and practical approaches to improve deflection *estimates*. As noted by ACI Committee 435 (2003), the accuracy of deflection *estimates* typically does not significantly improve with advanced analytical or mathematical modeling techniques.

¹ The term haunch refers to the concrete build-up used to fill the distance from the top of the girder to the bottom elevation of the bridge deck along the girder length.

Even these advanced *estimates* are still based on variables with random variability and, therefore, may not yield significantly more accurate estimations than simple calculations. In fact, in an effort to be seemingly *more accurate*, some advanced analytical approaches rely on the introduction of additional random variables and can therefore actually yield *less accurate* results (ACI Committee 435 2003). The pertinent question then becomes—with no easily identifiable single metric of camber accuracy to target in all cases, what is the most logical approach to attempt to improve the accuracy of deflection *estimates*?

Tadros et al. (2011) noted that the inherent variability in deflection calculations is often incorrectly used as a catch-all to justify the usage of theoretically-questionable analytic procedures and less than accurate assumptions of future material properties. It is important that the presence of random variability in deflection computations not be confused with that of systematic error introduced by incorrect assumptions of future material properties during the girder design phase. The differences between these two concepts is illustrated in Figure 2-2 for concrete modulus of elasticity.

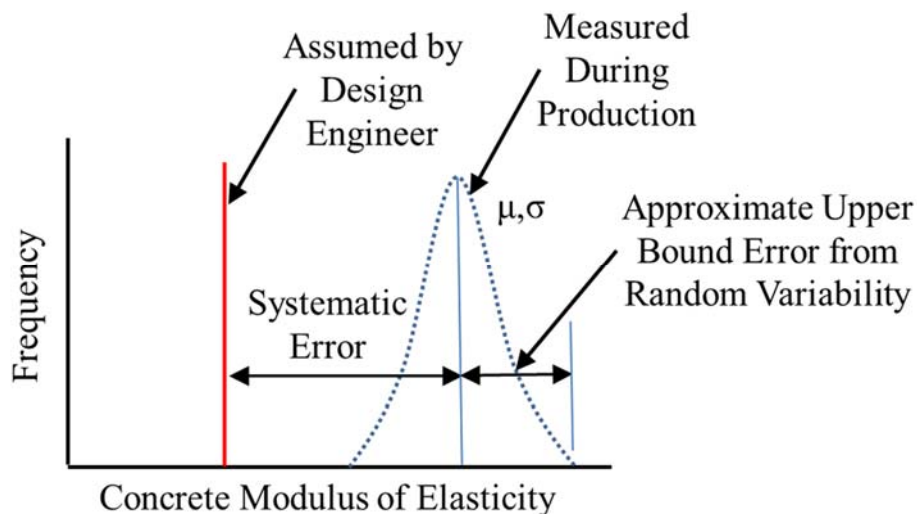


Figure 2-2: Systematic Error of a Random Variable

Similar to the previous example, the solid vertical line indicates the assumed modulus of elasticity used in deflection calculations, while the dashed curve denotes the sampling distribution of the random variable during production. A relatively widely dispersed normal distribution is indicated due to the large number of construction activities affecting this variable (compounding of random error) and the relatively large bias present in performing concrete material testing. For example, Tadros et al. (2011) note that the field measurements of the modulus of elasticity for identical concretes can vary by ± 22 percent at the time of

prestress transfer. In this case, the assumed value for modulus of elasticity does not coincide with the mean of the sampled distribution, indicating that the assumption of future material properties was inaccurate and fell well below the actual sampled value. This disparity represents a systematic error, independent from the random variability of the parameter. This concept of systematic error is also discussed by Buettner and Libby (1979).

With an understanding of the difference between systematic error and random variability, it becomes clear that the most logical and greatest potential for increases in the accuracy of camber predictions may be achieved by improving the assumptions of future material properties during the design phase, thereby minimizing certain sources of systematic error. The issue of improving camber predictions, as explored in this report, is not then one of a particularly advanced analytical nature, but instead predominately an issue of making more educated design phase assumptions regarding the material properties of the girder concrete expected to be used in girder production.

2.3 Deflections in One-Way Prestressed Flexural Members

Deflections in one-way prestressed flexural members can be divided into two primary categories: short-term deflections and long-term deflections. Each of these categories is defined and discussed in this section. For the purposes of this section and in accordance with regional design practices, the focus remains on computing deflections in uncracked prestressed concrete flexural members, that is, Class U (uncracked) sections as classified in ACI 318-14 (ACI Committee 318 2014).

The initial net camber (a short-term deflection) of a prestressed concrete girder is first observed during production upon transfer of the prestressing force to the bulk concrete section. This initial camber represents a superposition of two simultaneous effects: the tendency of the eccentric prestressing to induce negative bending and that of the girder self-weight to induce positive bending, as shown in Figure 2-3.

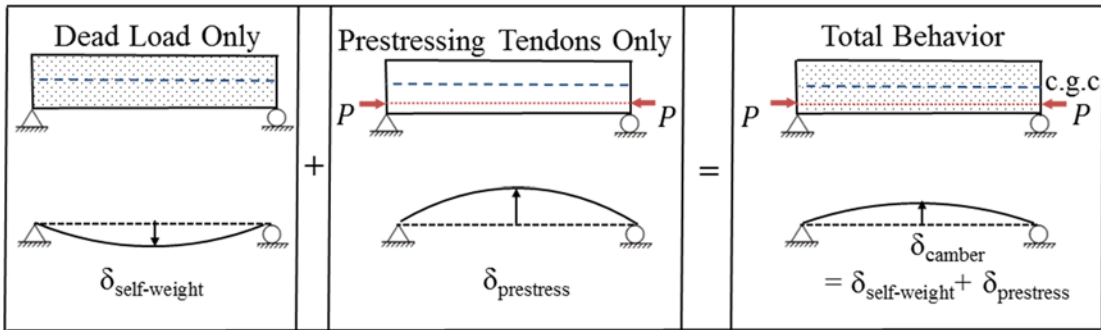
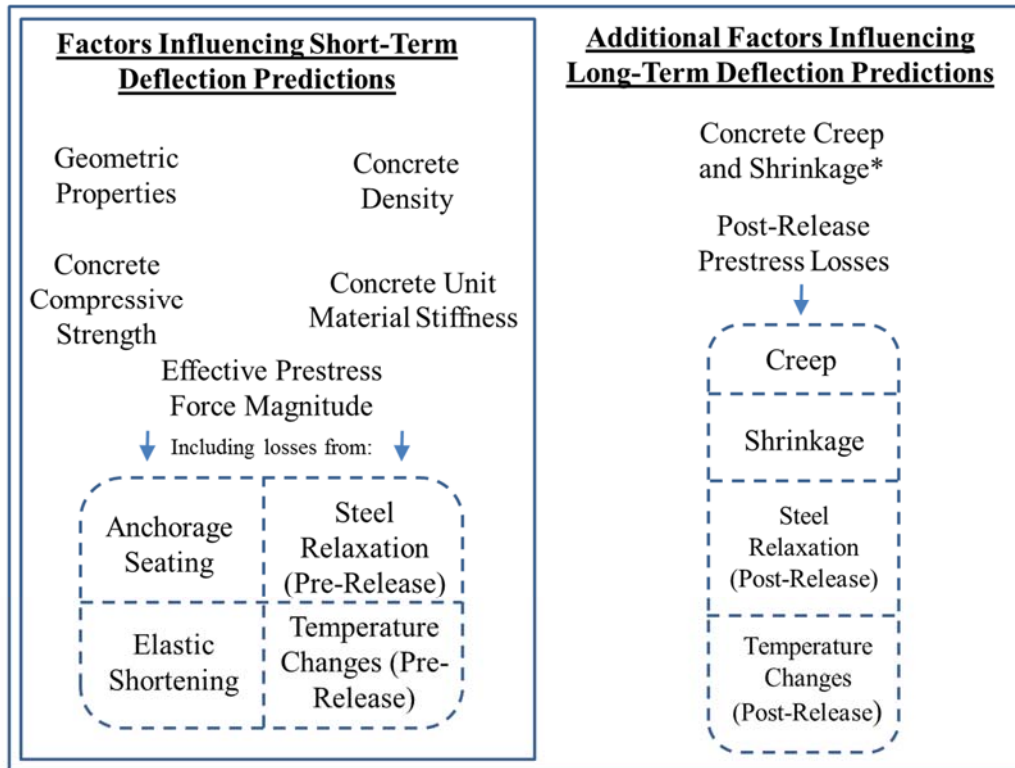


Figure 2-3: Net Instantaneous Deflections at Prestress Transfer in Prestressed Girders (adapted from Isbiliroglu 2014)

Immediately upon transfer of the prestressing force during girder production, the process of camber growth begins. The term camber growth refers to the tendency of the initial camber magnitude to experience a *net increase* with time as a result of various interrelated factors including the maturing of concrete properties, time-dependent deformations of concrete (creep and shrinkage), and relaxation of the prestressing steel (ACI 435 2003). Concrete creep is the factor primarily responsible for the camber growth tendency, while the simultaneous gradual loss of prestressing force (caused by a combination of creep, shrinkage, and strand relaxation) tends to have a mitigating effect, slightly reducing the initial rate of camber growth as time progresses (PCI 2011).

2.4 Primary Factors Influencing Flexural Deflection Predictions

This section includes a description of the primary factors influencing both short-term and long-term deflections in one-way prestressed flexural members. In the following sections, an effort is made to clearly differentiate between those quantities relevant to short-term deflections, long-term deflections, and both short- and long-term deflections, with a summary shown in Figure 2-4. For those topics that are of a primary focus of this investigation (i.e. concrete strength, concrete stiffness, concrete creep and shrinkage behavior), only a brief background is presented in this section in lieu of comprehensive treatment of these topics in standalone chapters later in this report.



Note: * = Concrete creep and shrinkage behavior are indicated separately from their contribution to post-release prestress losses due to their tendency to induce changes in time-dependent deformations independent of the presence of prestressing steel (i.e. in conventionally-reinforced concrete beams).

Figure 2-4: Primary Factors Influencing Deflections in Prestressed Concrete Girders

2.4.1 Geometric Properties

Precast, prestressed concrete girders are an economical choice for bridge construction due, in large part, to the use of standardized cross sections enabling efficient mass production (PCI 2011). Among the most commonly used cross sections are PCI bulb-tee shapes (most commonly used in three primary depths: 54, 63, and 72 in.) and AASHTO standard sections (Types I-VI). PCI bulb-tee shapes are of primary relevance to this report due to their widespread use in Alabama. Selected cross-sectional dimensions of various standard PCI bulb-tee shapes are shown in Figure 2-5. Also shown in this figure are standardized potential strand locations located in a 2 in. by 2 in. grid pattern.

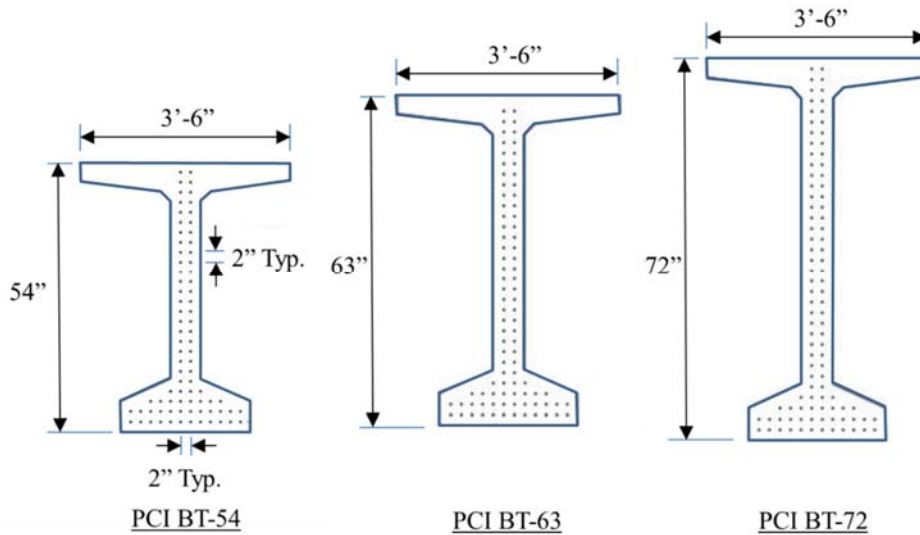


Figure 2-5: Standard Dimensions of PCI Bulb-Tee Cross-Sections (Adapted from PCI 2011)

More detailed dimensions, as well as various section properties of these standard sections, are shown in Figure 2-6.

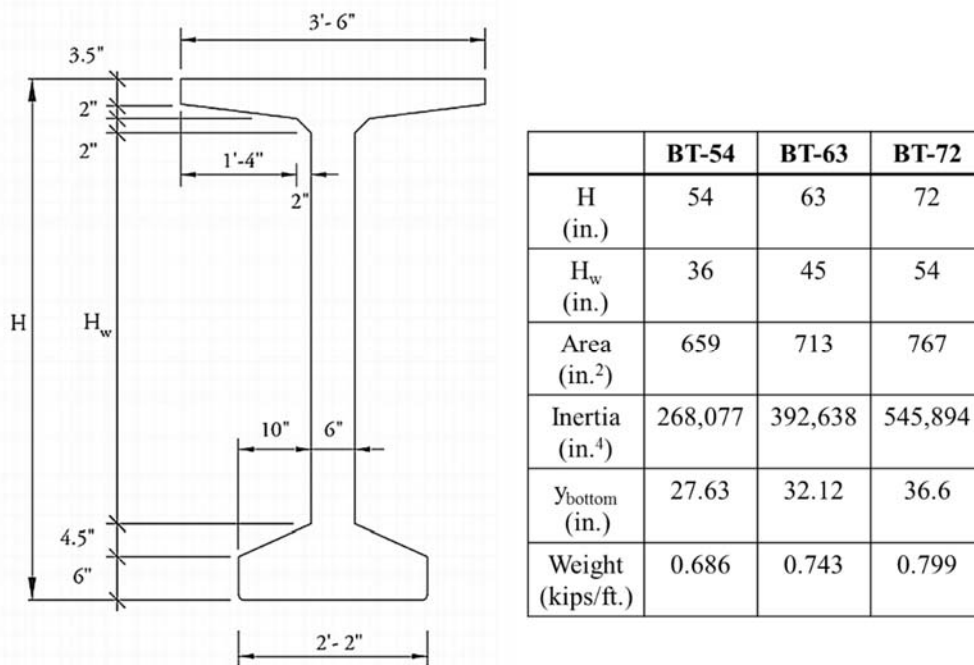


Figure 2-6: Detailed Section Properties of PCI Bulb-Tee Shapes (Adapted from PCI 2011)

Maximum design span length for each bulb-tee shape is primarily a function of the transverse lateral spacing of girders, due in large part to standardized bridge loadings and the maximum prestress force magnitude and orientation being somewhat prescribed by virtue of a limited number of strand

locations and orientations. BT-72 shapes are capable of the longest clear spans, approaching 160 ft in bridges with 6 ft transverse girder spacing. BT-63 girders typically span up to approximately 140 ft, while BT-54 girders are capable of spanning up to approximately 125 ft (PCI 2011). Generally speaking, increased span lengths correspond to increases in the magnitude of required prestressing forces, which in turn lead to higher design cambers in long-span bridge girders, as noted by Stallings et al. (2003).

2.4.2 Concrete Density

Concrete density influences the magnitude of initial and long-term girder deformations both directly and indirectly. The density of the concrete used in girder fabrication is relied on to compute the self-weight component of deflection at the time of prestress release and, therefore, directly affects the magnitude of net camber at both the time of prestress transfer and all subsequent girder ages. Concrete density is also indirectly related to concrete unit stiffness, which is a critical parameter in any deflection computation.

2.4.3 Concrete Compressive Strength

The compressive strength of concrete is the property most valued to design and quality control engineers and is generally defined as the ability of the concrete to resist compressive stress without failure (Mehta and Monteiro 2014). Not only essential for structural design and quality-assurance purposes, concrete strength also provides perhaps the most complete overall picture of the quality of a given concrete (Neville 2013). Concrete compressive strength is indirectly relevant to both short-term and long-term deflection predictions because it serves as a basis for estimating concrete stiffness. A full discussion of this topic, including a synthesized literature review and the experimental program on this topic, is included in Chapter 5 of this report.

2.4.4 Concrete Stiffness

Concrete unit material stiffness, as represented by the modulus of elasticity, is a parameter fundamental to the computation of both short-term and long-term deflections in prestressed concrete elements. Generally speaking, the modulus of elasticity of a given material is defined as the ratio between the applied uniaxial stress and instantaneous strain within an assumed proportional limit (Mehta and Monteiro 2014). It is this relationship that governs elastic material behavior and serves as the basis for deflection

computations in structural elements. A full discussion of this topic, including a synthesized literature review and an experimental program, is included in Chapter 6 of this report.

2.4.5 Concrete Creep

Naaman (2004) defines creep as “the time-dependent strain in excess of elastic strain induced in concrete subjected to a sustained stress.” While creep does not influence short-term deflections in prestressed concrete, it is the primary factor contributing to the tendency for camber growth to occur. If concrete did not exhibit creep under sustained compressive loading, camber growth would simply not occur. Instead, short-term camber would actually tend to decrease with time as a function of concrete shrinkage and steel relaxation. Full treatment of this topic is detailed in Chapter 7 of this report.

2.4.6 Concrete Shrinkage

The term shrinkage of concrete refers to the total time-dependent volume reduction experienced by concrete due to changes in the moisture content. In general, concrete shrinkage is assumed to not significantly influence short-term deflections, but is a factor that influences long-term deflections. The primary effect of shrinkage on deflections stems from its restraint by eccentric reinforcement, which accompanies a prestress loss in that reinforcement. In general, concrete shrinkage acts a mitigating factor, not directly contributing to the growth of long-term deflections, but actually reducing the rate of continued time-dependent camber growth. Full treatment of this topic is detailed in Chapter 7 of this report.

2.4.7 Steel Relaxation

The steel strands used to prestress concrete girders are prone to relaxation due to the relatively high levels of stress sustained over an extended time period. While steel relaxation can affect both short-term and long-term deflections, the effect of steel relaxation prior to prestress transfer is largely negligible when compared to post-transfer losses due to the relatively short time-period elapsed between strand stressing and transfer of the prestressing force (PCI 2011). Thereby, steel relaxation primarily affects long-term deflection computations by its contribution to the total magnitude of prestress losses, as discussed in the following section.

2.4.8 Prestress Losses

A discussion of the factors influencing deflection computations in prestressed concrete members is not complete without mention of prestress losses. The partial loss of the prestressing force occurs beginning at the time of prestress transfer and continues, theoretically, through the life of the girder. In order to compute anticipated member deflections, it is necessary to calculate the effective prestress force (that is, the jacking force minus losses) in a member as a function of time. Prestress losses affect both short-term and long-term deflection computations and can accordingly be divided into two primary groups: short-term prestress losses and long-term prestress losses.

Short-term prestress losses include losses caused by anchorage seating, steel relaxation, temperature effects, and elastic shortening (Tadros, Al-Omaishi, Seguirant, and Galt 2003). These short-term losses are graphically depicted in Figure 2-7 by letters A through D. While the contribution of anchorage seating losses, steel relaxation, and temperature effects are relatively minimal (often due to contractors actively compensating for these effects during production), elastic shortening is the primary contributor to short-term prestress losses (Tadros et al. 2003).

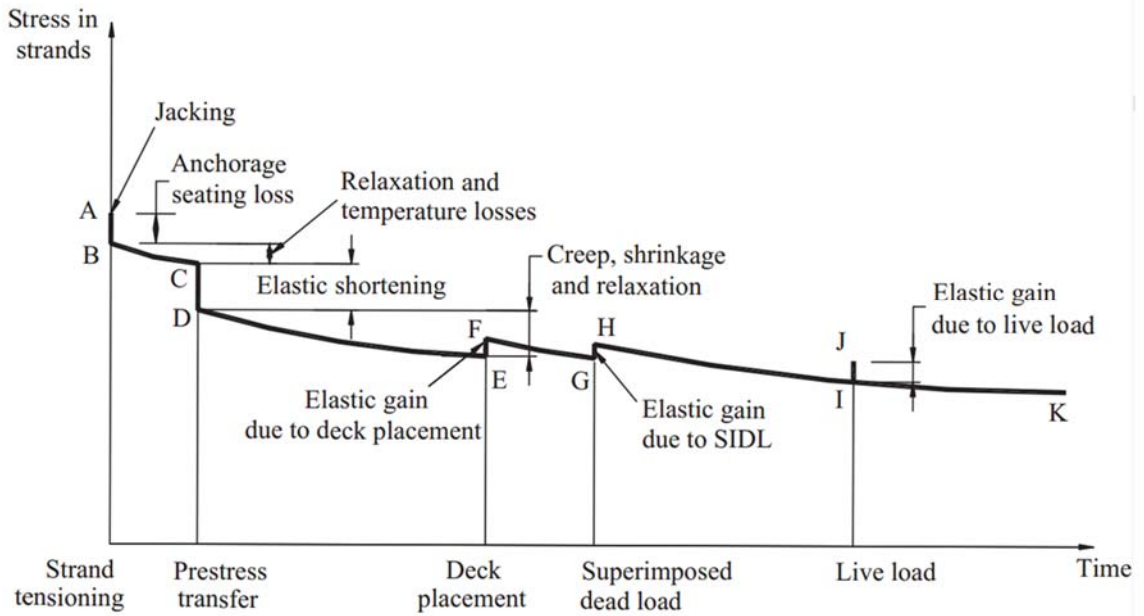


Figure 2-7: Graphical Representation of Prestress Loss Contributions (Adapted from Tadros et al. 2003)

In the context of this report, the term “long-term losses” is used to identify those losses occurring after the transfer of the prestressing force and prior to the time of deck placement. These long-term losses are caused by the complex interaction of creep and shrinkage behavior of concrete, steel relaxation, and temperature changes. Long-term losses are signified in Figure 2-7 by letters D through E. While many different techniques exist to estimate or compute long-term prestress losses, each of these techniques fundamentally relies on selecting accurate material models for concrete stiffness, steel relaxation, and creep and shrinkage behavior. Steel relaxation is fairly well-documented by others (i.e. Magura, Sozen, and Seiss 1964 and AASHTO 2014) and is generally not viewed as a major contributor to variability in estimating the effective prestressing force in concrete elements due to the relatively small magnitude of relaxation losses as compared to other prestress loss sources (PCI 2011). Conversely, concrete stiffness, and creep and shrinkage behavior are major contributors to variability in estimating the effective prestress force, and therefore have a large potential impact on the accuracy of deflection computations. More detail on the specific methods used to predict concrete material behavior and prestress losses in this research project, implemented as part of incremental time-steps analysis, is included in Chapter 9 of this report.

2.5 Techniques For Computing Short-Term Deflections

This section reviews three common techniques for computing short-term deflections in uncracked one-way prestressed flexural elements. The first two techniques, the moment-area method and tabulated equation method, are the techniques most commonly used. The third method detailed herein, an energy method, represents an effort to evaluate the feasibility of computing camber using a method not typically applied to deflection computations in prestressed concrete flexural elements. Each of the three techniques summarized here represent either a direct or in direct application of engineering beam theory.

2.5.1 Elastic Camber Computation by Moment-Area Theorem

One of the most commonly used analytical methods to compute design deflections in simple flexural elements is the moment-area theorems as originally developed by Otto Mohr and later refined by Charles E. Greene in 1873 (Hibbeler 2006). These theorems provide a semi-graphical technique for determining the slope of the elastic curve and corresponding beam deflections due to bending. Due to their importance and widespread use in predicting initial elastic camber, a summary of the application of the moment-area theorems follows. While these methods can equally be applied to member self-weight to compute the simultaneous downward deflection component, this discussion focuses on the computation of the upward camber component for some of the most common prestressing strand patterns.

In accordance with engineering beam theory, for a beam with a length much greater than its depth, the internal moment in a beam can be related to the displacement and slope of the elastic curve resulting from that moment by Equation 2-1 as follows:

$$\frac{1}{\rho} = \frac{M}{EI} \quad (2-1)$$

where

ρ = the radius of curvature at a specific point on the elastic curve;

M = the internal moment in the beam at the point where ρ is determined; and

EI = the flexural rigidity (the product of the elastic modulus of the material, E , and the moment of inertia of the beam computed about the neutral axis, I).

Using the geometry of the deformed beam and the arc-length relationship illustrated in Figure 2-8, the radius of curvature, ρ , can be approximated as $\frac{dx}{d\theta}$, where dx represents the infinitesimal portion of the elastic curve along the neutral axis for each cross section and $d\theta$ represents the change in angle between cross sections due to the internal moment, M .

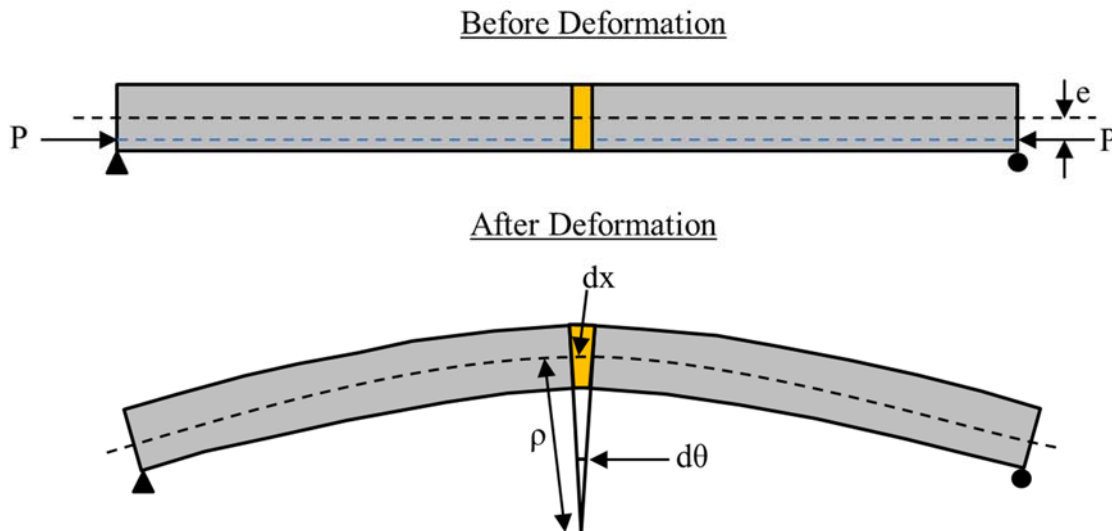


Figure 2-8: Engineering Beam Theory in a Flat-Strand Prestressed Girder (Adapted from Hibbeler 2006)

Substitution of this relationship into Equation 2-1 and simplification yields the following:

$$d\theta = \frac{M}{EI} dx \quad (2-2)$$

Equation 2-2 serves as the direct basis for development of the first moment-area theorem. By integrating Equation 2-2 along a length of beam, the first moment area theorem is derived, stating that the change in slope between any two points on the elastic curve equals the area of the M/EI diagram between these two points (Hibbeler 2006).

The second moment-area theorem expands on the first theorem and provides a method to determine the deviation between two tangents on a beam's elastic curve. The second moment-area theorem is stated by Hibbeler (2006) as follows:

“The vertical deviation of the tangent at [one point] on the elastic curve with respect to the tangent extended from another point... equals the moment of the area under the M/EI diagram between these two points... [taken about the first point].”

The primary factors making this theorem possible are the assumption of small deformation angles and the use of the arc-length formula. Generally, the second moment-area theorem does not yield a direct solution for the desired deflection within a beam. However, in the specialized case of a simple-span prismatic beam with symmetric loading (i.e. midspan camber in a precast, prestressed concrete element), the vertical deviation between a point at the girder end and midspan does indeed give the magnitude of the midspan deflection. This concept is graphically explained in subsequent sections detailing the application of the second moment-area theorem to computation of the upward component of camber at the midspan section.

A prestressed concrete beam with a uniform-eccentricity profile is shown in Figure 2-9 (top). In this simplified idealization, the net prestressing force (after losses), P , is assumed to be known and applied as a concentrated load at the end of the beam, thus the effects of debonding and end-region transfer length are neglected at present. A resulting curvature diagram is also shown in the figure, derived from constant internal moment along the length of the girder of magnitude Pe , where e is the eccentricity from the elastic centroid of the cross section.

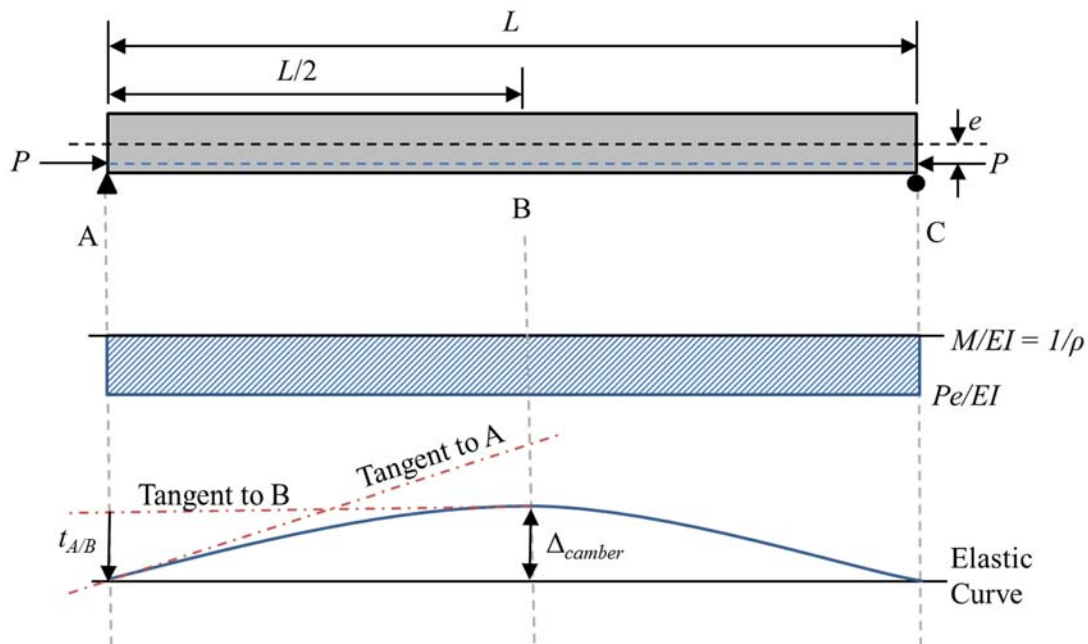


Figure 2-9: Application of Moment-Area Theorem to Calculate Elastic Camber in Flat-Strand Prestressed Girder

In the bottom of Figure 2-9, an exaggeration of the elastic curve is shown and tangent lines are shown intersecting the elastic curve at point A (left-support) and point B (midspan). By virtue of the symmetric

deflected shape, the vertical deviation of the two tangents at A, denoted $t_{A/B}$, is the same vertical distance as the upward midspan camber tendency, Δ_{camber} . The upward camber tendency in flat-strand prestressed girders can be calculated as:

$$\Delta_{camber} = t_{A/B} = \left[\left(\frac{L}{2} \right) \left(\frac{Pe}{EI} \right) \right] \left(\frac{L}{4} \right) = \frac{Pe}{EI} \left(\frac{L^2}{8} \right) = \frac{M}{EI} \left(\frac{L^2}{8} \right) \quad (2-3)$$

Another frequently used pattern of prestressing strands in prestressed concrete girders is that of a harped (draped) strand configuration. Harped strands can be present at any elevation within the cross section, but are typically positioned highest at the girder ends and lowest towards the girder center to counteract gravity-induced force effects (PCI 2011). A harped-strand profile is shown in Figure 2-10 (top), with the strands intersecting the elastic centroid at beam ends and exhibiting a known eccentricity, e , at the girder midspan. In this example, the strands follow a straight line harp pattern through a distance bL from the girder end.

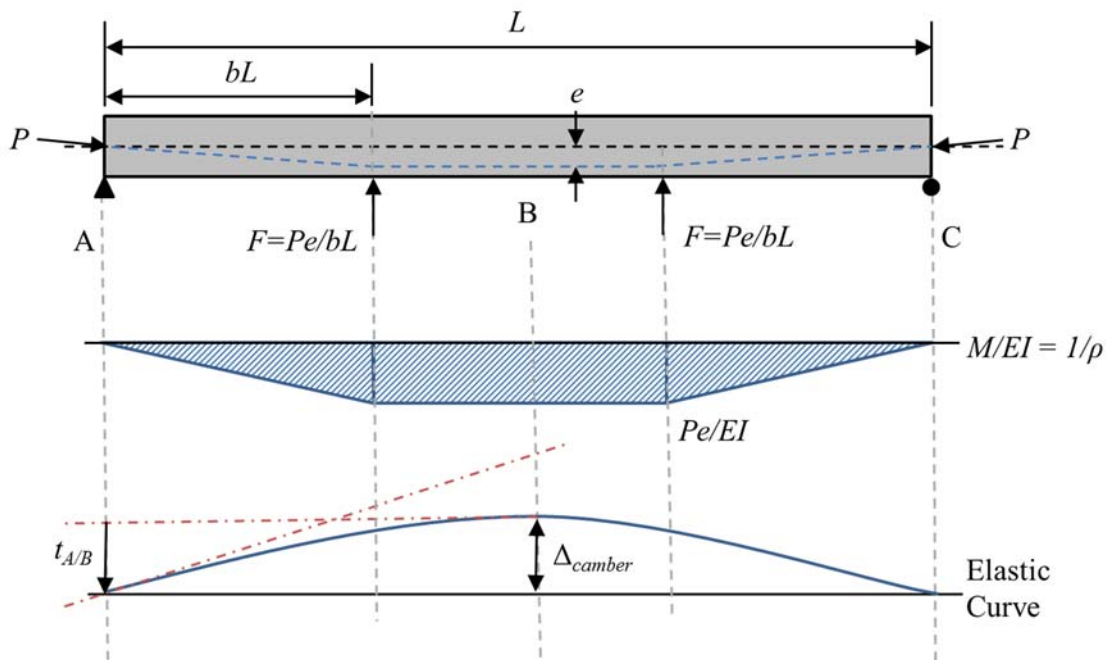


Figure 2-10: Application of Moment-Area Theorem to Calculate Elastic Camber in Simple Harped-Strand Prestressed Girder

A corresponding curvature diagram is also shown in Figure 2-10 (middle). In similar fashion to the previous example, the upward midspan camber tendency for this harped-strand girder can be then calculated as:

$$\Delta_{camber} = t_{A/B} = \left[\left(\frac{Pe}{EI} \frac{bL}{2} \right) \left(\frac{2}{3} bL \right) \right] + \left[\left(\frac{Pe}{EI} \right) \left(\frac{L}{2} - bL \right) \right] \left(bL + \frac{\left(\frac{L}{2} - bL \right)}{2} \right) \quad (2-3)$$

Due to the straight line nature of the curvature diagrams in the two preceding examples, it is possible to compute the desired midspan deflection relatively simply by discretizing the curvature diagram into three distinct sections. If a deflection at a location other than midspan (i.e. one-sixth span) is desired, the linear nature of the curvature diagrams discussed above again allow for simple computation of the required area under the curvature diagram. In other strand profiles representing higher-order curvature diagrams (e.g. parabolic draped strands), the solution for deflections at locations other than girder midspan (i.e. one-sixth span) can become more complex due to the higher-order nature of the curvature diagrams and the associated complexities in computing the required area of interest under the curvature diagram.

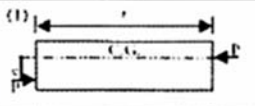
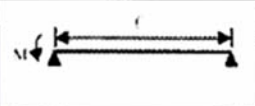
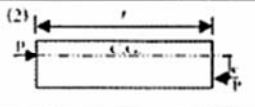

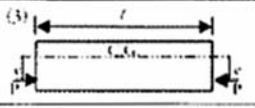
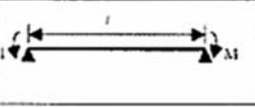
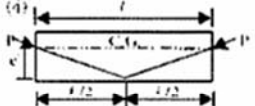
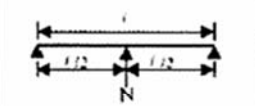
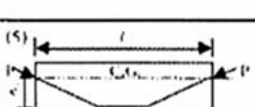
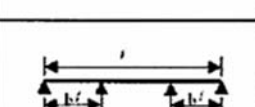
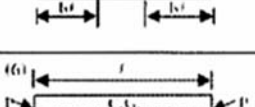
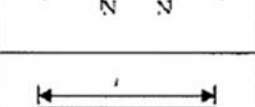
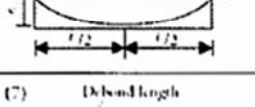
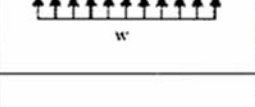
The moment-area method provides a robust, easily-programmable method, with the inherent flexibility to accommodate varying cross-sectional properties along the length of the girder. Among the most frequent refinements to the simplified procedures detailed above are the inclusion of debonding of prestressing strands and inclusion of the effect of transfer length at girder ends. The moment-area method is the primary technique for computing short-term deflections in two of the most popular prestressed concrete girder design software packages, *LEAP Conspan* by Bentley Systems, Inc. (Bentley Systems, Inc. 2012) and *PSBEAM* by Eriksson Technologies³.

2.5.2 Elastic Camber Computation by Tabulated Equation

In today's design environment, deflection computations for prestressed concrete members are seldom calculated by hand, but instead, are computed in advanced software packages. For those design engineers needing to verify the outputs of their computer analyses, the somewhat tedious direct application of engineering beam theory (either by the moment-area technique or other implementation of beam theory) is hardly a practical choice. Instead, the PCI Bridge Design Manual (PCI 2011) offers tabulated expressions of the upward camber tendency for seven of the most common prestressing patterns as shown in Figure 2-11. It is worthwhile to note that Cases 3 and 5 in the following table

³ As verified through author correspondence with Eriksson Technologies.

correspond to the two cases previously derived in this report by the moment-area method. Another convenience of the use of tabulated expressions is the simplicity with which the method of superposition may be applied to quickly solve for midspan camber magnitude for nearly any possible prestressing pattern and self-weight loading pattern. For instance, a design engineer attempting to compute the net design deflection due to a harped-strand prestress arrangement, not centered around the elastic centroid, including the effect of self-weight, might use a superposition of Cases 3, 5, and 6 (although the sign on Case 6 would become negative.)

Prestress Pattern	Equivalent Moment or Load	Equivalent Loading	Camber	End Rotation	
(1) 	$M=Pe$		$+\frac{M\ell^2}{16EI}$	$+\frac{M\ell}{3EI}$	$-\frac{M\ell}{6EI}$
(2) 	$M=Pe$		$+\frac{M\ell^2}{16EI}$	$+\frac{M\ell}{6EI}$	$-\frac{M\ell}{3EI}$
(3) 	$M=pe$		$+\frac{M\ell^2}{8EI}$	$+\frac{M\ell}{2EI}$	$-\frac{M\ell}{2EI}$
(4) 	$N = \frac{4Pe'}{\ell}$		$+\frac{N\ell^3}{48EI}$	$+\frac{N\ell^2}{16EI}$	$-\frac{N\ell^2}{16EI}$
(5) 	$N = \frac{Pe'}{b\ell}$		$+\frac{b(3-4b^2)N\ell^3}{24EI}$	$+\frac{b(1-b)N\ell^2}{2EI}$	$-\frac{b(1-b)N\ell^2}{2EI}$
(6) 	$N = \frac{8Pe'}{\ell^2}$		$+\frac{5w\ell^4}{384EI}$	$+\frac{w\ell^4}{24EI}$	$-\frac{w\ell^4}{24EI}$
(7) 	$M=Pe$		$+\frac{M\ell^2}{8EI}(1-2b_1^2-2b_2^2)$	$+\frac{M\ell^2}{2EI}[(1-2b_1)^2-b_2^2]$	$-\frac{M\ell^2}{2EI}[(1-2b_1)^2-b_2^2]$

* The tabulated values apply to the effects of prestressing. By adjusting the directional rotation, they may also be used for the effects of loads. For patterns 4 to 7, superimpose on 1, 2 or 3 for other C.G. locations

Figure 2-11: Camber and Rotational Coefficients for Prestress Force and Loads (Precast/Prestressed Concrete Institute 2011)

2.5.3 Elastic Camber Computation by Energy Method

Energy methods are commonly used for computing elastic deflections in the field of structural mechanics. In fact, as structural members and assemblages become more complex, the application of energy methods and their scalar nature make them an attractive choice for deflection computations in these complex systems (Boresi and Schmidt 2003). Through a comprehensive review of available literature on deflections and more specifically, camber in prestressed concrete girders, no evidence was found of any past attempt to compute camber by the use of an energy method. As such, an independent effort was undertaken to investigate the feasibility of employing energy methods to compute elastic design deflections in prestressed concrete girders. A full discussion of this effort is outside the scope of this document, but a description is included in Mante (2016) for the interested reader. While it did prove possible to calculate deflections in prestressed concrete members by the direct application of the conservation of energy principle, this approach was extremely complex and likely not practical for use by design engineers. It is interesting to note, however, when using energy principles to compute short-term camber, there may be unique opportunities afforded to account for second-order deformations typically neglected by other types of analyses.

2.6 Techniques to Compute Long-Term Deflections

The computation of long-term deflections is substantially more complex than that of short-term deflections due to the number of parameters involved and the time-dependent and interrelated nature of these parameters. ACI 435R-95 (2003) provides guidance on five methods appropriate for computing long-term deflections in one-way prestressed concrete flexural members. Of these five methods, the following four methods are applicable to computing deflections in uncracked flexural members: (1) PCI multiplier method, (2) incremental time-steps method, (3) approximate time-steps method, and (4) the prestress loss method. A brief review of each method is offered in this section. Readers may consult Chapter 9 for more advanced theory and implementation of the incremental time-step method as used in this study.

2.6.1 PCI Multiplier Method

Multiplier methods are the simplest available methods for predicting time-dependent deformations in precast, prestressed elements. The basic premise is that a multiplier is applied to amplify a computed

short-term deflection value to approximate the long-term deflection. Early published multiplier methods were arbitrarily assigned by design engineers based on experience and served primarily as rules of thumb. Then, a more logically-grounded multiplier method was proposed by Martin (1977) that is still widely used today and forms the basis for design guidance offered in the PCI Bridge Design Manual (PCI 2011).

The multiplier method, as proposed by Martin, was intended to reflect design equations available at the time for estimating additional long-term deflection of nonprestressed reinforced concrete members. ACI Committee 318 (1971) suggested the following expression for computing the factor representing the *additional* long-term deflections in doubly-reinforced non-prestressed sections:

$$\left[2 - 1.2 \left(\frac{A'_s}{A_s} \right) \right] \geq 0.6 \quad (2-4)$$

where

A'_s = the area of compressive steel reinforcement and

A_s = the area of tension steel reinforcement.

It is interesting to note that in present day, ACI Committee 318 (2014) recommends the use of a similar expression to that of Equation 2-4 as developed by Branson (1977). This current-day equivalent, shown below, includes an added factor, ξ , that allows for predictions of additional long-term deflections at various key ages of interest.

$$\lambda_{\Delta} = \frac{\xi}{1 + 50\rho'} \quad (2-5)$$

where

ξ = a time-dependent factor for sustained loads, with the recommended range from 1.0 to 2.0, and

ρ' = a ratio of the area of the compressive reinforcing steel, A'_s , to the gross area of the concrete section.

Both equations 2-4 and 2-5 suggest an ultimate multiplier of 2.0 be used for estimating long-term deflections in nonprestressed concrete members without compression steel.

Equations 2-4 and 2-5 are intended to operate on the design elastic deflection magnitude, typically calculated at a concrete age of 28 days. For these equations to be most useful to the precast, prestressed concrete industry, it is desirable for these equations to instead operate on the release elastic deflection magnitude, typically occurring approximately 18 hours after concrete placement. To accomplish this, Martin (1977) modified Equation 2-4 by the ratio of concrete stiffness at prestress release to concrete stiffness at 28 days. By assuming (1) the release strength of precast, prestressed concrete members is usually about 70 percent of the 28-day strength and (2) that concrete stiffness is proportional to the square root of concrete strength, Martin computed the following stiffness adjustment factor:

$$\sqrt{\left(\frac{f_{ci}}{f_c}\right)} = \sqrt{0.70} \approx 0.85 \quad (2-6)$$

Finally, combining Equations 2-4 and 2-6, while further modifying to transition from a factor for calculating *additional* long-term deflections to a convenient all-inclusive multiplier, Martin (1977) proposed the following multiplier to estimate long-term deflection due to member weight from the initial elastic deflection at the release of prestress:

$$1 + [0.85(2.0)] = 2.7 \quad (2-7)$$

Next, Martin computed a multiplier intended to estimate the long-term change in the initial upward camber component due to the prestress force. By assuming that an average of 15 percent of the prestressing force is lost after prestress transfer (85 percent remaining), Martin proposed the following multiplier to determine the upward camber component of the final camber:

$$1 + [0.85(2.0)(0.85)] = 2.45 \quad (2-8)$$

Similar expressions are derived by Martin (1977) for estimation of the time-dependent changes in both the self-weight component and the upward camber component occurring by the time of erection, assumed to be 30 to 60 days after production. Intrinsic in Martin's proposed multipliers is the assumption that approximately 50% of the ultimate creep and shrinkage behavior, and, therefore, the net camber, will have occurred by the time of erection. A summary of the multipliers as originally proposed by Martin (1977) and currently published in the PCI Bridge Design Manual (PCI 2011) is shown in Table 2-1.

Table 2-1: Long-Term Deflection Multipliers (Adapted from Martin 1977)

	Without Composite Topping	With Composite Topping
At Erection:		
(1) Deflection (downward) component – apply to the elastic deflection due to the member weight at release of prestress.	1.85	1.85
(2) Camber (upward) component – apply to the elastic camber due to prestress at the time of release of prestress.	1.80	1.80
Final:		
(3) Deflection (downward) component – apply to deflection calculated in (1) above.	2.70	2.40
(4) Camber (upward) component – apply to camber calculated in (2) above.	2.45	2.20
(5) Deflection (downward) – apply to elastic deflection due to super-imposed dead loads only.	3.00	3.00
(6) Deflection (downward) – apply to elastic deflection caused by the composite topping.	--	2.30

Although Martin (1977) also derived multipliers for composite topping assemblages and for the effect of superimposed dead loads, those multipliers of primary relevance to this report are the four multipliers emphasized in Table 2-1.

2.6.2 Incremental Time-Steps Method

The incremental time-steps method is a method of analysis based on combining the computation of deflections with those of prestress losses due to time-dependent creep, shrinkage, and relaxation (ACI Committee 435 2003). By dividing the life of the flexural element into discrete time intervals and dividing the girder length into discrete cross-sections, incremental changes in shrinkage, creep, and relaxation can be computed for each time interval and girder cross-section. Then, these incremental changes can be summed to yield strain distributions, curvatures, and prestressing forces for a particular time interval of interest, and ultimately used to compute girder deflection parameters of interest (ACI Committee 435 2003). The incremental time-steps method is particularly well-suited for computer solution (Stallings,

Barnes, and Eskildsen 2003). Further discussion of the theoretical derivation, assumptions involved, and implementation of the incremental time-steps method as used in this research effort is included in Chapter 9 of this report.

2.6.3 Approximate Time-Steps Method

The approximate time-steps method, as originally proposed by Branson and Ozell (1961) and refined shortly thereafter by the newly renamed ACI Committee 435⁴ (1963), is based on a simplified form of the summation of constituent deflections due to various time-dependent parameters (ACI Committee 435 2003). The summation of factors is completed twice, once at prestress release and at the final condition. Serving as a compromise between complexity and efficiency of calculation, the approximate time-steps method yields results comparable to the PCI multiplier method (Stallings and Eskildsen 2001).

2.6.4 Prestress Loss Method

The prestress loss method is a computation method for use in uncracked prestressed concrete sections that uses stress loss coefficients (to approximate the effect of creep and shrinkage losses) and a series of multipliers (similar to the PCI multiplier method) to compute the total deflection after prestress loss and before live-load application (ACI Committee 435 2003). While comparably simpler than the incremental time-steps method, the prestress loss method is heavily based on time-dependent multipliers and as such, may not yield substantially more accurate results than the PCI multiplier method.

⁴ Prior to 1963, the ACI Committee “Control of Deflection in Concrete Structures” was identified as ACI Committee 335, instead of the present-day designation of ACI Committee 435.

Chapter 3: Previous Camber Studies

3.1 Introduction

The intent of this chapter is to provide a concise introduction to various previous studies relating to camber and camber prediction in precast, prestressed one-way flexural elements. By the nature of the many interrelated variables involved in deflection predictions (i.e. geometric properties, concrete compressive strength, concrete stiffness, concrete creep and shrinkage behavior, steel relaxation, and prestress losses) and the varying extent to which different researchers explore each variable, it is extremely difficult to synthesize a single literature review organized by topic without first introducing each study. Accordingly, a concise introduction and summary of each past study is presented in chronological order in this chapter. Specific previous researcher findings relevant to the major scope areas of this report are presented by topic in synthesized literature reviews in later chapters as follows: concrete compressive strength (Chapter 5), concrete stiffness (Chapter 6), creep and shrinkage behavior (Chapter 7), and thermal effects (Chapter 8). Literature on the above topics, not conducted as part of a larger camber study effort, is also referenced in the synthesized literature reviews of future chapters.

3.2 Previous Camber Literature

Early literature (pre-1979) largely represents the development and refinement of various techniques for computing deflections in one-way prestressed flexural elements. Literature of this period is frequented by the names of early prestressed concrete pioneers including Branson, Ozell, Sozen, Corley, Martin, Seiss, Burns, Nawy, and Naaman who jointly laid much of the fundamental groundwork still reflected in present-day code provisions. Much of this historic work was referenced in Chapter 2, and thus, is not repeated here.

3.2.1 Buettner and Libby (1979)

As a result of discussions within ACI Committee 435 meetings, Buettner and Libby (1979) published a paper acknowledging the growing problem of inaccurate camber predictions in prestressed concrete girders and documented the various serviceability problems often resulting from these inaccurate predictions. This paper included a survey of 37 bridge girders produced in Fairfax County, VA to determine the percent variation between predicted and measured camber at various unspecified ages. It is important to note that by present-day standards, the girders included in this study had relatively short spans averaging approximately 50 ft. It was concluded that while there was consistent variability in the surveyed girders, there appeared to be a systematic error in the calculation procedures (a similar concept to that reflected in Figure 2-2) that tended to result in over-predictions of camber. Buettner and Libby suspected the systematic error was related to (1) an inaccurate prediction of concrete stiffness, (2) an incorrect assumption of uncracked behavior when the section may actually have been cracked, (3) inaccurate calculation of the prestress force and related parameters, (4) inconsistent or inaccurate time-estimates of shipping and erection events, and (5) the effects of temperature gradients. This paper suggested the development of code provisions as follow: (1) initial prestress deflection should be measured and recorded for all projects, (2) shop drawings should show anticipated deflections including some measure of required consistency between similar girders, and (3) the difference between the anticipated deflection and the actual deflection shall not exceed $L/1200$. Buettner and Libby's paper constituted the first documentation of widespread camber prediction issues in the precast, prestressed concrete industry and also correctly hypothesized many of the probable causes of these inaccuracies.

3.2.2 Tadros, Ghali, and Meyer (1985)

Tadros, Ghali, and Meyer (1985) conducted research work aimed at more precisely computing prestress losses and time-dependent deflections of prestressed concrete members. One of the main focuses of this work was to update the PCI multiplier method (originally proposed by Martin [1977]) to reflect assumptions more characteristic of high-strength concrete. In doing so, additional factors were introduced to represent the effect of relative humidity on creep and shrinkage, the effect of nonprestressed steel, and the effect of concrete cracking. The method proposed by Tadros et al. (1985), often called the revised PCI multiplier method, is substantially more complex than that proposed by Martin

(1977) and yields similar results for average environmental conditions in typical girders. Despite the recommendation of Tadros et al. (1985), the multipliers contained in the PCI Bridge Design Manual (Precast/Prestressed Concrete Institute 2011) remained unchanged and still reflects the original work by Martin (1977).

3.2.3 Kelly, Bradberry, and Breen (1987)

Kelly, Bradberry, and Breen (1987) documented the instrumentation and field monitoring of eight long-span (127 ft) pretensioned AASHTO Type IV bridge girders made with high-strength concrete and low-relaxation prestressing steel. This effort was part of a larger study aimed at evaluating the feasibility of utilizing high-strength concrete and low-relaxation steel in pretensioned bridge girders. Measurements of deformations and internal beam temperatures were recorded periodically beginning during girder production and ending one year after the bridge entered service. Deformation measurements included concrete surface strains, prestressing strand strains, and quarter- and mid-span deflections. The average camber of the eight girders included in this study was 3.3 in. The measured time-dependent camber was compared to the results of various period-specific analytical techniques for computing deflections. Most notable conclusions include: (1) the primary factors affecting time-dependent camber are concrete age-strength development, concrete creep, relative humidity, the age of concrete at release, and the construction schedule, (2) support conditions for girders in storage can dramatically affect camber and should be considered when calculating beam responses, (3) the camber of girders is very sensitive to the age and strength of concrete at prestress release, and (4) by adjusting the PCI multiplier method to reflect regional practices, increased accuracy of time-dependent camber predictions was achieved.

3.2.4 Brown (1998)

Brown (1998) examined the validity of camber growth computation methods used by the Idaho Department of Transportation (IDOT) for prestressed concrete girders. Camber measurement data was gathered from four different prestressed concrete girder manufacturers and compared to camber predictions computed by then-current IDOT design procedures. It was found that the standard IDOT prediction method tended to underestimate camber at the time of prestress release. Primary conclusions of this study included the following: (1) the primary contributor to prestress losses at release is elastic

shortening, while losses due to steel relaxation are minimal and can be neglected, (2) the incremental time-steps method provided an accurate prediction of camber after calibration of creep and shrinkage coefficients, (3) a modified PCI multiplier method was developed to include local concrete material properties and a regionally appropriate construction timeline, and (4) no clear correlation was observed between camber growth and relative humidity. Brown (1998) stressed that the camber prediction methods recommended in this study are based on estimates of the modulus of elasticity, ultimate creep coefficient, and ultimate shrinkage strain and should be validated by a future material testing program. Also noteworthy from Brown's work is the first historical discussion of various methods for camber control—that is, manually inducing a change in camber after production to meet a specified camber magnitude.

3.2.5 Wyffels, French, and Shield (2000)

Conducting a study for the Minnesota Department of Transportation (MnDOT), Wyffels, French, and Shield (2000) investigated the effect of pre-release cracking in precast, prestressed concrete bridge girders. Often observed during the fabrication process upon removal of formwork, pre-release cracking is typically assumed to have a negligible effect on prestressed girders due to the closing of cracks upon prestress release and the corresponding autogenous healing which may occur thereafter (Wyffels et al. 2000). The findings of various analytical techniques employed in this study suggested the following: (1) if discrete pre-release cracking occurs predominately above the girder neutral axis, it is possible that upon prestress release, the closing of these cracks may cause a reduced compressive stress at the bottom of a section, and thereby cause (2) a reduced camber effect in bridge girders exhibiting widespread pre-release cracking. This concept is illustrated in Figure 3-1. Despite evidence from various analytical models, this hypothesis by Wyffels et al. (2000) has not yet been verified by experimental work. Accordingly, some researchers are skeptical and contend that the effect of pre-release cracking is indeed negligible for precast, prestressed concrete bridge girders.

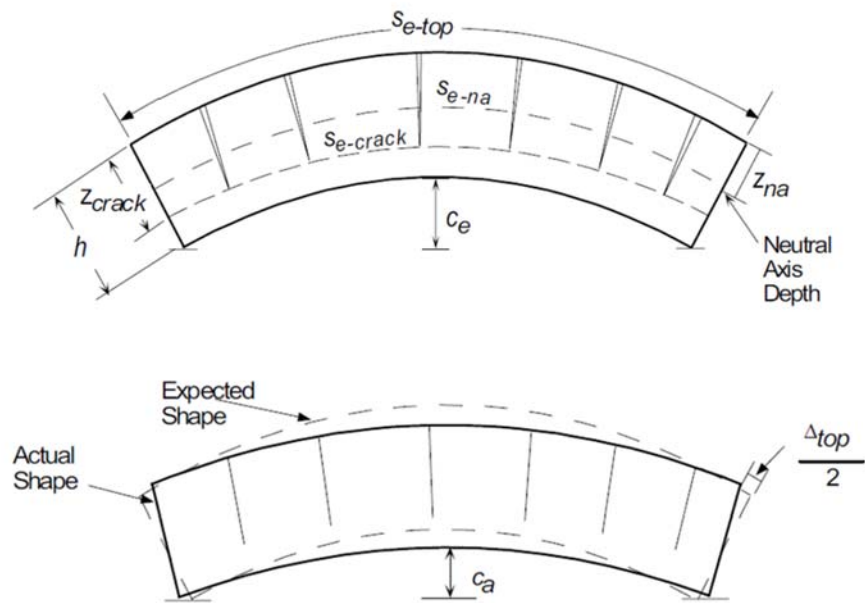


Figure 3-1: Effect of Pre-Release Cracking on Elastic Camber Magnitude (Adapted from Wyffels et al. 2000)

3.2.6 Stallings, Barnes, and Eskildsen (2003)

As part of a study conducted for the Alabama Department of Transportation (ALDOT), Stallings, Barnes, and Eskildsen (2003) investigated the accuracy of available camber and prestress loss prediction methods for bridge girders produced with high-performance concrete (HPC). This effort included a field instrumentation study of five BT-54 bridge girders used in Alabama's HPC Showcase Bridge. Field measurements included concrete strain, internal temperature, and midspan camber at various times throughout the early life of the girder. A complementary laboratory phase of this study was conducted to determine the creep, shrinkage, and elastic properties of the HPC concrete used in the field project. Primary conclusions of Stallings et al. (2003) included: (1) accurate predictions of camber can be achieved using the incremental time-steps method and approximate time-step method so long as material parameters representative of the actual concrete used in girder production are used, (2) measured camber values at erection were significantly less than those predicted by the PCI multiplier method (attributed to the tendency of HPC to exhibit reduced creep and shrinkage behavior), (3) concrete strains at the level of prestressing strands showed good agreement (within 20 percent) of predicted values for

times up to 300 days, and (4) time-dependent prestress loss predictions using the HPC material parameters were sufficiently accurate.

3.2.7 Cook and Bloomquist (2005)

Cook and Bloomquist (2005), funded by the Florida Department of Transportation (FDOT), conducted a study to verify the accuracy of camber estimates in prestressed concrete bridge girders in the state of Florida. As part of this effort, time-dependent deformations and concrete surface temperatures were monitored for 13 precast, prestressed concrete bridge girders and compared to camber values predicted by the software package *PSBEAM* developed by Eriksson Technologies. Cook and Bloomquist developed a curvature-based analytical procedure to compensate for the effect of varying temperature gradients on field-measured camber values, thereby providing more consistent comparisons between measurements regardless of varying ambient conditions.

The following primary conclusions were developed by Cook and Bloomquist (2005): (1) the observed camber increase with time for the field-monitored girders was significantly less than predicted by design software, (2) future work is needed to experimentally determine the creep and shrinkage properties of typical FDOT concretes, (3) the influence of thermal gradients on camber must be accounted for in field measurements, (4) storage conditions (namely, the height between the bottom of the girder and the ground) seem to affect the development of time-dependent concrete properties and, therefore, can affect the time-dependent development of camber, and (5) consistent differences were documented between camber measurements taken at prestress release and measurements taken shortly thereafter when girders were relocated to storage. A follow-up study (also sponsored by FDOT) was conducted by Tia, Liu, and Brown (2005) that focused on determining time-dependent properties (i.e. modulus of elasticity and creep and shrinkage behavior) for various FDOT concretes. This follow-up study is reviewed in the synthesized literature reviews of Chapter 6 (Concrete Stiffness) and Chapter 7 (Creep and Shrinkage Behavior).

3.2.8 Barr, Stanton, and Eberhard (2005)

Concurrent with the work of Cook and Bloomquist (2005), Barr, Stanton, and Eberhard (2005) also independently examined the effect of temperature variations on precast, prestressed concrete girders in a

project funded by the Washington Department of Transportation (WSDOT). By monitoring five precast, prestressed concrete girders during fabrication and service, Barr et al. (2005) were able to determine the effect of elevated curing temperatures on prestress losses and also validated a curvature-based temperature correction procedure. Primary findings of this work include the following: (1) a curvature-based approach for computing thermally-induced deformations and stresses was developed and verified to accurately predict observed girder thermal responses and (2) the elevated curing temperatures typical of precast, prestressed concrete can cause a significant reduction in the magnitude of the prestressing force (up to approximately 12 ksi), which corresponds to a significant decrease in observed midspan camber.

3.2.9 Hinkle (2006)

Hinkle (2006) conducted a study to identify the most accurate time-dependent material models for use in predicting time-dependent deflections of 27 high-strength prestressed concrete bridge girders in South Carolina. Girder deflections were periodically measured to determine camber growth and limited concrete materials testing (strength and stiffness) was conducted during girder production. An incremental time-steps method was implemented for predicting camber growth and allowed trial iterations to determine best-suited time-dependent material parameters for the analysis. Notable conclusions of Hinkle (2006) include the following: (1) same-day measured cambers tended to vary by up to ½ in. due to thermal exposures, (2) the PCI multiplier method (proposed by Martin 1977) tended to overestimate camber by 48 percent at an age of 60 days, (3) and the revised PCI multiplier method (proposed by Tadros et al. 1985) tended to overestimate camber by 21 percent at an age of 60 days. Specific recommendations relevant to key focus areas of this report are reviewed in later chapters.

3.2.10 Rosa, Stanton, and Eberhard (2007)

Sponsored by the Washington State Department of Transportation (WSDOT), Rosa, Stanton, and Eberhard (2007) conducted a research investigation to develop improved methods for predicting camber in prestressed concrete girders. As part of this project, prestressed girders were monitored from four WSDOT bridge projects (146 girders for short-term monitoring and 91 girders for long-term monitoring.) Typical measured data included deflections at various ages and selected concrete material properties

(compressive strength, modulus of elasticity, and creep and shrinkage behavior). Using a time-steps method for camber-growth analysis, Rosa et al. (2007) calibrated various constitutive models to reflect the field-observed deflections of girders and achieved much-improved predictions of camber. In addition, the effect of friction (between the girder and the prestressing bed) on the magnitude of initial elastic camber was investigated using a roller assembly placed under a girder end immediately after prestress release. Most notable conclusions by Rosa et al. (2007) included the following: (1) various noteworthy recommendations regarding concrete strength, stiffness, and creep and shrinkage behavior (which are included in the synthesized literature reviews of later chapters), (2) the effect of lifting and re-seating a girder tended to increase the measured camber by 0.15 in., and (3) girders stored on oak blocks tended to behave as if they were approximately 50 percent stiffer than those seated on elastomeric bearings (attributed to the partial restraint provided by oak blocks).

3.2.11 Jayaseelan and Russell (2007)

In a study funded by the Oklahoma Department of Transportation (OKDOT), Jayaseelan and Russell (2007) implemented a time-steps method to compute prestress losses of precast, prestressed concrete girders at varying ages. While this study was primarily a study of prestress losses, the effect of changes in prestressing forces were frequently extrapolated to the camber-growth behavior of the girder. For instance, for an AASHTO Type IV girder with a 105 ft span and a prestressing arrangement typical of an OKDOT girder, Jayaseelan and Russell (2007) concluded the following: (1) the addition of two top prestressing strands reduced the expected camber magnitude by 35 percent, while the addition of four top prestressing strands reduced the camber by 70 percent, (2) the addition of five #9 longitudinal mild steel reinforcement bars did not appreciably alter the values of long-term losses, but decreased the long-term camber by approximately 17 percent, (3) a 20 percent decrease in creep coefficient corresponded to a 6.8 percent decrease in long-term camber, and (4) a 20 percent increase in elastic modulus reduced the long-term prestress losses by 6 percent and the long-term camber by 12 percent.

3.2.12 Omar, Pui Lai, Poh Huat, and Omar (2008)

A study conducted in Malaysia by Omar, Pui Lai, Poh Huat, and Omar (2007) gives an international perspective on camber prediction in prestressed concrete girders. It is interesting to note that the beam

deflection domestically referred to as “camber” is referred to as “pre-camber” in Malaysia. Omar et al. identify the fundamental disparity between assumed and observed properties for concrete strength and stiffness and recommend the use of local concrete properties in pre-camber computations. Furthermore, a simplified expression is proposed (somewhat similar in principle to the PCI multiplier method) in order to approximate the time-dependent change in pre-camber occurring after girder production. This proposed expression relies on assumptions of an average prestressing force magnitude (and therefore an assumed prestress loss) and a creep coefficient parameter. Omar et al. found that by accounting for the time-dependent nature of concrete through the use of a creep coefficient and assumed prestress loss magnitude, improved accuracy of pre-camber predictions was achieved for early-life girder ages (up to 15 days).

3.2.13 Barr and Angomas (2010)

As a follow-up to the efforts of Barr, Stanton and Eberhard (2005), Barr and Angomas (2010) revisited the previous research work, revised certain portions of the analytical procedure, and more thoroughly compared the predicted behaviors to field-observed behaviors. Key findings by Barr and Angomas (2010) included the following: (1) high curing temperatures caused a corresponding reduction in computed camber of 33 percent, not 40 percent as previously reported, (2) changes in camber due to elevated curing temperature are a result of both a reduction in strand stress and a non-uniform temperature profile at the estimated time of bonding, (3) the time-steps method implemented using the material properties recommended in NCHRP Report 496 (Tadros et al. 2003) resulted in camber predictions within 10 percent of the measured long-term cambers, and (4) the PCI multiplier method (Martin 1977) yielded predicted cambers 22 percent lower than observed, while the modified multiplier method (Tadros et al. 1985) yielded predicted cambers 27 percent higher than observed.

3.2.14 Lee (2010)

Lee (2010) conducted an experimental and analytical study on a BT-63 concrete girder segment to investigate thermal effects on the girder. Using a two-dimensional finite element heat-transfer analysis model and a three-dimensional solid finite element analysis, vertical and lateral displacements due to measured environmental conditions were computed. After validation of the model, extremes in thermal

effects were used to predict the maximum thermal vertical and lateral movements in terms of span length for four PCI girder shapes. Finally, additional work focused on evaluating the effect that varying assumptions of thermal concrete properties had on the computed maximum deflections of the four PCI girder shapes. Conclusions and recommendations by Lee (2010) are presented in the synthesized literature review of Chapter 8 of this report.

3.2.15 Tadros, Fawzy, and Hanna (2011)

A study conducted by Tadros, Fawzy, and Hanna (2011) served largely as a review of the state-of-the-art on camber prediction in precast, prestressed concrete girders, but also included a valuable discussion on the anticipated variability in camber and best practices for accommodating this variability in design detailing efforts. Tadros et al. (2011) suggested the following: (1) designers should accommodate camber variation of up to 50 percent from the predicted value in detailing of bridges, (2) all bridges should be designed with a minimum girder haunch of 2.5 in., (3) shear reinforcement should be detailed to accommodate camber variability by keeping protruding bars vertical prior to erection and bending on-site to final elevations, (4) girder seats should be finalized near the time of girder installation to accommodate variable elevations, (5) contractor pay items based on concrete volume should be avoided and instead, the contractor should account for girder variability in their initial bid, and (6) designers should accommodate local material properties and storage and construction practices during design, if practical.

3.2.16 French and O'Neill (2012)

Sponsored by the MnDOT, French and O'Neill conducted a field study to validate beam deflections and camber estimates of prestressed concrete I-beams. Historical data gathered as part of this project representing 1,067 bridge girders showed that camber at release and erection was typically overpredicted by 74 percent and 83.5 percent, respectively. These inaccuracies in camber prediction were attributed primarily to under-predictions of the concrete compressive strength and corresponding modulus of elasticity of the concrete. This project included limited field concrete material testing (concrete strength and stiffness) and field monitoring of the time-dependent deflections in 14 girders of varying lengths and cross-sections through the time of shipping. An analytical model was developed to evaluate the influence of various time-dependent effects on long-term camber and used to develop a multiplier-based prediction

model for use by MnDOT. Primary conclusions from French and O'Neill (2012) relevant to the work of this report include the following: (1) various recommendations regarding predicting concrete compressive strength and modulus of elasticity during the design phase (as summarized in Chapters 5 and 6 of this report), (2) ambient relative humidity was found to be a primary contributor to camber variability (a change in relative humidity of 30 percent caused a corresponding change in long-term camber of 10 percent), (3) various changes to standard construction timing and practices were proposed to decrease the girder-to-girder variability, and (4) varying sets of revised multipliers were proposed to predict time-dependent changes in deflections more accurately.

3.2.17 Schrantz (2012)

Schrantz (2012) developed a visual-basic (VB) computer program that implemented an incremental time-steps method for computing initial and time-dependent camber in prestressed concrete girders. Various models for concrete modulus of elasticity and creep and shrinkage behavior were included in the software development allowing users to easily compute camber and camber-growth using these varying parameters. Schrantz (2012) validated the accuracy of the software program using measured strain and camber results from three previous research programs (Boehm 2008, Levy 2007, Stallings et al. 2003) and provided preliminary recommendations of the material models best suited for camber predictions in Alabama. Chapter 9 details the fundamental theory and development of the incremental time-steps method implemented in this report, largely based on the initial work by Schrantz (2012), later refined by Johnson (2012), and finally expanded and finalized by Isbilibiroglu (2014).

3.2.18 Johnson (2012)

As part of a comprehensive project evaluating the suitability of self-consolidating concrete (SCC) for precast, prestressed concrete applications, Johnson (2012) conducted comparisons of predicted and actual measured time-dependent deformations in 28 bulb-tee girders for an Alabama Department of Transportation (ALDOT) bridge replacement project. Data gathering efforts relevant to Johnson's work included the measurement of internal concrete strains and internal girder temperatures and the testing of selected time-dependent concrete material properties. The development of a curvature-based temperature correction procedure (similar to that of Barr et al. [2005]) was developed as part of Johnson's

work to remove the effect of varying temperature gradients on field camber measurements. By comparing measured field data to the predicted structural behavior, Johnson (2012) reached the following conclusions: (1) time-dependent strain predictions in the bottom-flange of girders were reasonably accurate for all creep and shrinkage models evaluated in this study, (2) there was a systematic over-estimation of concrete strains occurring at later girder ages, (3) the effective prestressing force was overpredicted in the first months after prestress transfer and underpredicted at later ages, (4) measured midspan camber magnitudes were generally less than predicted for ages up to 200 days, and (5) none of the creep and shrinkage models investigated as part of this study tended to predict time-dependent camber growth particularly well. Work by Johnson (2012) demonstrated the need for improved methods to predict time-dependent camber growth in ALDOT prestressed concrete girders and thus, partly spurred the research efforts contained in this report.

3.2.19 Precast/Prestressed Concrete Institute Committee on Bridges (2012)

In order to evaluate the appropriateness of the current PCI construction tolerance limits for camber of prestressed concrete bridge girders, the PCI Committee on Bridges (2012) gathered data representing the measured and predicted release camber values for 1,835 girders from eight states across the United States. Using these data, the PCI Committee on Bridges (2012) recommended changes to the permissible camber tolerance at release to more accurately represent the variability of the historical data set as shown in Figure 3-2. The blue-shaded areas represent those areas within the current camber tolerance limits, while the red-shaded areas show the expanded area proposed to be considered within tolerance. By increasing the tolerance limits as shown, the number of girders in the historical sample falling within tolerance increased from 66 percent to nearly 90 percent.

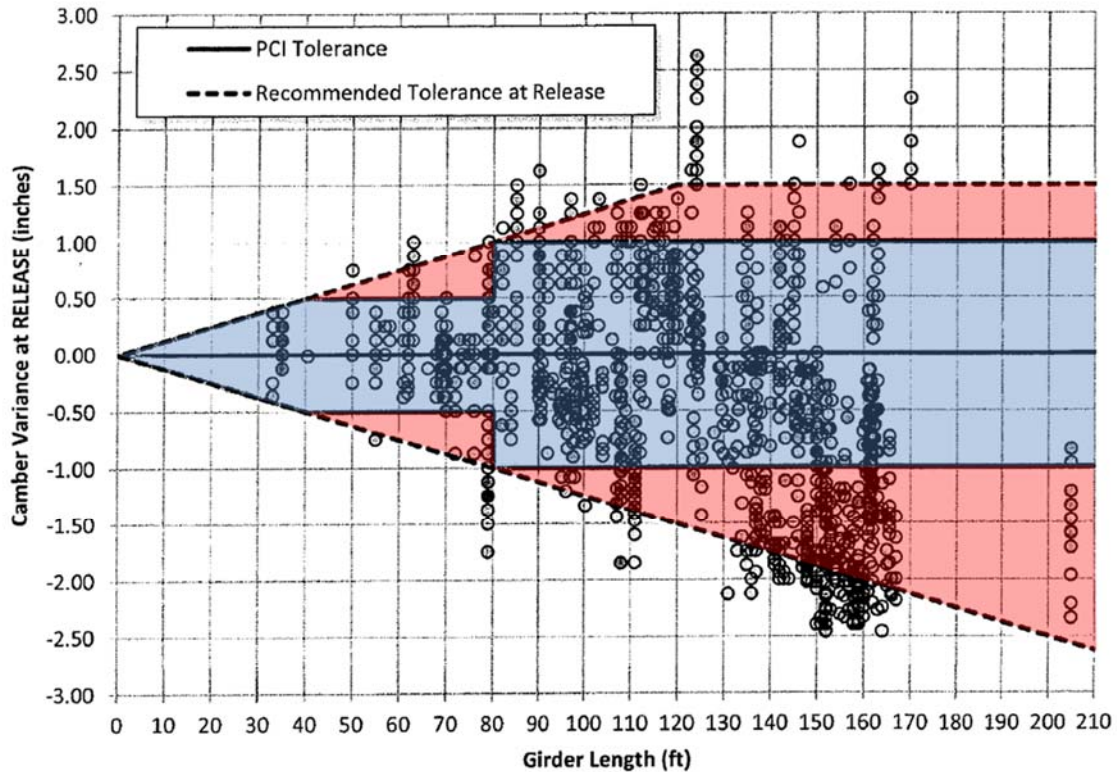


Figure 3-2: Proposed PCI Camber Tolerance Limit Revisions (Adapted from PCI Committee on Bridges 2012)

It is interesting to note that the revised camber tolerance upper limit is capped at a value of +1.5 in., reflecting the more severe consequence for a girder with underestimated camber as opposed to a girder with over-estimated camber. The efforts of the Committee on Bridges (2012) do not examine the procedures or assumptions used for computing camber and thus, may not address the root causes of inaccurate camber predictions in precast, prestressed concrete girders.

3.2.20 Storm, Rizkalla, and Zia (2013)

Storm, Rizkalla, and Zia (2013) conducted a field and laboratory study to examine the various parameters affecting camber predictions, with particular attention to factors related to girder production. As part of this study, camber measurements at the time of prestress transfer were collected for 382 pretensioned concrete girders from nine states and supplemental concrete material testing was conducted to determine compressive strength, elastic modulus, and unit weight at various concrete ages. Camber was measured immediately after prestress transfer, at the beginning of storage, prior to shipment, and after erection. Primary findings of Storm et al. (2013) relevant to this research effort included the

following: (1) recommendations are proposed to more accurately predict concrete strength and stiffness during the design phase (as referenced in Chapters 5 and 6 of this report), (2) neglecting the effect of debonding and transfer length at girder ends caused errors as high as 13 percent in camber computations, (3) the effect of thermal effects on the loss of prestressing prior to prestress transfer may be as high as 7 percent, and (4) both an approximate method (based on the PCI multiplier method) and an incremental time-steps method provided reasonably accurate camber predictions within 10-15 percent of measured values.

3.2.21 Mahmood (2013)

Mahmood studied the theoretical feasibility of using post-tensioned strands as a means of camber control in simply-supported prestressed concrete bridge girders and also explored the corresponding reduction in girder load capacity. Mahmood (2013) concluded that camber control by the use of post-tensioned strands was a viable method and resulted in minimal reductions to the load-carrying capacity of corrected members (the load-carrying capacity of an AASHTO Type IV member was reduced by 2.9 percent per 100,000 lb. of post-tensioning jacking force). Future work was recommended to investigate the effect of camber control on other girder types and to evaluate the practical feasibility of this proposed method.

3.2.22 He (2013)

To improve the accuracy of long-term camber predictions in prestressed concrete girders for the Iowa Department of Transportation (IDOT), He (2013) conducted a laboratory study to investigate selected time-dependent properties (modulus of elasticity and creep and shrinkage behavior) of seven regional concrete mixtures and later compared the results of various camber prediction techniques to the observed time-dependent camber behavior of 26 prestressed high-performance concrete bridge girders. He (2013) concluded the following: (1) the errors between the predicted and measured modulus of elasticity values were up to 20 percent, (2) sealed concrete specimens tended to represent the creep and shrinkage behavior of the full scale prestressed girder better than unsealed specimens, (3) when calculated by gross section properties instead of transformed section properties, girder camber was on average 13 percent higher, (4) the time-steps method implemented in this study predicted camber within

25 percent accuracy, (5) roughly 50 percent of ultimate camber growth had occurred one year after girder production. More specific recommendations and findings are reviewed in Chapter 7 of this report.

3.2.23 Nervig (2014)

Also funded by IDOT, Nervig (2014) focused on improving the predictions of instantaneous camber for prestressed concrete bridge girders through comparisons of measured and predicted release cambers for 105 prestressed concrete beams. Nervig concluded that a combination of inconsistent field measurement techniques and inaccurate estimates of material properties were the primary factors resulting in inaccurate camber predictions and accordingly, provided guidance to producers and designers in an attempt to improve the accuracy of camber predictions. Various specific recommendations by Nervig (2014) are referenced in Chapters 5 and 6 of this report.

3.2.24 Keske (2014)

Keske (2014) expanded on the previous efforts of Johnson (2012), exploring the time-dependent behavior of full-scale precast, prestressed girders. Specifically, Keske included the influence of measured concrete material properties (coefficient of thermal expansion and creep and shrinkage and behavior) on the accuracy of deflection predictions. While Keske's efforts were aimed predominately at evaluating the difference between conventionally-vibrated concrete (CVC) and self-consolidating concrete (SCC), the accuracy of various time-dependent property prediction models was evaluated. Specific recommendations of Keske (2014) are included in Chapters 6, 7, and 8 of this report.

3.2.25 Hofrichter (2014)

As part of the work of this report, Hofrichter (2014) completed an analysis of historical records representing more than 1,900 precast, prestressed girder pours to examine the common practices of the prestressed industry in Alabama and to recommend relationships for predicting concrete compressive strength and modulus of elasticity at the time of girder design. Hofrichter's efforts reflect earlier iterations of a portion of the work detailed in Chapters 5 and 6 of this report.

3.2.26 Isbilioğlu (2014)

Further refining the work of Schrantz (2012) and Johnson (2012), Isbilioğlu (2014) compiled a near-finalized version of the time-steps camber prediction software used in this report and validated this software using the results from previous experimental research including those of Johnson (2012), Schrantz (2012), Boehm (2008), Stallings et al. (2003), and Levy (2007). Improvements to the camber prediction software made by Isbilioğlu (2014) included: (1) development of a more user-friendly interface capable of importing and exporting project files and results, (2) implementation of new versions of design code parameters and material prediction models; and (3) implementation of various recommendations of Hofrichter (2014) and Keske (2014).

3.2.27 Davison (2014)

Davison (2014) developed a camber prediction algorithm that attempted to link time-dependent constitutive material models while also explicitly considering various discrete fabrication events in a computationally efficient manner. Advantages of the proposed method include: (1) the time-dependent concrete behavior, as well as its interdependence with strand relaxation and environmental loading in the form of shrinkage and thermal effects is analyzed explicitly at every step, (2) the analysis begins with the stressing of the strand and includes all pre-release activities relevant to camber, and (3) the developed algorithm is flexible and allows the exploration of alternative constitutive models for the material behavior. Preliminary comparisons of predicted behaviors from this algorithm and measured data show promising agreement, but additional work is needed to validate this algorithm and more accurately calibrate the various constitutive models.

3.3 Comments on Previous Camber Studies

From the brief review offered of the aforementioned camber studies, it is evident that a great deal of research effort has been devoted to improving the accuracy of short-term and long-term deflection predictions in prestressed concrete elements within the last 35 years. The following comments are offered as a general impression of these past efforts:

- Available methods for computing short-term and long-term deflections are capable of providing fairly accurate estimations of deflections in precast, prestressed concrete girders assuming that accurate values of material properties are known and utilized in computations;
- The constitutive materials in concrete are regionally-variable and thus, studies in various geographical areas are necessary to accurately capture local concrete material parameters;
- Design and production practices can greatly affect the accuracy of deflection computations in precast, prestressed concrete members and, therefore, designers should make educated assumptions of future material properties that reflect regional practice whenever possible;
- It is relatively rare for a single camber study to conduct thorough supplemental concrete materials research to thoroughly explore concrete strength, stiffness, creep and shrinkage behavior, and thermal properties;
- The majority of studies rely on measured camber as a metric of prediction accuracy and do not consider the accuracy of internal concrete strain predictions that are prerequisite computations in any curvature-based camber prediction procedure; and
- Despite the development and implementation of multiple incremental time-steps procedures for computing long-term camber in precast, prestressed concrete girders, software packages are rarely published or freely distributed for use by others.

Chapter 4: Current Design and Construction Practices for ALDOT Precast, Prestressed Concrete Bridge Girders

4.1 Introduction

A logical starting point for a study aimed at improving camber predictions in precast, prestressed concrete girders is to explore and document the existing procedures used for design and construction of precast, prestressed concrete bridge girders within the study region. Without intimate knowledge of these production practices and the often complex relationships among designers, material suppliers, producers, and erectors, it is difficult to propose viable and efficient solutions to real-world problems that are both convenient and agreeable to all vested parties. Accordingly, this report chapter documents the current state-of-the-art of the precast, prestressed concrete girder industry as applicable to ALDOT bridge projects. Included in this chapter is a general background of the prestressed concrete industry in Alabama, a review of typical girder design roles and procedures, a discussion of concrete mixture proportioning for regional prestressed applications, a brief review of girder production practices relevant to camber and camber-prediction, and a summary of the documentation required to be recorded during girder production. The majority of the information presented herein is derived from field visits to various prestressed concrete plants within the study region, a review of available historical plant records, and correspondence with ALDOT Bridge Bureau design personnel.

4.2 Background

The precast, prestressed concrete industry in Alabama and surrounding states actively manufactures concrete bridge girders and prestressed concrete piles for use in Alabama Department of Transportation (ALDOT) bridge construction projects. The work reflected in this study deals exclusively with precast, prestressed concrete bridge girders and focuses primarily on PCI bulb-tee standard shapes.

4.2.1 Prevalence of Precast, Prestressed Concrete Bridges in Alabama

The use of precast, prestressed concrete girders is fairly widespread in bridges throughout the State of Alabama. As of 2012, there were 1,113 prestressed concrete stringer/multi-beam bridges in service throughout the state, as compared to 2,104 steel stringer/multi-beam bridges (Svirsky 2015). Available data representing the frequency of prestressed concrete bridge girder usage in the five Alabama counties with more than 500 bridges is shown below in Table 4-1. This data is compiled by the Federal Highway Department (FHWA) as part of the National Bridge Inventory (NBI) program.

Table 4-1: Prevalence of Prestressed Concrete Bridges in Alabama (Baughn 2014)

Alabama County Name	Number of Prestressed Concrete Bridges In Service	Total Number of Bridges In Service	Prestressed Concrete Bridges as Percent of Total (%)
Montgomery	61	592	10.3
Mobile	83	576	14.4
Tuscaloosa	46	458	10.0
Jefferson	136	1,022	13.3
Madison	75	639	11.7
Total	401	3,287	12.2

Note: Data last compiled in 2013 from FHWA National Bridge Inventory.

As seen in Table 4-1, on average, 12.2 percent of the bridges in the five most bridge-populous counties in Alabama utilize precast, prestressed concrete girders as primary flexural elements. While this percentage may seem relatively low, it is important to note that the total number of bridges in service includes a disproportionately high number of short-span concrete culverts and concrete slab bridges. Without more detailed data available, the author estimates that roughly one-half of all bridges with span lengths exceeding 100 ft in Alabama are constructed using prestressed concrete elements.

4.2.2 Regional Precast, Prestressed Concrete Producers

Throughout the course of this research study, the precast, prestressed concrete industry proved to be rather dynamic with multiple production facilities closing, changing ownership, or ceasing to produce ALDOT bridge girder products altogether. In order to be eligible to produce ALDOT precast, prestressed bridge girders, a production facility must be certified by the Precast/Prestressed Concrete Institute (PCI) to a level of at least Category B4 (deflected strand bridge members) and also maintain pre-qualification from ALDOT. The PCI plant certification program ensures that each certified plant develops and

maintains an in-depth, in-house quality system based on time-tested national industry standards and requires two unannounced audits per calendar year (PCI 2011). Qualification by ALDOT is independent of PCI-certification and is based on a producer's ability to satisfy the requirements of all applicable ALDOT specifications and standards (ALDOT 2012). At the commencement of this study in 2012, there existed eleven PCI-qualified prestressed concrete plants in Alabama and the states directly adjacent as shown in Figure 4-1.

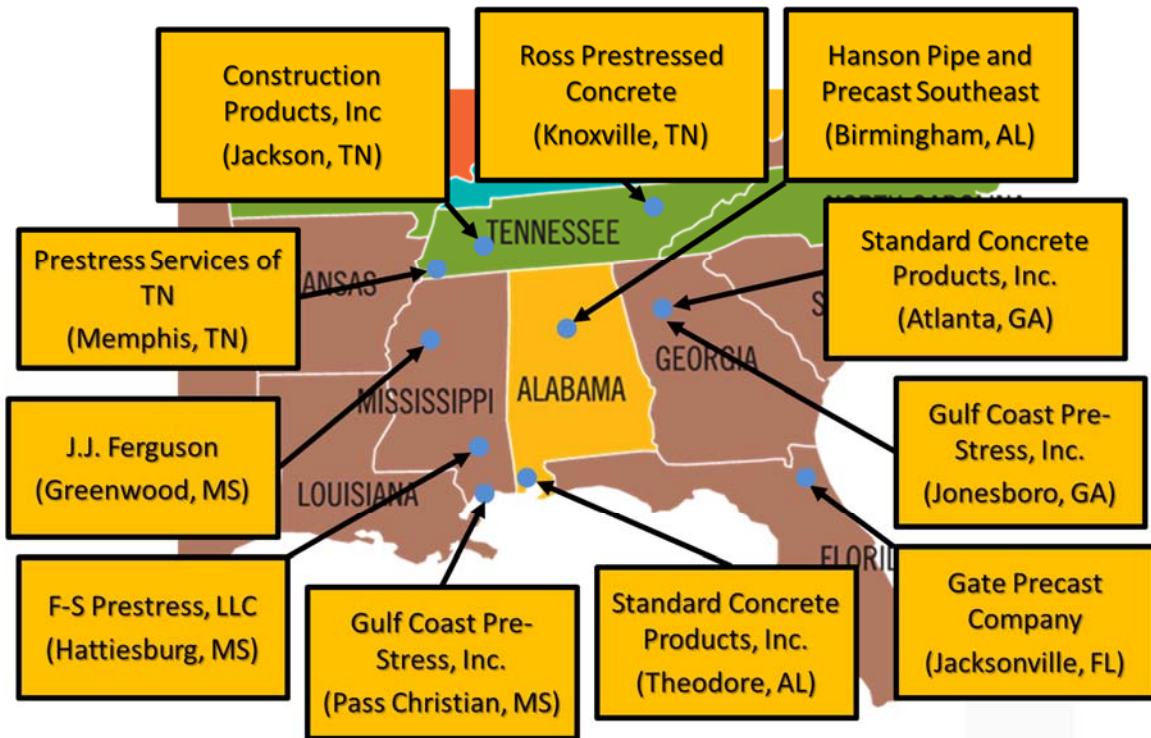


Figure 4-1: PCI-Qualified Prestressed Concrete Plants in Alabama and Neighboring States

Early discussions with ALDOT personnel identified five of the eleven precast, prestressed plants that maintained active ALDOT qualifications to bid precast, prestressed concrete bridge girder work. These five producers were the subject of plant visits by researchers early in this project and included two plants within Alabama, two in Georgia, and one in Mississippi, as shown in Figure 4-2.

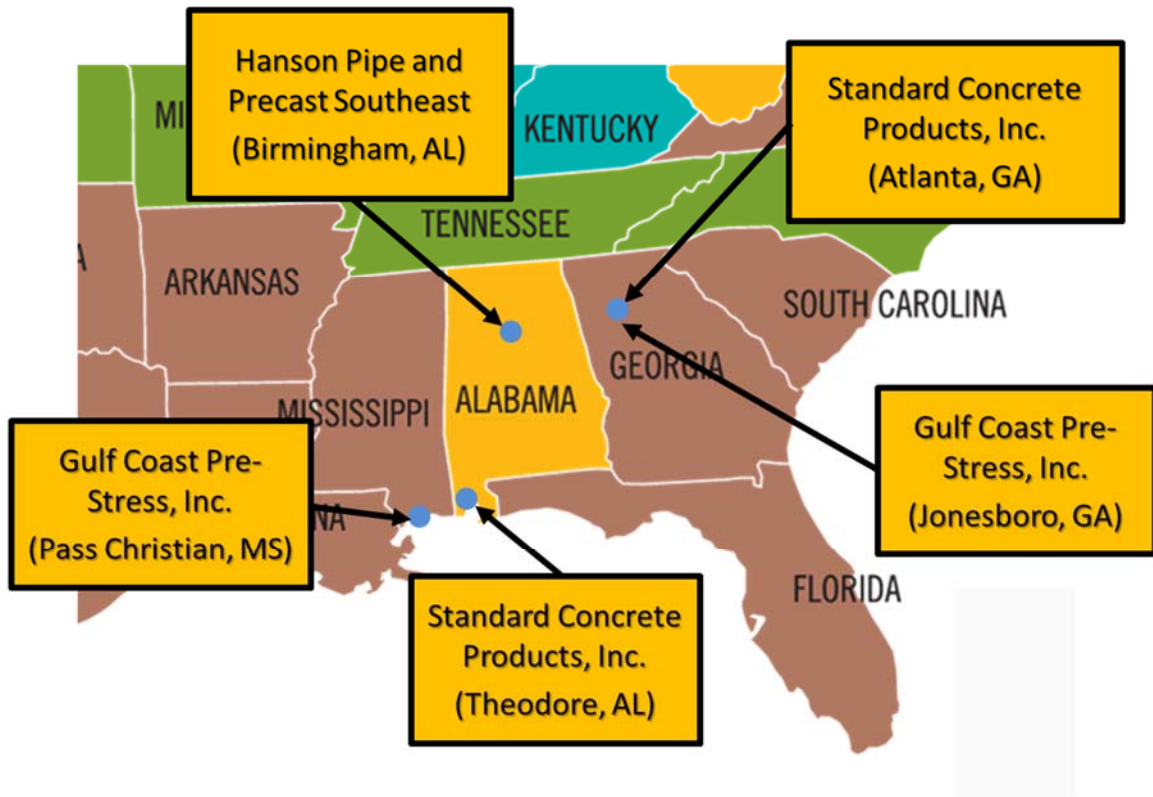


Figure 4-2: ALDOT Qualified Precast, Prestressed Concrete Producers in 2012

Throughout the course of this study, two of the five ALDOT-qualified plants would change ownership and ultimately close, while an additional plant would cease producing ALDOT bridge girders. At the conclusion of the data-gathering phase of this study in 2015, only two plants remained eligible to produce ALDOT precast, prestressed bridge girders: Hanson Pipe and Precast Southeast in Birmingham, Alabama and Gulf-Coast Pre-Stress, Inc. in Pass Christian, Mississippi. The dynamic nature of the prestressing industry in the study region would prove to hamper field-data gathering efforts to some extent and necessitate changes to the data-gathering methodology of the research effort.

4.2.3 Distribution of ALDOT Girder Types

As part of this research effort, historical data representing nearly 5,000 ALDOT precast, prestressed girders was collected from over 1,900 girder concrete placement events⁵ throughout the six-year period

⁵ The term “girder placement event” refers to the practice of producing multiple precast, prestressed concrete girders on a single production line. Typically, between 2 and 3 girders are produced in a single girder placement event.

spanning from 2007 to 2013. The frequency of usage for various standard girder shapes during this time period is shown in Figure 4-3.

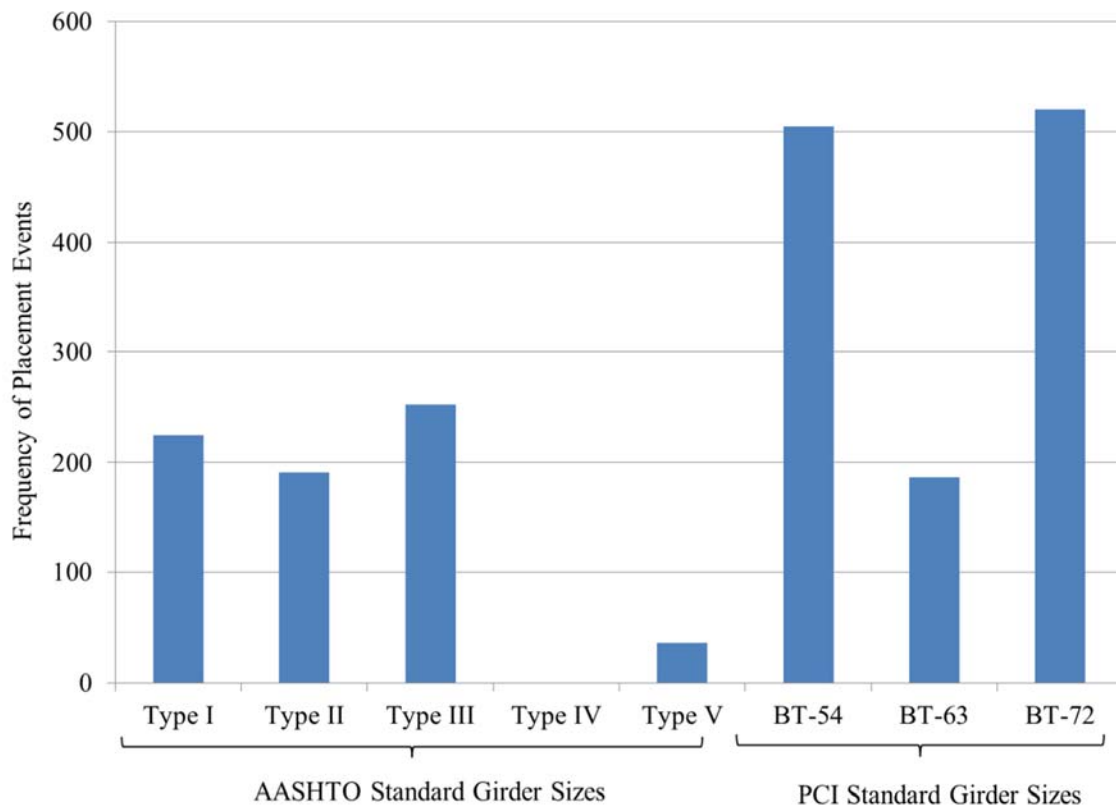


Figure 4-3: Frequency of ALDOT Girder Types from 2007-2013

The most common shapes for ALDOT prestressed concrete bridge projects are the PCI BT-54 and BT-72 shapes, with a lesser proportion of girders utilizing PCI BT-63 and standard AASHTO shapes. The increased incidence of BT-54 and BT-72 girders is likely attributed to the tendency of designers to use BT-72 sections for main spans and then default to the smallest bulb-tee shape, the BT-54, for shorter approach spans on bridge ends.

4.3 Design of Precast, Prestressed Concrete Bridge Girders in Alabama

The design and pre-construction planning of precast, prestressed concrete bridge girders in the state of Alabama is an interactive process typically involving both ALDOT in-house bridge designers and design staff at prestressing plants. First, a comprehensive prestressed concrete bridge design is completed in accordance with the ALDOT Structural Design Manual (ALDOT 2014) and other applicable design codes.

Approximately 85 percent of the time⁶, this comprehensive design is completed fully in-house by ALDOT bridge designers without the assistance of outside bridge consultants. After completion of the design and preparation of the contract documents, the project is let for competitive bidding by bridge erection contractors. Each bridge erector must include the cost of fabrication of the precast, prestressed concrete girders from an ALDOT-qualified prestressing plant. After award of the project, the engineering team at the awarded prestressing plant conducts independent design checks of the girders at varying stages of production and prepares shop drawings for ALDOT approval. The purpose of these shop drawings is to confirm the design intent of the project and expand the information on contract drawings as necessary for production of a component. The following sections summarize the requirements of structural design and detailing for ALDOT precast, prestressed concrete bridge girders and also discuss the role of shop drawings and the independent design review conducted by prestressing plant design engineers. The subsequent sections also attempt to highlight specific factors relevant to camber and camber-prediction within the following two phases of design: (1) preliminary design and (2) the design-review phase.

4.3.1 Preliminary Girder Design by ALDOT

This section aims to discuss (1) the requirements and code provisions applicable to the design of ALDOT prestressed concrete girders, (2) various design software typically used by ALDOT and procedures implicit to these software, and (3) the preparation of contract drawings, specifically with regards to noting camber magnitude and top-flange build-up (interchangeably referred to as “haunch”) requirements.

The requirements for the design of precast, prestressed concrete bridge girders for Alabama are set forth in the ALDOT Structural Design Manual (ALDOT Bridge Bureau 2014), most recently published in June 2014. This manual contains specific design criteria policies for the ALDOT Bridge Bureau and applies equally to ALDOT as well as to consultants completing structural designs on behalf of ALDOT. Noted in this manual is the adoption of the AASHTO LRFD Design Specifications, Sixth Edition (AASHTO 2012) as the code governing all bridge design within the state of Alabama. The following are specific design requirements of ALDOT prestressed concrete bridge girder projects—exceptions to which require the approval of the State Bridge Engineer:

⁶ Per discussions with ALDOT Bridge Bureau Bridge Design Personnel (February 2015)

- For prestressed concrete girders, specified design 28-day compressive strength of concrete shall be between 5.0 and 8.0 ksi;
- Standard shapes of AASHTO Type I, II, and III and PCI BT-54, BT-63, and BT-72 shall be used;
- Girder design shall be for simple span for all dead and live loads;
- The transformed area of bonded reinforcement shall not be included in the calculations of section properties;
- Standard pretensioning strand sizes shall be used;
- Members shall be designed such that no tension occurs (after losses) for the Service III load limit state;
- Girder shear reinforcing shall be at least #5 bars, spaced no greater than 18 in. on center, with 4 in. spacing in the girder ends for a distance equal to the girder depth;
- Confining steel shall be #3 bars spaced at 4 in. for a distance equal to the girder depth at each girder end;
- Calculation of camber at erection shall be based on a 60-day interval between release of the strand and erection of the girder;
- Debonding shall be permitted per AASHTO LRFD Section 5.11.4.3 (AASHTO 2012);
- For calculating losses, the AASHTO LRFD Approximate Method (neglecting gains) shall be used with the following parameters:
 - Time at release: 0.75 days
 - Age of deck placement: 60 days
 - Final age: 27,500 days (75 years)
 - Relative humidity: 75 percent;
- While the use of edge beams/end walls shall be a required typical detail, intermediate diaphragms shall only be used as required by calculation;
- A minimum 1 in. haunch shall be provided at girder midspan (as calculated at the critical edge of the girder flange);

- A prestress camber diagram shall be pictographically represented on bridge plans showing girder depth, haunch thickness, deck thickness, total deck plus haunch thickness, theoretical camber, and dead load deflection.

While the above design requirements have historically proven to yield safe and serviceable prestressed concrete bridges, constructability issues stemming from inaccurate camber predictions have been observed in bridges designed to the requirements summarized above.

Bridge designs complying with the above-summarized requirements are typically completed by ALDOT bridge designers with the assistance of various software packages including *LEAP CONSPAN* by Bentley Systems and *PSBEAM* by Eriksson Technologies. In general, ALDOT maintains subscriptions to both of these software to ensure compliance with current AASHTO code provisions and allows designers to choose a preferred software package for design and analysis. In order to ensure the research team could thoroughly understand the design procedures currently used by ALDOT design personnel and make recommendations compatible with these software, saved design files for previous ALDOT prestressed concrete bridge projects (in both *LEAP CONSPAN* and *PSBEAM* format) were acquired from ALDOT and reviewed thoroughly by the research team.

Both *CONSPAN* and *PSBEAM* have similar graphical user interfaces (GUI's) that allow bridge designers to input relevant material properties as shown in Figures 4-4 and 4-5, respectively. The value used by ALDOT design engineers for the unit weight of concrete in all reviewed project design files is 150 pcf. While a full discussion of various code provisions for computing the concrete modulus of elasticity is withheld until Chapter 6 of this report, it is interesting to note that both *LEAP CONSPAN* and *PSBEAM* allow the user to adjust the computed modulus of elasticity value to reflect regional calibration studies.

Concrete	Girder Release	Girder Final	Deck	
Unit weight	150.	150.	150.	pcf
Strength	6.5	6.5	4.	ksi
K1	1.	1.	1.	
Elasticity	4887.73	4887.73	3834.25	ksi
Poisson's Ratio	0.2			
Thermal coeff.	0.000006			1/°F

Figure 4-4: LEAP CONSPAN Material Input GUI

Concrete	f'c ksi	f'ci ksi	Density kcf	Normal Weight	Lightweight Sand	All	Stress Limits...
Beam:	8	7	0.15	<input checked="" type="radio"/>	<input type="radio"/>	<input type="radio"/>	Mcr Factors...
Deck:	4		0.15	<input checked="" type="radio"/>	<input type="radio"/>	<input type="radio"/>	Fr Factors...
Modulus of Elasticity, Ec							
<input checked="" type="radio"/> Compute per Spec Eq.							
Beam: Ec Factor:	33	wc,kcf:	0.15				
Deck: Ect Factor:	33	wct,kcf:	0.15				
<input type="radio"/> Compute using HS formula							
<input type="radio"/> Specify (ksi):							
Beam: Eci:	5072.240	Ec:	5422.453				
Deck: Ect:	3834.253						
Restraining Moment							
Continuity, days:	20						
Cast deck, days:	20						
Beam: e-su	600						
v-ult	2						
Deck: e-su	600						

Figure 4-5: PSBEAM Material Input GUI

LEAP CONSPAN accepts direct user input for a $K1$ parameter (a regionally calibrated factor used to represent the effect of aggregate stiffness) and PSBEAM allows users to modify the overall factor used to compute the modulus of elasticity.

Another key topic of interest in these software packages is the method used for computing long-term deflections for precast, prestressed concrete girders. Both programs default to the PCI multiplier method (as discussed in Chapter 2 of this report) and use the coefficients as originally proposed by Martin (1977). Within the GUI of each software program, it is possible to display the default long-term multipliers (as shown in Figure 4-6) and to change them as needed.

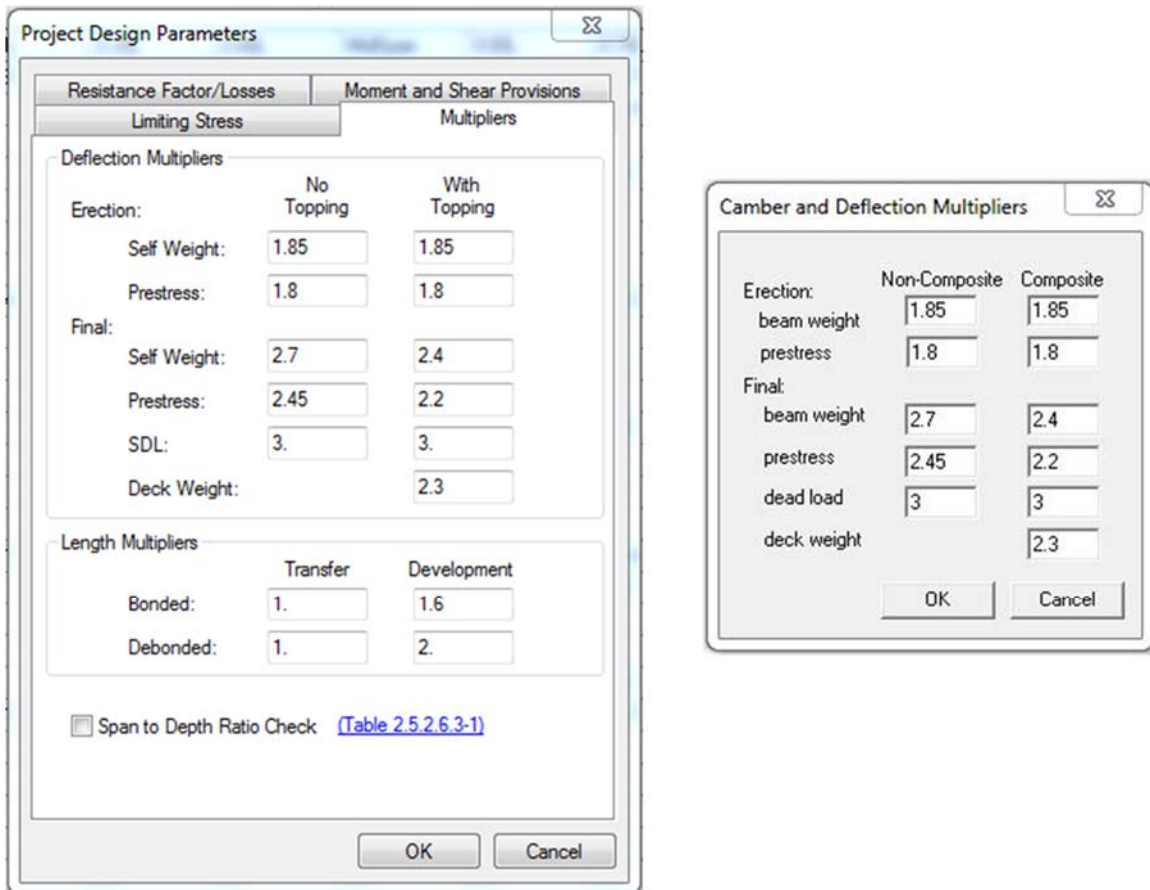
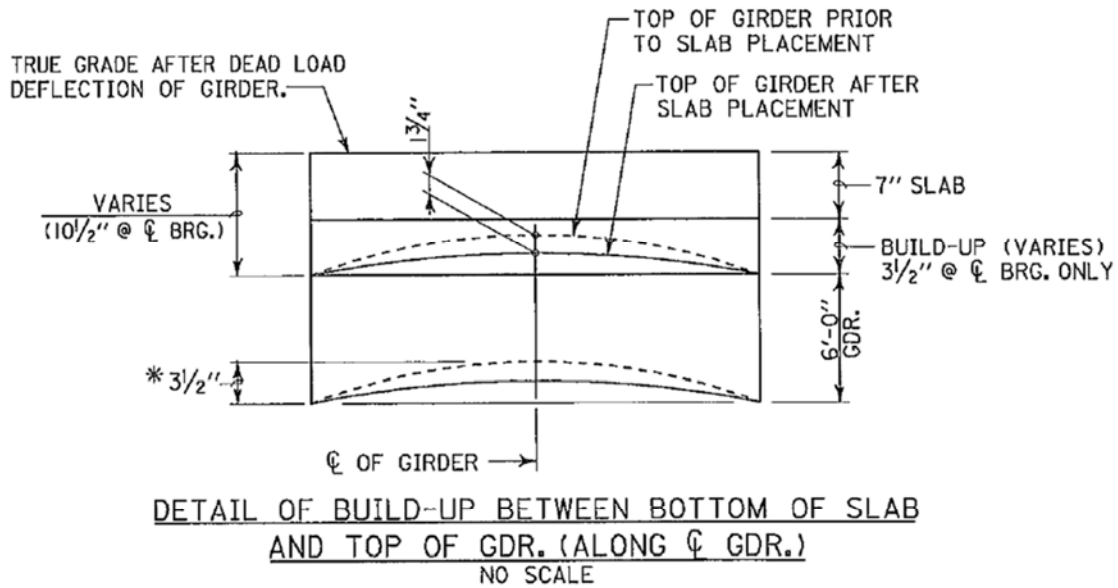


Figure 4-6: Long-term Deflection Multipliers in CONSPAN (left) and PSBEAM (right).

After the preliminary structural design is completed, a complete set of contract drawings is prepared in accordance with the ALDOT Bridge Plans Detailing Manual (ALDOT 2014) prior to the project proceeding to public bid. Included in this set of contract drawings is the following: plan view and elevations of the bridge, sections at bridge bents, typical cross sections and webwall details, and girder reinforcing details. As previously mentioned, the ALDOT Structural Design Manual (ALDOT 2014) also requires specific information regarding the build-up over top of prestressed concrete girders to be noted and visually displayed on contract drawings. A typical representation of the camber in a precast, prestressed concrete bridge is shown in Figure 4-7.



* **NOTE:** THEORETICAL CAMBER (UPWARD DEFLECTION) SHOWN. ACTUAL CAMBER OF GIRDER MAY VARY AND SHOULD BE DETERMINED BY THE CONTRACTOR PRIOR TO ORDERING MATERIAL AND SETTING FORMS.

Figure 4-7: Typical Camber Diagram on ALDOT Contract Drawings

In this case, the anticipated theoretical midspan girder camber at the instant before deck placement is $+3\frac{1}{2}$ in., where positive denotes upward. While placing a 7 in. thick concrete bridge deck, the girder is anticipated to deflect $-1\frac{3}{4}$ in. (downward) to a new net midspan camber of $+1\frac{3}{4}$ in. Accounting for the 1 in. minimum haunch thickness specified by the ALDOT Structural Design Manual (ALDOT Bridge Bureau 2014), the absolute minimum bridge build-up at the centerline of bearing is $2\frac{3}{4}$ in. The actual buildup specified on the drawing is $3\frac{1}{2}$ in., or $\frac{3}{4}$ in. greater than the minimum required for a level and flat deck. Hypothetically speaking, if the theoretical midspan girder camber was underpredicted and the true value exceeded $5\frac{1}{4}$ in. at the instant preceding deck placement, the specified $3\frac{1}{2}$ in. build-up in this scenario would be insufficient and the girder would impede on the bottom deck elevation. More common in Alabama, however, is that the theoretical midspan camber is overpredicted. In extreme cases, the true value of pre-deck placement camber may be less than $1\frac{3}{4}$ in, resulting in a situation where the downward dead load component from deck placement tends to reverse the net camber and cause a sagging under sustained dead loads. The preceding thought-exercise regarding the potential error that may be accommodated in camber prediction serves to demonstrate that the minimum 1 in. midspan haunch

requirement by ALDOT is technically a tolerance allowance, which safeguards against conflicts stemming from inaccurate camber predictions.

4.3.2 Design Review and Shop Drawing Submittal by Producer

Upon receipt of contract drawings for a precast, prestressed concrete project within Alabama, the prestressing plant engineering team begins the process of reviewing the design, proposing any necessary changes, and preparing shop drawings for submittal to ALDOT. Shop drawings typically contain an erection plan including a production sequence, precise dimensions and quantities necessary for girder fabrication, and a fabrication plan showing bed layout, elongation calculations, and detensioning sequences. In the experience of the research team, it is not uncommon for shop drawing submittals to also propose minor changes to contract drawings for ease of construction or to substitute more readily available components. Most typically, the design engineer at the prestress plant producing the girders also conducts a thorough structural analysis in order to verify the adequacy of the girder for design service loads and ultimate capacity and to confirm the deflection computations shown on contract drawings.

At the time of shop drawing preparation, the producer's design engineer likely knows substantially more about the probable material properties of girder concrete than the initial ALDOT bridge designer knew at the time of preliminary design. In addition, as a result of computing required quality-assurance calculations (i.e. anticipated girder shortening), the producer's engineer can also likely better estimate the prestress losses at different stages of production. For these reasons, it is common for girder producers to compute the expected initial camber at prestress transfer based on these refined parameters. Currently, ALDOT contract drawings typically do not publish expected camber at prestress transfer, and thus, girder producers are unable to either confirm or refute the anticipated prestress release camber as computed by the ALDOT bridge designer. In some cases, girder producers may even incorrectly compare their own refined estimation of camber at prestress transfer with the camber value published on ALDOT contract drawings, which is intended at a girder age of 60 days. Through discussions with girder producers, the research team learned that current industry practice dictates that the camber magnitude shown on producer shop drawings should reflect the same value as shown on ALDOT contract drawings. This

practice makes it difficult to identify inaccuracies in camber prediction soon after girder production and instead, encourages a delay in the evaluation of camber until an age of at least 60 days.

This research effort strives to make recommendations that allow ALDOT bridge designers and girder producers to improve the accuracy of both their initial camber calculations at prestress transfer (currently unpublished) and the camber-growth as the girder ages (published for 60 day value). By increasing the accuracy of these predictions in a transparent fashion, it is hoped that the girder producer's design staff will also participate in further refining the accuracy of camber predictions during the design review phase of a precast, prestressed concrete bridge project.

4.4 Concrete Mixtures for Precast, Prestressed Bridge Girders in Alabama

The intent of this section is to review ALDOT mixture design and approval provisions, summarize ALDOT requirements for concretes used in precast, prestressed bridge girders, review sample approved concrete mixtures typical within the study region, and discuss various fresh concrete properties as measured in the study region by girder producers.

4.4.1 ALDOT Mixture Design and Approval Procedures

ALDOT 170-82 (Method of Controlling Concrete Operations for Structural Portland Cement Concrete) (ALDOT 2009) is the primary specification governing approval of all concrete mixtures used within the state of Alabama including those used for precast, prestressed concrete applications. Outlined in this document are the following requirements for mixture design and approval:

- All concrete mixtures shall undergo a verification mixture design test at a laboratory certified by ALDOT with specific requirements as follow:
 - Mixture proportions shall be selected based on trial batches of at least three different water-cementitious materials ratios;
 - Trial mixtures shall use the exact materials intended to be used during actual production;
 - Target 28-day compressive strengths shall exceed specified requirements by 1,000 psi for compressive strengths less than 3,000 psi, by 1,200 psi for compressive strengths

greater than 3,000 psi but less than 5,000 psi, and by 1,400 psi for compressive strengths greater than 5,000 psi;

- Concrete cylinders shall be tested at the age of 7 days and 28 days in accordance with applicable ASTM and AASHTO testing standards;
- The formal submittal of the concrete mixture design shall contain all information related to the source and type of materials used, the aggregate material properties and geometric distributions, proportions for one cubic yard of concrete, freshly mixed concrete properties (including slump, air content, and temperature), and the results of the laboratory verification test summarized above; and
- Approved concrete mixtures are valid for a four-year period after which, they are subject to re-approval by ALDOT.

The mixture approval process as summarized above encourages producers to maintain a minimal inventory of approved concrete mixtures capable of satisfying a wide range of potential project requirements.

4.4.2 ALDOT Requirements for Concrete in Precast, Prestressed Bridge Girders

Specific requirements for concrete mixtures to be used in the construction of prestressed concrete bridge members are published within the *ALDOT Standard Specification* (ALDOT 2012) Section 513. Key requirements include the following:

- All constitutive materials shall meet ALDOT specifications and be from approved ALDOT source lists;
- Minimum 28-day strength of 5,000 psi (or as noted on plans);
- Minimum cementitious factor = 550 pcy;
- Maximum $w/cm = 0.45$;
- Air content between 2.5 percent and 6.0 percent by volume;
- Maximum slump (prior to admixture) = 4.0 in.;
- Maximum slump total (with admixture) for conventionally vibrated concrete = 9 in.; and
- Slump flow range for self-consolidating concrete = 25–29 in.

Supplementing the provisions of the *ALDOT Standard Specification*, ALDOT-367 (2015) (Production and Inspection of Precast Non-Prestressed and Prestressed Concrete) outlines requirements for the production and inspection of precast, prestressed concrete members and addresses some additional intricacies of girder fabrication. Included in this document are ALDOT requirements for the following: strand tensioning procedures, formwork, prestressing steel, reinforcing steel, concrete testing and acceptance, curing, strand detensioning, final approval of members, tolerances, and documentation procedures. While the provisions of the *ALDOT Standard Specification* are mainly relevant to pre-construction planning and approval, the requirements of ALDOT-367 are routinely referenced and enforced by on-site ALDOT field inspectors during girder production.

4.4.3 ALDOT-Approved Concrete Mixture Proportions

Concrete mixtures typically used in the precast, prestressed industry are characterized by low water-to-cementitious materials ratios (w/cm), relatively high total paste content, the use of Type III cement and supplementary cementing materials (SCMs), and medium- to high-dosages of chemical admixtures (PCI 2011). Producers attempt to optimize mixture designs to minimize raw material cost, concrete placement labor, and chronological time to prestress release, while simultaneously maximizing finish quality.

In the geographical study area, each ALDOT-approved prestressed girder producer tends to maintain between one and three approved mixtures at any given time. A comparison of typical mixture proportions representing four prestress producers included in this study is shown in Table 4-2.

Table 4-2: Typical Mixture Proportions for Alabama Precast, Prestressed Concrete

Label	Plant A		Plant B		Plant C		Plant D	
	#1	#2	#1	#2	#1	#2	#1	#2
Cement (lbs/yd ³)	639	751	788	765	788	600	697	765
SCM #1 Type	Slag Cement	Slag Cement	Class F Fly Ash	Class F Fly Ash	Class F Fly Ash	Class F Fly Ash	Class F Fly Ash	Class F Fly Ash
SCM #1 (lbs/yd ³)	113	133	173	100	150	170	123	135
SCM #2 Type	None	None	None	Silica Fume	None	Silica Fume	None	None
SCM #2 (lbs/yd ³)	0	0	0	75	0	85	0	0
Water (lbs/yd ³)	277	282	292	275	253	248	258	283
w/cm	0.37	0.32	0.30	0.29	0.27	0.29	0.32	0.32
Coarse Aggregate Type	#57/#67 Limestone (Dolomitic)	#57/#67 Limestone (Dolomitic)	#67 Granite	#67 Granite	#78 Limestone (Regular)	#67 Gravel	#67 Granite	#67 Granite
Coarse Aggregate (lbs/yd ³)	1860	1861	1345	1426	1720	1675	1655	1576
Source of Coarse Aggregate	Helena, AL	Helena, AL	Forest Park, GA	Forest Park, GA	Calera, AL	Pearl River, LA	Mulgrave, Canada	Mulgrave, Canada
Fine Aggregate	#100 Sand	#100 Sand	#100 Sand	#100 Sand	#100 Sand	#100 Sand	#100 Sand	#100 Sand
Fine Aggregate (lbs/yd ³)	1172	1048	1301	1278	1091	1048	1249	1189
Source of Fine Aggregate	Prattville, AL	Prattville, AL	Butler, GA	Butler, GA	Pearl River, LA	Pearl River, LA	Atmore, AL	Atmore, AL
Sand/total aggregate (by weight)	0.39	0.36	0.49	0.47	0.39	0.39	0.43	0.43
Max. AEA Dosage (oz/cwt)	0.13	0.11	0.21	0.21	0.42	0.47	0.40	0.40
Max. HSA Dosage (oz/cwt)	1.0	1.0	3.5	4.5	1.3	1.1	2.0	2.0
Max. HRWRA Dosage (oz/cwt)	10.0	10.0	5.9	7.0	5.1	5.0	6.5	5.5

Notes:

1. Admixture abbreviations: Air-Entraining Admixture (AEA), Hydration Stabilizing Admixture (HSA), and High-Range Water Reducing Admixture (HRWRA).
2. All aggregates in saturated-surface dry state.

From the mixture proportions shown in Table 4-2, the typical concrete mixtures used in the Alabama precast, prestressed industry can be characterized as follows:

- Average w/cm = 0.31;

- High cementitious materials content (on average = 881 pcy);
- Average water content = 270 pcy
- Average sand/total aggregate ratio = 0.42;
- Replacement of Type III cement with slag cement, fly ash, or a combination of fly ash and silica fume in varying percentages is common;
- The majority of producers use a #67 limestone or granite coarse aggregate;
- All producers use a #100 natural sand;
- Relatively low dosages of air-entraining admixtures (AEA) and hydration stabilizing admixtures (HSA); and
- Medium to high dosages of high-range water-reducing admixtures (HRWRA).

A more thorough discussion of mixture proportions as developed and used in the laboratory portion of this research study is included in Chapter 6 of this report.

4.4.4 Prestressed Concrete Fresh Properties

To further characterize the precast, prestressed concrete industry in Alabama, historical values were compiled for selected fresh concrete properties for the six-year period from 2007 through 2013. Frequency histograms for slump and percent air content (by volume) are shown in Fig. 4-8.

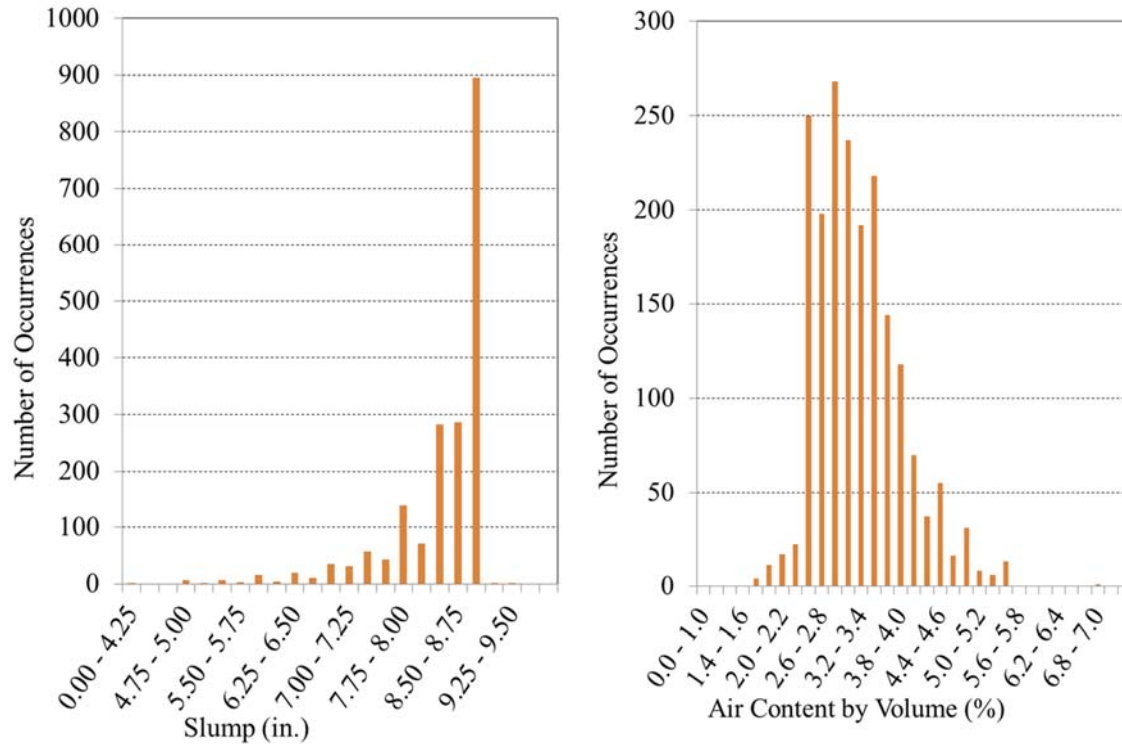


Figure 4-8: Historical Data for Select Fresh Concrete Properties: Slump (left) and Air Content (right).

It is not surprising that producers prefer to target the maximum allowable slump of 9 in. to maximize the workability of concrete. The mean slump value for all historical records considered was 8.5 in., with a most common measurement of 9 in. With regards to air content, it is most common for producers to target minimum requirements for air content (2.5 percent) given the relatively mild climate of the region. This minimal air content can typically be achieved without the need for air-entraining admixtures (AEA). The mean air content for the historical data was 3.3 percent, with a most frequent measurement of 3.0 percent.

4.5 Construction Practices Relevant to Camber

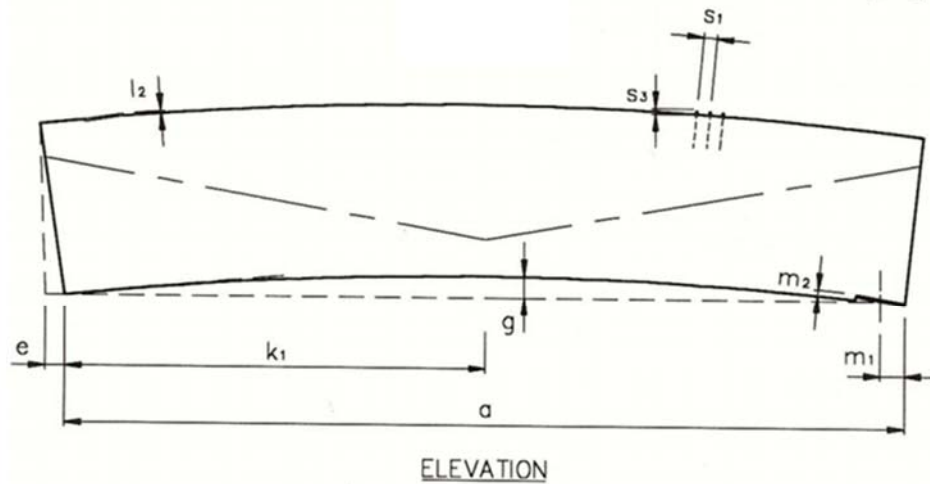
The construction procedures and practices used to produce ALDOT prestressed concrete girders at various girder producers have been thoroughly documented by others in recent years. These practices are fairly standardized and were found to be in accordance with the requirements of ALDOT specifications. Most recently, as part of this research effort, Hofrichter (2014) provided a detailed portrayal of typical construction procedures at four regional prestressed concrete producers. Previously, Dunham (2011) also documented the production of prestressed concrete girders within the study region.

Rather than providing a repetitive account of production procedures, the focus of this section remains on those construction factors most relevant to camber and camber prediction in precast, prestressed concrete bridge girders.

4.5.1 Production Camber Measurements and Permissible Tolerances

Pursuant to the requirements of ALDOT-367 (ALDOT 2015), girder camber is typically measured within 24 hours after strand detensioning for at least half of all members cast. These measurements of camber are intended to verify consistency among members of the same project and are not intended to confirm theoretical shop drawing camber. However, ALDOT-367 does require that significant variations from the camber shown on shop drawings be reported to the ALDOT for evaluation. In the experience of the research team (and in agreement with previous researchers' work summarized in Chapter 3), production camber measurement practices are quite inconsistent among girder producers and of little practical use from a research perspective.

Also included in ALDOT-367 (ALDOT 2015) are permissible tolerances for camber in precast, prestressed bulb-tee girders as shown in Figure 4-9. As noted, the variation from design camber is +/- 1/8 in. per 10 ft of girder length and the differential camber between adjacent members of the same design is 1/4 in. per 10 ft of girder length.



g = Camber variation from design camber* $\pm \frac{1}{8}$ in. per 10 ft.
g1 = Differential Camber Between Adjacent Members of the Same Design* $\frac{1}{4}$ in. per 10 ft.

Figure 4-9: Permissible Camber Production Tolerances (Adapted from ALDOT 367 2015)

The first requirement, camber variation from design camber, is difficult to evaluate because a specific age of measurement is not specified. While ALDOT contract drawings typically specify an anticipated theoretical camber at an age of 60 days after production (in accordance with the assumptions of Martin [1977]), the magnitude of camber is most commonly measured either directly after prestress release (0.75 days) or directly prior to shipping (frequently in excess of 60 days). The second requirement, differential camber between similar members, is a more useful and quantifiable metric because no specific age is necessary for evaluation. Most typically, differential camber is evaluated directly after prestress release, but also applies equally at any girder age.

4.5.2 Chronological Time to Prestress Release

The chronological time to prestress release is one of the most influential variables in determining concrete compressive strength at prestress release, and, therefore, is of the utmost relevance to this research effort. While the entirety of Chapter 5 is devoted to concrete strength considerations, this section discusses the average chronological time to prestress release in the context of field construction practices.

It is desirable for girder producers to maintain an average chronological time to prestress release of approximately 18 hours in order to maximize production efficiency and allow reuse of production beds

within 24 hours. As part of this research effort, Hofrichter (2014) compiled data for the chronological time to prestress release for 1,917 girder concrete placement events during the six-year period preceding 2013. A histogram of chronological ages at the time of prestress release for the full data set is shown in Figure 4-10. Two significant peaks occur in this histogram, demonstrating the two most common scenarios in which girder production and prestress release take place.

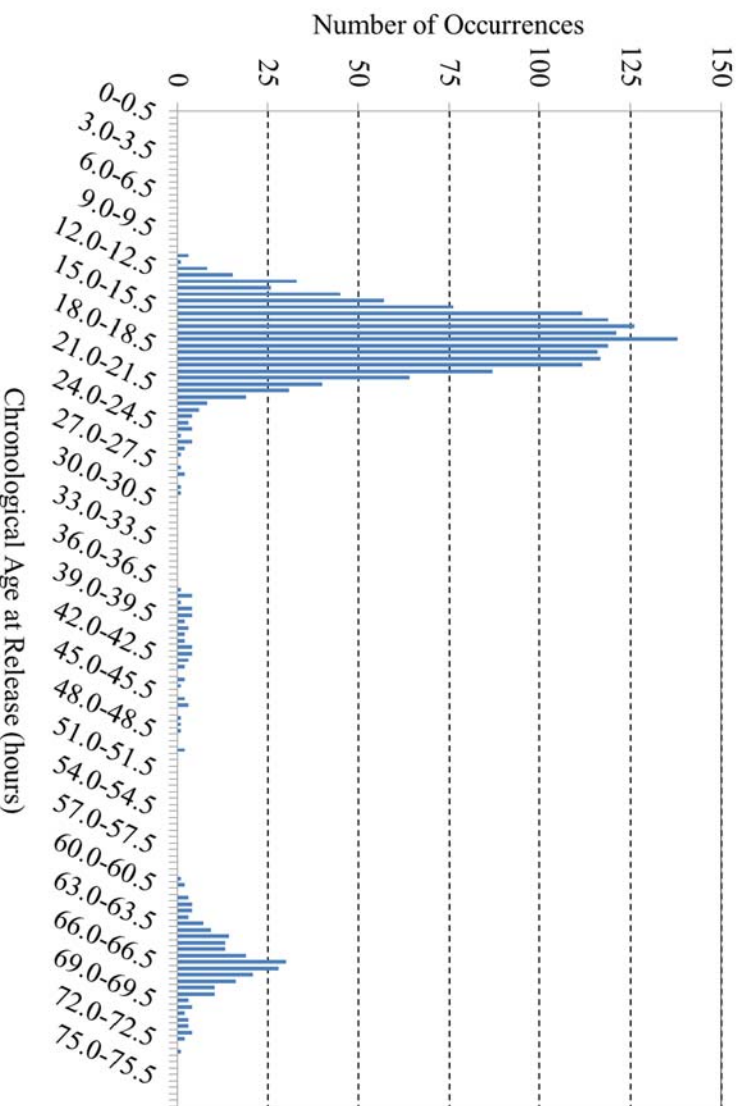


Figure 4-10: Frequency Histogram for Chronological Age at Release.

The first and primary peak occurs at the age of approximately 18 hours, which is representative of standard plant practices. Concrete is most often placed during the late morning or early afternoon, with the intent to transfer the prestressing force to the girders very early the next morning to facilitate the use of formwork on a 24-hour cycle. A second peak in the histogram is observed around 66 hours and represents non-standard pours typically taking place on Fridays and subjected to extended curing over the weekend prior to a Monday prestress release event. A cumulative percent occurrence plot of the same data set is shown in Figure 4-11. It can be seen that chronological ages at release of less than 24 hours represent roughly 84% of the full data set.

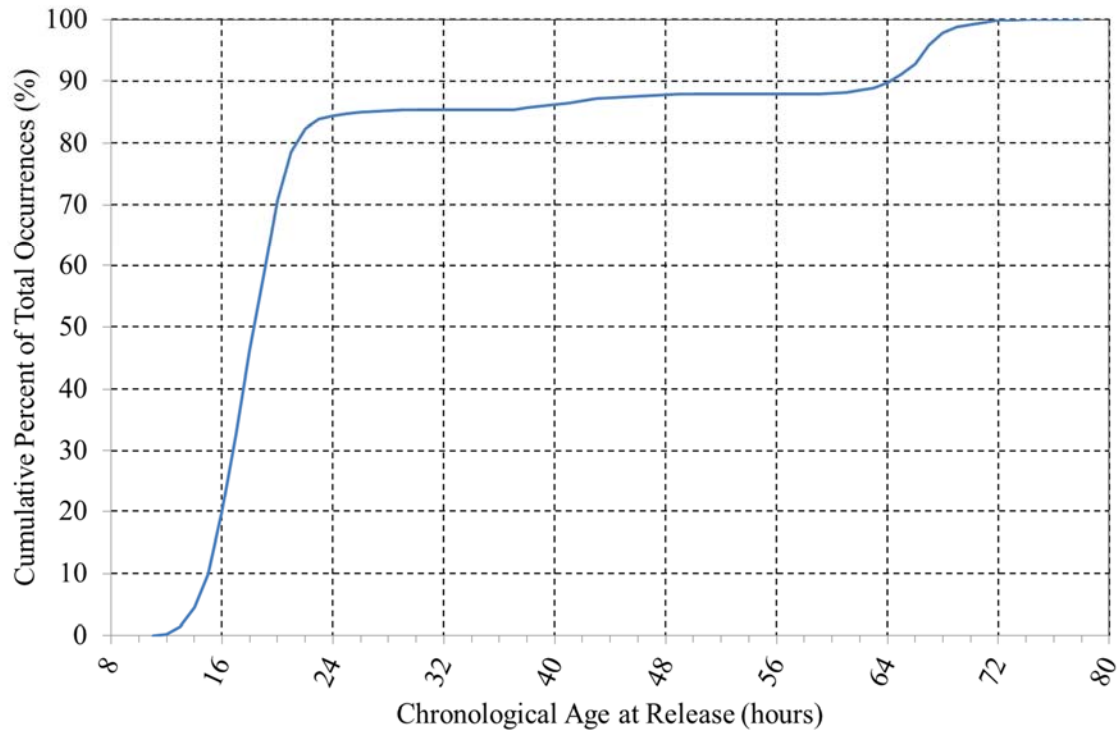


Figure 4-11: Cumulative Percent Occurrence for Chronological Age at Release.

The mean chronological age of release for the full data set is 25.1 hours, with a most frequently observed value of 17 hours. This disparity between the mean chronological age to release and the mode of the sampled data suggest that the sampled data represents two distinct populations, namely, standard plant practices and extended release practices. The sampled data was divided into two subgroups, those with release times less than or equal to 24 hours (identified as standard plant practices) and those with release times exceeding 24 hours (identified as extended release practices.) Statistical summaries for the reduced data sets are shown in Table 4-3.

Table 4-3: Statistical Summary of Chronological Age to Release by Subgroup

	Standard Plant Practices (≤ 24 hrs.)	Extended Release Practices (> 24 hrs.)
Number of Values	1602	226
Sample Mean, \bar{x} (hrs.)	17.7	66.2
Sample Mode, <i>Mo.</i> (hrs.)	17	66
Sample Standard Deviation, <i>s</i> (hrs.)	2.2	2.2

For standard plant practices, the mean chronological age at prestress release is 17.7 hours, with a sample mode of 17 hours, and a sample standard deviation of 2.2 hours. The summary statistics in Table 4-3 are offered as useful parameters for future designers of experimental research programs, in lieu of relying on anecdotal reports claiming a chronological time to release of 18 hours.

4.5.3 Maturity at Prestress Release

While the chronological time to release may be the most readily available parameter for timing in the precast, prestressed concrete industry, the widespread use of accelerated curing methods (i.e. steam curing) make it desirable to express average time to prestress release in terms of a concrete maturity or equivalent age. Steam curing protocols vary by region, but most often limit maximum exposure temperatures to approximately 150°F and specify the maximum rate at which the concrete temperature may change (typically 36-40°F/hour) (PCI 2011). Local ALDOT guidelines permit up to a maximum temperature of 160°F with a maximum rate of temperature change of 40°F/hour. For the purposes of this analysis, a reduced data set of 435 concrete placement events was randomly sampled from the full data set. To be eligible for selection for this reduced data set, a concrete placement event needed to have clear reliable temperature data recorded throughout fabrication, full fabrication records available, and belong to the standard plant practices (≤ 24 hour chronological age to release) data set.

Calculation of the equivalent age at release for each placement event was conducted based on ASTM C1074 (2011). For the analysis, a value of 45,000 J/mol was used for activation energy in accordance with the recommendations of Carino and Tank (1992) and a reference temperature of 22.5°C. A frequency histogram of the reduced data set for equivalent age is shown in Figure 4-12.

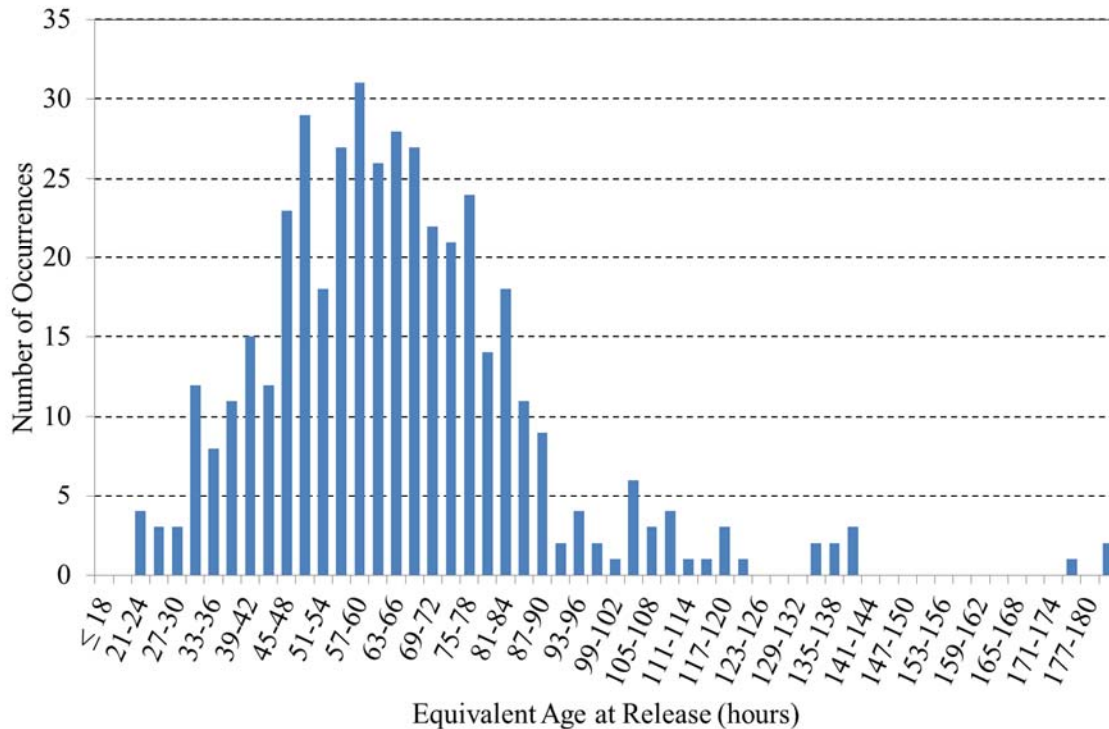


Figure 4-12: Frequency Histogram for Equivalent Age at Prestress Release.

The mean equivalent age at prestress transfer from the considered data set was 65.0 hours with a sample mode of 50 hours, and a sample standard deviation of 24.4 hours. A relatively large variance, as compared to the chronological age to release data set, was noted for the equivalent age distribution and may (1) question the reliability and consistency of in-plant temperature recording efforts or (2) suggest that the chronological time to transfer is intrinsically a more constrained parameter than the maturity at transfer.

4.5.4 Girder Handling and Storage Conditions

After production is complete, precast, prestressed concrete girders are typically stored at the girder production facility until transported to the bridge site for erection. As documented by Hofrichter (2014), a wide variety of storage conditions were observed in the four prestressed concrete plants included in this study. Most frequent was the use of timber dunnage or waste concrete piles (with a plywood bearing surface) located directly under the lifting points, approximately 5 ft from each girder end as required by ALDOT-367. With regards to camber and camber growth, ALDOT-367 (ALDOT 2015) specifies that all precast, prestressed concrete bridge members remaining in storage for a period in excess of 120 days

shall be repositioned every 120 days to ensure that deformations due to creep, shrinkage, loads, and uneven support conditions are kept to a minimum.

4.6 Required Girder Production Documentation and Data Reporting Formats

This section summarizes the documentation required by ALDOT during girder production and the most common recording formats. Of the information discussed in this section, historical concrete strength testing records proved to be the most useful and are thoroughly discussed and analyzed in Chapter 5 of this report.

In accordance with the requirements of ALDOT-367 (ALDOT 2015), the following field data are typically recorded during the production of precast, prestressed concrete bridge girders:

- Fresh concrete properties for each concrete placement and sampling location, including slump, air content, ambient air temperature, and fresh concrete temperature;
- Measured cylinder compressive strengths at the time of prestress release and at an age of 28 days;
- Prestressing strand force and/or elongation predictions and measurements; and
- Curing temperature records for the girder or cylinders produced.

Record keeping is a joint effort between ALDOT inspectors and girder producers, with each party maintaining independent copies of all records. In general, ALDOT on-site records tended to be thorough and consistent between all production facilities, while girder producer records tended to vary more in format and completeness.

4.7 Summary

In order to provide viable and efficient solutions to assist ALDOT to more accurately predict camber in precast, prestressed concrete girders, it was first necessary to explore and document the existing procedures used for the design and construction of precast, prestressed concrete bridge girders within the study region. In the context of girder camber, this chapter summarized the current state-of-the-art of the precast, prestressed girder industry in Alabama and included a general background, a review of typical girder design roles and procedures, a discussion of concrete mixture proportioning for regional

prestressed applications, a brief review of pertinent girder production practices, and a summary of typical record-keeping practices.

4.8 Recommendations

In order to assist with improving the accuracy of camber predictions, the following modification to current design and construction practices is proposed: ALDOT contract drawings should show the estimated *release* camber based on the bridge designer's calculations in addition to the 60-day erection camber currently included. By including this parameter on contract drawings, prestress plant engineers and quality-control personnel may be able to more readily confirm the accuracy of initial camber and identify troublesome discrepancies up to 60 days earlier than current practice allows. In addition, it may be advantageous to also show a 120-day estimate of camber to provide a metric of camber growth potential.

Chapter 5: Accurately Predicting Expected Concrete Compressive Strength

5.1 Introduction

Compressive strength is the concrete material property of paramount importance in structural design. Compressive strength is directly related to the structure of the hydrated cement paste and, therefore, provides an overall picture of the quality of concrete (Neville 2013). In typical structural design, the design engineer is primarily concerned with satisfying strength limit states (i.e. life-safety considerations) and places significantly less emphasis on the accuracy of serviceability calculations (i.e. deflections). Common practice for typical U.S. design engineers is to use specified concrete properties for both strength and serviceability limit state computations.

In reality, the specified concrete strength is a lower-bound value not intended to represent the average in-place concrete strength (alternately termed the “expected” strength) of a completed structural member. Instead, the expected concrete strength must always exceed the specified concrete strength by a statistically determined margin in order to ensure that the vast majority of the concrete strengths in the structure exceed the specified strength. The disparity between specified and expected concrete compressive strength is not presently accounted for in serviceability structural design computations.

For design engineers in certain practice areas, the accuracy of serviceability computations is of the utmost importance in order to avoid potential costly effects. Examples of engineers with an increased emphasis on serviceability may include the following: (1) engineers designing precast, prestressed concrete girders that must satisfy a minimum camber requirement, (2) design engineers for tall buildings estimating elastic shortening of columns and specifying corresponding tolerances/details, (3) designers of floor systems for owners with stringent deflection or floor flatness requirements. For these design engineers, it is essential that *expected* values for concrete material properties are used in serviceability computations in lieu of the common practice of using specified, lower-bound parameters. It is important to note that the *choice* to use expected parameters in serviceability computations is completely

independent of the *requirement* to use specified parameters for strength limit state designs. Specified parameters must always be used in strength limit state designs in order to ensure a sufficiently small code-intended probability of failure to safeguard life safety.

This chapter provides analyses and guidance to allow design engineers to more accurately predict the expected concrete compressive strength at various ages for the purposes of serviceability computations. By more accurately predicting the expected concrete strength, the accuracy of serviceability computations can be greatly improved. It is important to reiterate that the mean expected concrete compressive strength as predicted using the provisions of this chapter should not be used in strength limit state computations.

5.1.1 Chapter Objectives

The primary objective of this chapter is to improve the accuracy of design serviceability predictions by identifying relationships between specified concrete compressive strength and expected concrete compressive strength. Major tasks include the following:

- Review current code-provisions related to predicting expected concrete compressive strength in general and discuss the appropriateness of their usage in serviceability computations;
- Discuss recent research efforts within the precast, prestressed concrete industry aimed at predicting expected concrete compressive strength at the time of prestress release and 28 days after the start of production;
- Identify and discuss the primary causes of overstrength in the precast, prestressed concrete industry;
- Provide recommendations to more accurately predict expected concrete compressive strength at the time of prestress release in the precast, prestressed concrete industry; and
- Provide recommendations to more accurately predict expected concrete compressive strength 28 days after the start of production in the precast, prestressed concrete industry.

5.1.2 Chapter Outline

This chapter begins with a brief background section (Section 5.2) discussing concrete compressive strength. Next, Section 5.3 contains a discussion of current code provisions related to expected in-place

concrete compressive strength and an examination of the appropriateness of their usage in serviceability computations. Section 5.4 contains a synthesized literature review of previous efforts in the precast, prestressed industry to predict expected concrete compressive strength at the time of prestress release and 28 days after production. Next, Section 5.5 details a historical data set compiled as part of this effort and any subsequent post-processing. Section 5.6 contains details and recommendations of an analysis conducted to identify relationships between specified and expected concrete compressive strength at the time of prestress transfer. Section 5.7 contains the results of a similar analysis for 28-day strength. Finally, Section 5.8 provides a summary and conclusions of the research effort contained in Chapter 5 and highlights specific recommendations that address the study objectives listed in Section 5.1.1.

5.2 Background

5.2.1 Concrete Compressive Strength

Concrete compressive strength is defined as “the measured maximum resistance of a concrete specimen to axial compressive loading, expressed as force per unit cross sectional area” (ACI 2013). Compressive strength is commonly tested by applying a standard loading protocol to cylindrical concrete specimens as outlined in *ASTM C39: Standard Test Method for Compressive Strength of Cylindrical Concrete Specimens* (ASTM C39 2010). A tested specimen is judged to have reached failure when it is no longer capable of carrying increased load due to an advanced state of internal cracking and/or external fracture (Mehta and Monteiro 2014). Although non-standard testing ages may be specified to meet unique project requirements, the most common specified ages of testing are 24 hours, 3 days, 7 days, 28 days, and 90 days (ASTM C39 2010).

A large number of factors affect concrete compressive strength, but can be classified into two major groups: (1) characteristics and proportions of materials and (2) curing conditions. The first grouping, characteristics and proportions of materials, primarily affects concrete compressive strength by influencing the porosity of the hardened concrete. As porosity increases, the concrete compressive strength tends to decrease (Mehta and Monteiro 2014). The second grouping, curing conditions, tends to influence concrete compressive strength by governing the extent and rate of cement hydration. The following two paragraphs discuss the general effect of each of these groupings on concrete compressive strength.

Without doubt, the material parameter most influential to concrete compressive strength is the water-to-cement ratio, w/c . As documented by Duff Abrams in 1927 and shown in Figure 5-1, as the water to cement ratio decreases, the compressive strength of the concrete tends to increase exponentially. Perhaps next most important is the effect of air-entrainment on concrete compressive strength. As the volume of entrained air in the hydrated cement paste increases, the porosity of the concrete mixture as a whole also increases, tending to cause a decrease in concrete compressive strength. An approximate rule of thumb for the effect of air content on compressive strength is as follows: a one percent decrease in the air content of a given mixture corresponds to approximately a five percent increase in compressive strength. Additional material factors tending to affect concrete compressive strength, although to lesser extent than those outline above, are cement type, aggregate type and gradation, mixing water quality, and chemical admixture usage (Mehta and Monteiro 2014).

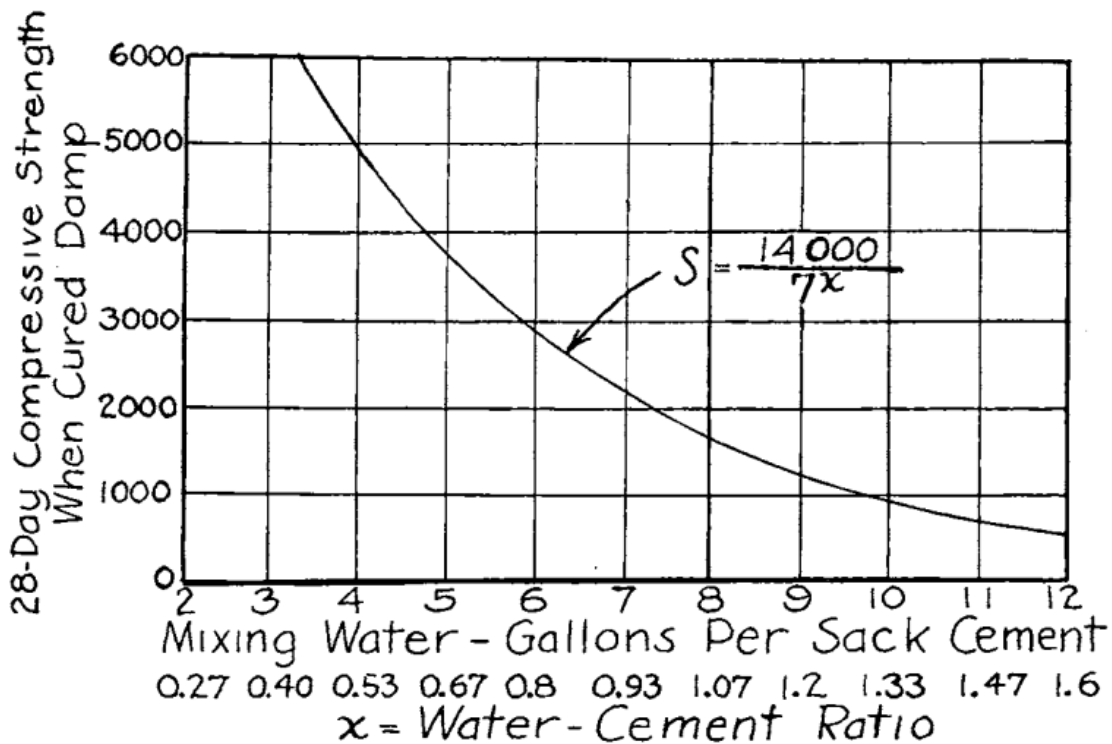


Figure 5-1: Relationship between water to cement ratio, w/c , and compressive strength as expressed by D. Abrams (1927)

Curing conditions, namely time, temperature, and humidity, are directly related to determining the total extent of cement hydration and the rate at which cement hydration occurs, thereby influencing concrete compressive strength. Time is a primary factor influencing concrete strength, as the hydration

process of cement is a time-dependent chemical reaction that essentially terminates at either the complete consumption of hydration reactants or in the global (or local) absence of available water. Owing to the importance of this topic with regards to this research effort, Section 5.2.3 includes a thorough discussion of the influence of time on concrete strength. With regards to temperature, increased temperature is generally correlated with more rapid hydration of cement, thereby causing an increased rate of strength development at early ages (Mehta and Monteiro 2014). Finally, the availability of moisture during early-age hydration (as measured by relative humidity) can also affect concrete strength by increasing the total degree of hydration achievable for a given concrete. In general, hydration slows or ceases when the vapor pressure in capillaries falls below 80 percent of the saturation humidity (Mehta and Monteiro 2014). By artificially maintaining a high external humidity, the hydration reaction is encouraged to continue for longer, thereby increasing the degree of hydration achieved.

5.2.2 Concrete Compressive Strength Nomenclature and Definitions

This section defines necessary nomenclature relating to concrete compressive strength and strength prediction models developed later in this chapter. In general, this section is heavily based on the definitions offered by Hofrichter (2014), although expanded to include additional quantifications of overstrength.

There are four “types” of strength at any given age that are discussed or used in the rest of this report. The system used for differentiating among these four types is as follows:

1. The strength level that is measured by cylinder testing at any given age is simply called the “measured strength” at that age. The variables used to describe this are the simplest of the four types, and are shown here:

f_{ci} = measured compressive strength of concrete at prestress release (psi)

f_c = measured compressive strength of concrete at 28 days (psi)

2. The strength level specified by the design engineer at a given time is called the “specified” strength at that age. The variables used to describe this type are shown here:

f'_{ci} = specified compressive strength of concrete at prestress release (psi)

f'_c = specified compressive strength of concrete at 28 days (psi)

The prime in the f' variable denotes it as a specified value.

3. The strength level that is expected or predicted based on the provisions recommended as part of this chapter and is called the “expected” strength at a given age. The variables used to describe this type are shown here:

f_{ci}^* = expected compressive strength of concrete at prestress release (psi)

f_c^* = expected compressive strength of concrete at 28-days (psi)

The asterisk in the f^* variable denotes it as an expected value.

4. The strength level that concrete producers target during mixture approval testing (discussed further in Section 5.3) and is called the “target” strength or “required strength” at a given age. The variables used to describe this type are shown here:

f'_{cir} = target compressive strength at prestress release (psi)

f'_{cr} = target compressive strength at 28 day (psi)

For the purposes of the analyses conducted in this chapter, the following derived nomenclature is also used to provide comparisons between some of the above strength parameters:

1. The ratio of the strength level that is measured by cylinder testing to the strength level specified by the design engineer at any given time. This is called the “actual overstrength factor” at any given age. The variables used to describe this type are shown here:

$OS_i = f_{ci} / f'_{ci}$ = actual overstrength factor at prestress release

$OS_{28} = f_c / f'_c$ = actual overstrength factor at 28 days

2. The ratio of the strength level that is expected or predicted to the strength level specified by the design engineer at any given time. This is called the “expected overstrength factor” at any given age. The variable form used to describe this type are shown here:

$OS_i^* = f_{ci}^* / f'_{ci}$ = expected overstrength factor at prestress release

$OS_{28}^* = f_c^* / f'_c$ = expected overstrength factor at 28 days

In general, the “actual overstrength factor”, (OS_i or OS_{28}) is a parameter based on the random variable “measured strength” (f_{ci} or f_c). Conversely, the “expected overstrength factor”, (OS_i^* or OS_{28}^*) is based on the result of an expected strength prediction computation, f_{ci}^* or f_c^* . In the case of a perfectly accurate prediction model, the “expected overstrength factor” would be equal to “actual overstrength factor”.

3. The difference between the strength measured by cylinder testing and the strength level specified by the design engineer at any given time is called the “difference statistic” ($dstat$).

The variables used to describe this type are shown here:

$$dstat_i = f_{ci} - f'_{ci} = \text{difference statistic at prestress release (psi)}$$

$$dstat_{28} = f_c - f'_c = \text{difference statistic at 28 days (psi)}$$

The “difference statistic” parameter serves an important role in the analysis procedure of Section 5.7.

5.2.3 Concrete Compressive Strength Growth Provisions

As discussed in Section 5.2.1, the nature of concrete is such that its mechanical properties change substantially over time. This section reviews two of the most common models for describing compressive strength development as a function of time—the ACI 209 method and the Model Code 2010 (MC 2010) method. Then, a summary of the research findings by Hofrichter (2014) conducted as part of this research effort is provided. These findings are later utilized in the analysis of Section 5.7, as well as the software implementation detailed in Chapter 9 of this report.

The nature of the two concrete strength growth provisions described herein is such that the strength development curve can be defined completely with knowledge of concrete strength at any two ages (chronological age or concrete maturity). If strength at only one age is known, published values of growth-rate coefficients may be used to apply the strength growth provisions to estimate strength at other ages of interest. The most typical application of strength growth provisions is for the estimation of concrete strength at any age other than 28 days given a known strength at 28 days. The standard form

of the equations in ACI 209R-92 (2008) and MC 2010 (fib 2010) are published with this intended use in mind.

Based on the independent work of six research groups, ACI 209 (2008) proposed an equation of the following form for modeling concrete strength growth as a function of time:

$$f_c(t) = f_{c28} \left(\frac{t}{\alpha + \beta \cdot t} \right) \quad (5-1)$$

where

$f_c(t)$ = concrete strength at any concrete age t (psi);

f_{c28} = concrete strength at a concrete age of 28 days (psi);

t = concrete age (days);

α = constant (days); and

β = constant (unitless).

Rearranging Equation 5-1 as follows, the strength growth term can be isolated on the right-hand side of the equation:

$$\frac{f_c(t)}{f_{c28}} = \left(\frac{t}{\alpha + \beta \cdot t} \right) \quad (5-2)$$

Setting the left-hand side of the equation equal to 1.0 at $t = 28$ days (synonymous to constraining the strength growth term to equal 1.0 at 28-days) gives the following:

$$1 = \left(\frac{28}{\alpha + \beta \cdot 28} \right) \quad (5-3)$$

Solving for the constant α yields:

$$\alpha = (1 - \beta)28 \text{ days} \quad (5-4)$$

Equation 5-4 denotes that α is dependent on β to ensure the strength growth factor equals 1.0 at $t = 28$ days. A plot of Equation 5-2 with varying combinations of α and β satisfying Equation 5-4 is shown in Figure 5-2. The series corresponding to $\alpha = 0.70$ and $\beta = 0.98$ reflects the ACI 209R-92 recommendation for steam-cured concrete containing Type III cement.

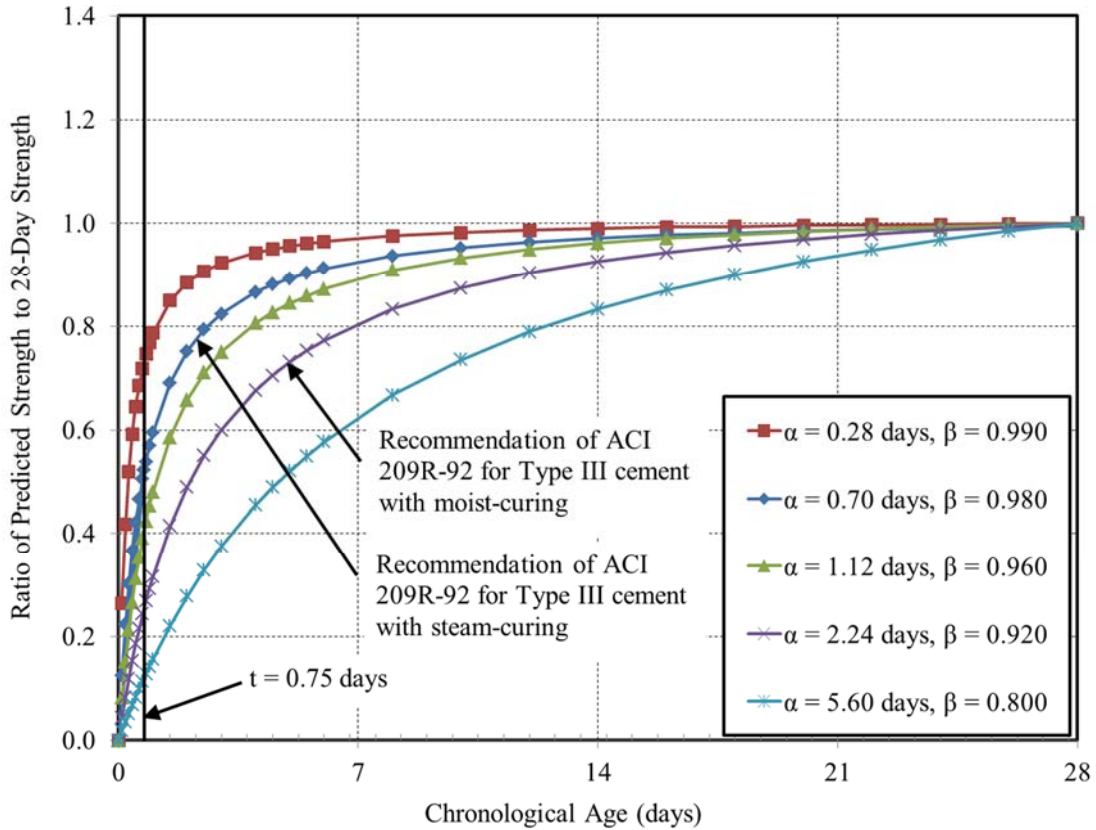


Figure 5-2: ACI 209R-92 Strength Growth Equation with Various Constants

As shown in Figure 5-2, the ACI 209R-92 recommendation implicitly assumes that at the typical chronological time of prestress release ($t = 0.75$ days), approximately 50 percent of the 28-day concrete strength has developed in steam-cured concrete.

The other primary strength growth equation, as proposed by MC 2010 (fib 2010), is given as:

$$f_{cm}(t) = \beta_{cc}(t) \cdot f_{cm} \quad (5-5a)$$

with

$$\beta_{cc}(t) = \exp \left\{ s \cdot \left[1 - \left(\frac{28}{t} \right)^{0.5} \right] \right\} \quad (5-5b)$$

where

$f_{cm}(t)$ = the mean compressive strength at temperature-adjusted age t (MPa);

$\beta_{cc}(t)$ = a function to describe strength development with time;

f_{cm} = the mean compressive strength at an age of 28 days (MPa);

s = coefficient that depends on the strength class of given cement; and

t = temperature-adjusted concrete age relative to 20°C. (days).

In Equation 5-5, the parameter $\beta_{cc}(t)$ is similar to the strength growth term of Equation 5-2, except unlike the ACI 209 method, it reflects the maturity of the concrete. Equation 5-5b is plotted in Figure 5-3 for varying values of the coefficient s . As shown, the growth curve is generally similar to the ACI 209 expression, with the exception of the horizontal-axis reflecting temperature-adjusted age instead of chronological age. The series corresponding to $s = 0.20$ reflects the recommendation of MC 2010 for the concrete type most similar to that used in the U.S. precast, prestressed industry.

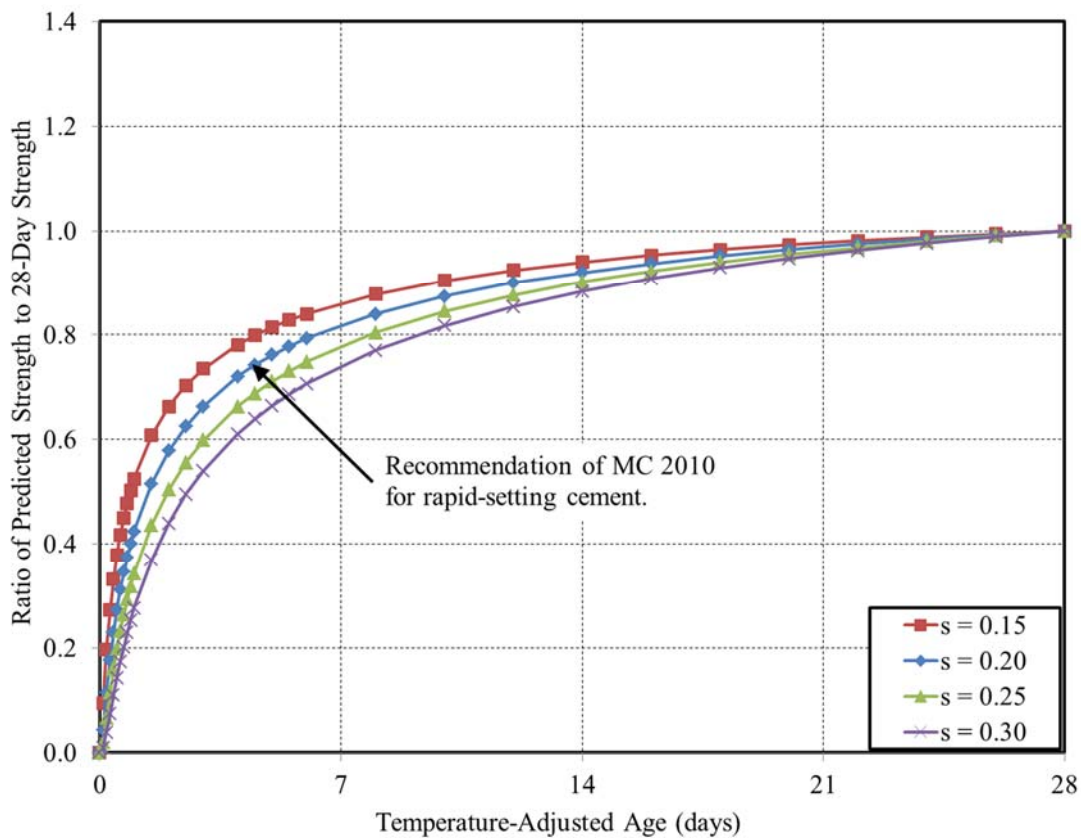


Figure 5-3: MC 2010 Concrete Strength Growth Provisions with Varying Constants

As part of this research effort, Hofrichter (2014) examined the applicability of the above strength growth provisions to concretes typical of the Alabama precast, prestressed concrete industry. By examining historical strength testing records of 435 concrete placement events for the production of

ALDOT precast, prestressed girders, Hofrichter (2014) proposed revised calibrations of the above strength growth as appropriate for the regional precast, prestress industry:

- A recommended form of the ACI 209-R92 strength growth equation appropriate for use in the precast, prestressed industry is as follows:

$$f_c = f_c(t) \cdot \left(\frac{\alpha + \beta \cdot t}{t} \right) \quad (5-6)$$

where

$f_c(t)$ = concrete strength at any concrete age t (psi)

f_c = concrete strength at 28 days (psi)

t = concrete age (days)

α = constant (days)

β = constant (unitless);

- A recommended form of the MC 2010 strength growth equation appropriate for use in the precast, prestressed industry is as follows:

$$f_{cm} = \frac{f_{cm}(t)}{\beta_{cc}(t)} \quad (5-7a)$$

with

$$\beta_{cc}(t) = \exp \left\{ s \cdot \left[1 - \left(\frac{28}{t} \right)^{0.5} \right] \right\} \quad (5-7b)$$

where

f_{cm} = the mean compressive strength at a temperature-adjusted time of 28 days (psi)

$f_{cm}(t)$ = the mean compressive strength at temperature-adjusted time t (psi)

$\beta_{cc}(t)$ = a function to describe strength development with time

s = coefficient which depends on the strength class of given cement

t = temperature-adjusted concrete age relative to 20°C. (days);

- Hofrichter recommended the use of Equation 5-6 in the absence of knowledge of curing temperatures and the use of Equations 5-7a and 5-7b when curing temperature information is known; and
- To accompany the above recommended strength prediction equations, Hofrichter (2014) provided updated values for the constants of Equations 5-6 and 5-7a and 5-7b for Type III accelerated-cured concretes as shown in Table 5-1.

Table 5-1: Recalibrated Constants for Strength Prediction Equations (Hofrichter 2014)

			Chronological Age	Equivalent Age
MC2010	Suggested based on Plant Data	s	NA	0.15
	Suggested by MC2010	s	NA	0.20
ACI 209	Suggested based on Plant Data	α (days)	0.34	NA
		β	0.99	NA
	Suggested by ACI 209	α (days)	0.70	NA
		β	0.98	NA

The findings of Hofrichter (2014) as summarized here are brief and aim only to provide the reader with the information necessary for understanding of subsequent sections of this report. Readers are encouraged to consult the complete work of Hofrichter (2014) for a comprehensive accounting of the strength growth analysis summarized here.

5.3 Current Overstrength Provisions in the Concrete Industry

The intent of this section is to review and explore existing available relationships to relate specified concrete compressive strength, f'_c , to expected concrete compressive strength, f_c^* for a given age. This section is applicable to the concrete industry as a whole and as such, any recommendations related to this section are not limited exclusively to the precast, prestressed concrete industry. Sections 5.7 and 5.8 discuss the applicability of these provisions to the precast, prestressed concrete industry in particular.

5.3.1 General Concept

By virtue of concrete production being a combination of tools, materials, methods, and people engaged in producing a measurable output, inherent statistical variability is expected and will always be present.

ACI 214 (2011) attributes the variability observed in measured concrete compressive strength to the following nine parameters: (1) variations in characteristics and proportions of ingredients, (2) changes in w/cm , (3) variations in concrete mixing, transporting, and sampling, (4) variations in placing and consolidation, (5) variations in concrete temperature and curing, (6) improper sampling procedures, (7) variations due to fabrication techniques, (8) differences in curing between sampled and in-place concrete, and (9) variations in sample testing procedures. These primary contributors to variability are defined more explicitly in Table 5-2.

Table 5-2: Principal Sources of Strength Variation Adapted from ACI 224R-11 (ACI Committee 214 2011)

Batch-to-batch variations	Within-batch variations
<p><i>Variations in characteristics and proportions of ingredients:</i></p> <ul style="list-style-type: none"> • Aggregates; • Cementitious materials, including pozzolans; and • Admixtures <p><i>Changes in w/cm caused by:</i></p> <ul style="list-style-type: none"> • Poor control of water; • Variation of aggregate stockpile moisture conditions; • Variable aggregate moisture measurements; and • Retempering. <p><i>Variations in mixing, transportation, and sampling:</i></p> <ul style="list-style-type: none"> • Mixing time and speed; • Distance between plant and placement; • Road conditions; and • Failure to obtain a representative sample from the batch <p><i>Variations in placing and consolidation:*</i></p> <ul style="list-style-type: none"> • Chute, pump, or buggy; • Internal or external vibration; and • Different operators <p><i>Variations in concrete temperature and curing:*</i></p> <ul style="list-style-type: none"> • Season; • Ambient humidity; • Wind speed 	<p><i>Improper sampling from the batch sample.</i></p> <p><i>Variations due to fabrication techniques:</i></p> <ul style="list-style-type: none"> • Substandard conditions; • Incorrect tools; • Poor quality, damaged or distorted molds; • Nonstandard molding and consolidation; and • Incorrect handling of fresh test samples. <p><i>Differences in curing:</i></p> <ul style="list-style-type: none"> • Delays in beginning initial curing; • Temperature variation; • Variable moisture control; • Nonstandard initial curing; • Delays in bringing cylinders to the laboratory; • Rough handling of cylinder in transport; and • Improper final curing. <p><i>Variations in sample testing</i></p> <ul style="list-style-type: none"> • Uncertified tester; • Specimen surface preparation; • Inadequate or uncalibrated testing equipment; • Nonstandard loading rate; and • Poor record keeping.

*Applies to in-place strength of the structure.

For a sufficiently large sample of tests for concrete compressive strength ($n \geq 30$), the sampling distribution (shown as a shaded histogram) approaches a Gaussian (normal) distribution as illustrated by Figure 5-4 (ACI Committee 214 2011). Cook (1982) contends that the assumption of a normal distribution

may not be correct for concrete compressive strengths exceeding 10,000 psi. However, Neville (2013) notes that the assumption of normality is conservative for high-strength concrete. This topic is explored further in Section 5.8 of this report.

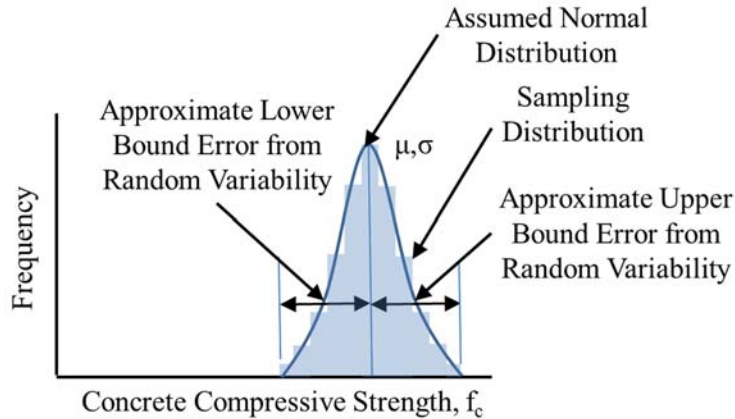


Figure 5-4: Gaussian Distribution of Sampled Concrete Compressive Strength

Any normal distribution can be described completely by a mean, μ , and a standard deviation, σ . For a normal distribution, approximately 68 percent of results fall within \pm one standard deviation of the mean and approximately 95 percent of the results fall within \pm two standard deviations of the mean, as illustrated in Figure 5-5 (ACI Committee 214 2011).

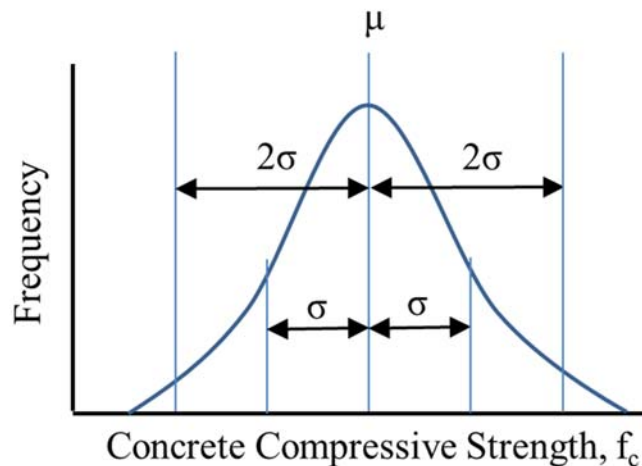


Figure 5-5: Relationship between Standard Deviation and Expected Data Spread

For this discussion, let us assume that given an engineer's specified concrete strength, f'_c , a concrete producer can proportion a mixture with a mean measured concrete strength, f_c , precisely matching the specified value. This case is illustrated graphically in Figure 5-6 (top). If this situation

occurred in a structure, it would be expected that approximately 50 percent of the concrete in the structure would have a strength falling below the specified strength, f'_c . A less extreme case is shown next in Figure 5-6 (middle). Here, the concrete producer arbitrarily targets a compressive strength 1.2 times the specified value. As evidenced by the reduced shaded area under the curve, the resulting structure would likely be safer than the first case (top) with a smaller proportion of concrete exhibiting insufficient strength. In the final case shown in Figure 5-6 (bottom), the concrete producer decides to target a compressive strength 1.7 times larger than the specified value hoping to ensure that all concrete within the final structure exceeds the specified concrete strength. While the probability of failure for the final case is indeed very low, it is still non-zero as a result of the probabilistic nature of random variables. In reality, the arbitrary proportions targeted above are code-dictated to promote a uniform level of minimum safety as is discussed further in Section 5.3.2.

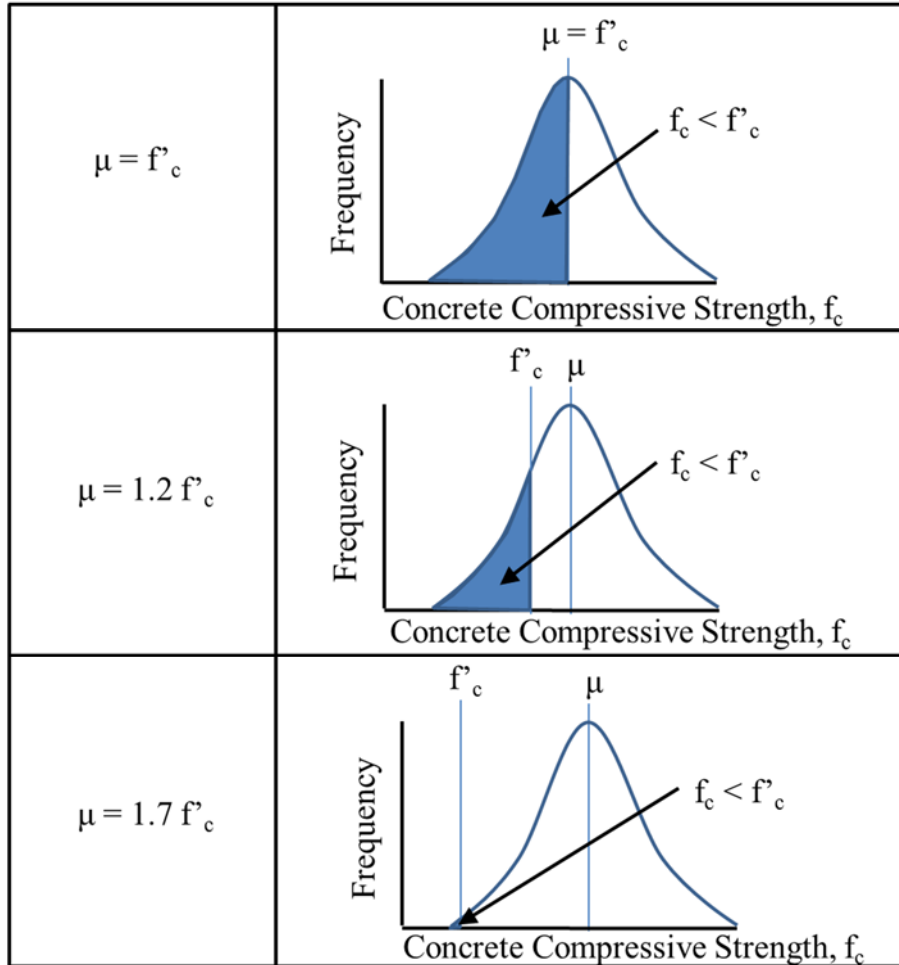


Figure 5-6: Concept of Probability of Failure

5.3.2 Measures of Variability

There are two main parameters suggested by ACI 214R-92 (ACI Committee 214 2011) to quantify the degree of dispersion of a normal distribution of sampled concrete strengths—the standard deviation and the coefficient of variation. The sample standard deviation for a series of concrete strength tests can be computed as follows:

$$s = \sqrt{\frac{\sum_{i=1}^n (X_i - \bar{X})^2}{n-1}} \quad (5-8)$$

where

n = the number of strength test results;

\bar{X} = the sample mean; and

X_i = the i th test result.

The coefficient of variation, also an indicator of the relative dispersion of a sampled distribution, is expressed as a percentage of the mean strength as follows:

$$V = \frac{s}{\bar{X}} \cdot 100 \quad (5-9)$$

where

s = the sample standard deviation; and

\bar{X} = the sample mean.

An obvious question regarding the above two metrics of variability is if one metric is more preferable than the other for use in the concrete community. This topic has been spiritedly debated in the literature for the last 35 years without clear consensus. ACI 214R-11 (ACI Committee 214 2011) allows the use of both standard deviation and coefficient of variation somewhat interchangeably, although Committee 214 supports the use of the coefficient of variation for comparisons of spread over a wide range of compressive strengths (in excess of 1,000 psi) and for overall variation of concrete strengths exceeding 5,000 psi. The recommendations of ACI Committee 214 are partly based on the work of Cook (1989) who concluded that the standard deviation approach may not be “a fair evaluation for higher strength concretes” and instead preferred the unitless coefficient of variation owing to the fact that it is less affected by the magnitude of the compressive strengths considered. Cook also concluded that for high-strength concretes, the coefficient of variation for varying concrete strengths tended to remain constant, while the standard deviation varied. In contrast, Neville (2013) points out that various laboratory studies have failed to consistently show that either the standard deviation or coefficient of variation remain constant for concretes of varying strength produced by the same facility and quality control practices. The common assumption, however, is that either standard deviation or the coefficient of variation remains constant for a given producer (regardless of strength level) as a product of control standards for concrete production. For varying mean target strength levels and varying constant standard deviations, the corresponding coefficient of variation is computed as shown in Figure 5-7.

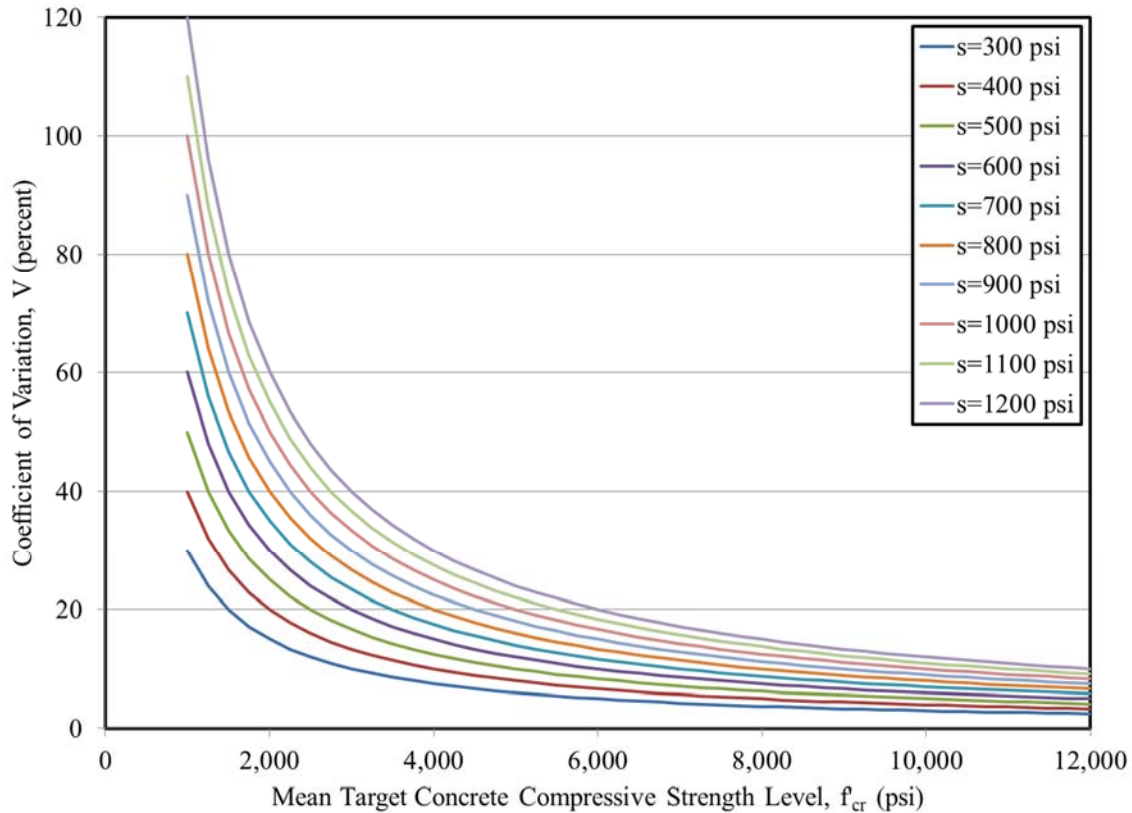


Figure 5-7: Relationship between Standard Deviation and Coefficient of Variation for Various Target Strength Levels

It can be seen that for concrete target strength levels exceeding approximately 6,000 psi, the computed coefficients of variation for various constant standard deviations tends to approach a horizontal line with a relatively small amount of vertical spread between curves. Therefore, for strength levels exceeding 6,000 psi, the choice to assume a constant variance (as promoted by Cook) or a constant standard deviation (as promoted by Neville) yields approximately identical results.

The use of a standard deviation approach offers a distinct advantage for the statistical analyses performed later in this chapter. If we recall the definition of the difference statistic, d_{stat} , from Section 5.2.2, this quantity represents the difference between the measured concrete strength, f'_c , and the specified concrete strength, f'_c , at a particular age. As previously discussed, for a concrete strength distribution of sufficient size, the probability distribution is expected to be approximately normal. This concept is reiterated in Figure 5-8 (top) for the hypothetical situation of the mean measured concrete strength precisely equaling the specified strength. In this example, a given concrete is prepared and

sampled 30 times, resulting in an assumed normal distribution with $\mu = 8,000$ psi and $\sigma = 400$ psi. Next, the difference statistic is computed and the distribution shown in Figure 5-8 (top right). As intuitively expected, computation of the difference statistic preserves the standard deviation of the initial distribution while shifting the mean. Next, the results of similar concrete trials are shown for two different strength mixtures in Figure 5-8 bottom. Here, each mixture is prepared and sampled 15 times for a total of 30 tests. In this example, it is assumed that the standard deviation is identical to that of the first example and remains 400 psi for each mixture. Notice that the height of each frequency curve is precisely half the height of the previous example, but the spread remains identical. By calculating the difference statistic for each of the two concrete mixtures and combining on the same plot by summing (Figure 5-8 bottom right), it is observed that the distribution of the difference statistic is again preserved at 400 psi.

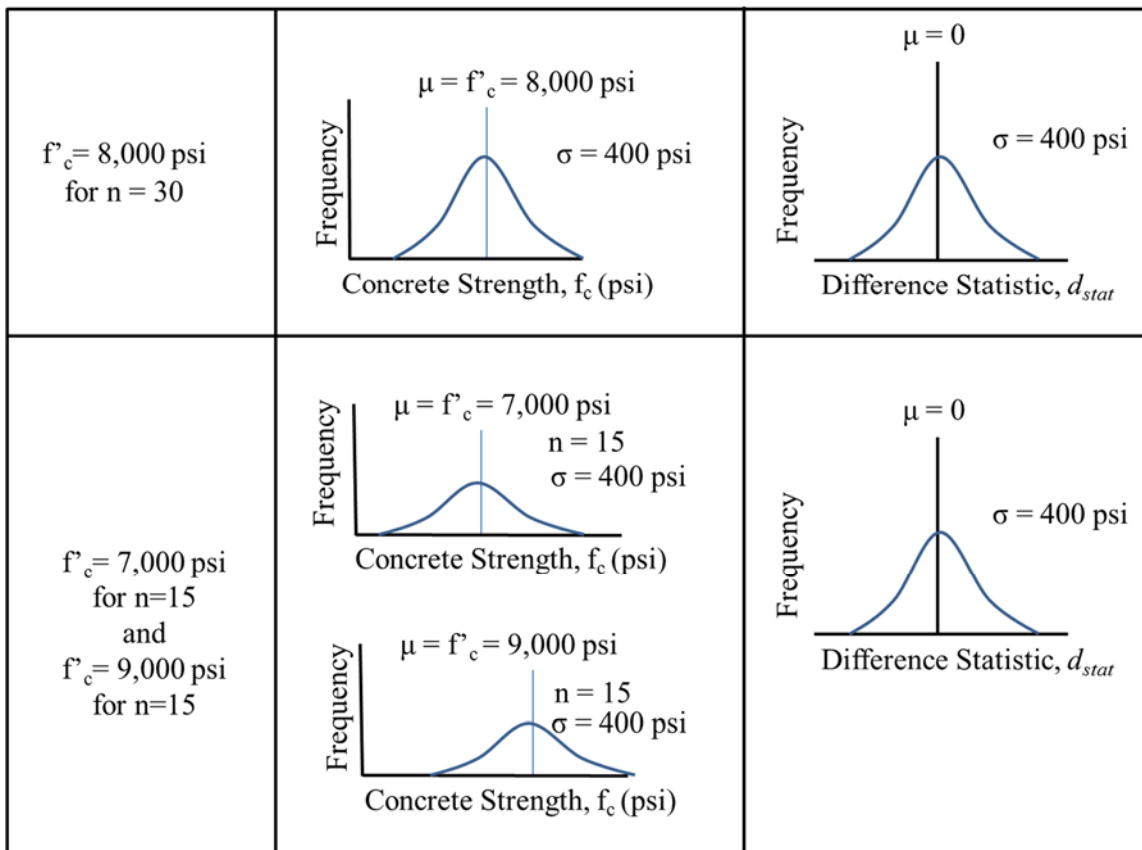


Figure 5-8: Concept of Preservation of Standard Deviation

The concept illustrated in Figure 5-8 was verified by performing statistical simulations with varying sample sizes, a varying number of constitutive mixtures, and varying distribution means. The concept can perhaps best be stated as follows:

For an assumed (or approximated) constant standard deviation value at all considered strength levels, the distribution of the difference statistic is identical regardless of the number of constitutive mixtures or the relative mean strength levels of each mixture.

The concept of preservation of standard deviation as summarized above does not equally apply to the coefficient of variance, V , due to the inclusion of the sample mean in the computation of this parameter. Statistical evidence of this concept is included in Mante (2016). The concept of preservation of standard deviation of the difference statistic is a convenient analysis tool used throughout the remainder of this chapter and is used to obtain a representative standard deviation from historical testing results (similar to Figure 5-8 bottom) that represents the standard deviation parameter (Figure 5-8 top) intended for use in existing published overstrength prediction equations.

ACI 363-R-11 *Report on High-Strength Concrete* (ACI Committee 363 2010), ACI 211.4-08 *Guide for Selecting Proportions for High-Strength Concretes Using Portland Cement and Other Cementitious Materials* (ACI Committee 211 2008), and ACI 301-10 *Specifications for Structural Concrete* (ACI Committee 301 2010) default to the use of a standard deviation to describe the spread of concrete compressive strength tests. Due to the (1) previously discussed similarities between standard deviation and coefficient of variation for concretes with compressive strength exceeding 6,000 psi, (2) the distinct analytical advantages offered by its use, and (3) the default of ACI guidance to its use, standard deviation is used as the preferred metric for describing dispersion in concrete strength testing results for the remainder of this report.

5.3.3 Relevant Design Code Provisions

As previously discussed, the relationship between the design engineer's specified concrete strength and the concrete producer's target strength is intrinsically related to the reliability and safety of a given building or structure. Accordingly, it is expected that design and building codes should dictate this relationship (based on an acceptable probability of failure) in order to ensure a minimum level of safety is preserved in all structures. This section reviews current design code provisions applicable to quantifying the relationship between specified design strength and expected strength or in-place mean strength. This discussion focuses on the provisions of ACI 318-14 (ACI Committee 318 2014) and the *fib* Model Code 2010 (fib 2010).

ACI 318-14 Section 26.4.3.1 summarizes the requirements for the proportioning of concrete mixtures for structural applications. In this section, it is required that a concrete mixture shall be proportioned either by the provisions of the *Specification for Structural Concrete* (ACI Committee 301 2010) or by some other method approved by the design engineer that preserves the minimum probability associated with the methods set forth in ACI 301⁷. ACI 318-14 also references the *Guide to Evaluation of Strength Test Results of Concrete* (ACI 214R-11) for further guidance on the probabilistic nature of this topic. The requirements for the ACI provisions regarding overstrength as outlined in ACI 301 are

1. For all concrete strengths ranges, the average of any three consecutive strength tests shall exceed the specified concrete strength, f'_c , 99% of the time. That is, failure to meet this criteria should not be anticipated more than 1 in 100 times;
2. For concrete strengths $\leq 5,000$ psi, on average no more than one percent of individual strength test results shall be permitted to fall below the specified strength, f'_c , by more than 500 psi; and
3. For concrete strengths $> 5,000$ psi, on average, no more than one percent of individual strength test results shall be permitted to fall below 90 percent of the specified strength, f'_c .

ACI 214R-11 offers two approaches to ensure that the above probabilistic requirements are satisfied. First, with sufficient knowledge of the variability typical for a specific concrete producer (based on historical test records), probabilistic equations may be used to compute the f'_{cr} as a function of f'_c . Equations for this purpose are summarized in Table 5-3 below, adapted from ACI 301-10. Equations 5-10a and 5-10c correspond to requirement one in the list above, Equation 5-10b corresponds to requirement two, and Equation 5-10d corresponds to requirement three.

Table 5-3: Required Average Compressive Strength, f'_{cr} , with Historical Data (Adapted from ACI 301-10)

f'_c (psi)	f'_{cr} (psi)	
	Use the larger of	
5,000 or less	$f'_{cr} = f'_c + 1.34s$	(Equation 5-10a)
	$f'_{cr} = f'_c + 2.33s - 500$	(Equation 5-10b)
Over 5,000	$f'_{cr} = f'_c + 1.34s$	(Equation 5-10c)
	$f'_{cr} = 0.9f'_c + 2.33s$	(Equation 5-10d)

⁷ The omission of the specific target strength provisions in ACI 318-14 is a departure from the previous ACI 318 building codes, which contained some of the information currently maintained in ACI 301.

The standard deviation, s , intended to be used in Equations 5-10 a through d is defined in ACI 214R-11 Section 5.2 as the sample standard deviation as computed by Equation 5-8 for a data set satisfying the following requirements:

- Historical strength testing records must reflect at least 30 tests (most commonly interpreted to mean at least 30 consecutive batches⁸ of concrete produced to meet a specified strength within 1,000 psi of the specified strength for the project at hand); and
- Historical concrete batches shall be similar in composition and production as those intended to be used for the project at hand;

ACI 214-R11 offers guidance on the interpretation of the standard deviation as computed according to the above requirements. In general, the standard deviation is regarded as a metric of the standard of control for a given concrete producer and represents the consistency of a producer's production and testing practices. A smaller standard deviation of strength testing results means there is less dispersion in the strength testing results and is generally correlated to better quality control during concrete production, placement, and testing. Various categories representing the standard of concrete control for general construction concrete applications are shown in Table 5-4.

Table 5-4: Standards of Concrete Control for General Construction (Adapted from ACI 214-R11)

Concrete Compressive Strength	Excellent	Very good	Good	Fair	Poor
$f'_c < 5,000$ psi	<i>Standard deviation for different control standards (psi)</i>				
	Below 400	400 to 500	500 to 600	600 to 700	Above 700
$f'_c \geq 5,000$ psi	<i>Coefficient of variation for different control standards (%)</i>				
	Below 7.0	7.0 to 9.0	9.0 to 11.0	11.0 to 14.0	Above 14.0
Strength level that above requirements are approximately equal (psi)	5,710	5,630	5,500	5,200	5,000

As shown and previously discussed, ACI 214-R11 prescribes the use of a standard deviation approach for compressive strengths below 5,000 psi and the use of a coefficient of variation for strengths exceeding 5,000 psi. For comparison between the two standards of concrete control, the strength level at which the provisions are equal is also shown in Table 5-4 (bottom). For example, at a concrete compressive

⁸ ACI 214R-11 allows for the computation of a sample standard deviation with fewer than 30 samples, but requires the use of a modification factor to account for increased uncertainty. This procedure was suggested by Philleo (1981).

strength of 5,710 psi, a coefficient of variation of 7.0 is approximately equal to a standard deviation of 400. In the absence of historical strength testing data, ACI 301-10 provides equations to directly compute the required concrete strength, f'_{cr} as summarized in Table 5-5.

Table 5-5: Required Average Compressive Strength, f'_{cr} , without Historical Data (Adapted from ACI 301-10)

f'_c (psi)	f'_{cr} (psi)
Less than 3,000	$f'_c + 1,000$ (Equation 5-11a)
3,000 to 5,000	$f'_c + 1,200$ (Equation 5-11b)
Over 5,000	$1.1f'_c + 700$ (Equation 5-11c)

It would appear that there must be an assumed level of variability implicit to the development of Equations 5-11. By systematically setting Equations 5-11a-c equal to Equations 5-10 a-d and solving for the implicit standard deviation at various strength levels, the results of Figure 5-9 can be computed. It is observed that for specified concrete compressive strengths less than 5,000 psi, an implicit value of $s = 730$ psi is assumed (corresponding to poor concrete control for general construction). For specified strength values exceeding 5,000 psi, s follows a linear trend with lower bound of $s = 730$ psi for $f'_c = 5,000$ psi and upper bound approaching $s = 1,330$ psi for $f'_c = 12,000$ psi. Accordingly, it can be concluded that when examining standard deviation as a metric of the dispersion of strength testing results, current ACI provisions include the implicit hypothesis that higher concrete strengths correlate to increased dispersion about the mean of strength testing results.

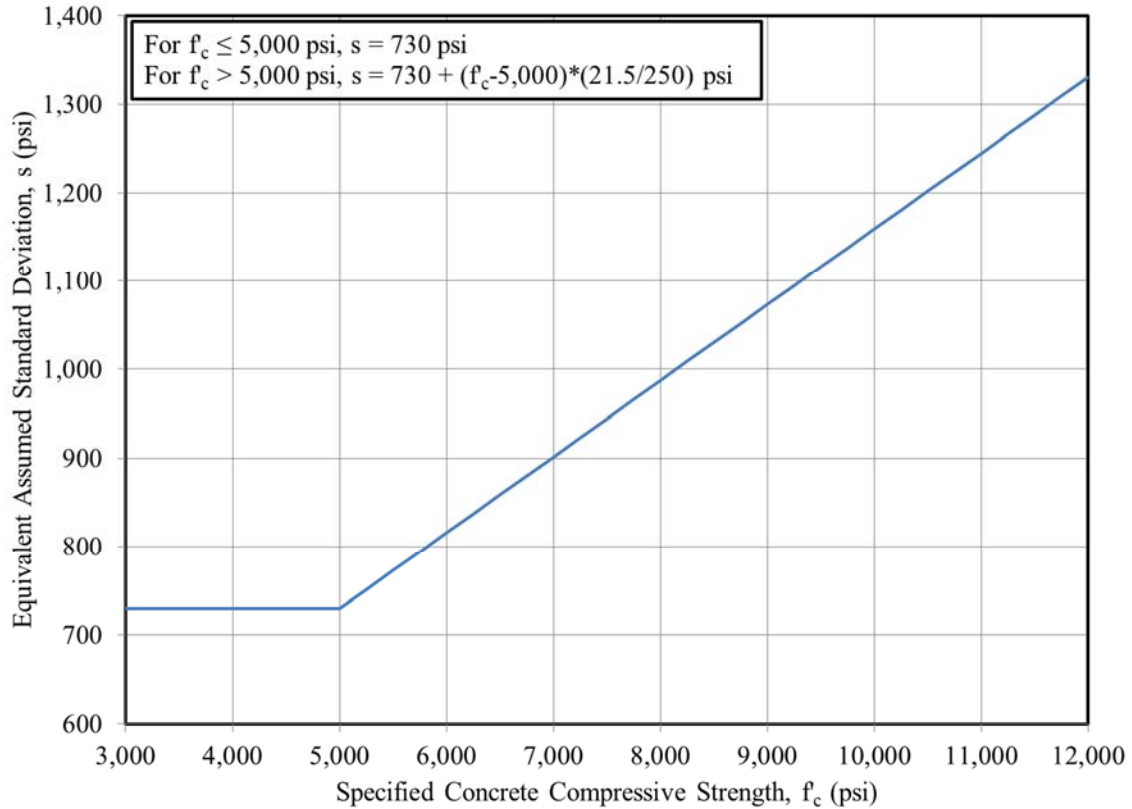


Figure 5-9: Implicit Standard Deviations for No Historical Data ACI Overstrength Provisions

The linear portion of Figure 5-9 affirms that current ACI provisions default to a coefficient of variation approach for specified concrete strengths exceeding 5,000 psi. A relative comparison of the provisions of Equations 5-10 a-d and 5-11 a-c is shown in Figure 5-10. As expected, Equations 5-11 a-c (denoted by “No Historical Data Available”) are verified to be conservative as compared to the lines of Equations 5-10 a-d (denoted by $s = \text{XXX psi}$), particularly for higher values of f'_c and the slope of the “No Historical Data Available” series exhibits a slight jog due to the use of coefficient of variation for strengths exceeding 5,000 psi as compared to the use of a constant standard deviation approach for all strength levels as discussed earlier in this section.

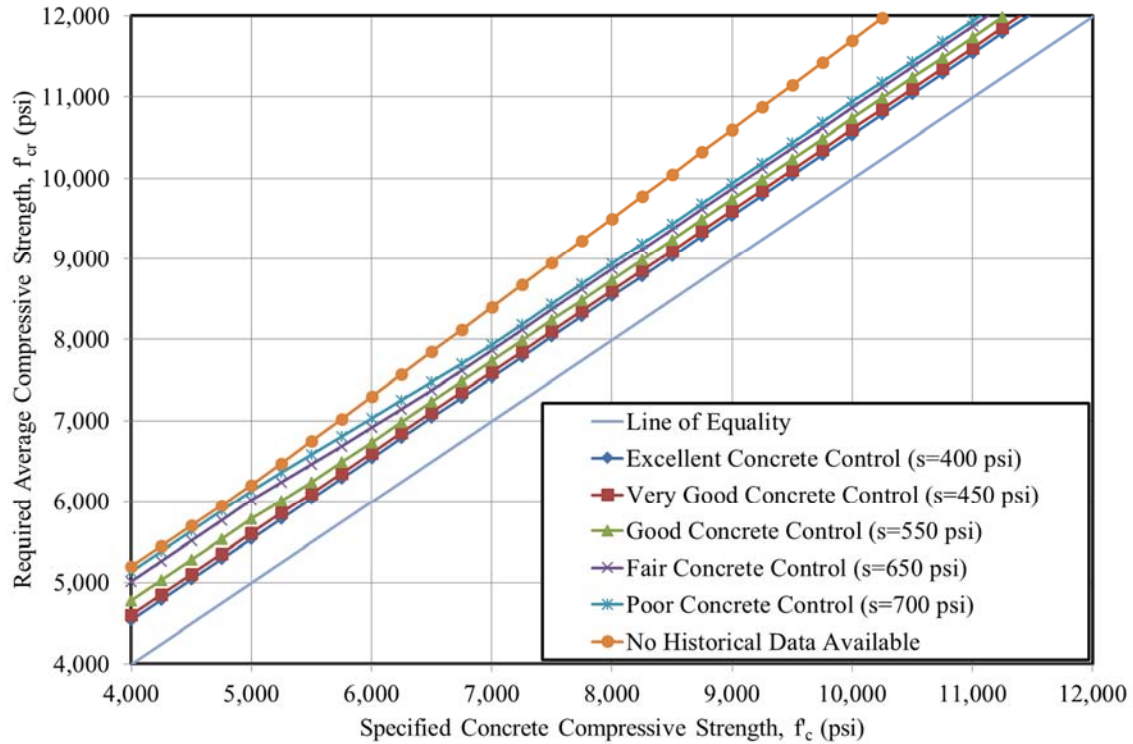


Figure 5-10: Comparison of Current ACI Overstrength Parameters

The *Model Code for Concrete Structures 2010* (fib 2010) contains provisions somewhat similar to those of the American Concrete Institute as reviewed above with a few marked differences. First, MC 2010 uses the term *characteristic compressive strength*, f_{ck} , in lieu of the ACI convention of specified concrete strength, f'_c . Both of these parameters are similar in that they represent a lower bound value of concrete strength, but represent different probabilities of failure for each code. In the Model Code, the characteristic strength, f_{ck} , is defined as the value below which 5 percent of all possible strength measurements are expected to fall (Muller et al. 2013) instead of the one percent probability of failure for three consecutive cylinders used in ACI 301-10 provisions. MC 2010 also includes an additional parameter, the mean compressive strength, f_{cm} , which represents the mean value of a sampled distribution of compressive strength tests. (This value is most similar to f'_{cr} in ACI terminology.) Muller et al. (2013) suggest the following relation between the characteristic strength, f_{ck} , and the mean compressive strength, f_{cm} :

$$f_{cm} = f_{ck} + 1.645 \cdot \sigma_s \quad (5-12)$$

where

σ_s = the standard deviation of the sample.

The 1.645 factor in Equation 5-12 is analogous to the 2.33 factor in the ACI equivalent equations of 5-10 b and d and is again derived from a Gaussian strength distribution. The MC 2010 code assumes a constant standard deviation of approximately 5 MPa (equal to 725 psi) regardless of strength level as is common practice in the European concrete industry (Muller et al. 2013). Substituting the assumed standard deviation value of 5 MPa into Equation 5-12 and rounding for simplicity gives the fib Model Code 2010 expression:

$$f_{cm} = f_{ck} + 8 \text{ MPa} \quad (5-13)$$

The predominant use of the overstrength provisions summarized above is for the proportioning of concrete mixtures to ensure that the code-prescribed level of life safety is achieved for strength limit states. For this life-safety application, it is essential that the standard deviation value used in specification equations must either accurately or else conservatively describe the distribution of strength tests of the produced concrete. The provisions above have been time-tested and repeatedly proven to provide satisfactory levels of safety for strength limit state design.

5.3.4 Regional Use of Overstrength in Serviceability Computation

Up to this point, the discussion on overstrength provisions has focused on relating the specified compressive strength, f'_c , to a target or required compressive strength, f'_{cr} in order to satisfy the probabilistic nature of the random variable concrete compressive strength. In order to extend this discussion further and to the main topic of this report, it is useful to recognize that the target or required compressive strength, f'_{cr} , at a given age is also equal to the best prediction of the expected compressive strength, f_c^* , at that age. Simply put, if a concrete mixture is proportioned to achieve a certain mean strength, f'_{cr} , at a given age, this mean strength is the value most reasonable to “expect” from a series of concrete strength tests performed at that age.

In general, serviceability computations are intended to provide the most accurate estimate or prediction of deflections and, therefore, do not use safety-related factors in computations. These

serviceability computations rely almost universally on a concrete modulus of elasticity value that is obtained from a correlation to the concrete compressive strength (as is explored in Chapter 6). Therefore, Model Code 2010 provisions suggest that the mean concrete strength, f_{cm} , be used in the computation of deflections instead of the characteristic strength, f_{ck} . The corollary to this Model Code provision in American design would be to recommend the use f'_{cr} or f_c^* in deflection computations for concrete structures in lieu of f'_c .

At the time of design, the f'_{cr} value cannot be precisely computed because the concrete producer and mixture proportions are not yet determined. However, even an imprecise estimate of the expected concrete strength, f_c^* , will yield a substantially more accurate serviceability computation than the use of the specified concrete strength, f'_c . An important distinction is necessary here—for strength or life-safety computations, the standard deviation must accurately or conservatively reflect the actual distribution of concrete strength tests for the given producer. However, for the purpose of serviceability computations, the accuracy of the standard deviation used to compute an expected value f_c^* is not as critical. Statistically speaking, even a relatively poor estimate of the expected value, f_c^* (incorrect by up to approximately 1.34 times the standard deviation) will still yield a more accurate estimation of the expected concrete strength than the incorrect usage of the specified strength, f'_c . Using the specified concrete strength in serviceability computations—as is currently done in U.S. practice, provides one of the *worst* possible estimations of expected mean concrete strength that is systematically and statistically an incorrect approximation.

A next logical discussion is the extent to which deflection computations might be improved if an expected concrete strength value, f_c^* , is used in lieu of the specified value, f'_c , in design computations. Although this topic is intrinsically related to multiple analyses and findings of this report, a brief discussion is offered here. The modulus of elasticity of concrete is typically correlated to the square root of the concrete compressive strength (ACI Committee 318 2014). Therefore, it seems logical to compare percent differences between the square root of the specified concrete strength and the square root of the

expected concrete strength computed according to ACI 301 provisions. This analysis is shown in Figure 5-11. It is evident that (1) the percent difference is greater for lower specified concrete strengths than for higher strengths, and (2) for the strength range considered, the percent difference ranges from 18 percent to 2 percent.

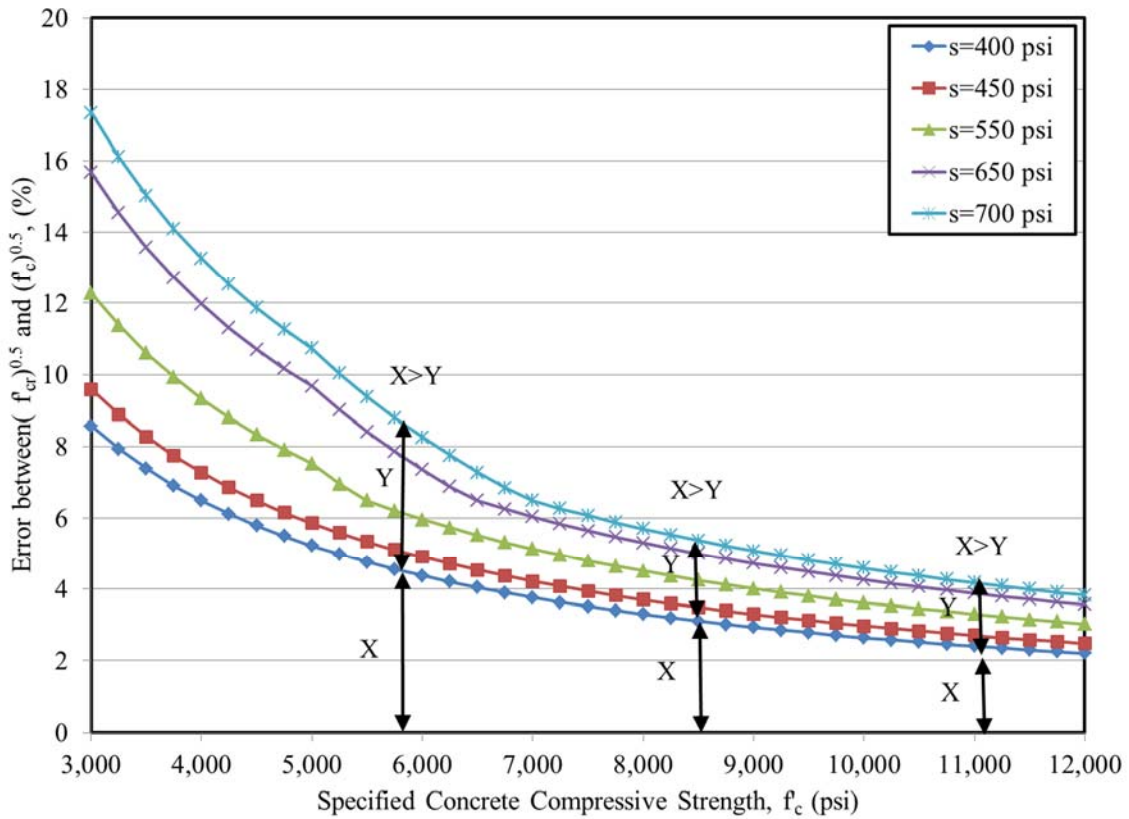


Figure 5-11: Percent Error in Square Root of Compressive Strengths

Notice in Figure 5-11 that two distances are denoted at various points along the plotted curves. The distance X represents the minimum percent difference for a given strength, while the distance Y represents the range of the percent differences at a given strength for a variety of practical standard deviation values. For strengths above approximately 6,000 psi, it is evident that $X > Y$, meaning that regardless of the accuracy of the standard deviation used to predict the mean strength (within a logical range), f'_{cr} , the percent error will be less than if the specified concrete strength were used in serviceability computations. Simply stated, any reasonable estimate of the standard deviation will cause a corresponding improvement in the accuracy of deflection computations for concrete strengths exceeding 6,000 psi.

Further discussion is contained in subsequent chapters of this report, but it is clear that the practice of using specified concrete strengths for serviceability computations is fundamentally flawed. While it is tempting to propose that all serviceability computations in American design should immediately adopt the practice of using an expected concrete strength, f_c^* , in design computations, this topic must be explored further in order to evaluate the effect of this potential recommendation on the concrete industry as a whole, specifically with regard to any previously empirically calibrated constants acting to modify either concrete compressive strength or concrete stiffness in existing design equations.

5.4 Overstrength in the Precast, Prestressed Concrete Industry

In contrast to the previous discussion that applied to the concrete industry as a whole, this section focuses solely on overstrength in the precast, prestressed industry. Included is a general discussion of the factors contributing to overstrength in the precast, prestress industry, a summary of previous work by others, and a discussion that examines the suitability of applying the overstrength provisions of Section 5.3 to the field of precast, prestressed concrete. It is important to note that while efforts to quantify overstrength at the time of prestress release are more relevant to the major objectives of this report, a limited discussion is also offered of efforts to quantify overstrength at the age of 28 days.

5.4.1 Overstrength at Prestress Release

At the time of the release of the prestressing force during girder fabrication, the concrete strength is required to have reached a specified concrete release strength, f'_{ci} . It is important to recognize that this requirement is primarily a serviceability requirement, owing to the fact that it is not directly tied to the life safety of the in-service structure. Accordingly, ACI 318-14 (ACI Committee 318 2014) includes specified values for maximum permissible stresses in prestressed members in Chapter 24: Serviceability Requirements. Here, the primary concern is ensuring that the concrete is strong enough, on average, to resist the internal stresses induced during prestress transfer without compromising the gross concrete section. A localized area with concrete strength falling slightly below f'_{ci} is not cause for concern because a failure of the concrete gross section remains unlikely. That being said, however, if the prestressing force was released at the precise moment when the girder concrete strength, f'_{ci} , were equal

to the specified strength, f'_{ci} , one would expect the concrete at approximately half of the critical locations within the girder to be of insufficient strength.

The primary causes of overstrength at prestress release include both those general factors contributing to variability previously discussed in Section 5.2 as well as a few additional factors unique to the precast, prestressed industry. Of the factors summarized in Section 5.2, it may be expected that certain factors will contribute to higher overall variation in the distribution of girder strength due to the large size and scale of precast, prestressed concrete plants. For example, one may expect more variability in concrete age, temperature, and curing conditions for a 150 ft long prestressed concrete girder placed over a three-hour period than would be expected for a smaller concrete placement taking place in a shorter time period with more consistent temperature control in place. In addition, there are two main factors unique to the precast, prestressed industry that are primary contributors to overstrength at prestress release—(1) the practice of using preapproved concrete mixtures and (2) the additional construction events required in the precast, prestressed industry as compared to cast-in-place concrete. As concluded in Section 4.4.1, the rigorous approval process for precast, prestress mixture designs encourages prestress producers to maintain a limited inventory of concrete mixtures suitable for a wide variety of projects. By making use of only a limited inventory of concrete mixtures, the expected concrete strength at prestress release, f_{ci}^* is not especially well matched to the specified release strength, f'_{ci} , but instead, errs on the conservative side and tends to provide a strength well in excess of f'_{ci} for many structures. Savvy prestress producers realize this and tend to either (1) capitalize on the reduced chronological time necessary to reach the specified release strength for lower strength designs or (2) subjectively adjust curing conditions (i.e. steam temperature or use of moist curing) as necessary to ensure the required release strength is met in a convenient chronological time period (most often 18 hours). A final cause of increased overstrength in the precast, prestressed industry is the increased variability in the distribution of concrete strengths caused by additional construction events contributing to a single final parameter. For instance, the standard deviations representing varying degrees of control for concrete previously discussed in Section 5.3.2 and shown in Table 5-4 (i.e. $s = 450$ psi for “very good”) are intended for concrete strength tests at a single chronological age (i.e. all test results for concretes

tested at 28 days). In the precast, prestressed industry, the testing of compressive strength at the time of release of the prestressing force does not adhere to a strict chronological time requirement. Instead, as shown in Figure 4-10, the distribution of the chronological age for concrete strength testing exhibits an approximately normal shape centered on an approximate age of 17.9 hours. This distinction is especially important due to the rapid strength gain occurring at prestress transfer as compared to 28 days after production. By adding in this additional source of variation, it is expected that the overall dispersion of strength testing results about the mean may increase for prestressed concrete as compared to a strictly single-age data set. Given the above discussion, it is reasonable to expect that a greater spread of strength testing results will likely be present at the time of prestress release in the precast, prestressed industry than may be expected in the general concrete industry¹⁰, and thus, higher amounts of *overstrength* may be observed in the precast, prestressed industry at prestress release.

Various previous researchers have conducted studies aimed at improving camber predictions in precast, prestressed concrete bridge girders and have similarly identified the importance of accurately predicting the expected concrete compressive strength at the time of prestress release during the girder design phase. Most typically, researchers perform a historical review of regionally available strength testing records and recommend a relationship between the specified concrete strength at release, f'_{ci} , and the expected concrete strength at release, f_{ci}^* . Conducting a study for MnDOT, French and O'Neill (2012) found that concrete cylinders exhibited an average strength 15.5 percent higher than the design release strength for that pour. Somewhat similarly, Storm et al. (2013) found that the average ratio of measured compressive strength to the specified strength at the time of prestress release was approximately 1.24 for girders produced for NCDOT. Rosa et al. (2007) suggested similar findings for WSDOT girders, finding that on average, the measured compressive strength at release was 10-11 percent higher than the specified release strength. Most recently, Nervig (2014) concluded that for IDOT bridge girders with specified release strengths between 4,500 and 5,500 psi, the measured value of compressive strength tended to exceed the specified value by approximately 39.5 percent; the specified

¹⁰ This trend is counter to the opinion that the increased quality-control practices in precast concrete production generally result in less variability in concrete as placed. While these practices likely do result in more consistent concrete delivered to the site (than in typical cast-in-place construction), the additional sources of variability discussed above likely outweigh any advantage gained by increased quality-control of concrete mixtures.

value was exceeded by 11.5 percent for specified concrete release strengths between 6,000 and 7,000 psi. The relatively large variability exhibited in the study results above seems to suggest that the research approach of conducting a historical review to determine a single indiscriminant overstrength multiplier may not be an ideal approach for quantifying overstrength due to its sensitivity to variations in regional practice or strength level.

The approach of this report research with respect to quantifying overstrength at the time of prestress release differs somewhat from previous efforts. While similar regressions of historical data to those detailed above are completed for the sake of comparison to previous work, the dominant approach employed in this report for predicting expected concrete strength at prestress release is a logical approach consistent with the concepts currently contained in by ACI 214R-11.

5.4.2 Overstrength at 28 Days

At the chronological age of 28 days after girder fabrication, the concrete compressive strength of a structural member is required to have reached a specified concrete strength, f'_c , prior to entering service. Unlike the concrete strength requirement at prestress release, this 28-day requirement is a strength limit state requirement. This section discusses the primary causes of overstrength at the chronological age of 28 days, previous research on this topic, and the research approach taken in this research study.

During the initial design of a precast, prestressed concrete girder, the design engineer must perform designs for both strength and serviceability limit states. While the primary serviceability limit state (allowable concrete stresses at prestress release) is evaluated using material properties from the time of prestress release, ultimate strength computations are performed using material properties at a chronological age of 28 days. In almost all cases, the serviceability limit state (strength at release) controls the proportioning of concrete for a given project (PCI 2011). More simply put, any concrete mixture that has the strength development characteristics capable of achieving the specified release strength, f'_{ci} , at 18 hours will typically hardly surpass the specified 28-day specified strength, f'_c (or more correctly any required 28-day strength, f'_{cr}), by the age of 28 days. This concept is primarily due to the fact that prestressed concrete producers aim to maximize productivity by minimizing the time

required to meet the specified concrete release strength. In doing so, producers can make maximum usage of a limited number of fabrication lines and steel formwork modules.

Given that the concrete strength at release is typically the controlling factor in mixture selection for precast, prestressed concrete products, it is most logical to “expect” the 28-day concrete strength to be that predicted in accordance with Equation 5-6.

$$f_c = f_c(t) \cdot \left(\frac{\alpha + \beta \cdot t}{t} \right) \quad (5-6)$$

Substituting a mean time to release of 0.75 days (18 hours) and using the recommendations of Hofrichter (2014) for constants α and β , Equation 5-6 simplifies to

$$f_c = f_{ci} \cdot 1.44 \quad (5-14)$$

The constant of Equation 5-14 can be interpreted to mean that for the precast, prestressed concretes typical of Hofrichter’s work, the 28-day strength is expected to be 1.44 times the release strength. In this way, the expected 28-day strength is dictated by a known controlling release strength and calibrated values of strength growth parameters (α and β).

Given the above discussion, it becomes evident that the magnitude of overstrength at 28 days is a function of two primary parameters—(1) the “expected” 28-day strength (which is a function of a known or expected release strength, f_{ci} , and calibrated growth parameters α and β), and (2) the choice by the design engineer of a specified 28-day strength, f'_c . This concept is shown more clearly in Figure 5-12 with the two primary parameters noted above shown in red. Notice that at the time of prestress release (0.75 days) there are two concrete strengths indicated—the specified release strength, f'_{ci} , and the measured release strength, f_{ci} . As expected, the measured value exceeds the specified value. The difference between these two values is shown on the plot (also called the difference statistic). Next, each of the two release values are extrapolated to 28 days, with the likely measured value denoted as f_c and the expected value based on the controlling specified release strength is denoted as f^*_c . Also pictured

are the choices of the specified 28-day strength by the design engineer, f'_c , and slightly amplified required value to satisfy the mixture design specification, f'_{cr} .

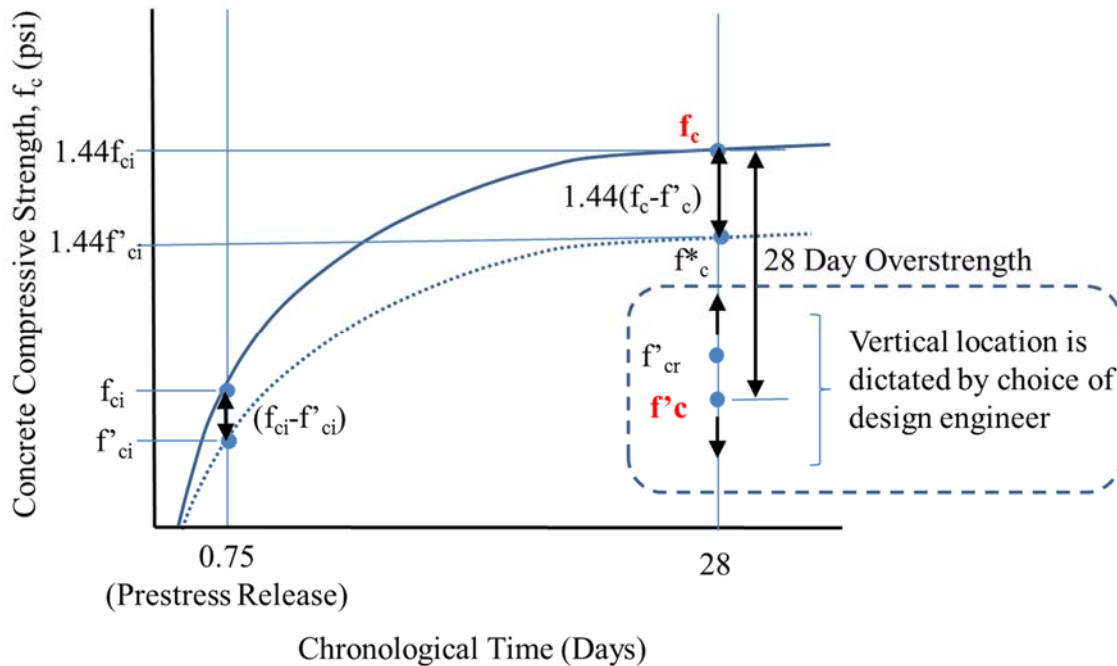


Figure 5-12: Concept of 28-Day Overstrength Derivation

The following conclusions can be drawn from the figure for the case of prestress release controlling concrete mixture proportioning (that is, $1.44 f_{ci} \geq f'_{cr}$):

- In the case that the design engineer specifies values precisely satisfying the ratio $f'_c / f'_{ci} = 1.44$, the magnitude of the overstrength (the difference statistic) at 28 days is expected to be approximately 1.44 times the difference statistic at prestress release;
- In the case that the design engineer specifies values resulting in the ratio $f'_c / f'_{ci} \leq 1.44$, the 28-day overstrength magnitude is expected to be substantially greater than 1.44 times the difference statistic at release; and

- In the case that the design engineer specifies values resulting in the ratio $f'_c/f'_{ci} > 1.44$, the 28-day overstrength is expected to be substantially smaller than 1.44 times the difference statistic at release.

The above general summary is expanded in later sections of this report, but is presented here to confirm that the magnitude of the 28-day overstrength present is not an independent parameter, but instead, is related to select parameters from the time of prestress release.

Given the above discussion, it is not surprising that the efforts of previous researchers to quantify overstrength at the age of 28 days have resulted in inconsistent conclusions. For instance, while Storm et al. (2013) found that the average ratio of measured compressive strength to the specified design strength at 28 days to be approximately 1.45, Rosa et al (2007) suggested that on average, the measured compressive strength at 28 days was 25 percent higher than the specified strength. This variability is likely due to the preference of design engineers in different regions to choose varying values of f'_c/f'_{ci} , thereby determining the degree of overstrength at 28 days.

5.4.3 Applicability of Existing Overstrength Provisions to Precast, Prestressed Industry

A final logical topic of the discussion regarding overstrength in the precast, prestressed concrete industry is to examine if the existing overstrength provisions of Section 5.3.2 are appropriate to apply to this industry. Without doubt, the concept of statistically adjusting the specified strength to some mean strength is a valuable tool presented by ACI 214-11. However, certain difficulties arise when one considers applying this concept to the precast, prestressed industry. Two of these key difficulties are summarized below.

1. Because release strength is a serviceability computation and not a strength limit state computation, it is not strictly *required* to apply the provisions of ACI 214-11 to concrete strength at prestress release. However, as discussed in Section 5.4.1, it seems proper to maintain some level of conservatism so that the likelihood of delay of prestress transfer is minimized and thus, the provisions of ACI 214-11 are an attractive option for consideration; and

2. The standards of control presented in ACI 214-11 (i.e. $s = 450$ psi for “very good”) are intended to describe the variability of strength testing results (and therefore also of concrete batch consistency) at a single age and do not account for the increased variability in strength testing results resulting from the varying chronological times to prestress release. Even if intentional trial batching is completed by a precast, prestressed producer, it will be difficult to capture the intrinsic variation in release timing, as this is often dictated by construction considerations, manpower availability, weather, etc.

Based on the above justification, the effectiveness of the provisions of ACI 214-11 for predicting overstrength in the precast, prestressed industry is evaluated in the remainder of this chapter. One should note that in order for this to be a feasible option, some alternative representation of the standard deviation, s , will need to be developed and recommended for use in the precast, prestressed industry.

5.5 Historical Data Set

As noted in Section 5.4, one of the most common approaches to explore the topic of overstrength in the precast, prestressed industry is to conduct a review of historical regional concrete strength testing records. During the course of this research effort, historical strength records representing nearly 5,000 precast, prestressed bridge girders were collected from 1,917 girder concrete placement events performed by four producers during the six-year period preceding 2013. While the work of Hofrichter (2014) thoroughly details the data gathering process, this report section provides a brief summary of the data set as applicable to subsequent analyses.

5.5.1 Historical Strength Data Set Description

The data set compiled by Hofrichter (2014) included a large number of parameters describing both the fresh and hardened properties of girder concretes and the timing of various construction activities. The findings of Hofrichter (2014) with regards to fresh concrete properties and average timing to prestress release were previously summarized in Chapter 4 of this report. For the purposes of the overstrength analyses contained in this chapter, Hofrichter’s complete data set is condensed to include only those parameters relevant to concrete strength. The format of the condensed database is shown in Table 5-6, with the complete data set provided in Mante (2016).

Table 5-6: Format of Condensed Raw Strength Data Set

Producer (A-D)	Specified Release Strength, f'_{ci} (psi)	Specified 28-Day Strength, f'_c (psi)	Measured Air Content (%)	Chronological Time to Prestress Release (days)	Average Measured Release Strength, f_{ci} (psi)	Average Measured 28-Day Strength, f_c (psi)
#	#	#	#	#	#	#

A logical first visualization of the raw data is a plot comparing the specified release strength, f'_{ci} to the measured release strength, f_{ci} as shown in Figure 5-13. It can be observed that the measured release strength exceeds the specified release strength in all cases as evidenced by all values being located above the line of equality. A similar comparison plot for the age of 28 days is shown in Figure 5-14.

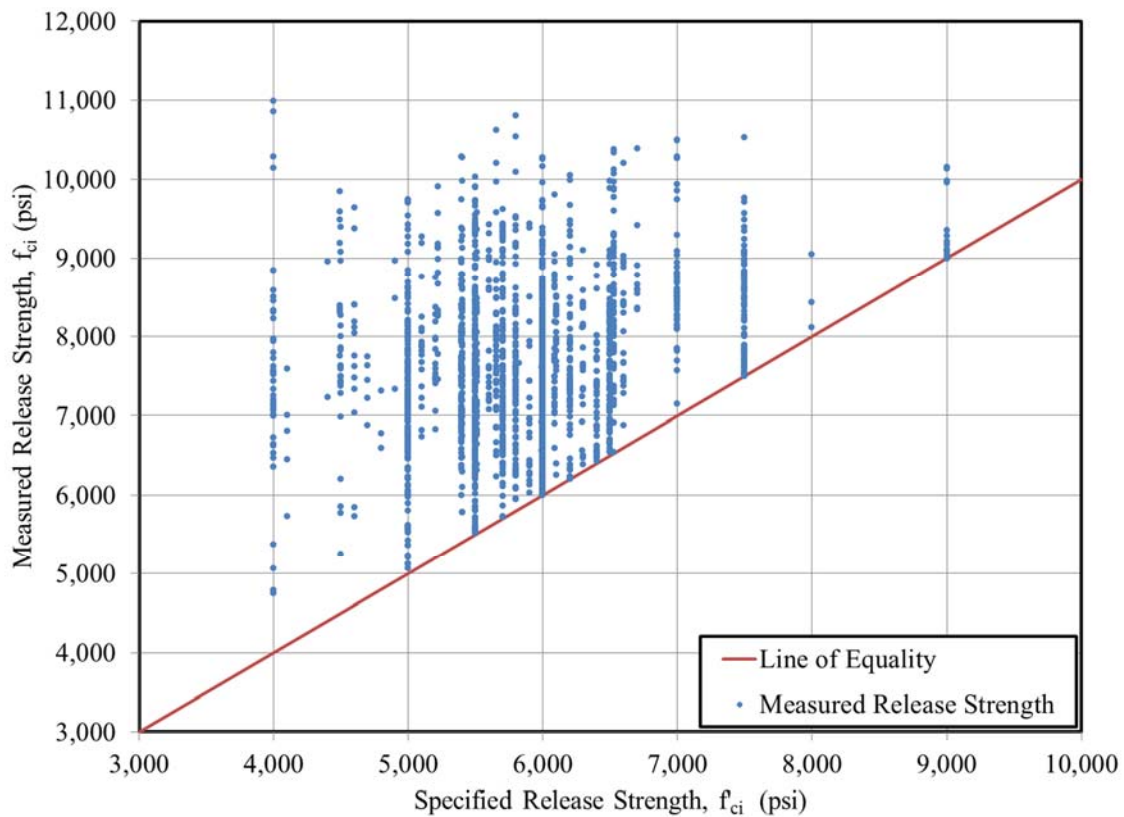


Figure 5-13: Comparison of Specified vs. Measured Release Strength for Historical Data Set

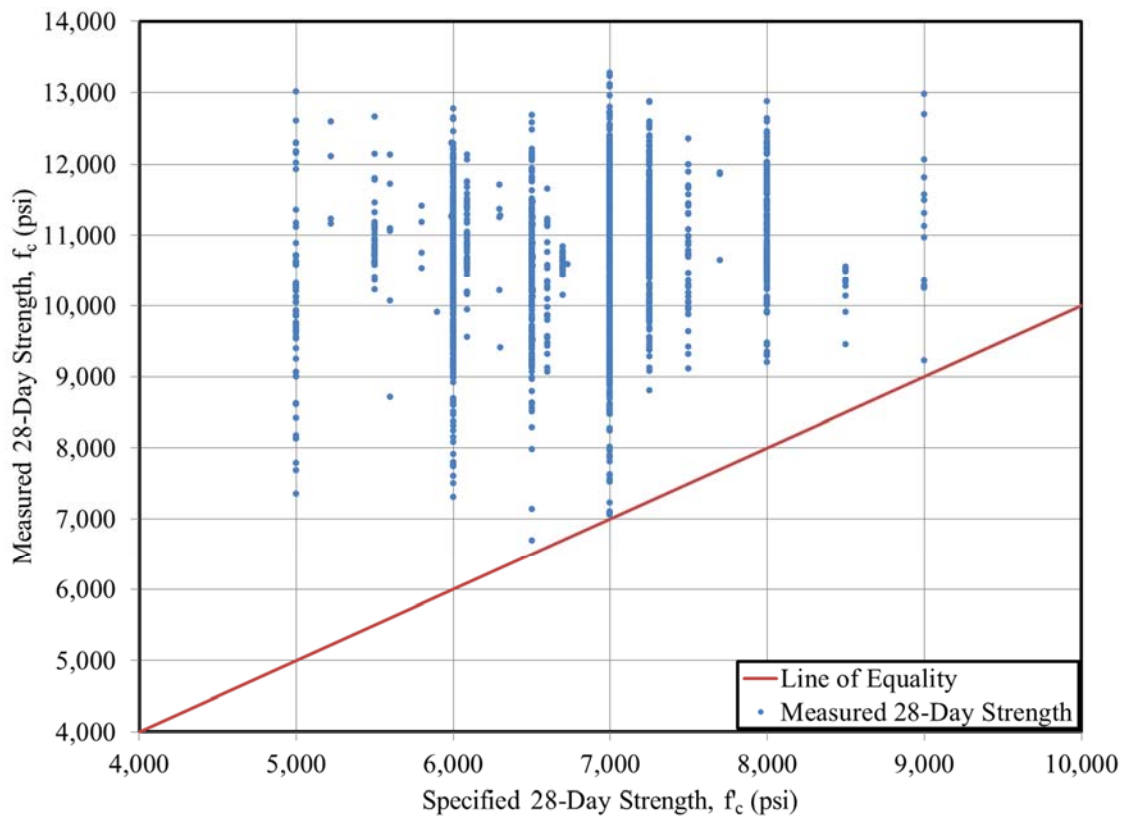


Figure 5-14: Comparison of Specified vs. Measured 28-Day Strength for Historical Data Set.

As demonstrated by the closer proximity of the data points to the line of equality in Figure 5-13 as compared to Figure 5-14, release strength requirements tend to control the selection of concrete mixture proportions in the precast, prestressed concrete industry. Figure 5-14 confirms this concept because the majority of data points fall well above the line of equality at 28 days.

Another logical visualization of the data set is to display the calculated value of overstrength in accordance with the nomenclature introduced in Section 5.2.2. Recall, overstrength at a given age is defined as the ratio of the measured strength to the specified strength and is denoted as OS_i , with the subscript denoting age. Computed overstrength ratios for the time of release and 28 days are shown in Figures 5-15 and 5-16, respectively.

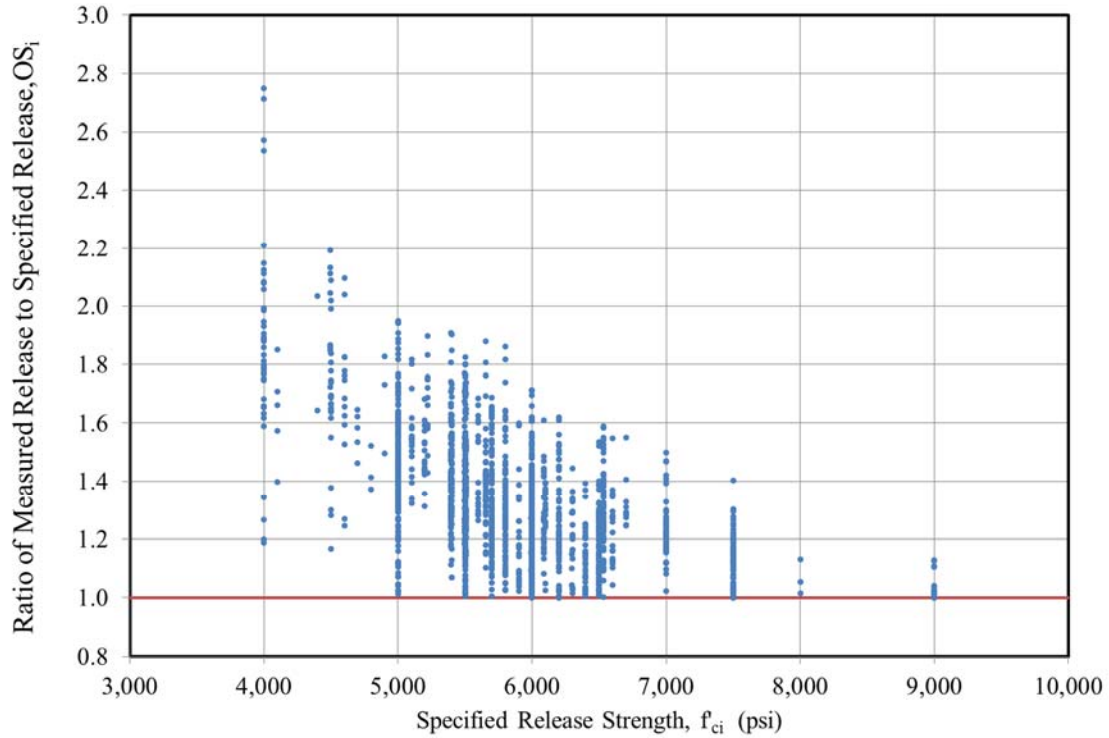


Figure 5-15: Overstrength Values at Prestress Release for the Historical Data Set

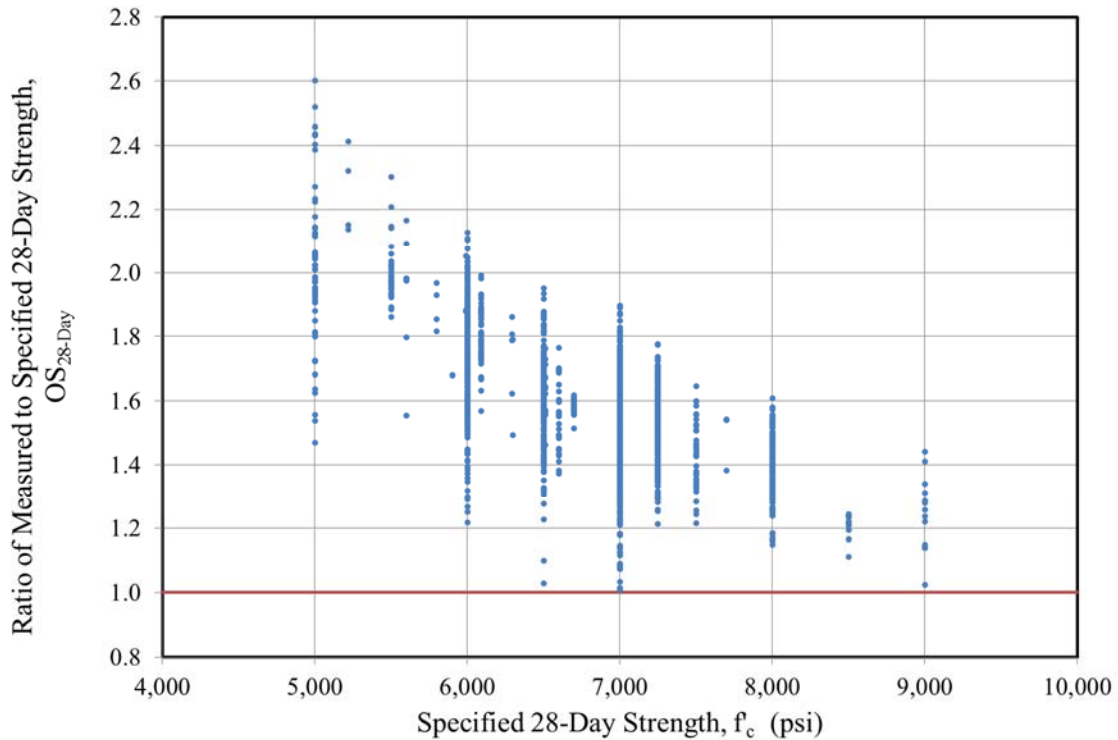


Figure 5-16: Overstrength Values at 28 Days for the Historical Data Set

As expected, all overstrength ratios exceed 1.0, meaning that the minimum strength requirements at both ages for all concrete placement events have been achieved. It is also interesting to note that the ratio of

overstrength for a given age tends to decrease with increasing specified strength requirements. Further visualizations and comprehensive analyses of the condensed data sets are presented in Sections 5.6 and 5.7 of this chapter.

5.5.2 Normalizing for Air Content

In the preliminary work of Hofrichter (2014), an effort was made to adjust the measured concrete strengths of the data set in accordance with the measured air content for each concrete placement event. Using the rule of thumb discussed in Section 5.2.1 (A one percent decrease in the air content of a given mixture corresponds to approximately a five percent increase in compressive strength), Hofrichter adjusted the values of measured compressive strengths to reflect those of a uniform target air content of 4.5 percent. This value was selected because it reflected the target air content from the ALDOT *Standard Specifications* (ALDOT 2012). In doing so, Hofrichter noted that the measured concrete strengths were generally adjusted downward because the mean air content of the full data set is 3.3 percent. The approach used by Hofrichter (2014), while successfully standardizing the air content of the data set, has the undesired consequence of artificially shifting the average air-content of the data set from 3.3 to 4.5 (and therefore, artificially shifting the mean compressive strength of the data set). The use of a target air content of 4.5 percent is undesirable in this case because it fails to account for the preference of the majority of concrete producers to target the bare minimum 2.5 percent air content by neglecting to use air-entraining admixtures (as discussed in Section 4.4.4). A more logical approach (as contained in this report) is to instead adjust measured strength values to a uniform target air content of the data set mean, 3.3 percent. In doing so, the artificial offsets of the data set mean air content and mean compressive strength noted by Hofrichter are avoided. The raw data set, as adjusted to a uniform target air content of 3.3 percent, is shown in Figures 5-17 and 5-18.

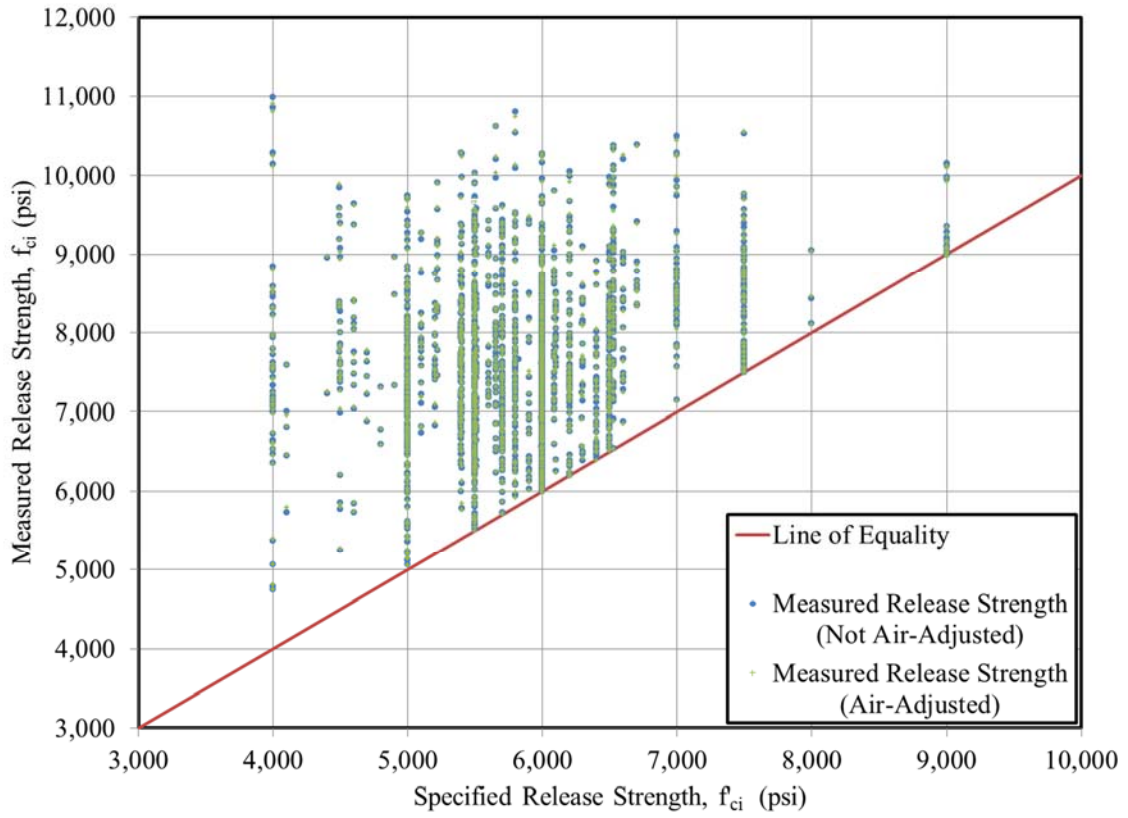


Figure 5-17: Comparison of Specified vs. Air Content Adjusted Measured Release Strength for Historical Data Set.

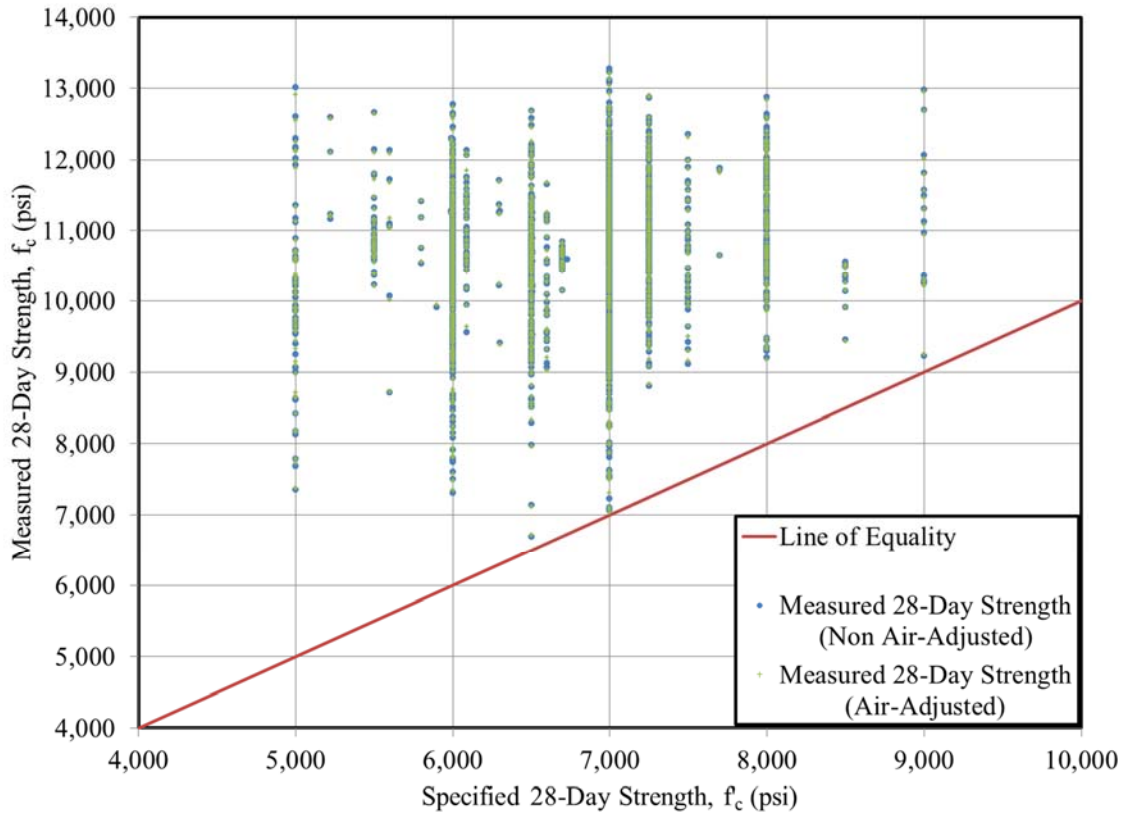


Figure 5-18: Comparison of Specified vs. Air Content Adjusted Measured 28-Day Strength for Historical Data Set.

Inclusion of the normalization for air content, performed in the manner discussed above, results in insignificant changes to the data set. The overall mean measured strengths of the nearly 1,900 data points remains unchanged and no significant changes in the dispersion of the data set (as evidenced by standard deviation) are evident¹¹. Accordingly, the data set used in the remainder of the analyses in this chapter is the raw data set without normalization for air content. This decision has the added benefit that the recommendations derived from the analyses of this data set intrinsically capture the anticipated small variations in air content likely to be observed in regional precast, prestressed plants.

¹¹ For the uncorrected data set, mean concrete compressive strengths of 7,660 psi and 10,600 psi and standard deviations of 980 psi and 986 were documented for release and 28 days, respectively. For air content corrected to 4.5 percent (Hofrichter's method), means of 7,200 psi and 9,950 psi and standard deviations of 910 psi and 910 were documented for release and 28 days, respectively. For air content corrected to 3.3 percent, means of 7,660 psi and 10,590 psi and standard deviations of 976 psi and 977 were documented for release and 28 days, respectively.

5.6 Predicting Expected Concrete Compressive Strength at Prestress Release

The primary goal of this section is to recommend a relationship that may be used at the time of girder design to more accurately predict the expected concrete compressive strength at prestress release, f_{ci}^* .

This report section begins by summarizing the analytical approach and criteria used to evaluate the goodness of fit for the various explored prediction models. Next, a logical mechanistic concept is hypothesized prior to its inclusion in subsequent prediction models. Finally, five major groupings of prediction models are explored and evaluated for their accuracy. Of these five groups of models, the first is purely empirical in nature, while the remaining four incorporate varying degrees of mechanistic concepts and existing design code provisions.

5.6.1 Analytical Approach

The general format of the analysis for predicting release strength as contained in this report is that various candidate prediction models are developed and evaluated against the measured concrete strength results of the condensed data set. The analytical approach is presented in an organizational chart as detailed in Figure 5-19.

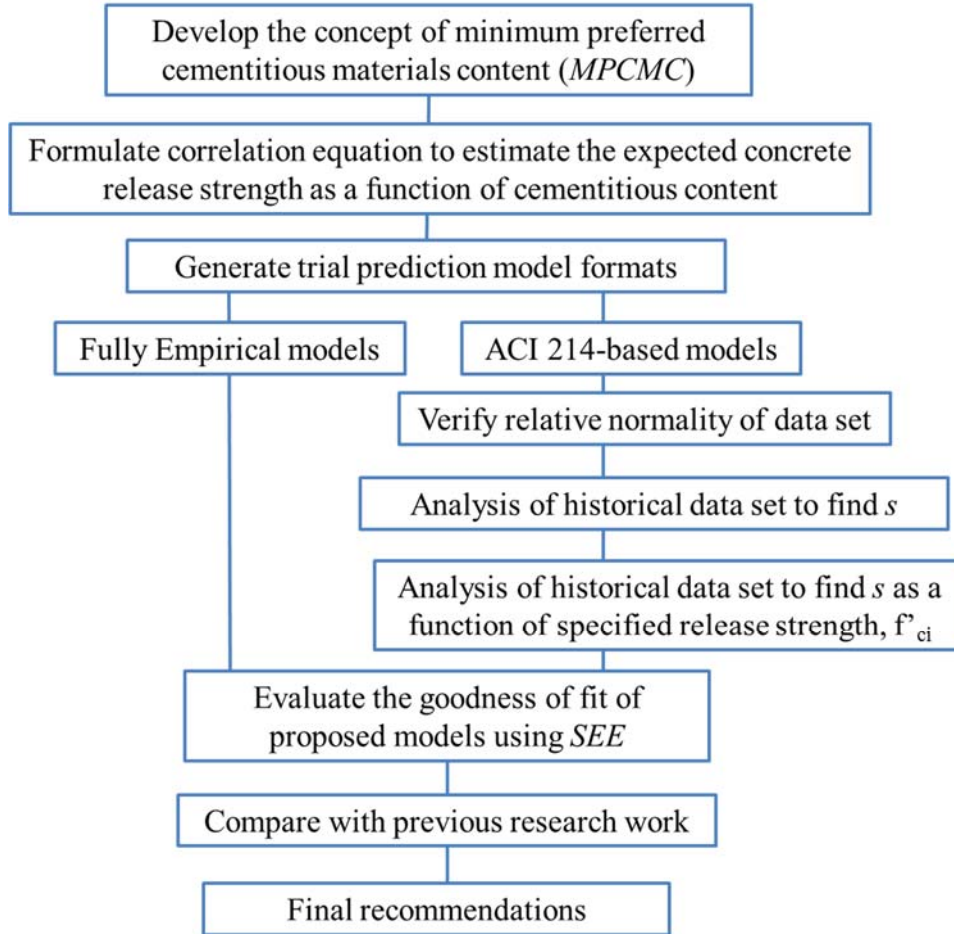


Figure 5-19: Analytical Approach of Release Strength Prediction Equation Development

First, the concept of a minimum preferred cementitious materials content (MPCMC) is developed and a correlated prediction equation is formulated. Next, the forms of various fully empirical models and semi-empirical models (those including the MPCMC concept) are selected by a combination of engineering judgment and the desire to maintain simplicity in recommended relationships. Next, using a GRG nonlinear solver, empirical and semi-empirical models are calibrated against the condensed data set by minimizing the standard error of the estimate, the *SEE*, denoted as follows (Vardeman and Jobe 2001):

$$SEE = \sqrt{\frac{\sum (f_c^* - f_c)^2}{N}} \quad (5-15)$$

where

f_c^* = the expected concrete compressive strength as predicted by a given model at a given age;

f_c = the measured concrete compressive strength at the corresponding age; and

N = the total number of data points the prediction model is being evaluated for.

For the code-based prediction models, the overstrength concepts of ACI 214-R11 (ACI Committee 214 2011) are used in conjunction with various sub-analyses aimed at quantifying typical measures of variability (in the form of a standard deviation) within the precast, prestressed industry. Finally, by comparing trial prediction models to each other and to previous work by others, a final relationship is recommended for use at the time of girder design to more accurately predict the expected concrete compressive strength at prestress release, f_{ci}^*

5.6.2 Concept of Minimum Preferred Cementitious Materials Content (MPMPC)

The PCI Bridge Design Manual (PCI 2011) notes that for concrete compressive strengths between 4.0 and 10.0 ksi, the total cementitious materials content typically varies between 600 and 1,000 pcy. Early in this research effort, it became evident that there existed a preference for precast, prestressed producers to use concrete mixtures with a high total cementitious materials content, often in excess of the content required to meet the governing specified strength for a given volume of mixing water. In discussions with girder producers, the research team learned that producers preferred targeting some minimum paste content in order to ensure a “creamy” mixture with sufficient workability and improved surface finish characteristics, as first documented by Hofrichter (2014). By maximizing workability and surface finish quality, labor costs associated with concrete placement and surface finishing are markedly reduced. The term, *minimum preferred cementitious materials content* (MPCMC) refers to the minimum content of cementitious materials that a producer tends to use, even if the strength provided by this cementitious content and the selected mixing water volume far exceeds the required specified strength. Although producers also rely on relatively high dosages of chemical admixtures to achieve sufficient workability, the preference to use a minimum cementitious materials content helps ensure that the paste volume is such that surface finish is improved (e.g. the potential for honeycombing is reduced) and the chemical admixtures are most effective in achieving the desired workability.

For the duration of the experimental portion of this project, the concept of a minimum preferred cementitious content remained a somewhat troublesome metric. While the MPCMC itself could be readily identified by either 1) asking a regional concrete producer or 2) conducting a statistical averaging of an

inventory of approved mixture designs, there did not exist a reliable method to correlate the MPCMC to a corresponding minimum expected concrete release strength, hereafter denoted $f_{c,\min}^*$ due to potential variations in the w/cm of different mixtures. Recognizing the need for this correlation, a conservative prediction equation was developed based on various ACI mixture proportioning guidance and the strength growth provisions of Hofrichter (2014).

Beginning with the ACI 211.4R-08: *Guide for Selecting Proportions of High-Strength Concrete Using Portland Cement and Other Cementitious Materials* (ACI Committee 211 2008), the expected mean concrete compressive strength at 28 days, f_c^* , can be predicted for typical plain cement mixtures with specific w/cm as shown in Table 5-7.

Table 5-7: Approximate Correlation between w/cm , Cementitious Materials Content, and Expected 28-Day Strength for Typical Concrete Mixtures (Adapted from ACI 211.4R-08 Table 6.5)

w/cm	Approximate cementitious materials content (pcy) for 285 pcy mixing water volume	Expected 28-day mean concrete compressive strength, f_c^* (psi)
0.45	633	7,000
0.40	713	8,000
0.35	814	9,000
0.31	919	10,000
0.27	1,056	11,000
0.25	1,140	12,000

Note: Values are for maximum-size coarse aggregate of $\frac{3}{4}$ in.

Using a first estimate of the mixing water volume of 285 pcy (in accordance with ACI 211.4R-08 for $\frac{3}{4}$ in. maximum-size aggregate [No. 67]), the approximate cementitious content can be computed as shown in the second column of Table 5-7. Next, the recommendations of Hofrichter (2014) may be used to relate the 28-day strength to the strength at the time of release using Equation 5-7 and corresponding calibrated coefficients. A finalized correlation between minimum preferred cementitious materials content (MPCMC) and an estimate of the minimum expected concrete release strength (also called the minimum mean concrete strength), $f_{ci,\min}^*$, are shown in Figure 5-20 with tabulated values superimposed at the lower right.

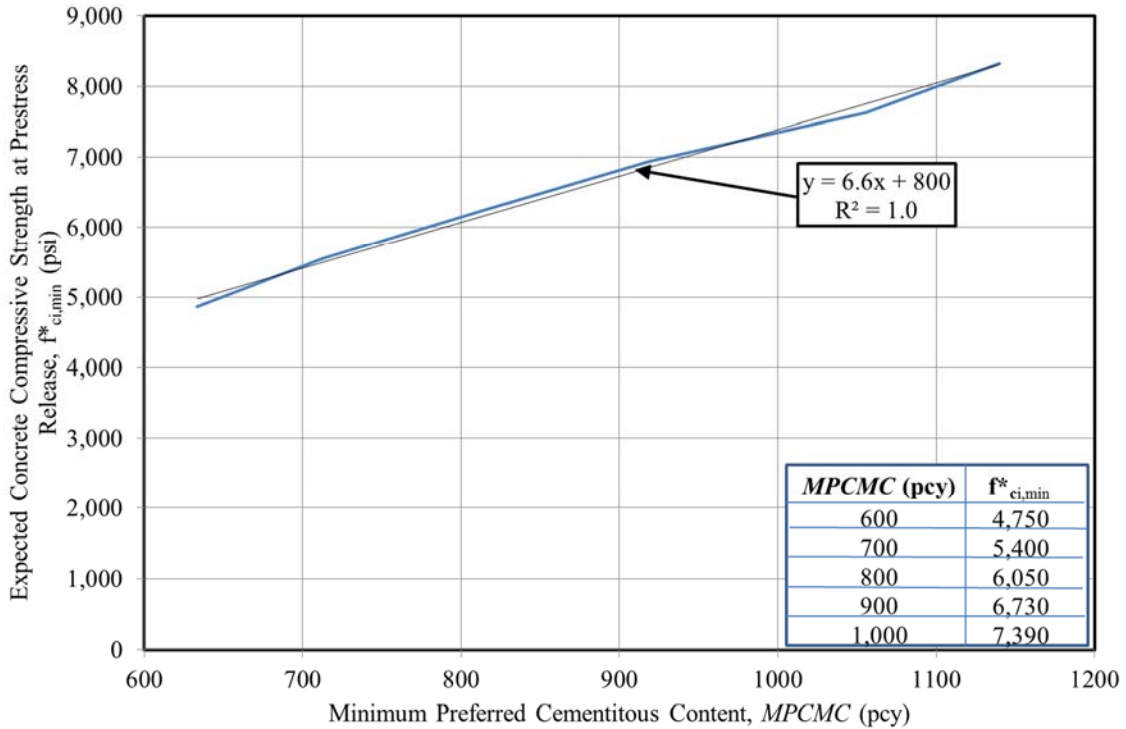


Figure 5-20: Correlation between MPCMC and Expected Concrete Compressive Strength at Prestress Release

For the state of Alabama, the average cementitious content for the sample approved mixtures in Section 4.4.3 is 881 pcy. Using the expression of Figure 5-20 that includes the implicit assumption of 285 pcy mixing water, this corresponds to an minimum expected concrete compressive strength at prestress release, $f_{ci,min}^*$, of approximately 6,600 psi.

The concept of a minimum preferred cementitious content, MPCMC, seems appropriate for the precast, prestressed industry and, therefore is incorporated into various trial models evaluated in subsequent sections of this report. In some cases, the value of $f_{ci,min}^*$ is determined by linear regression of experimental data (in the case of semi-empirical models), whereas in other trial cases, the ACI 211-based relationship of Figure 5-20 is used to systematically estimate the value of $f_{ci,min}^*$.

5.6.3 Simple Fully Empirical Models

The fit of purely empirical models to the condensed historical data set is completed primarily to allow valid comparisons to the work of previous researchers. Three primary prediction model formats were employed as shown below in Table 5-8.

Table 5-8: Simple Fully Empirical Model Description

Fully Empirical Model Designation	Format of Model (psi)	Description of Model	Calibration Constants
FE-1	$f_{ci}^* = a \cdot f'_{ci}$	Factor	$a = 1.30$
FE-2	$f_{ci}^* = b + f'_{ci}$	Offset	$b = 1,840$ psi
FE-3	$f_{ci}^* = a \cdot f'_{ci} + b$	Factor and Offset	$a = 0.34$ $b = 5,662$ psi

The format of FE-1 is deliberately similar to that used by French and O'Neil (2012), Storm et al. (2013), Rosa et al. (2007), and Nervig (2013). Each of these three models was calibrated by minimizing the *SEE* using a GRG nonlinear solver. The calibrated models for FE-1 through FE-3 are plotted in Figure 5-21, accompanied by the condensed data set.

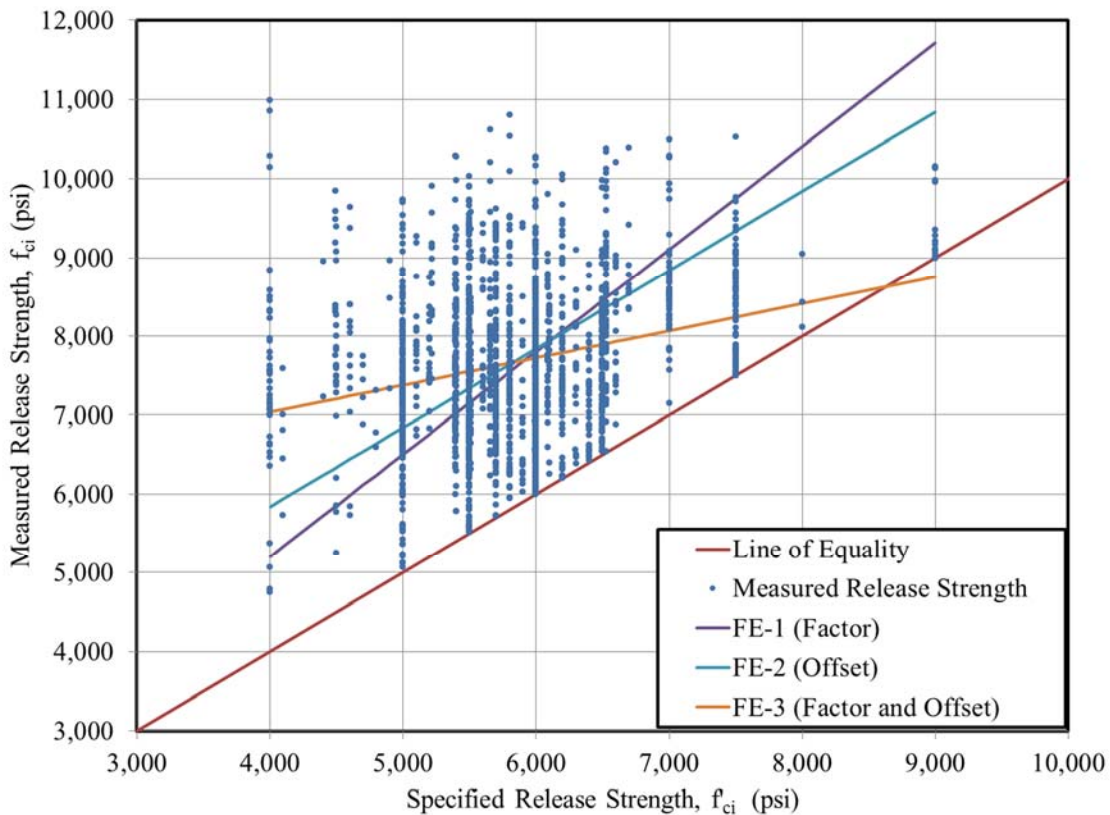


Figure 5-21: Calibrated Simple Fully Empirical Release Strength Prediction Models

The FE-1 and FE-2 model appear somewhat similar, although the FE-2 model tends to predict increased overstrength for higher specified release strengths. The fit of FE-3 is conceptually not desirable as it predicts insufficient strength for specified release strengths exceeding approximately 8,500 psi. For this reason, FE-3 is omitted from future comparisons between models. The single factor coefficient of 1.30 of

model FE-1 generally agrees with the range suggested by previous researchers of 1.15–1.40. Evaluation of the relative goodness-of-fit of each model to the historical data set is withheld until after development of all considered models in the following sections.

5.6.4 Piecewise Fully Empirical Models

The piecewise fully empirical fits were similar to the fully empirical simple models described above, except they also included the hypothesized concept of a minimum concrete strength fit to the historical data set. In order to completely define a model, the calibration of three constants was required as shown in Table 5-9. A GRG nonlinear solver was again used to calibrate the three constants against the historical data set. In this case, the algorithm minimized the error of the estimate by systematically varying combinations of the three variables until a minimum *SEE* value was obtained.

Table 5-9: Piecewise Fully Empirical Model Description

Fully Empirical Model Designation	Format of Model	Description of Model	Calibration Constants
FE-4	$f_{ci}^* = c$ when $f_{ci} \leq d$ $f_{ci}^* = b + f'_{ci}$ otherwise	Piecewise Constant and Offset	$c = 7,500$ psi $d = 6,100$ psi $b = 1,400$ psi
FE-5	$f_{ci}^* = c$ when $f_{ci} \leq d$ $f_{ci}^* = a \cdot f'_{ci}$ otherwise	Piecewise Constant and Factor	$c = 7,500$ psi $d = 6,300$ psi $a = 1.18$

The results of the calibration yielded piecewise continuous functions as plotted in Figure 5-22. Models FE-4 and FE-5 tended to predict similar results with an approximate minimum mean release strength of 7,500 psi (in contrast to the 6,600 psi estimate provided by the expression of Section 5.6.2).

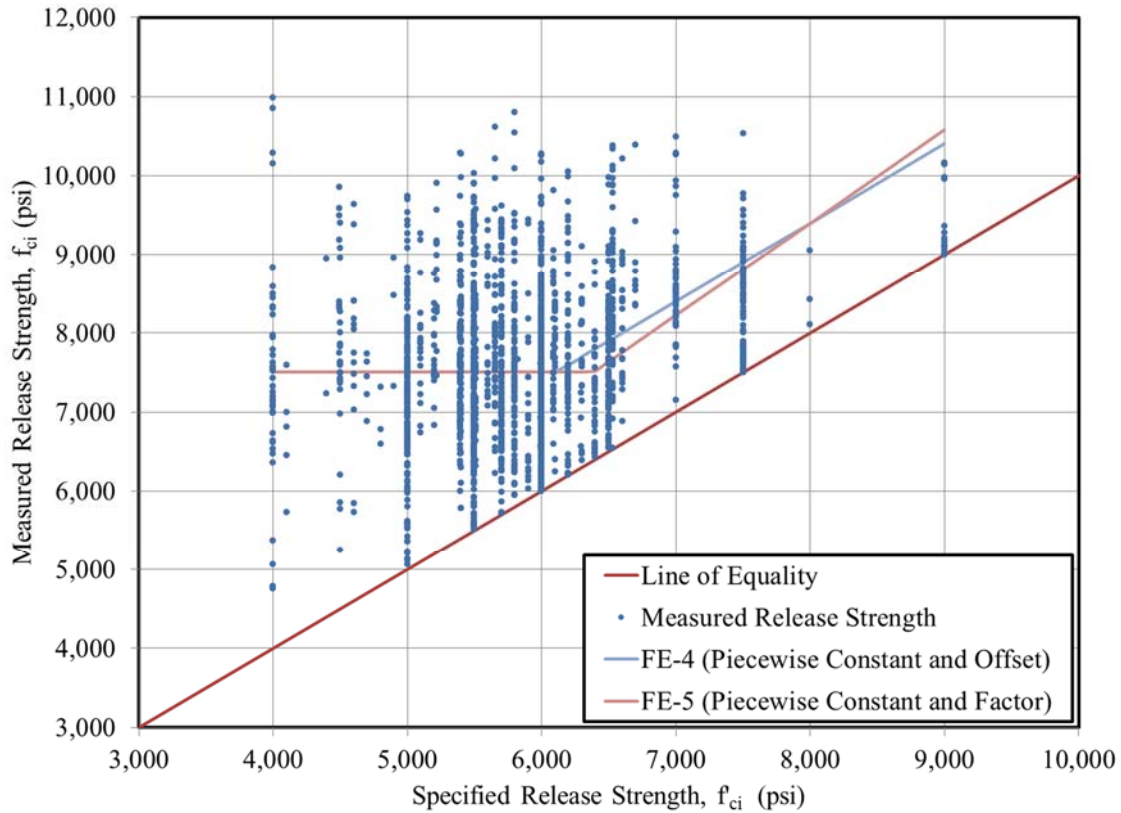


Figure 5-22: Calibrated Piecewise Fully Empirical Release Strength Prediction Models

5.6.5 Semi-Empirical Piecewise Data Fit with MPCMC Concept

In contrast to the fully empirical model development above, the use of a semi-empirical function to fit the data set was also explored. These semi-empirical models were similar to those of Section 5.6.4 in the linear empirical fit for higher strengths, but used the MPCMC prediction equation detailed in Section 5.6.2 to establish the minimum average strength, $f_{ci,min}^*$. The form of the two semi-empirical models, SE-1 and SE-2, and calibration constants are shown in Table 5-10 and plotted in Figure 5-23.

Table 5-10: Semi-Empirical Piecewise Model Description

Semi-Empirical Model Designation	Format of Model (psi)	Description of Model	Calibration Constants
SE-1	$\max(b + f'_{ci}, 6.6(MPCMC) + 800)$	Piecewise Constant and Offset	$b = 1,750$ psi $MPCMC = 881$ pcy (Alabama)
SE-2	$\max(a \cdot f'_{ci}, 6.6(MPCMC) + 800)$	Piecewise Constant and Factor	$a = 1.27$ $MPCMC = 881$ pcy (Alabama)

By forcing the SE model fits through a calculated *MPCMC* value (that is lower than the fully empirical mean minimum average), the tendency of the solver is to minimize the portion of the fit described by the horizontal line as shown in Figure 5-23.

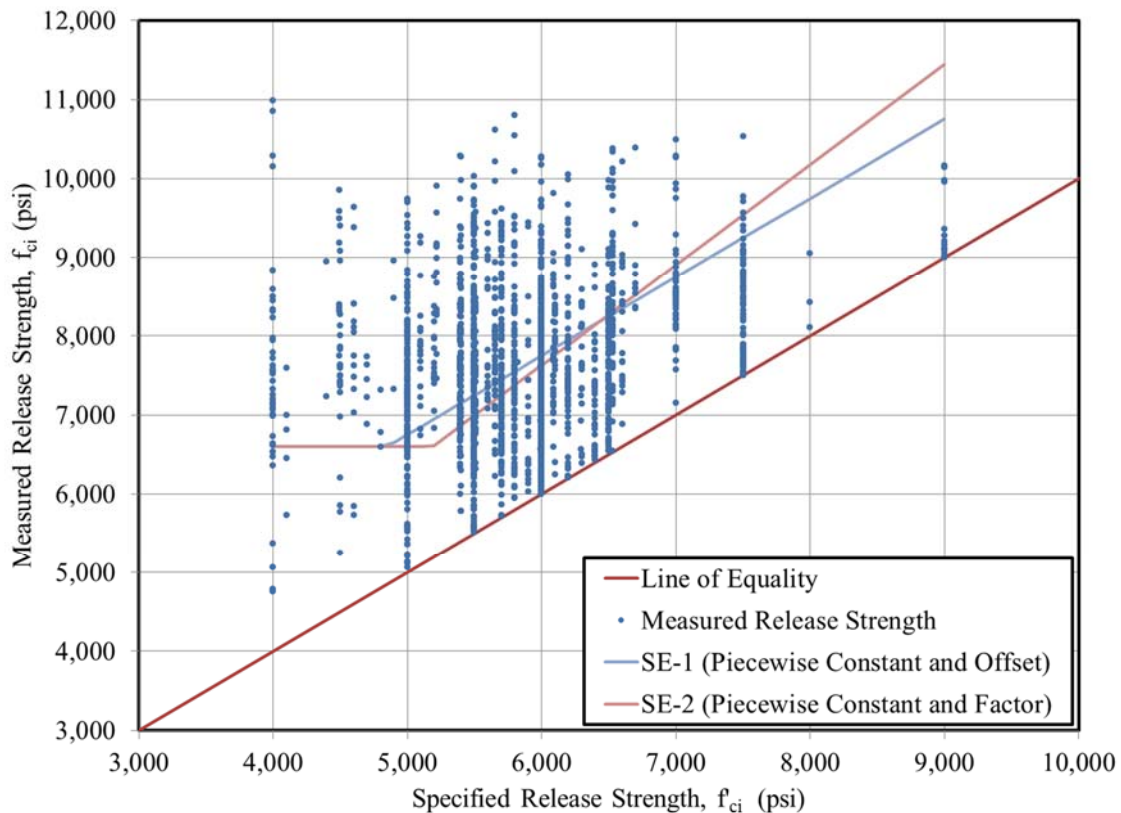


Figure 5-23: Calibrated Piecewise Semi-Empirical Release Strength Prediction Models

Overall, both models SE-1 and SE-2 yield similar results in the considered strength range, with the SE-2 model tending to predict higher strengths than the SE-1 model for specified concrete strength greater than approximately 6,500 psi.

5.6.6 ACI 214-Based Model (Constant s)

A more logical and universally applicable prediction model was desired than the fully empirical and semi-empirical fits previously developed. To achieve this goal, a prediction method based on the overstrength provisions of ACI 301 and ACI 224-R11 (detailed in Section 5.3.2) was explored. For the purposes of this discussion, ACI 301 overstrength provisions with historical data available are reproduced here in Table 5-11.

Table 5-11: Required Average Compressive Strength, f'_{cr} , with Historical Data (Adapted from ACI 301-10)

f'_c (psi)	f'_{cr} (psi)
	Use the larger of:
5,000 or less	$f'_{cr} = f'_c + 1.34s$
	$f'_{cr} = f'_c + 2.33s - 500$
Over 5,000	$f'_{cr} = f'_c + 1.34s$
	$f'_{cr} = 0.9f'_c + 2.33s$

Assuming that the target strength value, f'_{cr} is also the most likely concrete strength to expect, f_c^* , the use of the above provisions can be adapted to predict the expected strength as a function of specified strength. However, the issue remains of selecting or assuming an appropriate value of the standard deviation, s , for the precast, prestressed industry.

Recall, within the context of the ACI 301 and ACI 214 overstrength provisions, the standard deviation, s , is intended to be a function of the standard of control of a given concrete producer. A better standard of control by a producer corresponds to a narrower distribution of strength testing results about some target level, and, therefore, a smaller standard deviation, s . In the context of mixture proportioning, s is typically determined by considering a sample of at least 30 consecutive historical strength testing results all targeting a single concrete strength level. For the purposes of this report, it is advantageous to compute s using the large historical database generated as part of this research effort. For this purpose, a histogram was generated showing the frequency of occurrence for various ranges of measured release strengths, f_{ci} , in the historic data set as shown in Figure 5-24. The frequency distribution shown is relatively normal with a mean of 7,622 psi and a standard deviation of 967 psi.

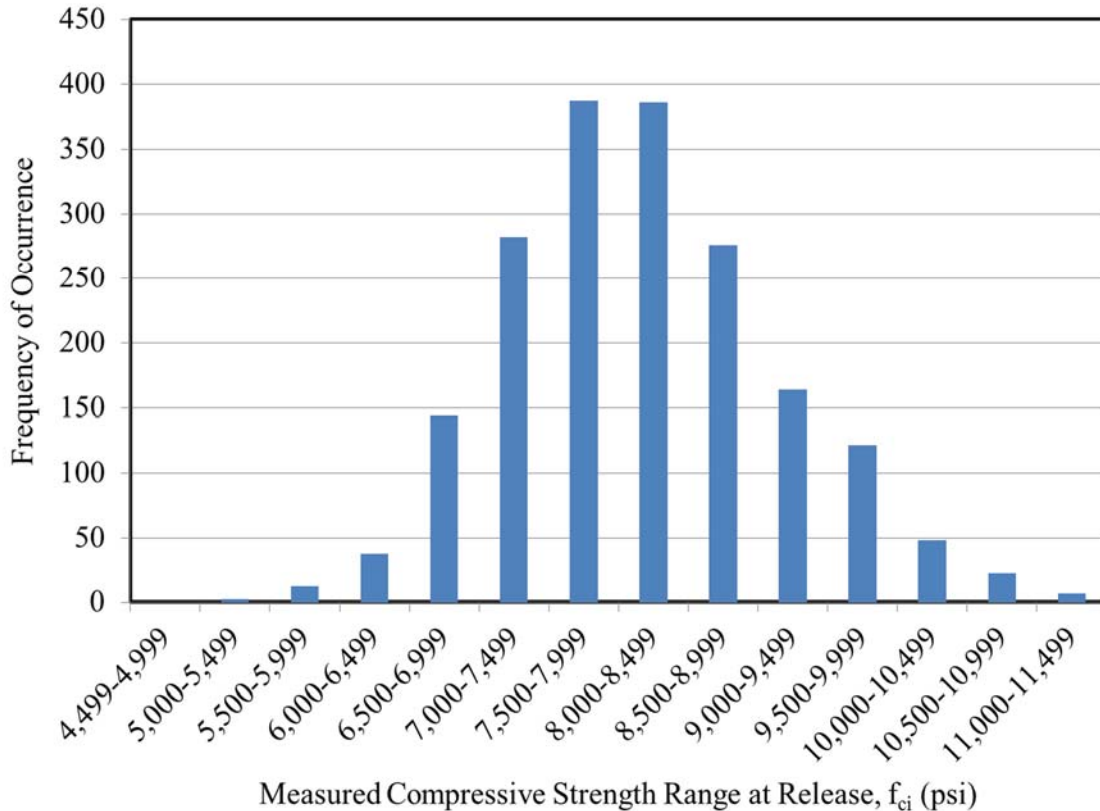


Figure 5-24: Frequency Histogram of Measured Release Strengths in Historical Data Set

While the standard deviation computed from the distribution pictured in Figure 5-24 does describe the general variability evidenced in *measured* concrete release strengths typical in Alabama for the previous 5 years, it is important to note that the historical strength testing results used to generate this distribution are not all for a single specified strength level. As such, it is difficult to differentiate between the portion of the variability attributed to a given typical producer’s standard of control and the portion of the variability due to differing target strengths of the historical data set. Accordingly, it is not appropriate to use the standard deviation representing the distribution of Figure 5-24 in an ACI 214-based models and instead, an alternate metric is required.

In order to determine an appropriate standard deviation, s , for use in an ACI 214-based model, the concept of the difference statistic, d_{stat} , is instead applied to the historical data set and a standard deviation of the difference statistic distribution computed accordingly. Recall, the difference statistic is a measure of the difference between the measured concrete strength and the strength level specified by the design engineer at a given time. Implicit to the use of this approach is the assumption that a single

typical standard deviation, s , is applicable regardless of varying concrete strength levels. The distribution of the difference statistic at prestress release for the combined historical data set representing four independent producers is shown in Figure 5-25.

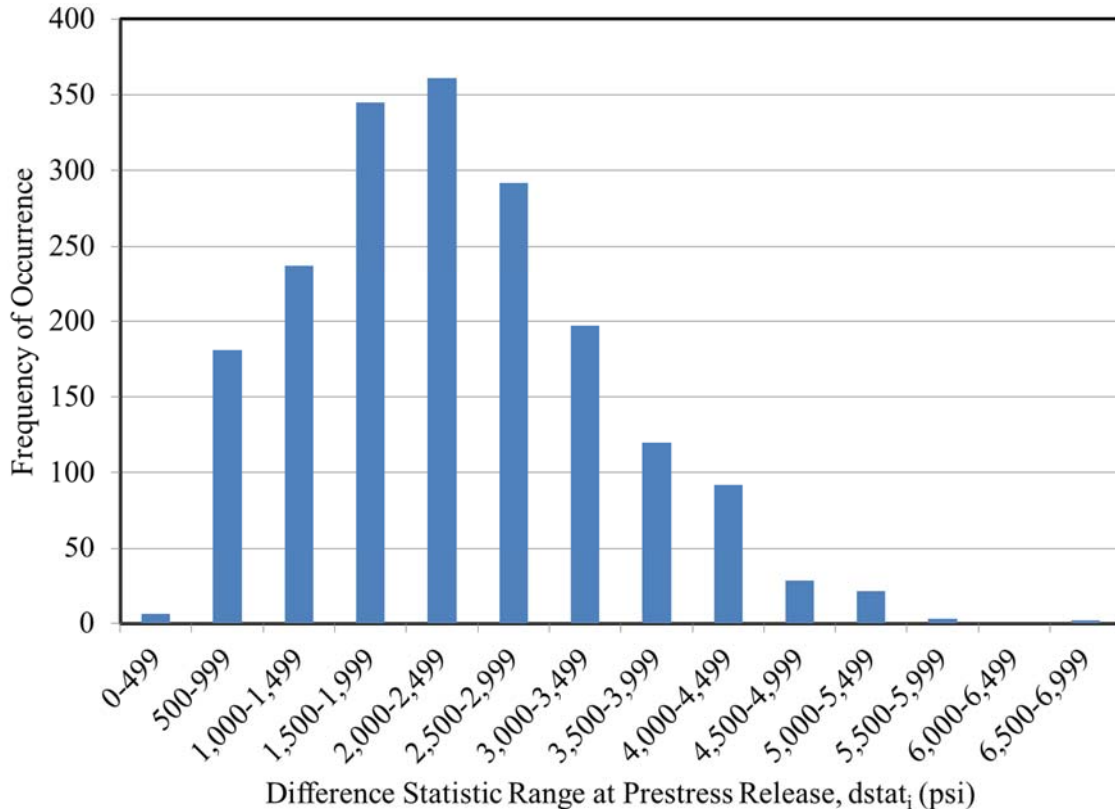


Figure 5-25: Frequency Histogram of Difference Statistic at Prestress Release in Historical Data Set

The standard deviation of the distribution of the difference statistic shown in Figure 5-25 is 1,063 psi. Relying on the concept of the preservation of standard deviation (as detailed in Section 5.3.1), it is evident that the standard deviation of 1,063 psi is a more appropriate metric to be used in conjunction with the ACI overstrength provisions than the previously discussed standard deviation of 967 psi.

To further validate and generalize the results of this section, it is desirable to examine the standard deviations of the difference statistic distributions independently for each of the four producers included in this research effort. If similar results are obtained independently from each plant, it may be possible to suggest a typical value of s appropriate for use by the precast, prestressed industry. The standard deviations of the difference statistic distribution for each plant are shown in Table 5-12.

Table 5-12: Standard Deviation of the Difference Statistic Distribution by Producer

Producer	Standard Deviation of the Difference Statistic Distribution, s (psi)		F-Test for Equal Variances Between Ages ($\alpha = 0.05$)	Curing Method
	Prestress Release	28 Days		
A	1,003	992	0.68 (True)	Steam
B	955	1,045	0.06 (True)	Steam
C	887	1,019	0.13 (True)	Steam
D	1,258	1,268	0.90 (True)	Moist
Full Data Set	1,063	1,132		

As shown, the standard deviations of the difference statistics appear quite similar for each of the four producers at the time of prestress release and at 28 days. Using an F-test to test for equivalent variances ($\alpha = 0.05$), it is shown that the distribution of the difference statistic for a given plant is not substantially different regardless of the age of consideration (as evidenced by F-test results greater than $\alpha = 0.05$). Next, a series of F-tests are used to evaluate the similarity of the variances among the four plants, with results shown in Table 5-13.

Table 5-13: Results of Statistical Analysis of Variances of the Difference Statistic among Plants

Combination	F-Test for Equal Variances At Prestress Release ($\alpha = 0.05$)	F-Test for Equal Variances At 28 Days ($\alpha = 0.05$)
A+B	0.23 (True)	0.18 (True)
A+C	0.09 (True)	0.61 (True)
A+D	<0.01 (False)	<0.01 (False)
B+C	0.35 (True)	0.76 (True)
B+D	<0.01 (False)	<0.01 (False)
C+D	<0.01 (False)	0.01 (False)

As shown, the variance of the difference statistic appears to be significantly different for Plant D, but similar for plants A, B, and C. A possible reason for this difference is that Plant D (which has since ceased operation) was the only plant included in the study without steam-curing capabilities. If the standard deviation of the difference statistic is computed for Plants A, B, and C only, values of $s = 1,039$ psi for prestress release and $s = 1,126$ psi for 28 days are obtained.

In accordance with the above analysis, the standard deviation value, s , used in the preliminary development of the ACI 214-based model (constant s) is rounded to the value of 1,050 psi. While this value does greatly exceed the typical range of standards of quality control recommended by ACI 214-R11 (between 400 and 700 psi) for conventional concrete work, it is not entirely unexpected based on the previous discussion of the unique causes of variability of concrete strength at the time of prestress

transfer in the precast, prestressed concrete industry (Section 5.4.1). Substituting the value of $s = 1,050$ psi into the equations of Table 5-11 and recognizing the controlling equation for each strength interval, the preliminary ACI 214-based model equations of Table 5-14 are derived and plotted in Figure 5-26.

Table 5-14: Preliminary ACI 214-Based Model (Constant $s = 1,050$ psi)

f'_{ci} (psi)	f_{ci}^* (psi)
5,000 or less	$f_{ci}^* = f'_{ci} + 1,950$
Over 5,000	$f_{ci}^* = 0.9f'_{ci} + 2,450$

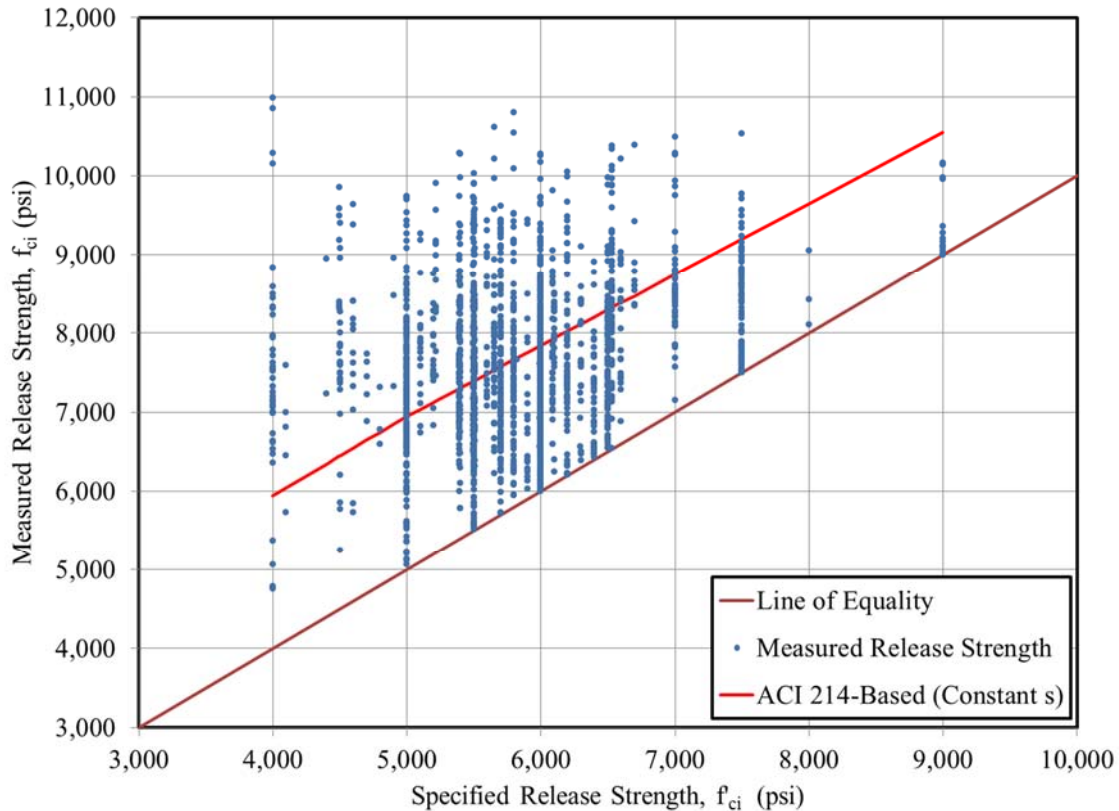


Figure 5-26: Preliminary ACI 214-Based Prediction Model (Constant $s = 1,050$ psi)

For an input value of $f'_{ci} = 5,000$ psi, both equations from Table 5-13 yield $f_{ci}^* = 6,950$ psi as shown in Figure 5-26.

5.6.7 ACI 214-Based Model (Constant s and MPCMC Concept)

In an attempt to improve the accuracy of the previous prediction model for lower specified concrete strengths, the MPCMC concept was incorporated into the previous model resulting in an ACI 214-based model with constant s and the MPCMC concept. The MPCMC prediction equation of Section 5.6.2 was

used to predict the minimum mean concrete strength, which was then extended to the point of intersection with the ACI 214-Based Model (Constant s) as shown in Figure 5-27.

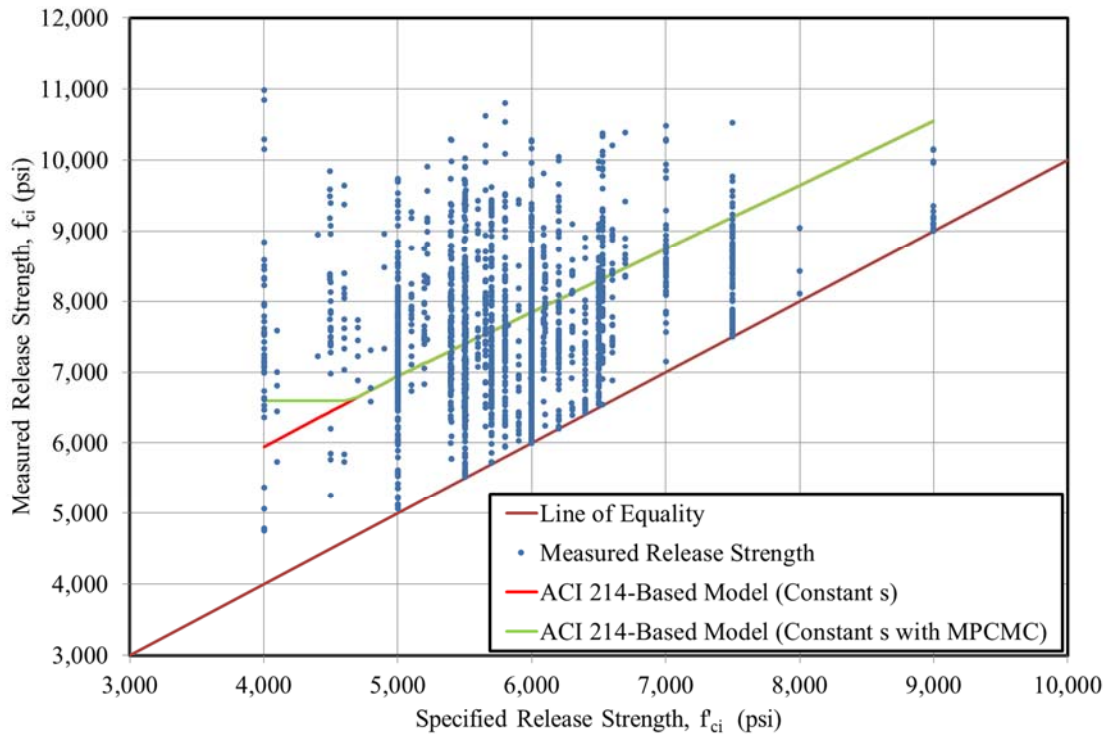


Figure 5-27: ACI 214-Based Prediction Model with MPCMC (Constant $s = 1,050$ psi)

5.6.8 ACI 214-Based Model (Variable s and MPCMC Concept)

In the previous ACI 214-based model, the implicit assumption was included that a single standard deviation representative of a typical producer standard of concrete control was appropriate for use at all specified strength levels. In the final model developed in this section, this assumption is further explored by allowing the standard deviation, s , to vary for different ranges of specified release strengths, f'_{ci} . The d_{stat} is still used in this analysis, but on a more limited level than in previous analyses. Previously, the d_{stat} was used to normalize the difference between specified and actual strength into a single distribution representing the full range of specified strengths. In this analysis, the difference statistic is used on individual subsets of historical data corresponding to a range of specified strengths within 500 psi of each other.

For this analysis, the historical strength data was divided by specified release strength, f'_{ci} , into eight data subsets each representing a range of specified release strengths of 500 psi. The difference

statistic was then computed for each data point within each subset at the time of prestress release and at 28 days. For each subset, statistical descriptive parameters including means and standard deviations were computed as shown in Table 5-15.

Table 5-15: Analysis of Standard Deviation by Specified Release Strength Subsets

f _c Range (psi)	n	Prestress Release		28 Days		F-Test for Equal Variances at both ages (α =0.05)	Pooled Standard Deviation (psi)
		Mean of the Difference Statistic Distribution (psi)	Standard Deviation of Difference Statistic Distribution (psi)	Mean of the Difference Statistic Distribution (psi)	Standard Deviation of Difference Statistic Distribution (psi)		
4,000- 4,499	55	3,585	1,312	5,050	1,452	0.23 (True)	1,384
4,500- 4,999	49	2,984	953	4,555	1,123	0.13 (True)	1,042
5,000- 5,499	402	2,313	920	4,504	915	0.45 (True)	918
5,500- 5,999	509	1,888	1,014	3,840	1,047	0.23 (True)	1,031
6,000- 6,499	553	1,482	856	3,514	1,077	<0.01 (False)	972
6,500- 6,999	179	1,522	887	3,772	884	0.48 (True)	886
7,000- 7,499	43	1,643	723	3,365	679	0.34 (True)	702
7,500- 7,999	79	869	667	2,795	695	0.36 (True)	681

It is interesting to note that there appears to be a decreasing mean value of the difference statistic distribution for increasing specified strengths at both prestress release and at 28 days. Furthermore, F-tests ($\alpha=0.05$) confirm that with the exception of one subset, the subset variances at prestress release and at 28 days are not substantially different. Accordingly, it is appropriate to compute a pooled standard deviation, a single parameter representing the distribution of the difference statistic for a given subset. Much of the data from Table 5-15 is shown graphically in Figure 5-28.

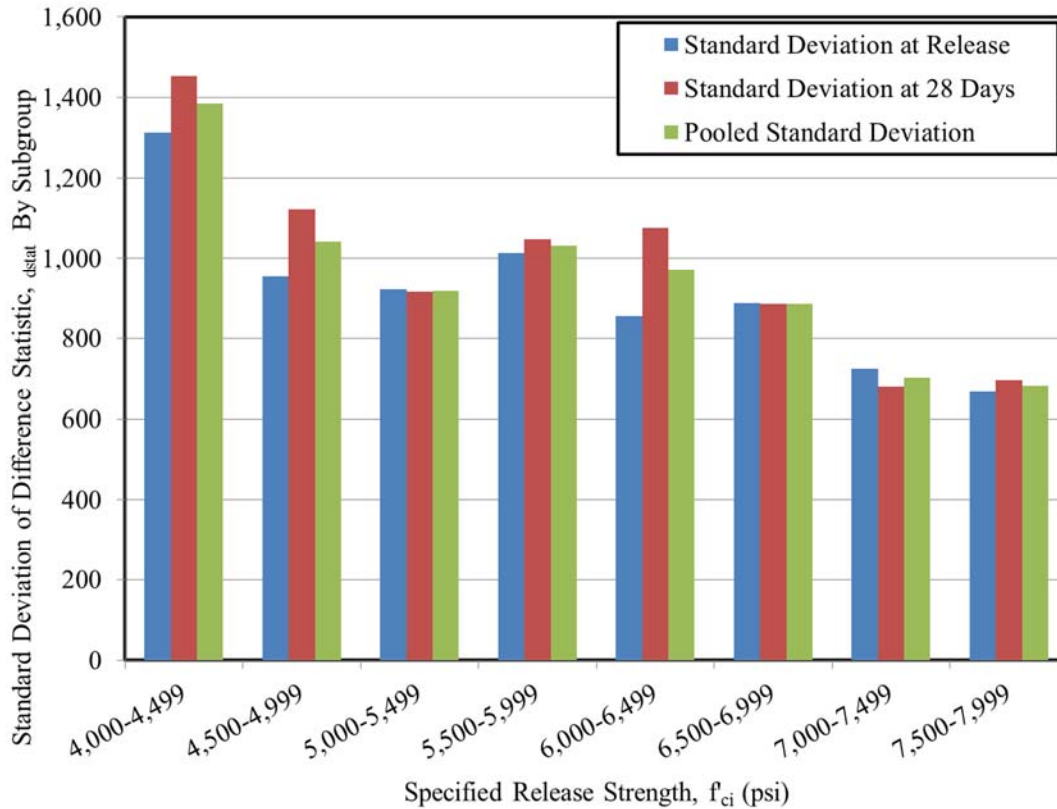


Figure 5-28: Standard Deviation of Difference Statistic by Subgroup

As shown in Figure 5-29, the pooled standard deviation tends to decrease with increasing specified release strengths, f'_{ci} . This decreasing tendency¹² is in contrast to the trend of the implicit assumed standard deviation included in the ACI 224 overstrength provisions for use without historical data as plotted in Figure 5-9. In order to facilitate the use of the pooled standard deviation trend with respect to specified release strength, a linear regression of the pooled standard deviation values was completed with results shown in Figure 5-29. Also shown on the plot is the line representing the simplified constant s used in the two ACI 214-based models discussed in Sections 5.6.6 and 5.6.7.

¹² This offered conclusion may be different if the coefficient of variation approach is relied on instead of the standard deviation. In this case, the primary interest is in the dispersion of the data set around the mean—independent of the magnitude of the mean.

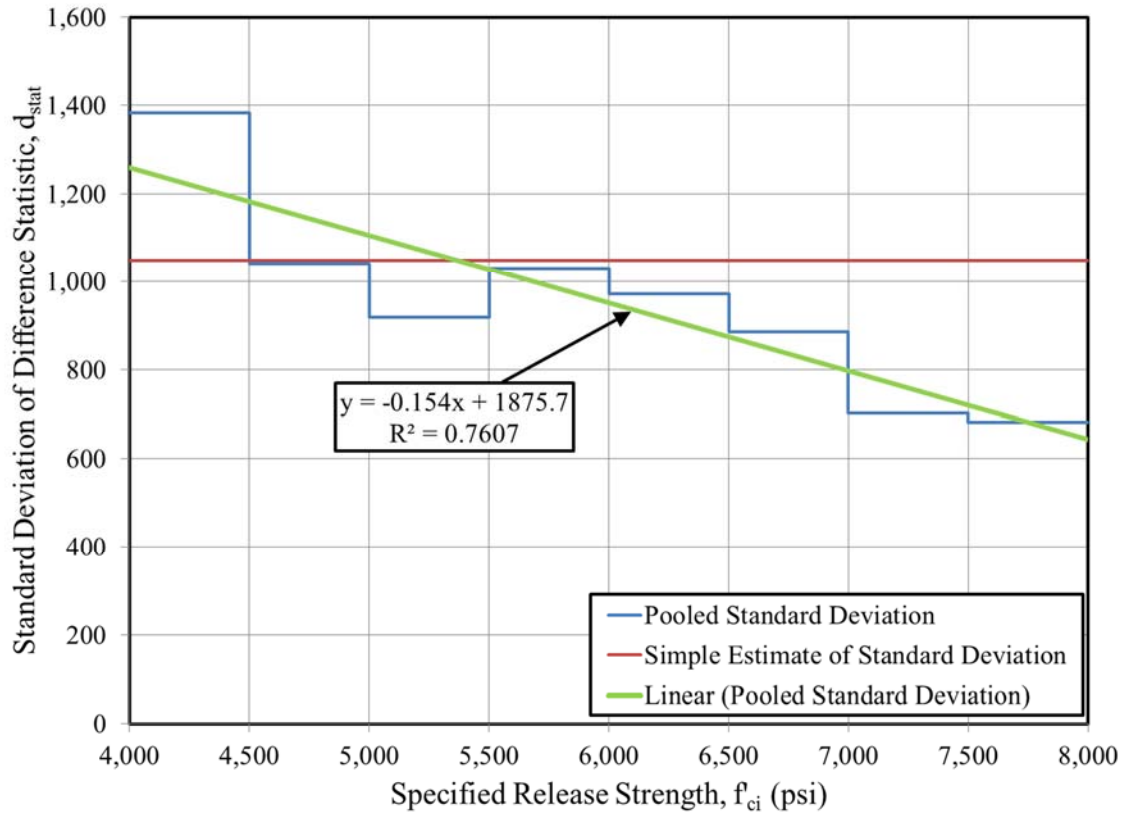


Figure 5-29: Linear Regression of Standard Deviation of Difference Statistic

While the explicit form of the model is withheld until Table 5-16, the completed model is defined by use of the following:

- the MPCMC prediction equation of Section 5.6.2;
- the overstrength provisions of ACI 301 as discussed in Section 5.3; and
- the linear regression equation for s as a function of f'_{ci} as shown in Figure 5-29.

The completed ACI 214-based model (variable s and MPCMC concept) is shown in Figure 5-30, alongside the previous ACI-based models for comparison.

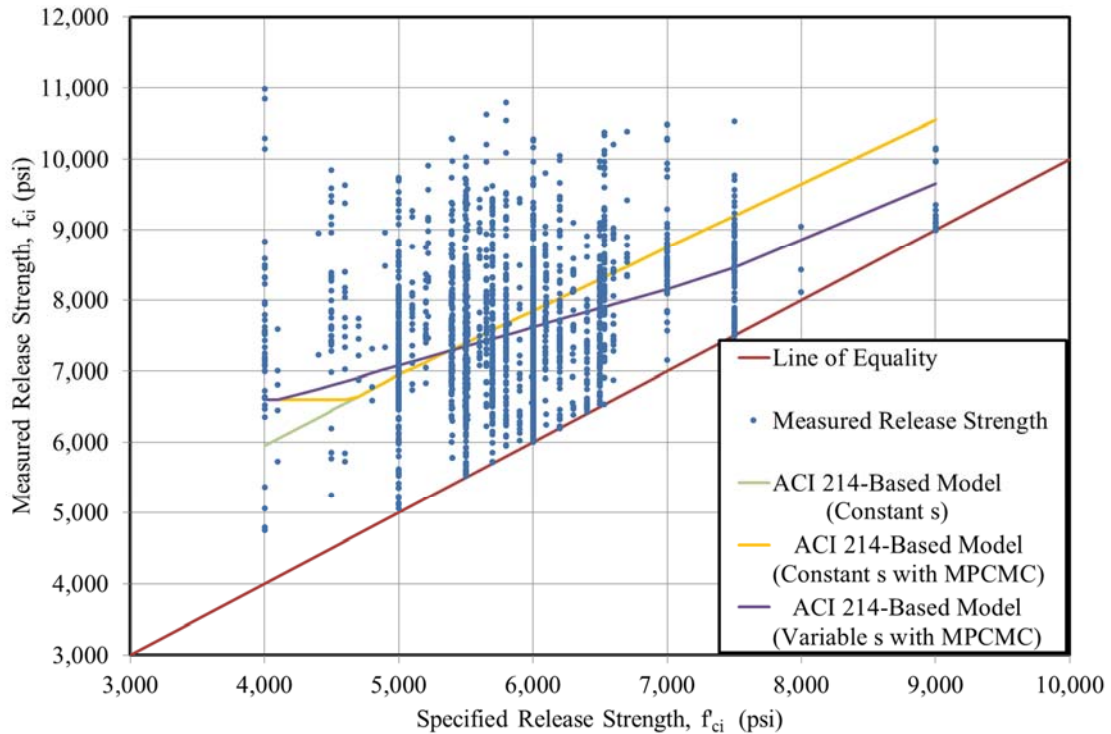


Figure 5-30: ACI 214-Based Model (Variable s with MPCMC)

5.6.9 Comparison of Trial Models

The standard error of the estimate (SEE) was used to evaluate and compare the goodness-of-fit of the trial models developed in this chapter. This section compares and contrasts the trial prediction models and provide final recommendations to be used during the design phase for predicting the expected concrete compressive strength at the time of prestress release, f'_{ci}^* as a function of the specified compressive strength, f'_{ci} .

For reference, each of the trial models, with the exception of FE-3 (previously dismissed in Section 5.6.3), is tabulated in Table 16 and shown in Figure 5-31. The corresponding SEE for each model is shown in Table 5-17. For comparison, the recommendation of Hofrichter (2014) is also included.

Table 5-16: Trial Prediction Equations for Prestress Transfer

Model Designation	Model Definition	Calibration Constants
FE-1	$f_{ci}^* = a \cdot f'_{ci}$	$a = 1.30$
FE-2	$f_{ci}^* = b + f'_{ci}$	$b = 1,840$ psi
FE-3	$f_{ci}^* = a \cdot f'_{ci} + b$	$a = 0.34$ $b = 5,662$ psi
FE-4	$f_{ci}^* = c$ when $f'_{ci} \leq d$ $f_{ci}^* = b + f'_{ci}$ otherwise	$c = 7,500$ psi $d = 6,100$ psi $b = 1,400$ psi
FE-5	$f_{ci}^* = c$ when $f'_{ci} \leq d$ $f_{ci}^* = a \cdot f'_{ci}$ otherwise	$c = 7,500$ psi $d = 6,300$ psi $a = 1.18$
SE-1	$\max(b + f'_{ci}, 6.6(MPCMC) + 800)$	$b = 1,750$ psi $MPCMC = 881$ pcy (Alabama)
SE-2	$\max(a \cdot f'_{ci}, 6.6(MPCMC) + 800)$	$a = 1.27$ $MPCMC = 881$ pcy (Alabama)
ACI 214-Based (Constant s)	$f_{ci}^* = f'_{ci} + 1,950$ psi when $f'_{ci} \leq d$ $f_{ci}^* = 0.9f'_{ci} + 2,450$ psi otherwise	$d = 5,000$ psi (Implicit assumptions $s = 1,050$ psi)
ACI 214-Based (Constant s and MPCMC)	$\max(f'_{ci} + 1,950$ psi, $6.6(MPCMC) + 800$) when $f'_{ci} \leq d$ $\max(0.9f'_{ci} + 2,450$ psi, $6.6(MPCMC) + 800$) otherwise	$d = 5,000$ psi (Implicit assumptions $s = 1,050$ psi) $MPCMC = 881$ pcy (Alabama)
ACI 214-Based (Variable s and MPCMC)	$\max(f'_c + 1.34s, f'_c + 2.33s - 500, 6.6(MPCMC) + 800)$ when $f'_{ci} \leq d$ $\max(f'_c + 1.34s, 0.9f'_c + 2.33s, 6.6(MPCMC) + 800)$ otherwise	$d = 5,000$ psi $s = -0.154f'_{ci} + 1876$ psi $MPCMC = 881$ pcy (Alabama)
Recommendation of Hofrichter (2014)	$f_{ci}^* = c$ when $d \leq f'_{ci} \leq e$ $f_{ci}^* = b + f'_{ci}$ otherwise	$c = 7,500$ psi $d = 4,000$ psi $e = 7,000$ psi $b = 500$ psi

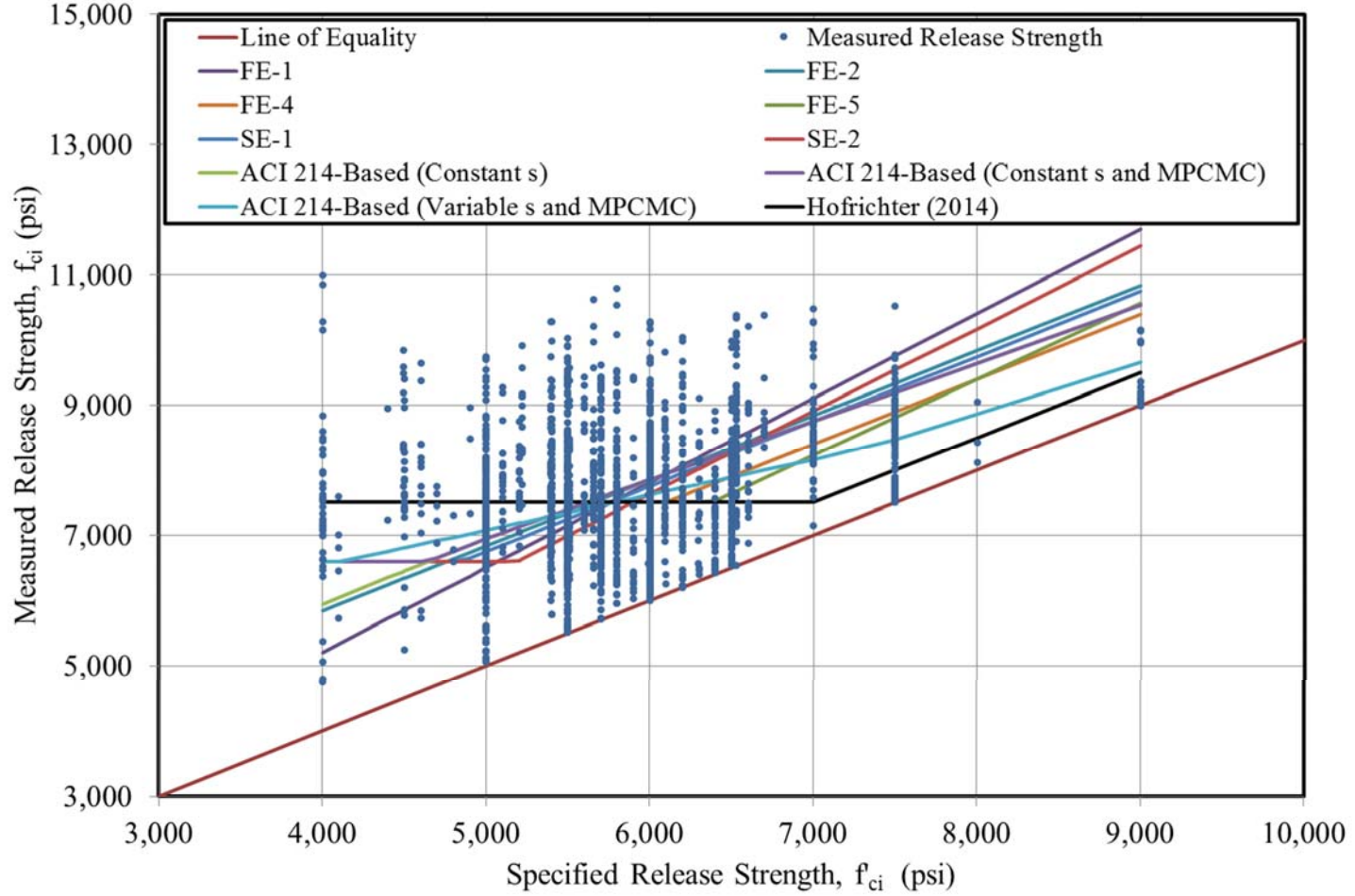


Figure 5-31: Trial Prediction Models for Expected Concrete Release Strength at Prestress Release

Table 5-17: Goodness-of-Fit for Trial Prediction Equations at Prestress Release

Prediction Model Label	Standard Error of Estimate (SEE) (psi)
Current Practice ($f_{ci}^* = f'_{ci}$)	2,126
FE-1	1,185
FE-2	1,064
FE-3	947
FE-4	945
FE-5	950
SE-1	1,032
SE-2	1,097
ACI 214-Based (Constant s)	1,038
ACI 214-Based (Constant s and MPCMC)	1,016
ACI 214-Based (Variable s and MPCMC)	968
Hofrichter (2014)	966

As a metric for comparison, the SEE corresponding to the current design practice of assuming $f_{ci}^* = f'_{ci}$ is shown prior to the SEE for the nine trial models. In general, all trial models represent a large improvement over current design practice. For the simple fully empirical models (FE-1 to FE-3), it is evident that the combination multiplier and constant offset formulation of FE-3 tends to be most accurate form to fit the historical data set. This is not surprising, as the ACI 301 recommendations for concrete strengths exceeding 5,000 psi follow the same multiplier and constant offset formulation as shown in Equation 5-11d. The introduction of the piecewise formulation in the fully empirical models of FE-4 and FE-5 does not significantly increase the accuracy of the prediction models when compared to the historical data set. In general, the fully empirical fits represent the most accurate prediction equations of the nine trial expressions. However, due the empirical nature of these equations, their usefulness is rather narrow, likely confined only to the geographic region from which the historical strength data set was compiled.

The semi-empirical models of SE-1 and SE-2 utilize the MPCMC concept and thus, are somewhat more logically based prediction models than the fully empirical model set. However, it appears that the use of the MPCMC prediction equation included in these models offers a conservative estimate of the minimum mean concrete strength at release for the region represented by the historical data set and, therefore, results in larger SEE values. While the fully empirical models suggest a minimum mean concrete strength of approximately 7,500 psi, the MPCMC prediction equation estimates the minimum

mean concrete strength at 6,600 psi. Recall that the MPCMC concept included certain implicit assumptions of a fixed volume of mixing water (285 pcy), a fixed w/cm (0.32), and the absence of any supplementary cementing materials. Accordingly, use of the MPCMC prediction equation should be used as an approximation of the minimum mean concrete strength only as a last resort, in the absence of designer knowledge of local concrete mixture properties and corresponding minimum mean concrete strengths. Put more simply, if a designer considers estimating the paste content of a likely to be used concrete mixture, he or she is likely better served to estimate the minimum mean concrete strength directly based on region-specific plant practices.

If capable of accurately estimating the expected concrete release strength, f_{ci}^* , the ACI 214-based prediction models may be the most preferable of all the trial models considered in this report due to their potential for more widespread implementation than the fully empirical models. Because these models are largely based on the existing overstrength concepts of ACI 214-R11 and ACI 301, they require little or no calibration from a historical strength data set. For the constant standard deviation models, the rounded value of $s = 1,050$ psi was confirmed as an appropriate value for precast, prestressed construction in historical data subsets from three independent producers at two varying ages. Both of the ACI 214-based constant s models (with and without the MPCMC concept) tend to provide predictions on the same approximate accuracy level as the semi-empirical models and many of the fully empirical models. The slightly lower SEE of the ACI 214-based constant s model with MPCMC suggests that for most accurate results with a constant s model, it is may be appropriate to include the concept of a minimum preferred compressive strength. Finally, for most accurate results of the ACI 214-based trial models, the variable s and MPCMC concept model offers prediction accuracy on par with some of the most accurate fully empirical models. This is not surprising, as the equation for determining s as a function of specified concrete strength, f'_{ci} , (variable s) is somewhat more tailored to the historical data set than the constant s prediction equations. Overall, due to the historical data set in this study containing a relatively few data for comparison at the upper extremes of the strength range (strengths in excess of $f'_{ci} = 7,500$ psi), the increased complexity of the variable s equation does not seem justified for most typical applications.

Prior to determining a final prediction recommendation, it was desirable to compare a leading candidate prediction model from this research (ACI 214-based [constant s with MPCMC]) to previous work by others. As detailed in Section 5.4.1, the predominant research efforts conducted to date tend to rely on the use of a single amplification factor method. Findings of previous researchers are shown in Table 5-18 and Figure 5-32, accompanied by the ACI 214-based (constant s with MPCMC) prediction equation of Section 5.6.7. Where explicit bounds of applicability were not available for previous researcher's recommendations, a range of 4,000 psi to 9,000 psi was assumed. In addition, it is important to note that recommendations of Nervig (2014) are undefined between the specified strength range of 5,500 psi and 6,000 psi.

Table 5-18: Findings of Previous Researchers for Overstrength at Prestress Transfer

Model Reference	Model Definition¹	Calibration Constants
French and O'Neill (2012)	$f_{ci}^* = a \cdot f'_{ci}$	$a = 1.16$
Storm et al. (2013)	$f_{ci}^* = a \cdot f'_{ci}$	$a = 1.24$
Rosa et al. (2007)	$f_{ci}^* = a \cdot f'_{ci}$	$a = 1.11$
Nervig (2014)	$f_{ci}^* = a_1 \cdot f'_{ci}$ for $4,500 \leq f'_{ci} \leq 5,500$ $f_{ci}^* = a_2 \cdot f'_{ci}$ for $6,000 \leq f'_{ci} \leq 8,000$	$a_1 = 1.40$ $a_2 = 1.12$

Note: ¹ = Where explicit bounds of applicability were not available for previous researcher's recommendations, a range of 4,000 psi to 9,000 psi was assumed.

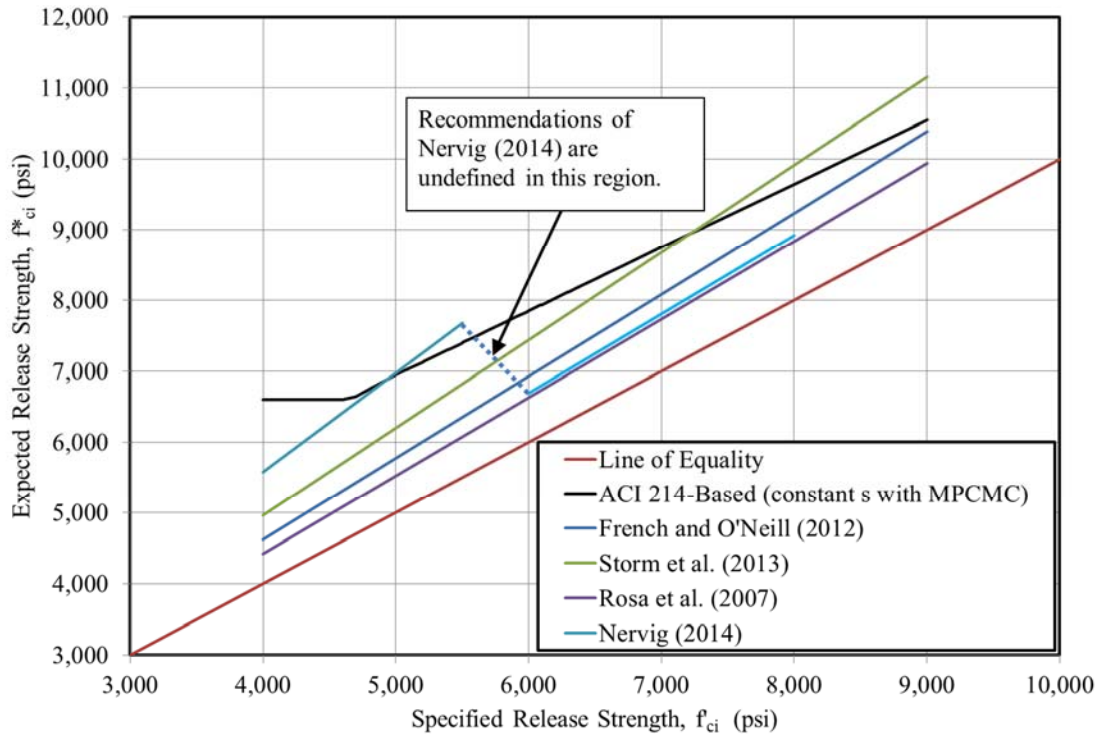


Figure 5-32: Comparison of ACI 214-Based Prediction Equation with Previous Findings by Others

For specified strengths in the lower range, the work of Nervig (2014) provides similar expected release strengths. For higher specified strengths, the ACI 214-based prediction equation yields similar results to those of Storm et al. (2013) and Nervig (2014). A quantitative comparison of the goodness-of-fit of each equation is shown in Table 5-19.

Table 5-19: Comparison of Trial Prediction Equations at Prestress Release Suggested by Previous Researchers to Experimental Data

Prediction Model Label	Standard Error of Estimate (SEE) (psi)
Current Practice ($f_{ci}^* = f'_{ci}$)	2,126
ACI 214-Based (Constant s and MPCMC)	1,016
French and O'Neill (2012)	1,445
Storm et al. (2013)	1,238
Rosa et al. (2007)	1,630
Nervig (2014)	See Note 1.
Hofrichter (2014)	966

Note 1: In the historic strength data set, 323 f_{ci} values were contained in the undefined interval of Nervig's recommendation (i.e. between 5,500 psi and 6,000 psi) making computation of an SEE not possible.

As demonstrated in Table 5-19, the fully empirical recommendations of previous researchers calibrated for regions outside of Alabama (i.e. all noted models with the exception of Hofrichter [2014]) generate less

accurate predictions of release compressive strength than the recommendation of Hofrichter (2014) or the ACI 214-based model recommended as a result of this research effort. This affirms the prior discussion that fully empirical recommendations are limited in application and may not represent the most efficient means of predicting overstrength factors.

5.6.10 Final Recommendations

As a result of the analyses contained in this report section, the design relationship of Section 5.6.6 (ACI 214-based model [constant s]) as displayed in Table 5-16 is proposed for predicting the concrete compressive strength at the time of prestress release, f_c^* . This recommendation is consistent with the discussion of Section 5.3.3 that indicates existing overstrength provisions should logically be applied to all design deflection computations (predictions) in order to avoid a major source of systematic error and to improve the accuracy of these computations. Major conclusions of Section 5.6 are as follow:

1. For the purposes of predicting the expected concrete compressive strength at the time of prestress release, f_c^* , the overstrength provisions of ACI 301 and ACI 214 should be applied with a standard deviation as determined by the distribution of the difference statistic for historical records from production cycles of precast, prestressed products within the region. In the absence of historical data, the standard deviation, s , may be assumed to be 1,050 psi, resulting in the following expressions for predicting compressive strength at the time of prestress release:

$$\text{For } 4,000 \text{ psi} \leq f_{ci} \leq 5,000 \text{ psi} \quad f_{ci}^* = f'_{ci} + 1,950 \text{ psi}$$

$$\text{For } 5,000 \text{ psi} < f_{ci} \leq 9,000 \text{ psi} \quad f_{ci}^* = 0.9 f'_{ci} + 2,450 \text{ psi}$$

2. The overstrength factor at release, OS_i , for concrete strengths exceeding 5,000 psi (without inclusion of the MPCMC concept) can be expressed as:

$$OS_i = \frac{f_{ci}^*}{f'_{ci}} = 0.9 + \frac{2,450}{f'_{ci}}$$

where

OS_i^* = expected overstrength ratio at prestress release;

f_{ci}^* = the expected concrete strength at prestress release (psi); and

f'_{ci} = the specified concrete strength at prestress release (psi).

5.7 Predicting Expected Concrete Compressive Strength at 28 Days

Accurately predicting overstrength at the time of 28 days after girder production is of somewhat less importance to design engineers in the precast, prestressed industry than the accuracy of overstrength predictions at the time of prestress release due to the critical role of the initial modulus of elasticity in determining deformations (camber) and prestress losses over the life of the girder. The primary goal of this section is to recommend a relationship for use at the time of girder design to more accurately predict the expected concrete compressive strength 28 days after girder fabrication, f_c^* . This section is structured similarly to that of Section 5.6 as shown below in Figure 5-33.

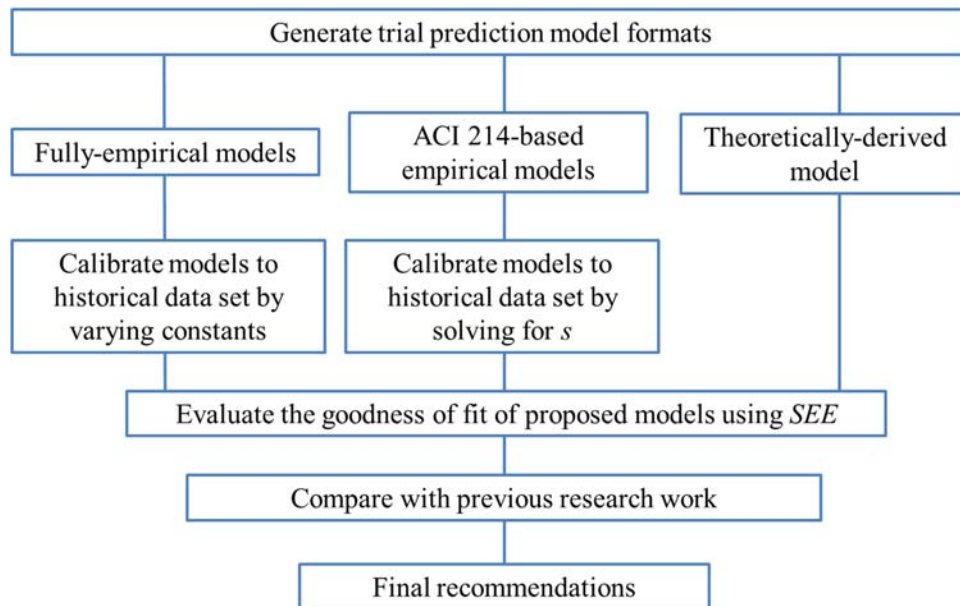


Figure 5-33: Analytical Approach of 28-Day Prediction Equation Development

First, various fully empirical and ACI 214-based trial models are developed and calibrated using the historical data set. While these calibrated trial models do offer relatively good agreement with the 28 day expected strengths of the historical data set, it is important to note that these trial models omit the effect of two important regional variables: (1) the level of overstrength at prestress release and (2) the ratio of the specified release strength, f'_{ci} , to the specified 28-day strength, f'_c . By including the effect of these

parameters in a final prediction model (based on the concepts depicted in Figure 5-12), a more theoretically-correct and logical model capable of capturing regional variations in design practices is investigated and found to be a preferable prediction method.

5.7.1 Fully Empirical Models

The format and calibration constants for each of the five fully empirical models are shown in Table 5-20.

The format of these equations is similar to those prestress release models discussed in Section 5.6.3.

Each of the five models is plotted, alongside the historical data set, in Figure 5-34.

Table 5-20: Fully Empirical Model Description

Fully Empirical Model Designation	Format of Model (psi)	Description of Model	Calibration Constants
FE-1	$f_c^* = a \cdot f'_c$	Factor	$a = 1.56$
FE-2	$f_c^* = b + f'_c$	Offset	$b = 3,862$ psi
FE-3	$f_c^* = a \cdot f'_c + b$	Factor and Offset	$a = 0.21$ $b = 9,172$ psi
FE-4	$f_c^* = c$ when $f'_c \leq d$ $f_c^* = b + f'_c$ otherwise	Piecewise Constant and Offset	$c = 10,500$ psi $d = 7,300$ psi $b = 3,330$ psi
FE-5	$f_c^* = c$ when $f'_c \leq d$ $f_c^* = a \cdot f'_c$ otherwise	Piecewise Constant and Factor	$c = 10,500$ psi $d = 7,450$ psi $a = 1.43$

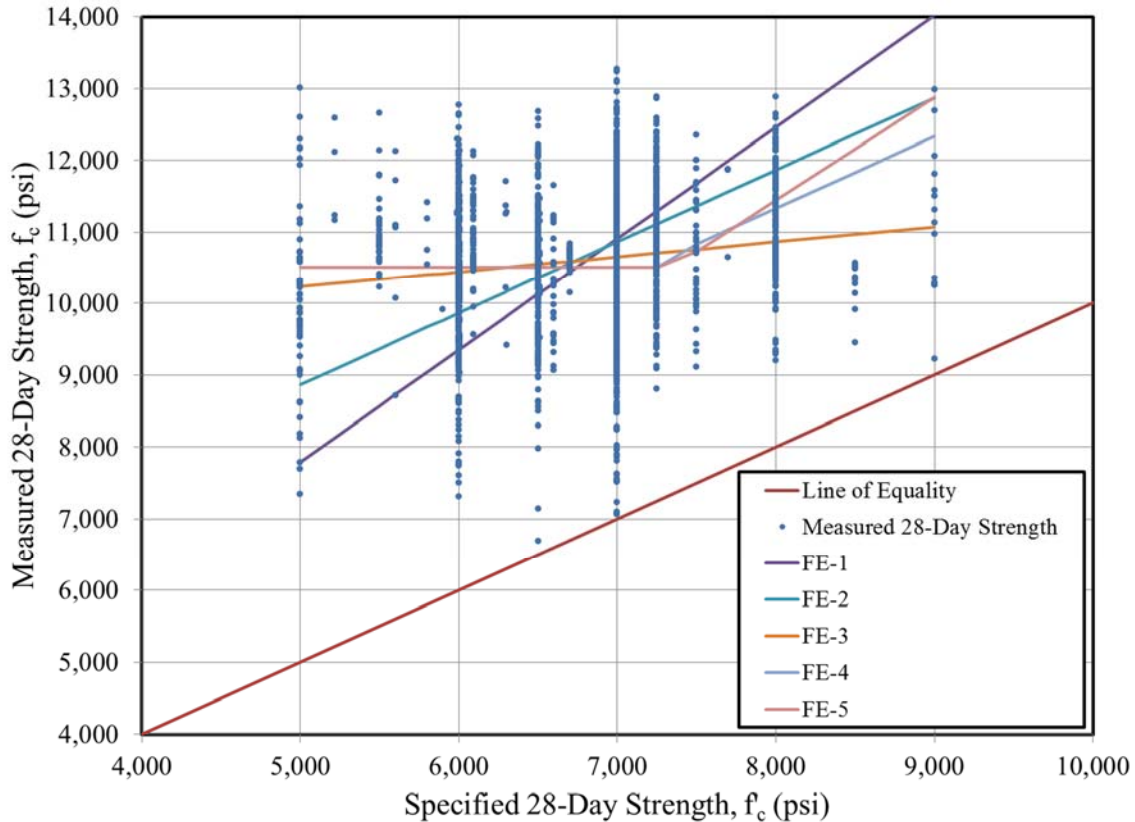


Figure 5-34: Calibrated Fully Empirical 28-Day Strength Prediction Models

Although there is a large variety in the best-fit equations, certain trends are evident. Examining Figure 5-34, it seems that a minimum mean concrete strength, $f_{ci,min}^*$, of approximately 10,500 psi is suggested by Models FE-3, FE-4, and FE-5. In addition, all models yield similar results for specified strengths of approximately 6,700 psi, which corresponds to the mean specified 28-day strength of the historical database.

5.7.2 ACI 214-Based Empirical Models

Two trial models of the ACI 214-based format were investigated for predicting expected 28-day concrete strength. The first model, the ACI 214-based with constant s , was calibrated to the historical data set by varying the standard deviation, s , and minimizing the SEE . The second model, the ACI 214-based with constant s and MPCMC, was calibrated similarly, although an additional parameter, the minimum mean concrete strength, $f_{c,min}^*$, was also fit to the historical data set. The form and calibration constants for these trial models are shown in Table 5-21 and plotted in Figure 5-35.

Table 5-21: ACI 214-Based Empirical Model Description

	f'_c (psi)	f_c^* (psi)	Calibration Constants
		Use the larger of:	
ACI 214-Based (Constant s)	5,000 or less	$f_c^* = f'_c + 1.34s$	$s = 1,950$ psi
		$f_c^* = f'_c + 2.33s - 500$	
	Over 5,000	$f_c^* = f'_c + 1.34s$	
		$f_c^* = 0.9f'_c + 2.33s$	
ACI 214 (Constant s and MPCMC)	5,000 or less	$f_{c,min}^* = a$	$a = 10,500$ psi
		$f_c^* = f'_c + 1.34s$	$s = 1,050$ psi
		$f_c^* = f'_c + 2.33s - 500$	
	Over 5,000	$f_{c,min}^* = a$	$a = 10,500$ psi
		$f_c^* = f'_c + 1.34s$	$s = 1,050$ psi
		$f_c^* = 0.9f'_c + 2.33s$	

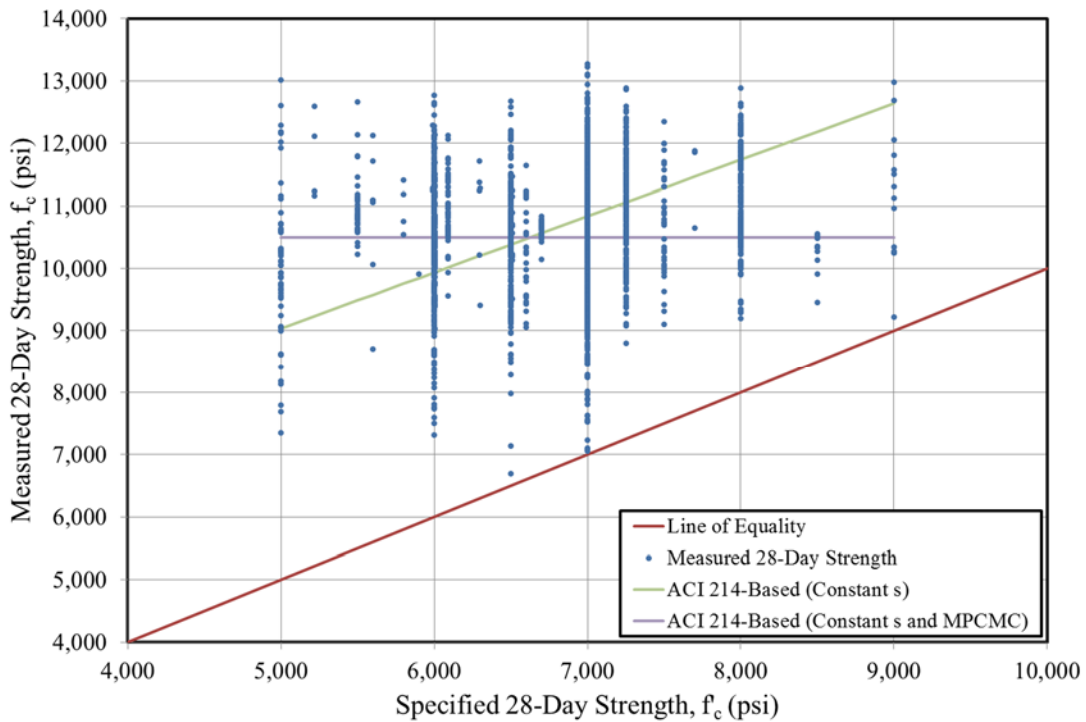


Figure 5-35: ACI 214-Based Empirical Models for 28-Day Concrete Strength

Upon introduction of the MPCMC concept in the second considered model, the model simplifies to a single horizontal line at the value of 10,500 psi, suggesting a constant expected value may be appropriate for all concrete mixtures. This finding is in agreement with the recommendation of Hofrichter (2014)

derived in a similar manner. The calibrated standard deviation, s , therefore, has no effect on the second model (with MPCMC), but does play a role in defining the first model. The calibrated value of s for the first model (ACI 214-based [Constant s]) does not agree with the computed value representing the historical data set for the age of 28 days ($s = 1,132$ psi from Table 5-12). For these reasons, the ACI 214-based empirical models may not be preferable for computing the expected 28-day concrete strength, f_c^* .

5.7.3 Theoretically-Derived Strength Growth Model

Given the previous discussion on the probable causes of 28-day overstrength (Section 5.4.2), it seems appropriate to develop a prediction model incorporating certain logically-relevant parameters. Recall, it was discussed that two key parameters are required to fully define the overstrength ratio present at 28 days: (1) the “expected” 28-day strength computed as a function of the expected release strength, f_{ci}^* , and various strength growth parameters and (2) the selection of a specified 28-day strength, f'_c , by the design engineer to ensure adequate service and strength limit state performance. It would seem that a series of prediction equations for both release and 28 days omitting these parameters would tend to be (1) overly restrictive by definition (i.e. implicitly assuming a strength growth model) and (2) not suitable for widespread usage due to regionally varying ratios of f'_{ci}/f'_c by design engineers¹³. The theoretically-derived model explored herein includes the relevant parameters discussed above, and thus, is more suited to widespread usage than a fully empirical.

The basic hypothesis explored here is that the actual 28-day compressive strength for typical precast, prestressed girders has very little to do with the magnitude of the specified 28-day concrete strength, f'_c , but instead, is solely a result of the expected release strength, f_{ci}^* , and the strength growth parameters relating the two ages (α and β). A logical first step to evaluate this hypothesis is to validate the applicability of the strength growth provisions suggested by Hofrichter (2014) on the measured concrete strengths of the historical data set. As shown in Figure 5-36, there is close

¹³ The ratio of specified concrete release strength to specified 28-day strength is expected to vary regionally in accordance with state-specific allowable design stresses (i.e. Alabama girders are designed as zero-tension members at service—likely requiring higher specified strengths than a state that permits in-service tensile stresses.)

agreement between the values of (1) the expected 28-day strength, f_c^* , computed by applying Hofrichter's strength growth recommendations (i.e. $f_c = f_{ci} \cdot 1.44$) to measured values of release strength, f_{ci} , and (2) the measured value of 28-day strength, f_c .

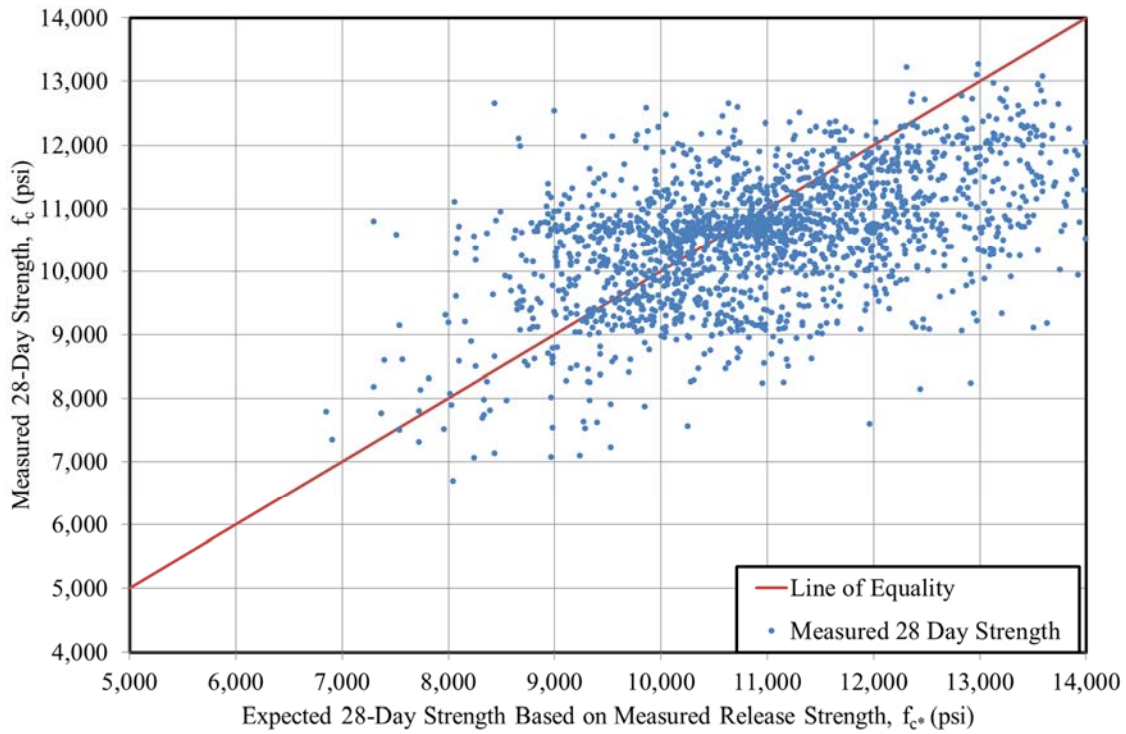


Figure 5-36: Comparison of Expected 28-Day Strength Based on Measured Release Strength and Measured 28-Day Strength.

The measured 28-day strengths tend to be clustered around the line of equality somewhat symmetrically indicating that a relationship may exist between these parameters. The next logical comparison to explore is the relationship between (1) measured 28-day strength, f_c , and (2) expected 28-day strength, f_c^* , based on the combination of the previously proposed equations for computing the expected concrete strength at prestress release, f_{ci}^* (as a function of f'_{ci}), as modified by the strength growth provision by Hofrichter (2014). The results of this analysis are plotted in Figure 5-37.

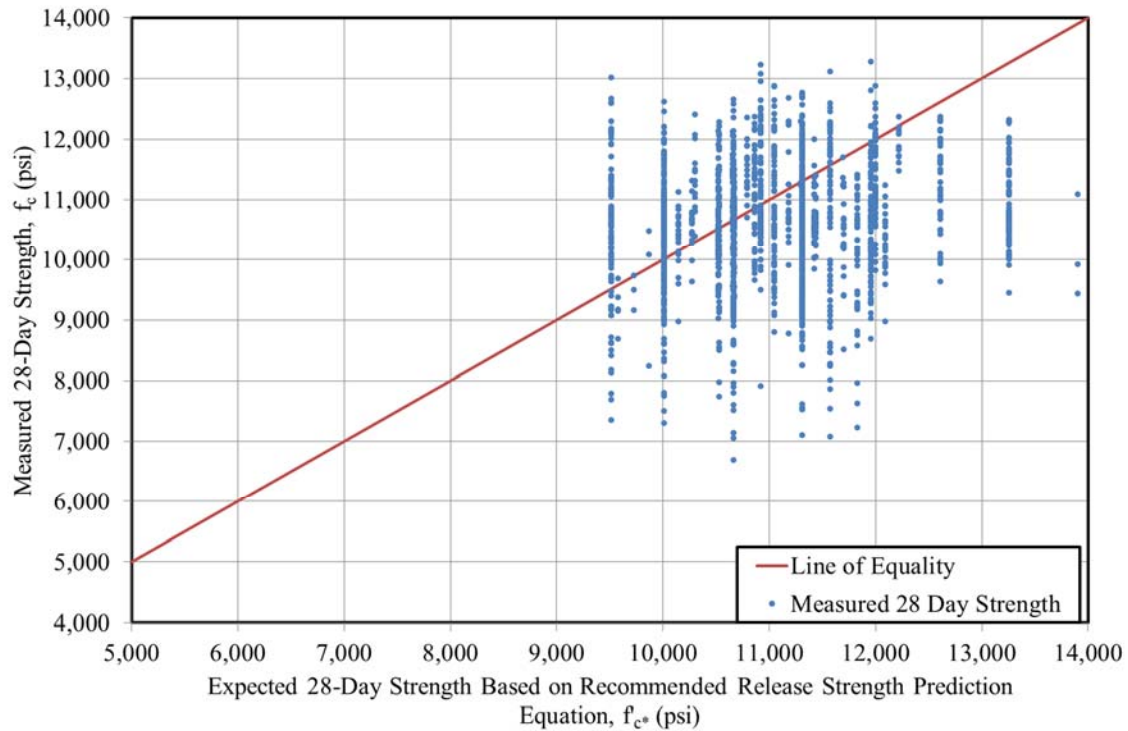


Figure 5-37: Comparison of Expected 28-Day Strength Based on Expected Release Strength and Measured 28-Day Strength.

Again, relatively good agreement is shown between the compared parameters as evidenced by the close proximity of the measured data points to the line of equality. Finally, the measured 28-day strength, f_c , (for the historical 28-day data set) and the expected 28-day strength, f_c^* , (for the release data set adjusted by the strength growth model explored in this section) is plotted versus the specified 28-day strength, f'_c in Figure 5-38. On the plot, it is evident that the values predicted by the theoretically-derived model do not form a continuous line, but instead, are represented by a discrete value for each data point of the historical data set. As shown, there is relatively good agreement between the values predicted by the theoretically-derived model and the measured values of historical data set.

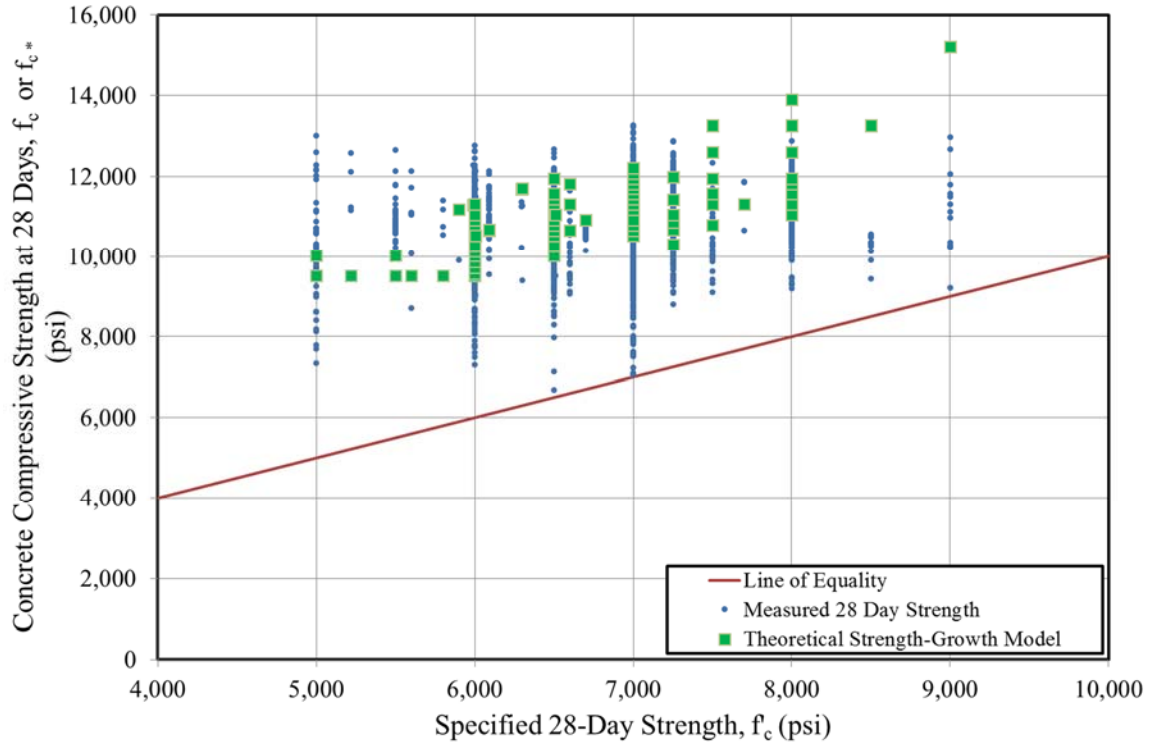


Figure 5-38: Theoretical Strength Growth Model Predictions for 28-Day Concrete Strength Compared with Measured Values of Historical Data Set.

As presented in this section, the theoretically-derived strength growth model is a relatively simple concept in application, but is likely too cumbersome for use by a design engineer. In order to simplify the above procedure, a simple expression for the expected overstrength ratio at 28 days, OS_{28}^* , can be derived. As previously defined, OS_{28}^* can be expressed as:

$$OS_{28}^* = \frac{f_c^*}{f'_c} \quad (5-16)$$

where

f_c^* = the expected concrete strength at 28 days (psi) and

f'_c = the specified concrete strength at 28 days (psi).

Combining with Equation 5-14 (derived from Hofrichter [2014]) yields:

$$OS_{28}^* = \frac{f_c^*}{f'_c} = \frac{1.44 f_{ci}^*}{f'_c} \quad (5-17)$$

Substituting in Equation 5-18b (limiting solution to $5,000 \text{ psi} < f_{ci} \leq 9,000 \text{ psi}$):

$$OS_{28}^* = \frac{1.44f_{ci}^*}{f'_c} = \frac{1.44(0.9f'_{ci} + 2,450)}{f'_c} \quad (5-18)$$

Simplifying and grouping terms yields:

$$OS_{28}^* = 1.3 \left(\frac{f'_{ci}}{f'_c} \right) + \frac{3,500}{f'_c} \quad (5-19)$$

where

$\left(\frac{f'_{ci}}{f'_c} \right)$ = the ratio of specified strength at prestress release to 28 days as selected by design engineer.

Examination of Equation 5-19 shows that the expected overstrength 28 days after production is then theoretically a function of only the ratio of specified strengths (as chosen by design engineer) and the specified 28-day strength, f'_c . Equation 5-19 is a multi-variate expression and can be perhaps best visualized in tabulated form as shown in Table 5-22. For ease of the use, values that are not realistic (i.e. specified release strength exceeding 28-day strength or overstrength values less than 1.0) are omitted, values prohibited by ALDOT design specifications are marked in yellow, and possible combinations to be specified by ALDOT are marked in green. Implicit in the table are both (1) the overstrength predictions for prestress release and (2) the strength growth provisions for precast, prestressed concrete as proposed by Hofrichter (2014).

Table 5-22: Expected Overstrength Factor at 28 Days as a Function of Specified Release Strength and Specified 28-Day Strength

		Specified 28-Day Concrete Strength, f'_c (psi)																
		4,000	4,500	5,000	5,500	6,000	6,500	7,000	7,500	8,000	8,500	9,000	9,500	10,000	10,500	11,000	11,500	12,000
Specified Release Concrete Strength, f'_i (psi)	4,000	2.19	1.94	1.75	1.59	1.46	1.34	1.25	1.17	1.09								
	4,500		2.09	1.88	1.71	1.56	1.44	1.34	1.25	1.17	1.10	1.04						
	5,000			2.01	1.82	1.67	1.54	1.43	1.34	1.25	1.18	1.12	1.06					
	5,500				1.94	1.78	1.64	1.53	1.42	1.34	1.26	1.19	1.12	1.07	1.02			
	6,000					1.89	1.74	1.62	1.51	1.42	1.33	1.26	1.19	1.13	1.08	1.03		
	6,500						1.84	1.71	1.60	1.50	1.41	1.33	1.26	1.20	1.14	1.09	1.04	
	7,000							1.80	1.68	1.58	1.49	1.40	1.33	1.26	1.20	1.15	1.10	1.05
	7,500								1.77	1.66	1.56	1.48	1.40	1.33	1.26	1.21	1.15	1.11
	8,000									1.74	1.64	1.55	1.47	1.39	1.33	1.27	1.21	1.16
	8,500										1.71	1.62	1.53	1.46	1.39	1.32	1.27	1.21
9,000											1.69	1.60	1.52	1.45	1.38	1.32	1.27	

Not Realistic Values or Invalid by Assumption
 Prohibited by ALDOT Specifications
 Predictions for ALDOT Possible Combinations

Table 5-22 is a useful design aid for the precast, prestressed concrete industry, allowing an engineer to first complete strength-limit state design according to current practice and then use Table 5-22 to estimate the magnitude of the expected 28-day overstrength factor, thereby allowing more accurate 28-day deflection computations. For instance, consider the case when a given initial structural design (satisfying allowable stress requirements) warrants a specified release strength, f'_{ci} , of 5,000 psi and a specified 28-day strength, f'_c , of 6,000 psi. Using Table 5-22, a design engineer can determine that an overstrength factor of 1.67 should be applied to the specified 28-day strength, f'_c , for use in computing 28-day deflections of interest.

5.7.4 Comparison of Proposed Models

The standard error of the estimate (*SEE*) for each of the trial models discussed in this section is shown in Table 5-23. Recall, the *SEE* is a measure of the relative goodness-of-fit of a prediction model to measured data from the historical data set.

Table 5-23: Goodness-of-Fit for Trial Prediction Equations at 28 Days

Prediction Model Label	Standard Error of Estimate (<i>SEE</i>) (psi)
Current Practice ($f_c^* = f'_c$)	4,026
FE-1	1,391
FE-2	1,133
FE-3	974
FE-4	988
FE-5	1,001
ACI 214-Based (Constant <i>s</i>)	1,097
ACI 214-Based (Constant <i>s</i> and MPCMC) / Hofrichter (2014)	991
Theoretically-Derived Strength Growth	1,349

As shown, each of the trial models represents a significant improvement in accuracy when compared to current design practice. The fully empirical models, when calibrated to the historical data set, yield relatively good fits of the historical data with Model FE-3 being the most preferable due to its simplicity. While these fully empirical models are appropriate for use in the study region, they may not be suited for use in other areas due to differing design and production practices. The ACI 214-based methods were not preferable due to the lack of agreement between the standard deviation of the historical data set calibrated empirically and the standard deviation previously computed directly from the historical data

set—likely suggesting that form of the ACI 214 overstrength equations are not suit for application at 28 days. Despite being somewhat less accurate for the historical data set, the theoretically-derived strength growth model is the most mechanistic model for predicting concrete overstrength at 28 days in steam-cured concrete and thus, is most well suited for widespread applicability.

5.7.5 Final Recommendations

As a result of the analyses of the preceding report sections, the theoretically-derived strength growth model is selected as the most appropriate model for design estimates of the 28-day concrete compressive strength, f_c^* . While fully empirical models may be useful on a somewhat limited regional basis, the nature of the theoretically-derived strength growth model is conducive to capturing variations in regional design practices (the effect of varying specified strength ratio) by using strength growth provisions appropriate for the curing application. For accelerated-cured concretes (containing Type III cement) typical of the precast, prestressed concrete industry, the strength growth provisions of Hofrichter (2014) are recommended for use (as summarized in Section 5.2.3) and implicitly included in the overstrength prediction expression of Equation 5-23 as represented in Table 5-22.

5.8 Summary and Conclusions

5.8.1 Summary

The primary objective of this report chapter is to identify design relationships between specified concrete compressive strength and expected concrete compressive strength in order to allow engineers to improve the accuracy of design phase serviceability predictions. After a brief background discussion, current relevant code provisions of ACI 301 and *fib* Model Code 2010 are reviewed, compared, and recommended for general usage in structural concrete design serviceability computations. Next, overstrength in the precast, prestressed industry is discussed—including probable causes of overstrength at two key ages of interest and an evaluation of the suitability of applying the provisions of ACI 301 for estimating overstrength in the precast, prestressed industry. Subsequently, the details of a historical concrete strength data set compiled as part of this research effort are presented and discussed prior to its usage in various analyses. The first major analysis is aimed at evaluating various fully empirical, semi-empirical, and ACI 214-based prediction equations for estimating the expected concrete compressive

strength at the time of prestress release. Finally, a similar set of analyses is conducted to yield a recommended design relationship for estimating expected concrete strength at 28 days.

5.8.2 Conclusions and Recommendations

Several key conclusions of the work presented in this report chapter are applicable to the concrete industry as a whole:

1. For the purposes of design deflection computations, it is appropriate to use an estimate of the “expected” concrete compressive strength rather than the current practice of using the specified strength.;
2. The existing provisions of ACI 301 and ACI 214R-11 are an appropriate and convenient method for estimating the expected concrete compressive strength as a function of the specified strength;
3. The “difference statistic” and the concept of preservation of standard deviation as summarized below offer a convenient method to compute a standard deviation from a historical data set with varying specified concrete strengths that is appropriate to be used with the provisions of ACI 301 and ACI 214R-11:
 - a. *For an assumed (or approximated) constant standard deviation value at all considered strength levels, the distribution of the difference statistic is identical regardless of the number of constitutive mixtures or the relative mean strength levels of each mixture.*

Several key conclusions of the work presented in this report chapter are applicable specifically to the precast, prestressed concrete industry:

1. For the purposes of predicting the expected concrete compressive strength at the time of prestress release, f_c^* , the overstrength provisions of ACI 301 and ACI 214 should be applied with a standard deviation as determined by the distribution of the difference statistic for historical records from production cycles of precast, prestressed products within the region. In the absence of historical data, the standard deviation, s , may be assumed to be 1,050 psi based on the results of this study. The overstrength provisions of ACI 301 and ACI 214 are recommended for predicting compressive strength at the time of prestress release, simplified as follows for the value of $s = 1,050$ psi:

$$\text{For } 4,000 \text{ psi} \leq f_{ci} \leq 5,000 \text{ psi} \quad f_{ci}^* = f'_{ci} + 1,950 \text{ psi}$$

$$\text{For } 5,000 \text{ psi} < f_{ci} \leq 9,000 \text{ psi} \quad f_{ci}^* = 0.9 f'_{ci} + 2,450 \text{ psi}$$

2. Based on Equation 5-18, the overstrength factor at release, OS_i , for concrete strengths exceeding 5,000 psi (without inclusion of the MPCMC concept) can be expressed as:

$$OS_i = \frac{f_{ci}^*}{f'_{ci}} = 0.9 + \frac{2,450}{f'_{ci}}$$

where

OS_i^* = expected overstrength factor at prestress release;

f_{ci}^* = the expected concrete strength at prestress release (psi); and

f'_{ci} = the specified concrete strength at prestress release (psi).

3. For the purposes of predicting the expected concrete strength at the age of 28 days after production, the theoretically-derived strength growth model of Section 5.7.3 is recommended. This method consists of using the above recommendations to estimate the expected concrete strength at release and then applying appropriate strength growth provisions to compute expected 28-day strength. For accelerated cured concretes typical of precast, prestressed industry, the expected overstrength at 28 days, OS_{28}^* , can be approximated

$$OS_{28}^* = 1.3 \left(\frac{f'_{ci}}{f'_c} \right) + \frac{3,500}{f'_c}$$

where

$\left(\frac{f'_{ci}}{f'_c} \right)$ = the ratio of specified strength at prestress release to 28 days as selected by design

engineer.

Rearranging, the expected 28-day compressive strength, f_c^* , can be computed directly as a function of specified release strength, f'_{ci}

$$f_c^* = 1.3 f'_{ci} + 3,500 \text{ psi}$$

where

f'_{ci} = the specified concrete strength at prestress release (psi).

Chapter 6: Concrete Modulus of Elasticity Relationships

6.1 Introduction

Concrete material stiffness, as represented by modulus of elasticity, is a parameter intrinsically related to the computation of both short-term and long-term deflections in prestressed concrete elements. Generally speaking, the modulus of elasticity (also called the elastic modulus) of a given material is defined as the ratio of the applied stress to the instantaneous strain within an assumed proportional limit (Mehta and Monteiro 2014). It is this relationship that governs elastic material behavior and serves as the basis for deformation computations in structural elements.

This report chapter focuses on correlating a known (or expected) concrete cylinder compressive strength to a corresponding modulus of elasticity for typical precast, prestressed concrete. Using a robust regional data set compiled from a laboratory and concurrent field data collection effort, various available elastic modulus prediction equations were first calibrated and then evaluated for potential use by bridge designers. It is assumed that the compressive strength values used in modulus of elasticity prediction models represent either a known (measured) value or a best-estimate of the concrete compressive strength at a given time. While based on a relatively robust regional data set, the concretes considered in this study are all for similar precast, prestressed application and represent a relatively narrow range of compressive strengths and constitutive materials. Therefore, the focus of this chapter remains on fitting those prediction models with built-in constants to the compiled data set in an effort to appropriately capture regional concrete behavior.

6.1.1 Chapter Objectives

The primary objective of this chapter is to establish the most appropriate relationships for use by design engineers to accurately characterize the elastic modulus of concrete as a function of compressive strength and other relevant variables likely to be known during the preliminary design phase. Tasks completed in pursuit of this primary objective include the following:

- Review relevant background regarding concrete modulus of elasticity and the primary mixture-dependent factors hypothesized to affect elastic modulus;
- Review and discuss various available concrete stiffness prediction equations, their application at various ages, and the results of similar previous research studies;
- Summarize an experimental program consisting of a laboratory and concurrent field data collection effort to compile a robust regional data set;
- Calibrate various available prediction equations to experimental results for two primary ages of interest (prestress release and 28 days after production) and evaluate the effectiveness of various candidate models; and
- Explore and discuss the time-dependent nature of the effect of aggregate stiffness on concrete modulus through consideration of a reduced data set.

6.1.2 Chapter Outline

This chapter begins with a brief background detailing the definition of the modulus of elasticity of concrete and the primary factors affecting concrete material stiffness. Next, various available prediction equations are introduced and discussed. The work of previous researchers is also discussed in an effort to identify those prediction equations most universally recommended and utilized in design. Then, an experimental program consisting of a laboratory and field data collection effort is presented, which culminated in the compilation of a data set including many variables hypothesized to affect elasticity modulus. By calibrating available prediction models and comparing the accuracy of these prediction equations to measured data, recommendations are then made for use of the most appropriate prediction equations. Finally, a discussion of a potential source of uncontrolled variability in the experimental data is included.

6.2 Background

6.2.1 Modulus of Elasticity Definition

As previously defined, the elastic modulus of a given concrete is the ratio of the applied stress to the instantaneous strain when the concrete is subjected to uniaxial compression up to an assumed proportionality limit (Mehta and Monteiro 2014). For the purposes of this report, the term modulus of

elasticity (or elastic modulus) refers exclusively to the static modulus of elasticity (as opposed to the dynamic modulus.) Most commonly, concrete is assumed to exhibit relatively linear-elastic behavior through roughly 40 percent of its ultimate compressive strength. Thereafter, the development of microcracking at interfaces between hydrated cement paste and aggregate particles tend to cause a curved stress-strain relation (Neville 2013) as shown below in Figure 6-1.

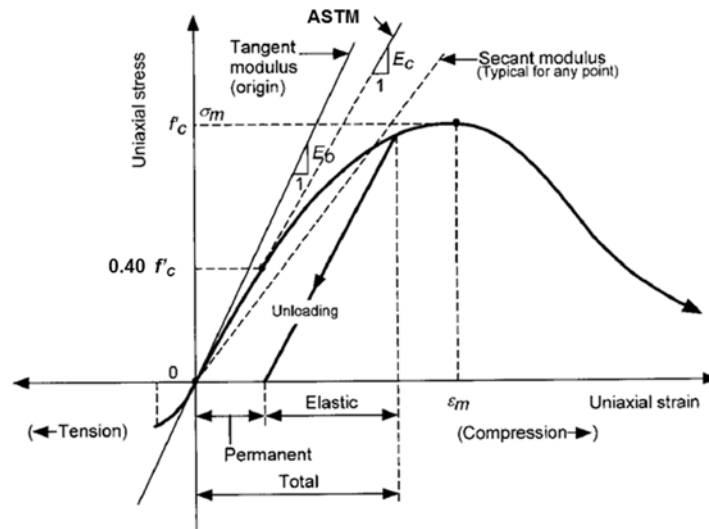


Figure 6-1: Stress-Strain Curve and Elastic Modulus Depictions (Adapted from Naaman 2004)

As expected, the stress-strain response of concrete specimens exhibits no permanent deformation upon unloading in the range of linear-elastic behavior. Also shown in Figure 6-1 are three common representations of elastic modulus including (1) initial tangent modulus, (2) chord modulus, and (3) secant modulus. A tangent modulus is defined for any given point on the stress-strain curve and represents a localized portion of the response. In this case, the initial tangent modulus is depicted, representing the initial stiffness response of the concrete. However, as noted by Neville (2013), the tangent modulus may not accurately describe the overall stiffness response and therefore is of little practical importance. The secant modulus (shown for a stress range of approximately 90 percent of f'_c) offers an improved characterization of stress-strain behavior, but is prone to being skewed by initial response nonlinearities commonly observed at lower stress ranges. The third metric, the chord modulus, is the preferable metric for elastic modulus testing in concrete and the method designated by the standardized testing method ASTM C-469 (2010). This metric, represented by the slope of a line joining two pre-defined points within the elastic portion of a stress-strain curve, is able to avoid the previously mentioned effect of initial

nonlinearities, while also characterizing the elastic response range relatively accurately. In accordance with the requirements of ASTM C-469, the chord modulus of elasticity, E_c , can be computed from test parameters as follows:

$$E_c = (S_2 - S_1) / (\varepsilon_2 - 0.000050) \quad (6-1)$$

where

S_2 = stress corresponding to 40 percent of ultimate load (psi);

S_1 = stress corresponding to a longitudinal strain, ε_1 , of 50 millionths (psi); and

ε_2 = longitudinal strain produced by stress S_2 (in/in).

6.2.2 Primary Factors Affecting Concrete Modulus of Elasticity

This section provides a general discussion of four of the mixture-dependent factors most commonly correlated to concrete elasticity including (1) concrete compressive strength, (2) concrete unit weight, (3) aggregate stiffness, and (4) the use of supplementary cementing materials (SCMs). This discussion is intended to remain general in nature and leads into Section 6.2.3, which introduces candidate prediction equations for E_c .

6.2.2.1 Concrete Compressive Strength

In contrast to other construction materials that tend to exhibit a relatively uniform elasticity regardless of proportional limit (i.e. most structural metals), it was recognized quite early that the stiffness of a given concrete correlates well with the compressive strength. In fact, it is clear that available prediction equations used prior to 1960 relied on a direct correlation between elastic modulus and compressive strength (Pauw 1960). Prediction equations of this time period were typically were of the following forms:

$$E_c = a \cdot f'_c \quad (6-2a)$$

$$E_c = a \cdot f'_c + b \quad (6-2b)$$

where

f'_c = concrete compressive strength; and

a , b = empirically calibrated constants.

Pauw (1960) observed that each E_c prediction equation of the period tended to apply only to a specific narrow range of concretes (i.e. lightweight aggregate only or compressive strengths not exceeding 3,000 psi), and each equation consistently overpredicted concrete stiffness for higher values of compressive strengths. Citing a previously unpublished study, Pauw (1960) suggested that it may be more accurate to correlate concrete stiffness to the square root of concrete compressive strength—recognizing that this approach might help to curtail over-estimates of E_c for higher strength concretes. By empirically calibrating an E_c prediction equation to a compiled data set, Pauw demonstrated that an equation of the following form more accurately correlated concrete compressive strength to stiffness:

$$E_c = a\sqrt{f'_c} \quad (6-3)$$

where

a = empirically calibrated constant.

While the format of Equation 6-3 and the work of Pauw is still largely in use today in U.S. concrete design, European concrete practice has historically tended to correlate the modulus of elasticity of concrete to $\sqrt[3]{f'_c}$. Recently, Noguchi et al. (2009) examined the possibility of modifying the exponent of Equation 6-3 to increase the accuracy of modulus correlations. Results of the analysis of a large historical data set are shown in Figure 6-2.

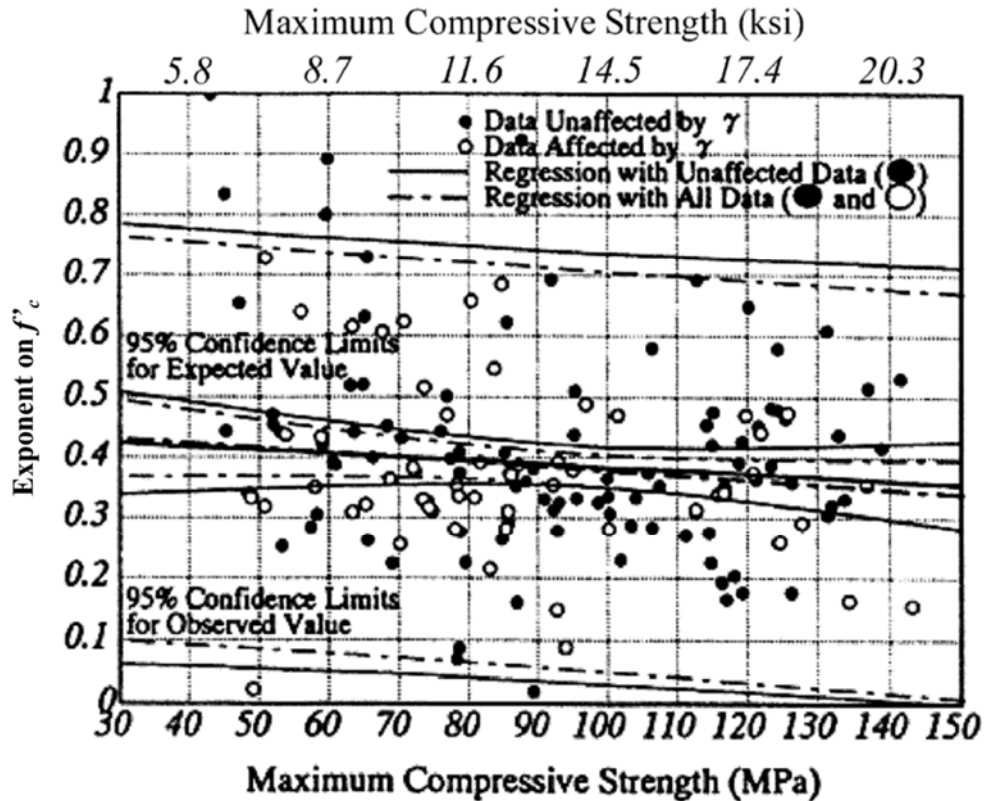


Figure 6-2: Experimental Results of Noguchi et al. (2009)

Noguchi et al. (2009) concluded that the ideal exponent on concrete compressive strength tends to decrease linearly from approximately 0.5 to approximately 0.3–0.4 for higher than typical concrete compressive strengths. Accordingly, Noguchi et al. proposed a revised prediction equation for U.S. practice that correlated concrete stiffness to $\sqrt[3]{f'_c}$, effectively mirroring European practice. Despite the motivation for the proposed change being very similar to that of Pauw in 1960 (correcting over-estimation of E_c for high-strength concretes), the work of Noguchi et al. has attracted little attention from the American concrete design community.

6.2.2.2 Unit Weight

In addition to suggesting the relationship to $\sqrt{f'_c}$, Pauw (1960) also postulated that concrete modulus of elasticity appeared to be a function of concrete weight. He reasoned that differences in concrete weights were primarily the result of voids within the concrete (either purposely entrained air or vesicles in lightweight aggregate), which would logically also affect concrete stiffness. By empirically exploring

correlations among concrete stiffness, unit weight, and compressive strength, Pauw (1960) proposed that concrete stiffness also correlated well to $w^{1.5}$, that is, the equilibrium unit weight of the hardened concrete at the time of testing (w) raised to the exponent of 1.5. The majority of Pauw's work examined structural lightweight aggregate, and as such, Pauw insisted that the unit weight in the above correlation be the equilibrium unit weight, otherwise known as the air-dry unit weight. While the difference between fresh unit weight and air-dry unit weight is negligible for normal-weight concrete, the air-dry unit weight can be up to 12 pcf less than the fresh unit weight for concrete made with lightweight aggregates (Neville 2013). Users of Pauw's prediction equations should be aware of the requirement¹⁴ to use the air-dry density in stiffness computations to provide more accurate estimates of elastic modulus for concrete with lightweight aggregate. Although other researchers since Pauw have proposed that the elastic modulus of concrete may better correlate to the square (exponent of 2.0) of the unit weight (Noguchi et al. 2009), data sets used in these revised analyses do not cover the range of unit weights represented by Pauw's compiled data set.

For the purposes of this report, a discussion of the unit weight of concrete mixtures typical of the precast, prestressed industry is warranted. Historically, the unit weight of plain concrete (excluding steel reinforcing) is most typically assumed to be 145 pcf for cast-in-place concrete applications and 150 pcf for precast concrete (Al-Omaishi et al. 2009). As an alternative, for cases when the 28-day strength of a concrete is known, Al-Omaishi et al. (2009) recommend the following expression for predicting unit weight, w , as a function of concrete compressive strength:

$$w = 0.140 + \frac{f'_c}{1000} \leq 0.155 \quad (6-4)$$

where

w = concrete unit weight (kcf); and

f'_c = concrete compressive strength (ksi).

Work by Keske (2014) and Storm et al. (2013) both independently confirmed the recommendation of Al-Omaishi et al. (2009) that designers of precast, prestressed concrete assume a unit weight of 150 pcf

¹⁴ ACI 318-14 (2014) does require the use of equilibrium unit weight in the computation of modulus of elasticity for lightweight concretes, as noted in the notation definitions of ACI 318-14.

in the absence of other information to account for the generally increased paste content of precast, prestressed concrete mixtures. Somewhat similarly, Hofrichter (2014) concluded that an assumed value of 152 pcf may be more appropriate based a review of historic precast, prestressed concrete mixture designs.

6.2.2.3 Aggregate Stiffness

Early research results published by Thoman and Raeder (1934) suggested that the modulus of elasticity of concrete varied with the coarse aggregate used. Work by Alexander and Milne (1995) also demonstrated the effect of aggregate type on the E_c of various concretes. Alexander and Milne (1995) concluded that stiffer concretes are likely to be produced using dolomite or andesite aggregates, while granite and quartzite aggregates tend to produce less stiff concretes. Later, Wu et al. (2001) concluded somewhat contradictory results, finding that quartzite aggregates tend to produce concretes with much greater stiffness than those of granite, limestone, or marble. The major conclusions of these early studies were qualitative in nature.

In 2003, as part of an effort to more accurately estimate prestress losses in pretensioned high-strength concrete bridge girders, Tadros et al. (2003) recognized that despite existing prediction equations for modulus of elasticity accounting for concrete compressive strength and unit weight, there still existed a rather large range of error in experimental data sets. Tadros et al. (2003) concluded that the remaining variation observed between predicted and measured E_c was primarily due to the regional effect of aggregate stiffness. Although this view is widely supported qualitatively in traditional literature (Neville 2013 and Mehta and Monteiro 2014), Tadros et al. (2003) appears to be the first to propose a multiplier, K_1 , used to modify elastic modulus predictions in high-strength concrete to account for the difference between national average and local average aggregate stiffness. In the related work of Tadros et al. (2003) and Al-Omaishi et al. (2009), the K_1 factor is referred to as an aggregate stiffness factor—without differentiating between the effect of coarse and fine aggregate. While some believe the effect of aggregate stiffness is primarily seen in coarse aggregate stiffness variations (Noguchi et al. 2009), others acknowledge the importance of the effect of variations in fine aggregate stiffness (Donza, Cabrera and

Irassar 2002; Limeria, Etxeberria and Molina 2011; Shi-Cong and Chi-Sun 2009). Aggregate stiffness factors have been widely studied and most typically range between 0.7–1.2. A full discussion of specific recent work on this topic is included in Section 6.2.3 of this report.

6.2.2.4 Use of Supplementary Cementing Materials

Alexander and Milne (1995) and Noguchi et al. (2009) also explored the effect of the use of varying supplementary cementitious materials (SCMs) on concrete elastic stiffness. Both researchers concluded that the effect of SCMs on E_c also varies according to aggregate type. Although Noguchi et al. (2009) did not track the relative SCM substitution percentages in their data set, they concluded that on average, mixtures containing fly ash tend to be approximately 10 percent stiffer than control mixtures and those mixtures containing silica fume and/or slag cement tended to be roughly 5 percent less stiff than control mixtures. Conversely, Alexander and Milne (1995) concluded that for mixtures with identical aggregates, substitution of silica fume tended to produce stiffer mixtures when compared to control mixtures while substitution of fly ash tended to produce less stiff mixtures. He (2013) provides an extensive discussion of this topic, ultimately citing previous research results tending to agree with those of Alexander and Milne (1995). The experimental efforts of the research program detailed in later sections of this chapter shed further light on this topic.

6.2.3 Available Prediction Equations

In this section, various available prediction equations for concrete modulus of elasticity are presented and discussed. These equations represent the most common relationships used by design engineers to correlate concrete stiffness to concrete compressive strength and other parameters. This section focuses primarily on those relationships most suited for use at the time of preliminary design and contains only a limited discussion of more detailed prediction equations. Many of the expressions reviewed herein contain calibration constants that can be used to tailor expressions to capture regional material variations relevant to E_c .

6.2.3.1 Pauw (1960) / ACI 318-14 / ACI 209 Method

As previously discussed, Pauw (1960) proposed an empirical relationship that correlated the modulus of elasticity of concrete to the square root of compressive strength and unit weight to the 1.5 power. The data set compiled by Pauw, shown in Figure 6-3, comprised mostly structural lightweight concretes with only 52 data points representing normal-weight concrete. The prediction equation recommended by Pauw, approximately represented by the linear regression displayed in Figure 6-3, is as follows:

$$E_c = 33w^{1.5}\sqrt{f'_c} \quad (6-5)$$

where

E_c = static elastic modulus of concrete (psi);

w = equilibrium unit weight of concrete (pcf); and

f'_c = concrete compressive strength (psi).

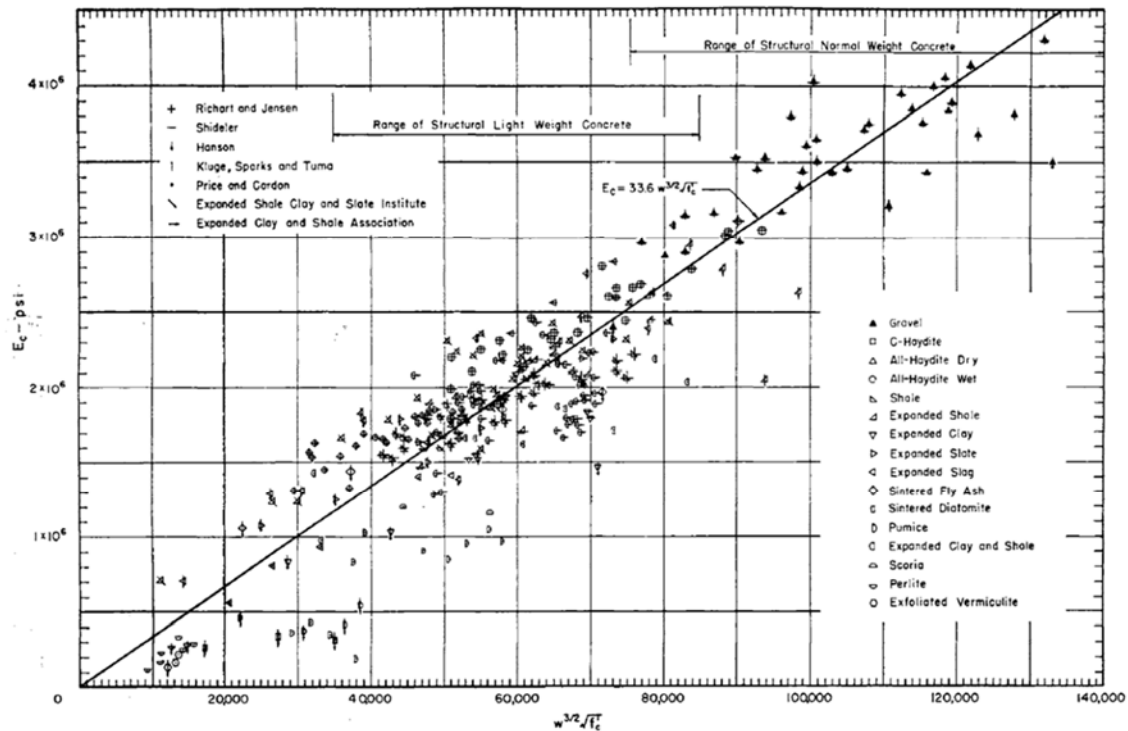


Figure 6-3: Historic Data Set Compiled by Pauw (1960)

Equation 6-5 in its original form is still specified in the building code requirements of ACI 318-14 (ACI Committee 318 2014) as well as in the guidance of ACI 209R-92 (ACI Committee 209 2008). While the original work of Pauw did not explicitly specify the appropriateness of the proposed equation for different

concrete ages, ACI 209R-92 clarifies that Equation 6-4 may be applied to concrete strengths at any given age (either known or estimated by the time-development expressions previously discussed in Section 5.2.3). Equation 6-5 can be further simplified to the form of Equation 6-3 by including an assumption of concrete unit weight, as is explored later in this chapter. Hinkle (2006), Brown (1998), and French and O'Neill (2012) recommended the use of Equation 6-5 for precast, prestressed concrete as a result of independent experimental work.

6.2.3.2 AASHTO LRFD (2014) / NCHRP Report 496 Method

As a result of work conducted by Tadros et al. (2003) as part of NCHRP research project 18-07, the following prediction equation for elastic modulus was adopted in the 2005 edition of the AASHTO LRFD Bridge Design Specifications:

$$E_c = 33,000 \cdot K_1 \cdot w^{1.5} \sqrt{f'_c} \quad (6-6)$$

where

E_c = static elastic modulus of concrete (ksi);

K_1 = correction factor for source of aggregate;

w = unit weight of concrete (kcf); and

f'_c = concrete compressive strength (ksi).

Equation 6-6 remains in its original form in the 2014 edition of the AASHTO LRFD Bridge Design Specifications (AASHTO 2014). With the exception of the inclusion of a K_1 factor to account for aggregate stiffness variations, Equation 6-6 is functionally identical to Equation 6-5, and therefore may be used with the same time-dependent strength growth provisions previously reviewed.

As part of the work of NCHRP Report 496, Tadros et al. (2003) also proposed an additional modifier, K_2 , intended to provide either an upper or lower-bound statistically-based value depending on the purpose of the computation. While an upper bound value corresponding to a 90th percentile would yield conservative results for a crack control analysis, a lower bound 10th percentile value may be more appropriate for prestress loss or deflection computations. Tadros et al. (2003) recommended various

empirically calibrated values for K_2 —although the lack of continuity among K_2 values calibrated for four geographic regions instills little confidence in the usefulness of this concept to designers. Recent research by Nervig (2014) and Storm et al. (2013) supported the use of Equation 6-6 for precast, prestressed concrete as a result of independent experimental work.

6.2.3.3 Carrasquillo et al. (1981) / ACI 363 Method

Noting that existing prediction methods of the time period tended to overestimate the stiffness of high-strength concrete by as much as 15 percent, Carrasquillo et al. (1981) proposed the following expression:

$$E_c = (40,000\sqrt{f'_c} + 10^6)(w_c/145)^{1.5} \quad (6-7)$$

Despite literature frequently claiming that Equation 6-7 is the preferred method of ACI 363R-10 (ACI Committee 363 2010), it is important to note that ACI 363R-10 presents eight differing prediction methods without showing clear preference for any particular one. However, to provide continuity with the work of previous researchers, Equation 6-7 is hereafter referred to as the ACI 363 method. Experimental work conducted by He (2013) has supported the use of Equation 6-7 for designers of precast, prestressed concrete.

6.2.3.4 *fib* Model Code 2010 Method

The provisions of the *fib* Model Code 2010 (*fib* 2010) are somewhat fundamentally different from the three previously reviewed prediction equations in two primary ways: (1) E_c is correlated to the cube root of concrete compressive strength instead of the square root and (2) the code includes a prediction equation intended only for use with 28-day concrete compressive strength values. While the first dissimilarity is of little consequence to this effort, the second makes it somewhat difficult to accurately predict the elastic modulus of a given concrete at the time of prestress release. To explicitly follow the requirements of the *fib* Model Code to compute E_c at prestress release as a function of expected concrete release strength¹⁵, it would seem that a designer must do the following:

¹⁵ An alternate approach is to rely on the prescribed 28-day overstrength by the *fib* Model Code in lieu of first estimating the expected concrete release strength and using the prescribed strength growth provisions. However, the later approach is included in the discussion above due to its similarity in form to the other prediction equations summarized in this section.

1. Estimate the expected concrete release strength for a given project (based perhaps on the recommendations of Chapter 5) or code-prescribed guidance;
2. Utilize a code prescribed strength growth method to project an expected 28-day compressive strength;
3. Compute the elastic modulus using a code-prescribed equation based off the result of Step 2; and
4. Utilize a code prescribed elastic modulus-growth method to estimate the E_c at the time of prestress release.

To further complicate matters, the strength- and modulus-growth parameters contained in the *fib* Model Code (used in Steps 2 and 4) rely on a metric of equivalent age-making it impractical to use the above procedure at the time of design without accurate knowledge of a future curing temperature profile of the concrete. While earlier iterations of this analysis conducted by Hofrichter (2014) on a limited data set attempted to accommodate the above requirements, the results proved no more accurate than the approximation of the above procedure discussed next. For these reasons, the above procedure is judged impractical for design purposes and, therefore, excluded from the remainder of the analysis effort in this chapter.

As an alternative to the above procedure, Rosa et al. (2007) suggested that the Model Code 2010 modulus prediction equation—although intended for use only with 28-day compressive strengths—be used to compute E_c at any age. This approach is analogous to U.S. practice, where Equations 6-5, 6-6, and 6-7 may be used for any given value of concrete compressive strength. After modifying accordingly and converting to U.S. Customary units, the Model Code 2010 prediction equation for elastic modulus is as follows:

$$E_c = 276,000 \cdot \alpha_E \cdot \sqrt[3]{f'_c} \quad (6-8)$$

where

E_c = static elastic modulus of concrete (psi);

α_E = aggregate correction factor (analogous to K_1); and

f'_c = concrete compressive strength (psi).

Recent research by Rosa et al. (2007) has supported the use of Equation 6-8 for precast, prestressed concrete as a result of experimental work.

6.2.3.5 Noguchi et al. (2009) Method

As a result of an examination of more than 3,000 relevant data points, Noguchi et al. (2009) proposed the following prediction equation for elastic modulus:

$$E_c = k_1 \cdot k_2 \cdot 4,860 \cdot \left(\frac{w_c}{150} \right)^2 \sqrt[3]{\frac{f'_c}{8.7}} \quad (6-9)$$

where

k_1 = correction factor for aggregate stiffness, and

k_2 = correction factor for supplementary cementing materials.

Simplifying Equation 6-9, assuming a unit weight of 150 pcf, and converting to equivalent units of Equation 6-8 gives:

$$E_c = k_1 \cdot k_2 \cdot 236,000 \cdot \sqrt[3]{f'_c} \quad (6-10)$$

where

E_c = static elastic modulus of concrete (psi);

k_1 = correction factor for aggregate stiffness;

k_2 = correction factor for supplementary cementing materials; and

f'_c = concrete compressive strength (psi).

It is interesting to note that the form of Equation 6-10 is similar to that of Equation 6-8 with a different coefficient.

6.3 Experimental Program

An experimental program was undertaken to compile a regionally robust data set of hardened concrete property data for use in evaluating existing E_c prediction equations and recommending the most suitable

equation for regional use in precast, prestressed applications. This effort consisted of both an in-plant¹⁶ testing effort and a companion laboratory phase, each of which are described separately in subsequent sections. While the concrete mixtures evaluated in the in-plant monitoring effort represented those mixtures used in commercial production of ALDOT bulb-tee products, the mixtures examined in the laboratory study, although similar, were intentionally proportioned to isolate the effect of certain key variables of interest. For the purposes of this work, no distinction is made between test data obtained from self-consolidating concrete (SCC) versus data obtained from vibrated concrete (VC). This is because (1) a designer is unlikely to know whether a product will be fabricated with SCC or CVC and (2) previous researchers established only a small difference in elastic modulus between SCC and VC (Keske 2014) independent of unit weight and compressive strength.

6.3.1 Laboratory Study

This report section details the efforts of a companion laboratory study completed as part of this research effort. While this laboratory effort was designed to yield data useful for both the analyses of this chapter (Chapter 6: Concrete Stiffness-Strength Relationships) as well as Chapter 7 (Creep and Shrinkage Behavior), only those parameters relevant to elastic modulus prediction are reported herein.

6.3.1.1 Summary of Work

In this laboratory study, six concrete mixtures were proportioned to represent typical mixtures currently used in Alabama precast, prestressed work. These six mixtures included three regional coarse aggregates and three varying combinations of supplementary cementing materials (SCMs) in typical substitution percentages. By maintaining a uniform target 18-hour compressive strength, uniform paste content, and uniform sand-to-total aggregate ratio (by volume) for all mixtures, it was possible to isolate certain key variables of interest in this study. Sampled specimens were exposed to either accelerated curing practices mimicking those of steam-curing methods used in precast, prestressed work or a standard curing protocol. Fresh concrete properties and hardened properties at various key ages of

¹⁶ Here the term in-plant is used to mean testing conducted by researchers on-site at a regional precast, prestressed concrete producer.

interest (18 hour, 24 hour, and 28 days) were tested in accordance with ASTM C39 (2010) and ASTM C469 (2010) for each mixture.

6.3.1.2 Concrete Mixtures and Raw Materials

Upon making the decision to supplement the in-plant testing work with a concurrent laboratory phase, the question arose as to whether ALDOT-approved mixtures should be prepared strictly from approved proportions or if there may be potential advantages to further tailoring approved mixtures in order to isolate certain key variables. Recognizing that it was unlikely the much smaller mixer of the laboratory (8 cubic foot volume) could impart similar mixing energy to the larger mixing equipment of field producers, it was decided that further tailoring of approved mixtures would be required regardless to yield similar concretes to those observed in the field. For this reason, it was decided that six concrete mixtures would be proportioned according to the following criteria:

- Laboratory mixtures should be similar to typical ALDOT-approved mixtures (as discussed in Section 4.4.3) while also satisfying the requirements of ALDOT 170-82 (ALDOT 2009);
- Laboratory mixtures should use constituent materials identical to those most frequently used (or anticipated to be used in the future) by field producers including:
 - Three regional coarse aggregates;
 - Three combinations of supplementary cementing materials (SCMs) along with a full Type III cement control mixture;
- Mixtures should achieve a uniform compressive strength at the time of prestress release (using accelerated curing practices typical of the local precast, prestressed industry) of approximately 6,700 psi as reported as the regional average by Hofrichter (2014); and
- Because these mixtures would later also be used for creep and shrinkage testing, all mixtures should have a uniform paste content and sand-to-total aggregate ratio (by volume).

As a consequence of the above criteria, the compressive strengths, while nearly identical at 18 hours, may vary differentially at other times of measurement. In addition, the water-cementitious materials ratio, w/cm , may vary between mixtures to account for different strength-development properties of various

SCMs and the requirement to preserve a uniform paste content. As a result of extensive trial batching, the six mixtures shown in Table 6-1 were successfully proportioned to meet the above criteria.

Table 6-1: Laboratory Phase Concrete Mixture Proportions

Mixture ID	Type III Cement (pcy)	Grade 120 Slag Cement (pcy)	Class F Fly Ash (pcy)	Silica Fume (pcy)	Water (pcy)	w/cm	Coarse Agg. (pcy)	Fine Agg. (pcy)	sand/total agg. (volume)	total agg. vol. (%)	paste vol. (ft ³ /cy)	HRWRA (oz/cwt)	HSA (oz/cwt)
DL-III	878	0	0	0	281	0.32	1,860	1,048	0.37	64	9.0	7.50	1
CL-III	878	0	0	0	281	0.32	1,860	1,048	0.37	64	9.0	7.75	1
GG-III	878	0	0	0	281	0.32	1,823	1,038	0.37	64	9.0	7.50	1
DL-SL	746	130 (15%)	0	0	278	0.32	1,860	1,048	0.37	64	9.0	6.75	1
DL-FA	754	0	132 (15%)	0	262	0.30	1,860	1,048	0.37	64	9.0	7.50	1
DL-FA/SF	606	0	142 (18%)	63 (8%)	276	0.34	1,860	1,048	0.37	64	9.0	7.75	1

Notes:

1. Percent substitutions noted for supplementary cementing materials (SCMS) are by weight of total cementitious materials.
2. High-range water reducer admixture (HRWRA) = Glenium 7700 and hydration-stabilizing admixture (HSA) = Masterset Delvo.
3. All aggregate weights in saturated-surface dry state.

The target 18-hour strength (accelerated cure), paste volume, and sand-to-aggregate ratio for the laboratory mixtures were determined by first preparing the DL-SL mixture. This mixture was closely based on an ALDOT-approved mixture used in a large percentage of precast, prestressed work within Alabama in recent years and seemed a logical choice to determine these target parameters. The DL-SL mixture contains a #67 dolomitic limestone, a #100 river sand, and a 15% (by weight) cement replacement with grade 120 slag cement. Next, the DL-III mixture was proportioned by (1) eliminating the slag cement substitution to arrive at a full cement mixture, and (2) modifying mixture proportions to meet the target 18-hour strength (while preserving uniform paste content and sand-to-aggregate ratio). The DL-III mixture uses the same #67 dolomitic limestone and #100 river sand as the DL-SL. Next, the proportions of the CL-III mixture were determined by trial batching. The CL-III mixture is essentially identical to the DL-III mixture, except the coarse aggregate is a different #67 dolomitic limestone. The proportions of GG-III were then determined in a similar manner—except the coarse aggregate included was a #67 crushed granite. Next, the proportions of the DL-FA and DL-FA/SF mixtures were determined by trial batching, both using the same #67 dolomitic limestone and #100 river sand as the DL-SL and DL-III mixtures. The DL-FA mixtures used a 15% by weight cement replacement with a Class F fly ash and the DL-FA/SF uses a ternary blend of 18% by weight cement replacement by Class F fly ash and 8% by weight silica fume.

The intent of the six mixtures described above (and shown in Table 6-1) was to isolate the effect of coarse aggregate types and SCM substitution on various hardened concrete properties. While it was judged impractical to include a fully expanded experimental matrix ($3 \times 4 = 12$ mixtures) as shown in Table 6-1, those combinations designated by a check mark were included in the experimental design. By comparing the relative effect of SCM variants on the DL-III control mixture, it was hoped that the effect of SCM substitution, if any, on the CL-III and GG-III mixtures could be estimated from experimental results.

Table 6-2: Experimental Matrix of Laboratory Mixtures

		Cement Replacement Variants			
		Type III Cement	15% Slag Cement Replacement	15% Class F Fly Ash Replacement	18% Class F Fly Ash and 8% Silica Fume Replacement
Coarse Aggregate Variant	DL	√	√	√	√
	CL	√			
	GG	√			

6.3.1.3 Mixture Preparation

Laboratory concrete mixing activities conducted as part of this research project were completed in accordance with the general requirements of ASTM C-192: *Standard Practice for Making and Curing Concrete Test Specimens in the Laboratory* (ASTM 2014). The specific mixing procedure employed for all mixtures was as follows:

1. Butter mixer
2. Add rock and sand
3. Start mixer on high speed
4. Add headwater (80%)
5. Mix for 2 minutes, stop mixer
6. Add cementitious materials, start mixer
7. Add tailwater (20%)
8. Add Hydration-stabilizing admixture (HSA)
9. Mix for 1 minute
10. Add high-range water reducer admixture (HRWRA) initial dose
11. Mix for 2 minutes
12. Rest for 3 minutes
13. Mix for 2 minutes
14. Sample fresh properties, if acceptable – done.
15. Re-dose HRWRA

16. Mix for 1 minute
17. Rest for 1 minute
18. Mix for 1 minute
19. Sample fresh properties, if acceptable – done.
20. Repeat 15-19 as necessary.

An important consideration in the laboratory mixing program was whether the above mixing procedure would generate sufficient mixing energy to break down the agglomerations of the bulk-densified silica fume typically used in field-batching of precast, prestressed concretes. While Holland (2005) notes that a modification to the mixing time noted in ASTM C192 can be used to ensure sufficient dispersion of bulk-densified silica fume for laboratory operations, changes to the above mixing durations for silica fume mixtures may be undesirable due to their potential alter mixture air content (and therefore potentially shift compressive strengths). To avoid this potential source of uncontrolled error, a density-controlled silica fume (a less dense form of silica fume) was selected for use for mixing operations to preserve the above mixing durations for all mixtures.

6.3.1.4 Sampling and Curing Procedures

For each mixing cycle, thirteen 6" x 12" cylinder specimens were sampled in accordance with ASTM C192. After initial set (approximately 4 hours after concrete production), ten of these cylinders were exposed to an elevated curing temperature profile by the use of a *SURECURE* control system, as shown in Figure 6-4. In accordance with the requirements of ALDOT 367 (ALDOT 2010) and typical practice observed plant production, specimens were exposed to a linearly increasing temperature profile (increasing at a rate of 20.5°F hourly) up to a maximum temperature of approximately 150°F.



Figure 6-4: SURECURE Jacket for Accelerated Curing

After the maximum temperature was reached (approximately 8 hours after sampling), this temperature was maintained through the time of cylinder testing—either 18 or 24 hours after mixing. Chapter 7 (Early-Age Creep and Shrinkage Behavior) includes computed maturities for each loading event. The three remaining 6" x 12" cylinder specimens were exposed to standard curing conditions in accordance with ASTM C192 (2014) until the time of testing at 28 days after production.

6.3.1.5 Fresh and Hardened Concrete Properties Testing Plan

As noted in the mixing procedure of Section 6.3.1.3, fresh properties including temperature, slump, air content, and unit weight were sampled for each mixing iteration performed in the laboratory. While fresh properties were mainly documented for quality-control purposes, the unit weight recorded for each

mixture is instrumental to the analysis efforts of this chapter. Where unit weights were not recorded (due primarily to equipment malfunction), estimates of unit weight were computed from mixture proportions and adjusted for measured air content.

The laboratory portion of this research effort was intended to simulate plant operations as closely as possible. Accordingly, two ages of simulated prestress release were selected based on the historical data set compiled by Hofrichter (2014) documenting the chronological time to prestress release for 1,917 girder concrete placement events. These two chronological ages were 18.0 hours (the approximate average of the primary peak of Figure 4-10) and 24.0 hours (an upper-bound value capturing 99.5 percent of the data of the same primary peak). At both of these ages, concrete compressive strength and modulus of elasticity were measured (in accordance with ASTM C39 and ASTM C469, respectively) for the accelerated-cured specimens. In addition, these same hardened properties were tested at 28 days for the cylinders receiving subjected to standard curing conditions. A concrete cylinder prepared for modulus of elasticity testing is shown in Figure 6-5.



Figure 6-5: Cylinder Prepared for Elastic Modulus Testing

6.3.1.6 Ungrouped Laboratory Data Set

The ungrouped data set compiled as a result of experimental effort described above is shown below in Figures 6-6 and 6-7. For the purposes of this section, both the 18-hour and 24-hour release measurements are combined. The measured relationship between modulus of elasticity and concrete compressive strength (independent of unit weight) is shown in Figure 6-6. Also shown for reference is the prediction equation proposed by Pauw (1960) assuming a unit weight of 150 pcf.

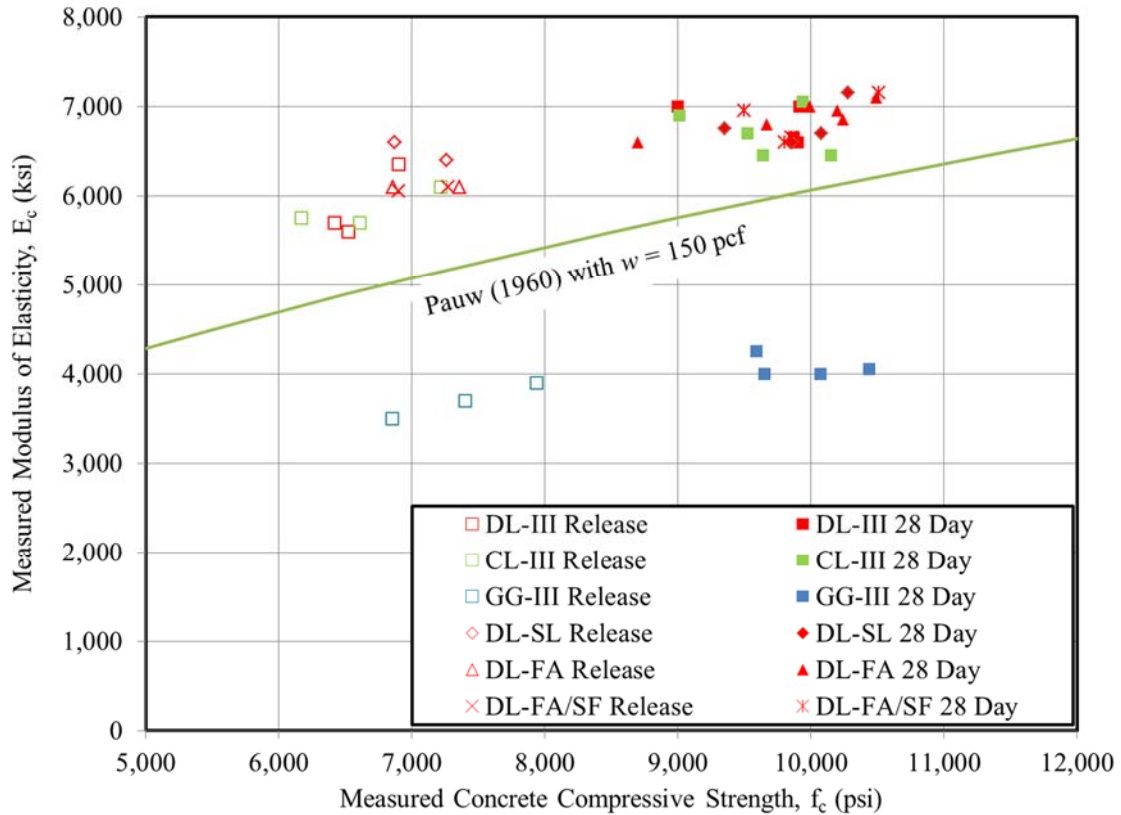


Figure 6-6: Ungrouped Stiffness-Strength Data from Laboratory Study Neglecting Effect of Unit Weight

The same data shown above is displayed in a somewhat different form in Figure 6-7. While the vertical axis remains the measured modulus of elasticity, E_c , the horizontal axis is now the quantity $(w^{1.5} f_c^{0.5})/10^3$. Recall, this is the method Pauw used (Figure 6-3) in order to perform a simple linear regression to determine the long-used coefficient of 33.0.

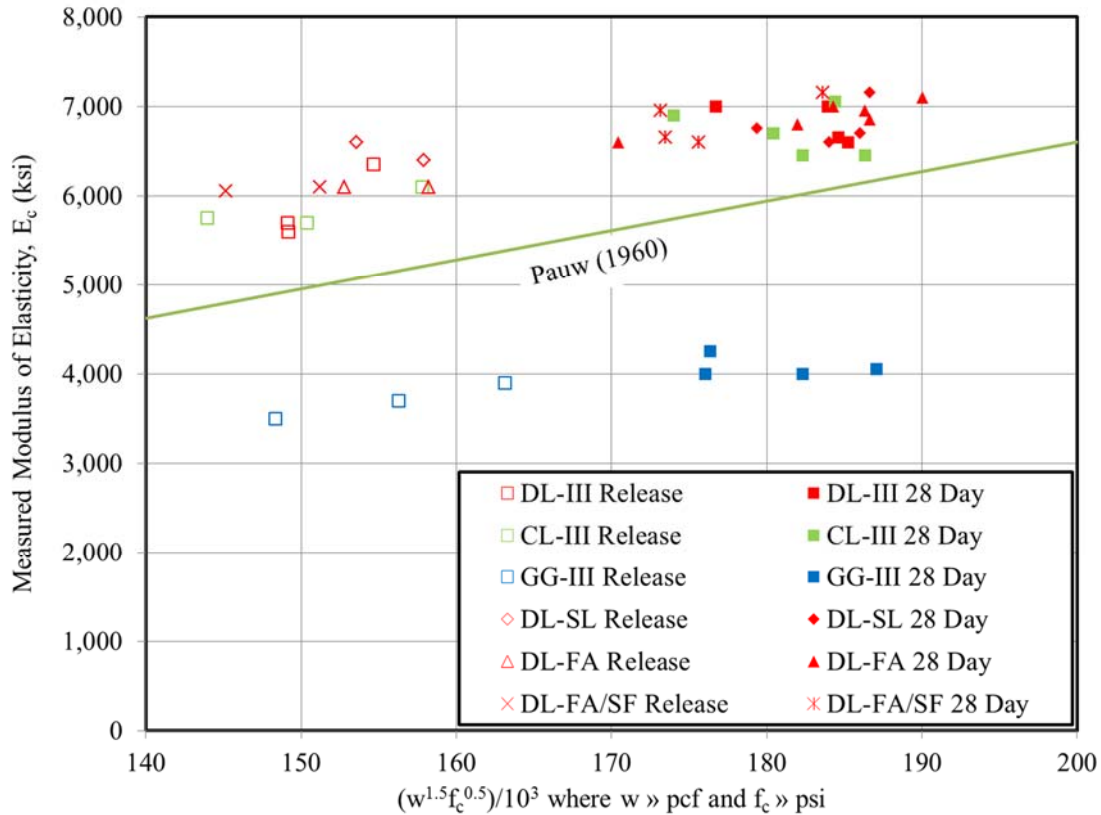


Figure 6-7: Raw Stiffness-Strength Data from Laboratory Study Including Effect of Unit Weight

6.3.2 Field Data Collection

The field data collection effort of this investigation consisted of in-plant monitoring of nine production cycles of ALDOT bulb-tee precast, prestressed concrete bridge girders occurring with the three year period spanning from 2012 to 2015. These in-plant efforts consisted of sampling fresh and hardened properties, the installation and monitoring of sensors in bridge girders both during and after fabrication, and measurement of girder cambers by surveying at various ages of interest. While select fresh and hardened properties of sampled girder concretes are discussed in this section, the remainder of the field-monitoring work is discussed in its entirety and used as a basis for comparison against girder behavior predictions in Chapter 10 of this report.

6.3.2.1 Summary of Work

In this field data collection effort, nine production cycles of ALDOT bulb-tee precast, prestressed bridge girders occurring at two different producers were monitored by researchers. For each production cycle, girder concretes were randomly sampled twice—at least once for every 50 cubic yard of production in

accordance with the requirements of ALDOT-367 (ALDOT 2015). Sampled specimens were then subjected to a variety of curing treatments (including steam field curing, standard lime-bath curing, field lime-bath curing, and selected combinations thereof) until the time of hardened property testing. Testing for compressive strength and modulus of elasticity (in accordance with ASTM C39 and ASTM C469, respectively) was conducted at (1) the time of field girder release, (2) 24 hours after girder production, and (3) 28 days after girder production. Research procedures were designed to minimize impact on the typical girder production cycle.

6.3.2.2 Mixtures and Raw Materials

Girder concretes for the field-monitored projects were produced by precast, prestressed producers using typical production practices and mixtures with no influence from the research team. Mixture proportions for the field-monitored projects are summarized in Table 6-3. The mixture used by Plant C in field production most closely resembled the DL-FA/SF mixture of the laboratory portion of this study. Both mixtures contained a crushed dolomitic limestone coarse aggregate, a #100 natural sand, and preserved similar ratios of sand-to-total aggregate (by volume), total aggregate volume (percent), and paste volume. However, the mixture used by Plant C in field production had a lower w/cm than the laboratory mixture (0.27 versus the 0.34) and used a #78 dolomitic limestone instead of the #67 used in the DL-FA/SF laboratory mixture. The mixtures used by Plant A in production cycles 2-6 and 7-9, respectively, most closely resembled the laboratory mixture DL-SL. In fact, by virtue of the DL-SL being based off earlier iterations of the field mixtures used by Plant A, these three mixtures were essentially identical—containing equal proportions of Type III cement, Grade 120 slag cement, #67 dolomitic limestone, #100 natural sand, and water.

While the field monitoring effort of this study allows for comparisons between only the two types of mixtures shown in Table 6-3 (essentially the DL-SL and DL-FA/SF mixtures), the laboratory study allows for comparisons to be among a range of mixtures (DL-FA, DL-III, CL-III, and GG-III) that either have historically been used or could be used in the future for precast, prestressed concrete production within Alabama.

Table 6-3: Mixture Proportions for On-site Production Cycles

Mixture ID	Type III Cement (pcy)	Grade 120 Slag Cement (pcy)	Class F Fly Ash (pcy)	Silica Fume (pcy)	Water (pcy)	w/cm	Coarse Agg. SSD (pcy)	Fine Agg. SSD (pcy)	sand/total agg. (volume)	total agg. vol. (%)	paste vol. (ft ³ /cy)	HRWRA #1 (oz/cwt)	HRWRA #2 (oz/cwt)	HSA (oz/cwt)
Plant C (Field Production Cycle 1)	745	0	135 (14%)	75 (8%)	258	0.27	1,665 (#78 Dolomitic Limestone)	1,085 (#100 River Sand)	0.40	61	9.4	5.25	N/A	1.25
Plant A (Field Production Cycles 2-6)	751	133 (15%)	0	0	282	0.32	1,861 (#67 Dolomitic Limestone)	1,048 (#100 Natural Sand)	0.37	62	9.1	6.0	4.50	1.0
Plant A (Field Production Cycles 7-9)	751	133 (15%)	0	0	277	0.31	1,861 (#67 Dolomitic Limestone)	1,048 (#100 Natural Sand)	0.38	63	9.0	9.0	N/A	1.0

Notes:

1. Percent substitutions noted for supplementary cementing materials (SCMS) are by weight of total cementitious materials.
2. Plant C (All Cycles): HRWRA #1 = Glenium 7700 and HSA = Pozzolith 100-XR.
3. Plant A (Cycles 2-6): HRWRA #1 = ADVA Cast 575, HRWRA #2 = ADVA Cast 555, HSA = Recover
4. Plant A (Cycles 7-9): HRWRA #1 = Glenium 7700, HSA = Delvo

6.3.2.3 Sampling and Curing Procedures

The sampling effort detailed herein is independent and in addition to that completed by the producer and ALDOT quality control personnel. For each on-site production cycle, the research team randomly sampled two sets of thirteen 6" x 12" cylinders (26 cylinders total) in accordance with ASTM C31 (ASTM 2009). Twenty of the sampled cylinders were stored within the girder formwork and exposed to the field steam curing of the girder product. The other six cylinders were immediately transported to the on-site testing laboratory after completion of sampling and exposed to standard curing conditions by immersion in a lime-saturated water bath regulated to 73.5°F. At the time of form removal, the 20 field-cured cylinders were transferred into a preheated lime-saturated water bath¹⁷ to allow for a gradual transition to ambient temperature until the time of testing.

6.3.2.4 Fresh and Hardened Concrete Properties Testing Plan

Upon delivery of the concrete from the on-site mixing facility, fresh properties (including temperature, slump, and air content) were tested by plant quality control and ALDOT personnel to determine the acceptability of the concrete batch in accordance with the requirements of ALDOT 367 (ALDOT 2010). Due to the large number of concurrent activities required to be completed by researchers, it was not possible to measure the unit weights of the girder concretes during production and thus, unit weights used in the analyses of this chapter are computed based on ALDOT-approved mixture designs and adjusted for measured air content.

The timing of prestress release was determined by plant and ALDOT personnel. At the approximate time of prestress release, concrete compressive strength and modulus of elasticity were tested by the researchers for the first set of sampled cylinders (3 cylinders per sampling location = 6 cylinders total). Approximately 6 hours thereafter (at a time of 24 hours after girder production), compressive strength and modulus of elasticity were again tested for a second set of sampled cylinders (3 cylinders per sampling location = 6 cylinders total). The two remaining cylinder sets (6 field cure + 6

¹⁷ The method used for preheating the field lime-saturated water bath was to store the bath adjacent to the girder product under the tarp during steam curing. This practice resulted in varying temperatures of the lime-saturated water bath, but resulted in temperatures approaching those of the girder concrete for a given placement event.

standard cure = 12 cylinders total) were transported back to the laboratory for compressive strength and modulus of elasticity testing at the age of 28 days. Once transported back to the laboratory, field-cured cylinders were stored in a covered outdoor lime-saturated bath (to capture relative ambient temperature variations similar to those experienced by the actual girders) while standard-cure cylinders were stored in a moist room until the time of testing.

6.3.2.5 Field Data Set

The data set compiled as a result of the experimental effort described above is shown in Figures 6-8 and 6-9. As shown, there is significantly more variation in the strengths observed for the plant-produced concrete than for the laboratory concrete. The E_c prediction equation recommended by Pauw (1960) is also shown for reference.

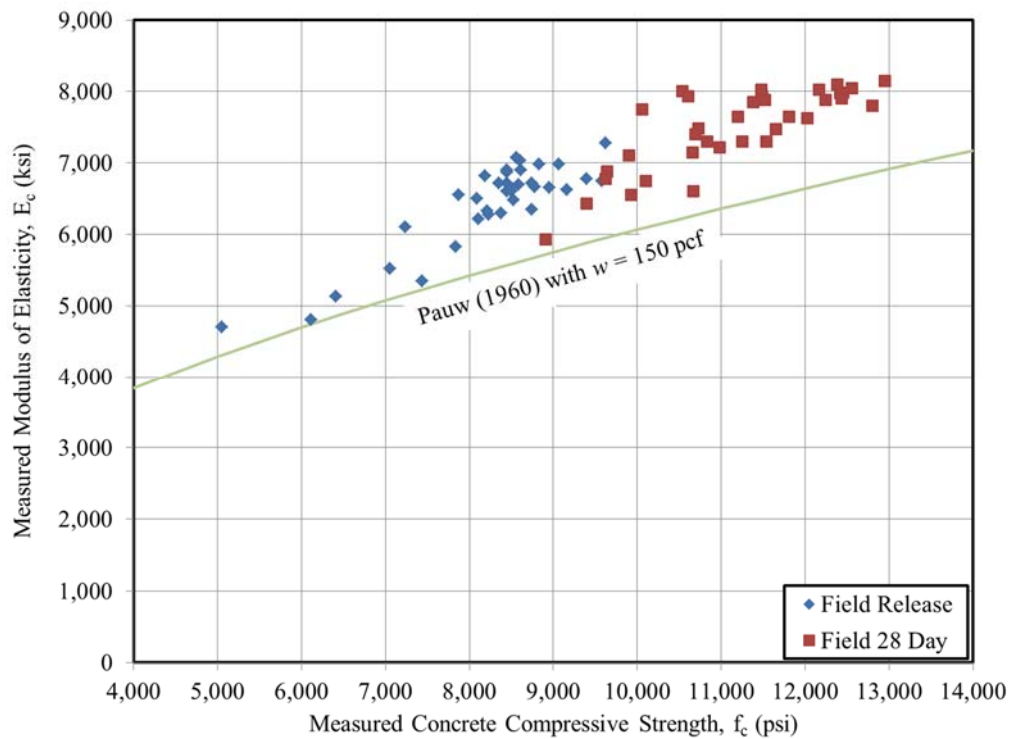


Figure 6-8: Stiffness-Strength Data from Field Study Neglecting Effect of Unit Weight

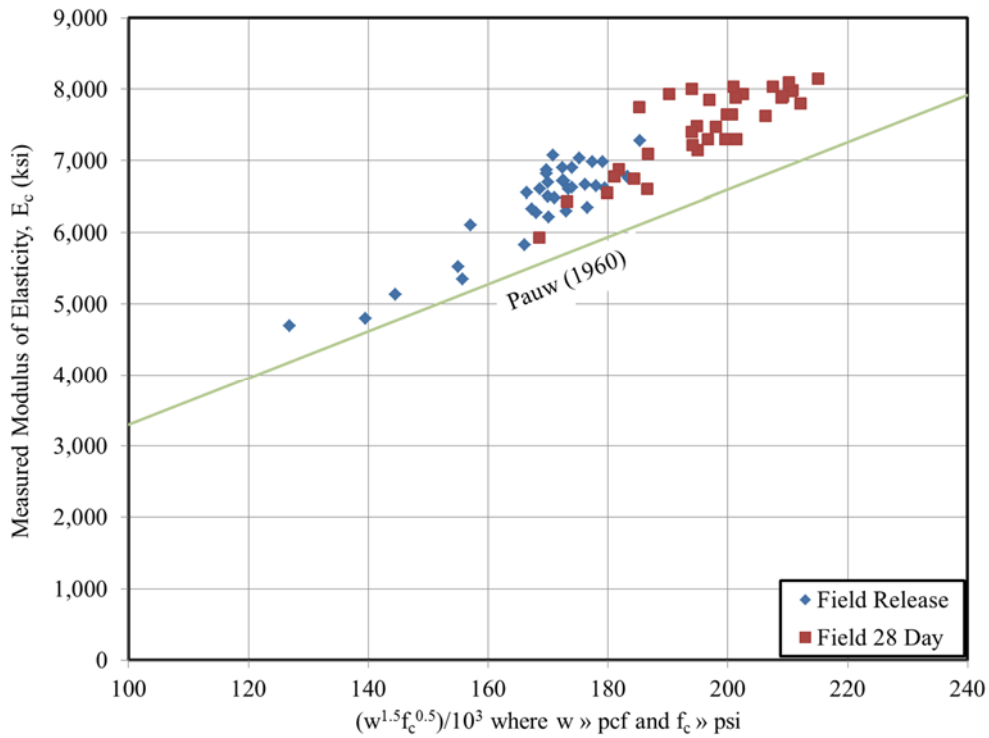


Figure 6-9: Stiffness-Strength Data from Field Study Including Effect of Unit Weight

6.3.3 Additional Data Sources

As a result of the experimental efforts detailed in the laboratory phase of this project and the in-plant testing phase, 110 elastic modulus data points were compiled. While this sample represents a relatively robust data set, two researchers (Keske 2014] and Boehm et al. [2010]) previously gathered similar field data as part of independent experimental efforts. This section provides a brief summary of the experimental efforts and data collection techniques employed by Keske (2014) and Boehm et al. (2010) to compile their respective data sets.

6.3.3.1 Keske (2014)

As part of the experimental effort to investigate the differences between SCC and VC in precast, prestressed bridge girders, Keske (2014) monitored 13 girder placement events at Plant A—conducting hardened material property testing (both compressive strength and E_c) at the time of prestress release and 28 days after casting. Sampled cylinder specimens were field cured (within the girder formwork) until the time of prestress release. Specimens were then exposed directly to ambient conditions until the time of 28-day testing. In this project, two sampling locations were selected for each placement event—

yielding a total of 26 additional data points useful to the stiffness-strength analysis performed later in this chapter.

6.3.3.2 Boehm et al. (2010)

Prior to the work of Keske (2014), Boehm et al. (2010) monitored a girder production effort at Plant A as part of a study aimed at evaluating the structural performance of SCC in precast, prestressed bridge girders. Cylinder sampling and curing methods were identical to those used by Keske (2014), resulting in a total of 12 data points useful to supplement the data set used in this chapter.

6.3.4 Complete Compiled Data Set For Stiffness-Strength Analysis

The full data set compiled as a result of the work described in Sections 6.3.1 through 6.3.3 consists of 148 total data points as shown in Figures 6-10 and 6-11. This complete data set is also included in Mante (2016) for reference.

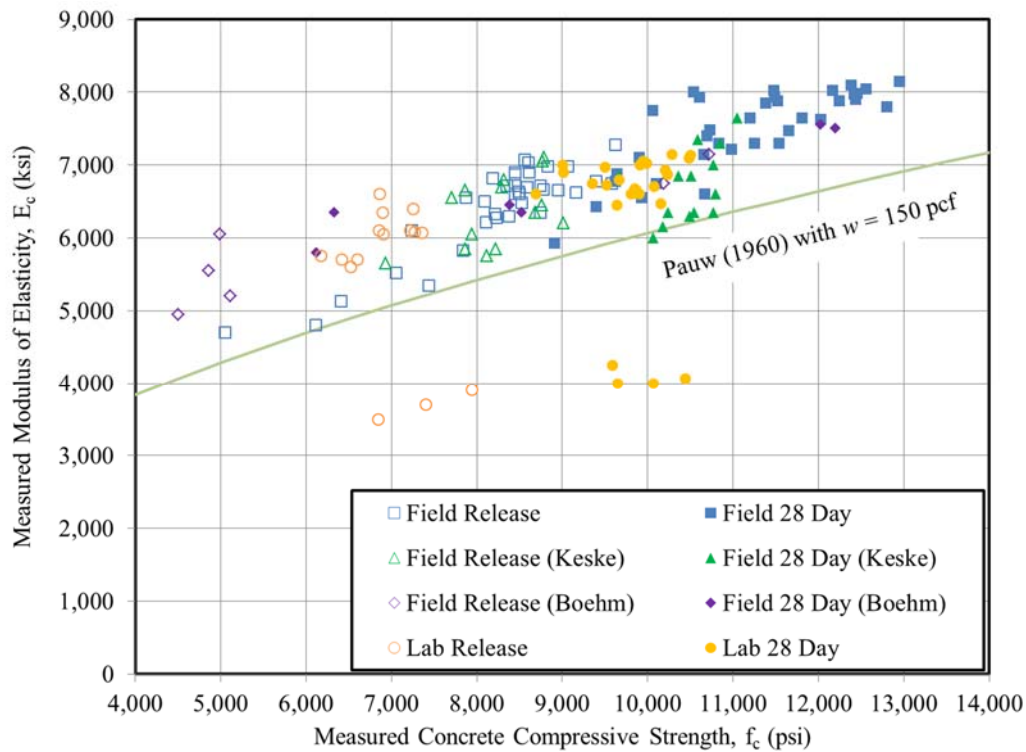


Figure 6-10: Stiffness-Strength Data Neglecting Effect of Unit Weight

The data set shown in Figures 6-10 and 6-11 represents a wide range of compressive strengths and appears to be a relatively robust regional data set.

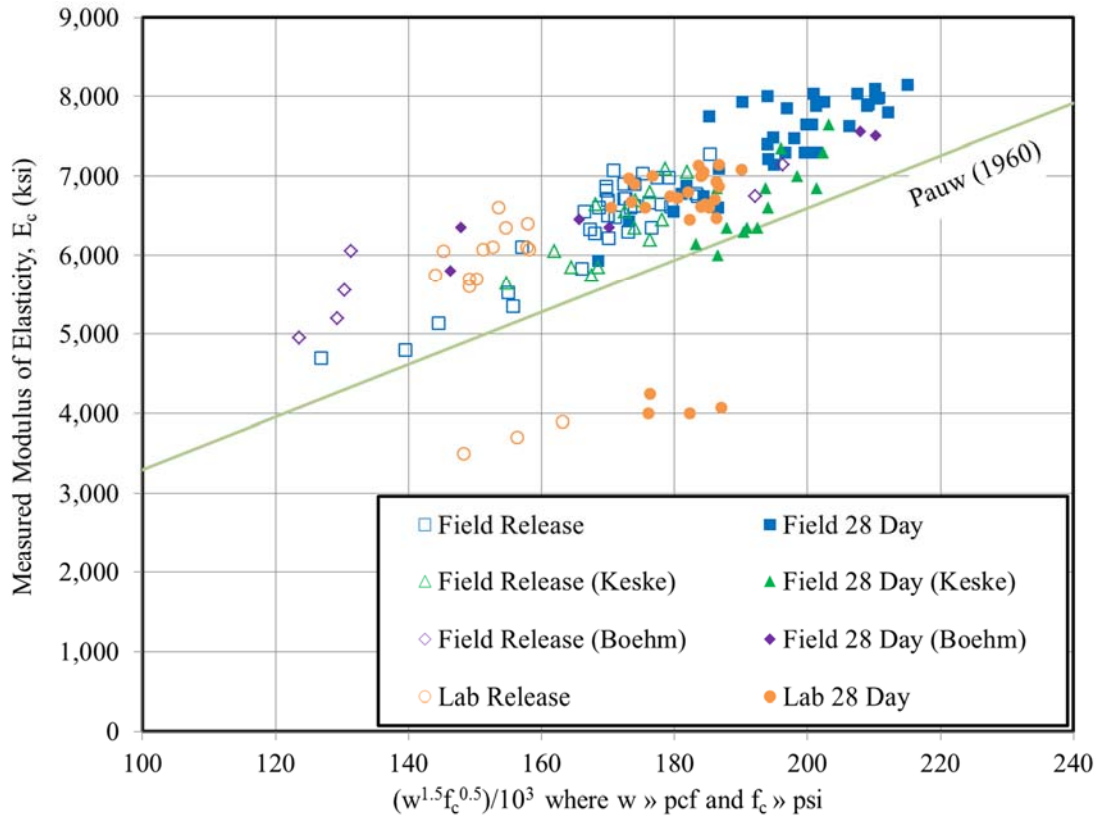


Figure 6-11: Stiffness-Strength Data Including Effect of Unit Weight

6.4 Presentation and Analysis of Results

This section details the methodology used to analyze the compiled stiffness-strength data set. First, a preliminary statistical analysis is performed on selected variables of the raw data set to establish logical groupings for use in the remainder of the analysis of this chapter. Then, for each grouping, the experimental data set is used to appropriately calibrate any of the four previously discussed prediction models capable of calibration. Finally, the results of the prediction equations for E_c are compared to the measured data in an effort to identify the most accurate prediction equations for use by designers. A brief discussion follows the analysis, identifying an uncontrolled variable in the project that may be responsible for an unexpected trend observed in both this research project and previous work by others.

A brief discussion on the analysis approach selected in this study is warranted. Recall, the goal of this work is to identify the E_c prediction equation most appropriate for use in predicting the stiffness of concrete typical of precast, prestressed concrete elements. A common approach by previous researchers (in the absence of a standardized test method) is to (1) generate or compile a data set similar

to that of this study, (2) select an E_c prediction equation—most commonly the AASHTO LRFD Equation in American practice, and (3) calibrate the candidate equation by selecting a value of K_1 providing the best agreement between predicted and measured modulus values. While this is a convenient approach, this methodology does little to explore the correctness of the mathematical form of the prediction equation and also tends to incorrectly attribute all prediction error to the aggregate stiffness correction factor, K_1 . This practice may be partially unavoidable, it is a troublesome flaw of not having a standardized test method to calibrate K_1 factors. Other researchers (e.g. Hofrichter 2014) have attempted to calibrate the AASHTO LRFD Equation to specified strength levels, f'_c , instead of measured strength levels, f_c . This practice results in a “calibrated” K_1 aggregate stiffness factor that incorrectly includes the effect of strength amplification (as discussed in Chapter 5 of this report). The inconsistencies discussed above make it difficult and unreliable to compare K_1 factors as calibrated by previous studies.

In an effort to avoid the complications discussed above, the following precautions have been taken in this research effort: (1) the effect of overstrength (as explored in Chapter 5) is wholly decoupled from the Chapter 6 efforts of calibrating stiffness prediction equations, and (2) a variety of prediction models are first calibrated to the experimental data (by linear regression) and then evaluated for relative accuracy by a comparison of the standard error of the estimate (SEE). Using this approach not only facilitates accurate calibrations of existing prediction equations to the experimental data set, but also allows for comment on the relative correctness of the mathematical form of the four candidate prediction equations explored herein.

6.4.1 Preliminary Analysis and Data Groupings

Prior to calibrating the candidate prediction equations, it was first necessary to perform an analysis of the raw data set to identify statistically significant variables for grouping. The final data set (as shown in its final form in Mante [2016]) consisted of 148 data points each including time of measurement, coarse aggregate type, curing method, unit weight, measured compressive strength, and measured modulus of elasticity. While convenient to have so many variables in the data set, it made it difficult to perform a statistical analysis involving the variables suspected to be significant. It was decided that a single

coefficient would be computed to represent a hypothesized relationship between unit weight, compressive strength, and E_c for each data point. Rearranging a portion of Pauw's expression (Equation 6-5), the following coefficient, c , was computed for each data point:

$$c = \frac{E_{c,measured}}{\left(\frac{w_{measured}^{1.5} \sqrt{f_{c,measured}}}{1000} \right)} \quad (6-11)$$

Where

$E_{c,measured}$ = measured modulus of elasticity for a given data point (ksi);

$w_{measured}$ = measured unit weight for a given data point (pcf); and

$f_{c,measured}$ = measured compressive strength for a given data point (psi).

The c value of Equation 6-11 represents the calibrated coefficient of Pauw's equation, equal to a value of 33 from his analysis. The use of Pauw's empirical relationship here is an analytical technique to allow simplification of this statistical analysis. By comparing the relative values of the coefficient c for varying experimental treatments, standard statistical tests (i.e. two-sample two-sided t-tests and ANOVA-tests) may be used to identify statistically significant groupings of the data set.

The first hypothesis explored using this technique was that the type of coarse is a statistically significant predictor of elastic modulus. Using the three hypotheses shown in Table 6-4 (1a to 1c) and the corresponding statistical tests of the compiled data set, there was strong evidence (at a significance level of $\alpha = 0.05$) that the mean of the coefficient c for concrete mixtures with dolomitic limestone was different than for those mixtures with crushed granite.

Table 6-4: Effect of Coarse Aggregate Type on Elastic Modulus

Null Hypothesis:	Result ($\alpha = 0.05$)
1a. The difference in means of the coefficient c between concrete mixtures produced using dolomitic limestone and crushed granite is zero for the entire data set.	Reject ($p \leq 0.001$) (paired t-test assuming unequal variances)
1b. The difference in means of the coefficient c between concrete mixtures produced using dolomitic limestone and crushed granite is zero for the release data set.	Reject ($p \leq 0.001$) (paired t-test assuming unequal variances)
1c. The difference in means of the coefficient c between concrete mixtures produced using dolomitic limestone and crushed granite is zero for the 28-day data set.	Reject ($p \leq 0.001$) (paired t-test assuming unequal variances)

The above hypothesis testing suggested that the compiled data set should be divided by coarse aggregate type for the remainder of analysis efforts.

The next question was whether the time of measurement of a data point (either at prestress release or 28 days) was a significant variable in predicting E_c of a given concrete. For this purpose, the statistical procedure outlined in Table 6-5 was used—essentially comparing the likelihood that the mean value of the coefficient c was identical for the two ages of testing.

Table 6-5: Effect of Time of Measurement on Elastic Modulus

Null Hypothesis:	Result ($\alpha = 0.05$)
2a. The difference in means of the coefficient c between the time of release and 28 days is zero for concrete mixtures using dolomitic limestone.	Reject ($p = 0.005$) (paired t-test assuming unequal variances)
2b. The difference in means of the coefficient c between the time of release and 28 days is zero for concrete mixtures produced using crushed granite.	Fail to Reject ($p = 0.13$) (paired t-test assuming unequal variances)

Note: For hypothesis 2b, $n=3$ and 4 , respectively, making the results questionable due to small sample size.

The analysis of hypothesis 2a affirmed strong statistical evidence that the coefficient c differed between the two measurement ages considered for concretes produced using dolomitic limestone. A similar analysis conducted for the crushed granite aggregate (hypothesis 2b) however, failed to detect a significant difference in means between testing ages. Due to the extremely small sample sizes available for use in hypothesis 2b ($n=3$ and $n=4$), the validity of this analysis is questionable. To be conservative, it was assumed that the failure to detect a difference in analysis 2b may be a Type II statistical error caused

by the small sample size. As a result of the work summarized in Table 6-5, the stiffness-strength data set is grouped by time of measurement for the analysis efforts of the remainder of this chapter.

Another logical question to explore prior to combining the data compiled from four independent efforts was if curing method was a significant factor in predicting concrete stiffness. Because different curing regimes were only used for the 28-day time of testing, the analysis summarized in Table 6-6 focuses only on this measurement time.

Table 6-6: Effect of Curing Conditions on Elastic Modulus

Null Hypothesis:	Result ($\alpha = 0.05$)
3a. The difference in means of the coefficient c at 28 days among the four curing conditions is zero for concrete mixtures using dolomitic limestone.	Reject ($p \leq 0.001$) (ANOVA single factor)
3b. The difference in means of the coefficient c at 28 days among the three curing conditions (omitting that used by Keske [2014] and Boehm et al., [2010]) is zero for concrete mixtures using dolomitic limestone.	Fail to Reject ($p = 0.37$) (ANOVA single factor)

Using two ANOVA single factor tests with varying input groupings, it was affirmed that, for concretes containing dolomitic limestone aggregate, there existed strong statistical evidence that the means of the coefficient c differed between (1) the work of Keske (2014) and Boehm et al. (2010) and (2) the experimental work conducted in this research study. However, it is also important to note that the work of Keske (2014) and Boehm et al. (2010) included SCC in addition to VC, while the experimental work conducted in this research effort included only VC. The work reflected in Table 6-6 suggests that either (1) curing method (specifically, the difference between air-dried specimens versus all other moist curing methods used in this work) is likely a statistically significant predictor of concrete stiffness, (2) the difference detected above is due to differences between the elastic modulus of SCC and VC, or (3) a combination thereof. For the purposes of this project, the above difference was disregarded in order to provide a data set including both VC and SCC mixtures—as is likely most representative of the precast, prestressed industry in Alabama in future years.

A final consideration for grouping of data was to investigate if the presence of varying supplementary cementing materials (SCMs) was a significant predictor of the variability in E_c . For this

purpose, the subset of the stiffness-strength data set generated by the controlled laboratory portion of this study was examined as shown in Table 6-7.

Table 6-7: Effect of Supplementary Cementing Material (SCM) on Elastic Modulus

Null Hypothesis:	Result ($\alpha = 0.05$)
4a. The difference in means of the coefficient c at the time of release for the four variants of supplementary cementing materials (SCMs) is zero for concrete mixtures produced in the laboratory using dolomitic limestone.	<i>Fail to Reject</i> ($p = 0.27$) (ANOVA single factor)
4b. The difference in means of the coefficient c at 28 days for the four variants of supplementary cementing materials (SCMs) is zero for concrete mixtures produced in the laboratory using dolomitic limestone.	<i>Fail to Reject</i> ($p = 0.51$) (ANOVA single factor)

Note: For hypothesis 4a/b, results are questionable due to small sample size.

At both times of measurement, differences in the means of the coefficient c were unable to be detected as a result of the use of varying supplementary cementing materials. Due to the small sample sizes available for these analysis ($n=3$ and $n=4$ typically), the failure to detect a statistical difference by varying SCM shown in Table 6-7 is regarded as inconclusive—as opposed to a clear conclusion that varying SCM does not influence concrete stiffness. A study by Brooks (1999) similarly concluded that SCM usage in modest replacement percentages failed to cause an appreciable effect on E_c .

In summary, preliminary statistical manipulation of the stiffness-strength data set confirmed that it is logical to group the compiled data set by both aggregate type and time of testing for analysis purposes. This grouping approach is used in the analysis of Section 6.4.2 (Concrete Stiffness at Prestress Release) and the analysis of Section 6.4.3 (Concrete Stiffness at 28 Days).

6.4.2 Concrete Stiffness at Prestress Release

This section details the analysis conducted in order to provide a recommendation of the most appropriate modulus of elasticity prediction equation for use during preliminary design to estimate the elastic stiffness at the time of prestress release. The analysis procedure used in this Section is outlined in Figure 6-12.

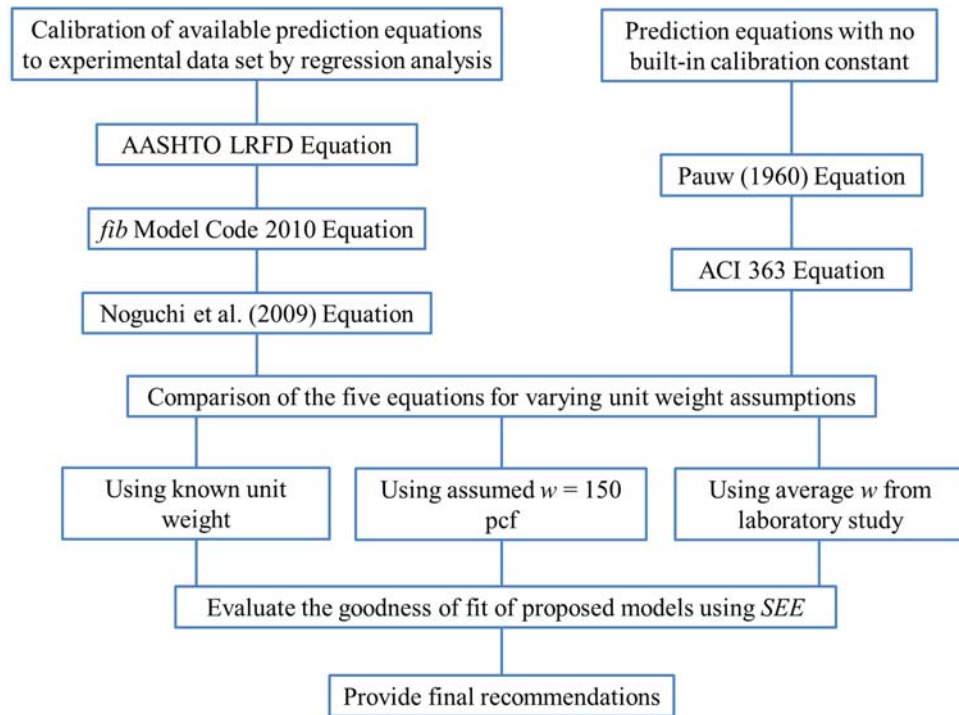


Figure 6-12: Analytical Procedure for Stiffness-Strength Data Set

As noted, first the three prediction equations that include potential calibration constants (AASHTO LRFD, *fib* Model Code 2010, and Noguchi et al. [2009]) are calibrated to the experimental data set. Next, the accuracy of the five available prediction equations is evaluated using the standard error of the estimate (SEE) for differing assumptions of unit weight.

6.4.2.1 Calibration of AASHTO LRFD Equation

The AASHTO LRFD prediction equation, as used in this report, is calibrated in practically the same way Pauw (1960) empirically calibrated his equation. The experimental data for E_c at the time of prestress release, grouped by aggregate type, is shown below in Figure 6-13.

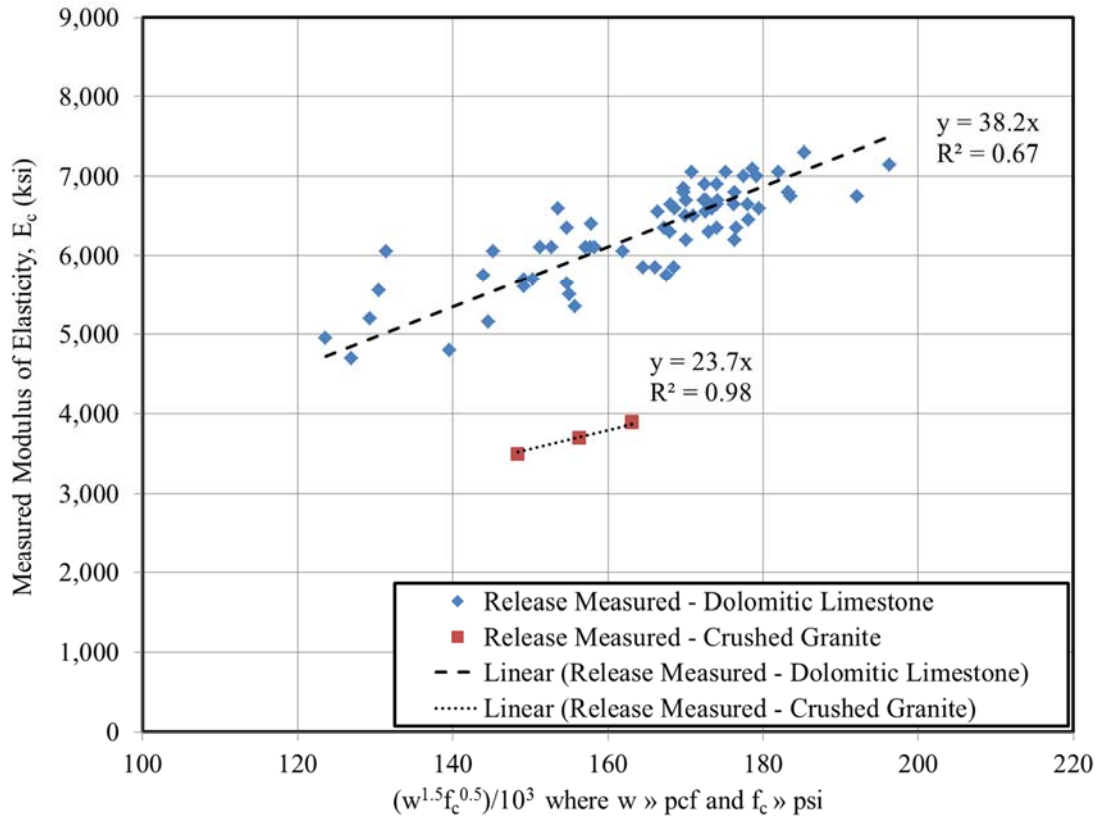


Figure 6-13: Calibration of AASHTO LRFD Equation for Prestress Release

Presenting the data on these axes allow for the use of a simple linear regression to calibrate the prediction equation. As shown, the appropriate coefficient for dolomitic limestone and crushed granite at the time of prestress release are 38.2 and 23.7, respectively. To determine the appropriate K_1 factor for each aggregate type, the previously noted coefficients need simply be divided by 33.0, yielding $K_1 = 1.16$ for dolomitic limestone and $K_1 = 0.72$ for crushed granite at the time of prestress release. While the value for dolomitic limestone ($K_1 = 1.16$) agrees with typical ranges referenced by Mehta and Monteiro (2014) and the Model Code 2010 (fib 2010) for dense limestone aggregates, the calibrated value for crushed granite ($K_1 = 0.72$) is less than the $K_1 = 1.0$ typically expected for quartzitic aggregates (Mehta and Monteiro 2014). The topic of the crushed granite aggregate exhibiting less than expected stiffness is addressed in Section 6.4.5.

6.4.2.2 Calibration of *fib* Model Code 2010 Equation

In similar fashion to above, the *fib* Model Code 2010 prediction equation was also calibrated by a simple linear regression analysis as shown in Figure 6-14. By dividing the slope of the regression lines for each aggregate type by the leading coefficient of Equation 6-7, α_E values of 1.15 and 0.69 are computed for dolomitic limestone and crushed granite, respectively.

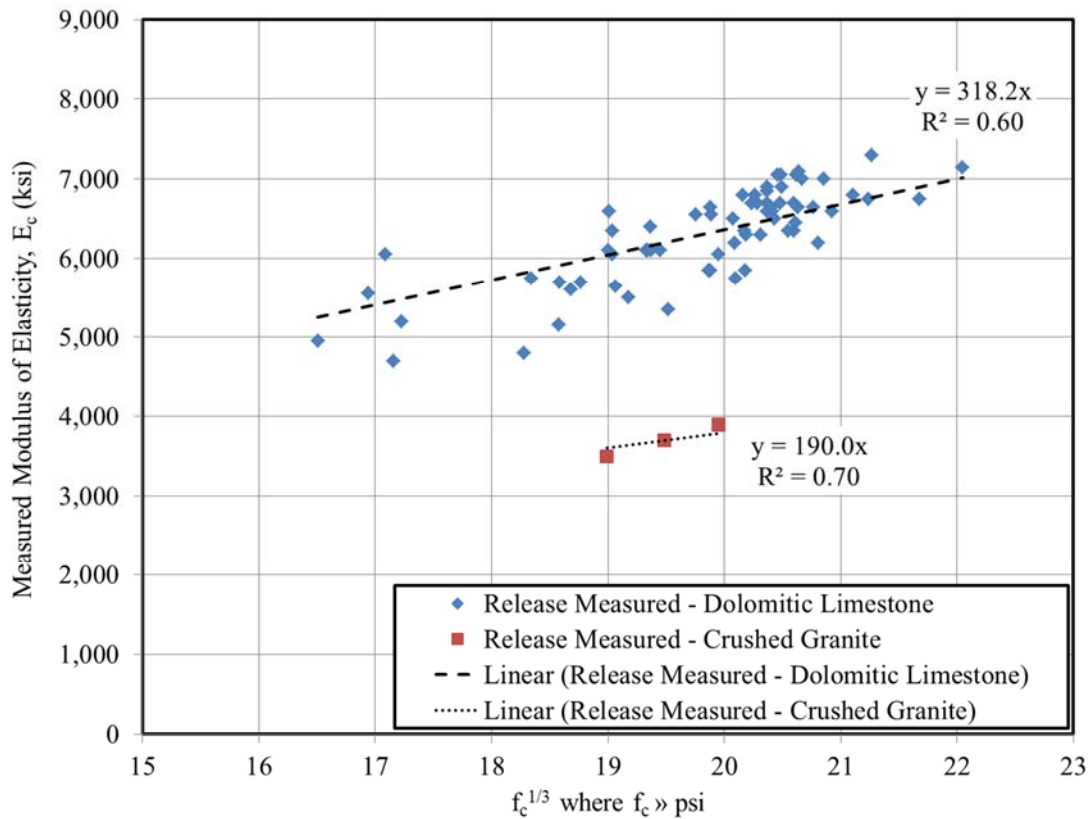


Figure 6-14: Calibration of *fib* Model Code 2010 for Prestress Release

6.4.2.3 Calibration of Noguchi et al. (2009) Equation

Finally, the Noguchi et al. (2009) prediction equation is calibrated in a similar manner. Recall, this prediction equation has two calibration factors— k_1 that accounts for the effect of aggregate stiffness variations and k_2 that accounts for the effect of supplementary cementing materials (SCMs). The factor k_2 is taken as 1.0 as a result of the statistical analysis of the laboratory data set reviewed in Section 6.4.1, that failed to detect a significant difference among SCM type. The factor k_1 is calibrated similarly to that of the *fib* Model Code 2010 as shown in Figure 6-15. Again, by dividing the slope of the regression

line for each aggregate type by the leading coefficient of Equation 6-8, k_1 values for the dolomitic limestone and crushed granite were determined as 1.32 and 0.82, respectively.

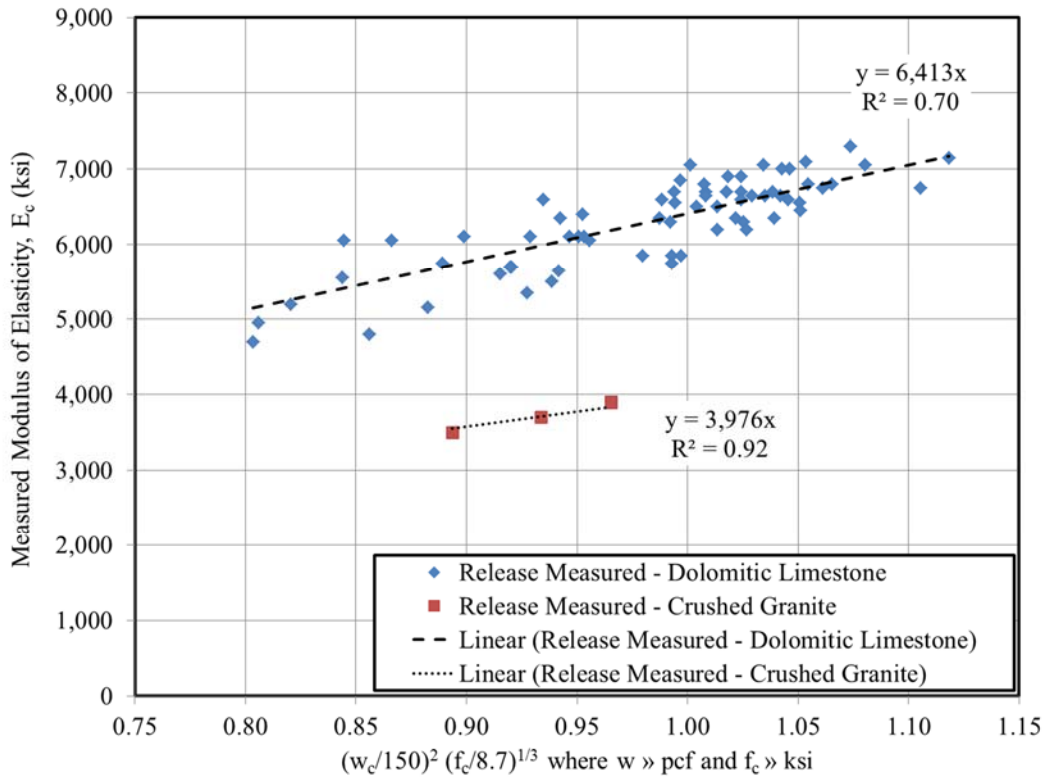


Figure 6-15: Calibration of Noguchi et al. (2009) for Prestress Release

6.4.2.4 Comparison of Available Prediction Equations

The final form of each of the five candidate prediction equations included in this study, as calibrated for use at the time of prestress release, is summarized in Table 6-8. The standard error of the estimate, SEE , is used to evaluate the relative goodness-of-fit of each prediction model to the stiffness-strength data set for varying assumptions of unit weight, w . An independent analysis is conducted for each aggregate type.

While the stiffness-strength data set compiled in this effort includes a known unit weight for each data point, this information is not available at the time of preliminary design. Therefore, the design engineer must estimate the unit weight of the concrete likely to be used in constructing the structural element. Possible assumptions for this purpose include (1) assume a unit weight of 150 pcf for precast concrete as recommended by Tadros et al. (2003), (2) assume a unit weight based on knowledge of

typical regional mixtures, or (3) attempt to correlate the expected concrete strength, f_c^* , to unit weight using Equation 6-4, reproduced below, as developed by Al-Omaishi et al. (2009) and included in the 2014 AASHTO LRFD Bridge Design Specifications (AASHTO 2014).

$$w = 0.140 + \frac{f_c^*}{1000} \leq 0.155 \quad (6-4)$$

Conveniently, alternative (1) and (2) are essentially identical, as the average of the mixtures included in the laboratory study is 149.9 pcf. Therefore, the following three assumptions for unit weight are used for the analyses of this section: (1) use known unit weight from data set, (2) assume unit weight of 150 pcf, and (3) use Equation 6-4 to estimate unit weight from expected (or measured in this case) compressive strength.

Table 6-8: Candidate Modulus Prediction Equations Calibrated for Prestress Release

Source	Prediction Equation	Nomenclature
Pauw (1960) / ACI 318-14 / ACI 209	$E_c = 33w^{1.5}\sqrt{f'_c}$	E_c = static elastic modulus of concrete (psi) w = equilibrium unit weight of concrete (pcf) f'_c = concrete compressive strength (psi)
AASHTO LRFD (2014)	$E_c = 33,000 \cdot K_1 \cdot w^{1.5} \sqrt{f'_c}$	E_c = static elastic modulus of concrete (ksi) K_1 = correction factor for source of aggregate = 1.16 for dolomitic limestone = 0.72 for crushed granite w = unit weight of concrete (kcf) f'_c = concrete compressive strength (ksi)
ACI 363 Method	$E_c = (40,000\sqrt{f'_c} + 10^6)(w_c/145)^{1.5}$	E_c = static elastic modulus of concrete (psi) w_c = unit weight of concrete (pcf) f'_c = concrete compressive strength (psi)
fib Model Code 2010	$E_c = 276,000 \cdot \alpha_E \cdot \sqrt[3]{f'_c}$	E_c = static elastic modulus of concrete (psi) α_E = aggregate correction factor = 1.15 for dolomitic limestone = 0.69 for crushed granite f'_c = concrete compressive strength (psi)
Noguchi et al. (2009)	$E_c = k_1 \cdot k_2 \cdot 4,860 \cdot \left(\frac{w_c}{150}\right)^2 \sqrt[3]{\frac{f'_c}{8.7}}$	E_c = static elastic modulus of concrete (ksi) k_1 = correction factor for aggregate stiffness = 1.32 for dolomitic limestone = 0.82 for crushed granite k_2 = correction factor for supplementary cementing materials = 1.0 w_c = unit weight (pcf) f'_c = concrete compressive strength (ksi)

The results of the *SEE* analysis to evaluate the relative goodness-of-fit for the five prediction equations for two varying aggregates with three assumptions of unit weight are displayed in Table 6-9. For each varying assumption of unit weight, the most accurate prediction model is shaded for reference. Of these shaded models, the standard errors of the estimates represent less than 10 percent of typical values for elastic modulus. Caution is warranted when evaluating the results for crushed granite due to the small sample size. The calibrated AASHTO LRFD, *fib* Model Code 2010, and Noguchi et al. (2009) methods each represent a significant improvement when compared to current practice (represented by Pauw [1960]). For the dolomitic limestone data grouping evaluated with measured unit weights, the Noguchi et al. (2009) method provides a more accurate prediction of modulus ($SEE = 323$ ksi) when compared to the AASHTO LRFD Method ($SEE = 341$ ksi) suggesting that the form of the Noguchi et al. (2009) equation may be slightly theoretically better suited for prediction of elastic modulus at the time of prestress release. When considering the dolomitic limestone grouping for unit weight computed according to Equation 6-4, the *fib* Model Code 2010 prediction equation is identified as most preferable despite this equation not varying as a function of unit weight. For a unit weight assumption of 150 pcf, the AASHTO LRFD equation yields the most accurate predictions ($SEE = 364$ ksi as compared to the next closest of 372 ksi). Another interesting trend is identified by comparing the assumed unit weight of 150 pcf subgroup and the unit weight computed by Equation 6-4 subgroup for dolomitic limestone. The use of Equation 6-4 generates significantly less accurate predictions than does a simple assumption of a unit weight of 150 pcf for the precast, prestressed concretes considered in this study.

Table 6-9: Standard Error of the Estimate, *SEE* for Calibrated Modulus Prediction Equations at Prestress Release

Prediction Model	Dolomitic Limestone			Crushed Granite		
	<i>SEE</i> Using Assumed $w = 150$ pcf (ksi)	<i>SEE</i> Using Measured w (ksi)	<i>SEE</i> Using w Predicted from f_c (Al-Omaishi 2009) (ksi)	<i>SEE</i> assuming $w = 150$ pcf (ksi)	<i>SEE</i> Using Measured w (ksi)	<i>SEE</i> Using w Predicted from f_c (Al-Omaishi 2009) (ksi)
Pauw (1960) / ACI 318-14 / ACI 209 / Uncalibrated AASHTO LRFD (2014)	1,008	923	1,109	1,512	1,446	1,377
Calibrated AASHTO LRFD (2014)	364	341	422	73	22	58
ACI 363	1,579	1,500	1,670	972	911	850
<i>fib</i> Model Code 2010	372	372	372	89	89	89
Noguchi et al. (2009)	392	323	455	114	48	88

For the crushed granite data set, similar trends are found, except in this case, the relative level of prediction accuracy agrees with that logically expected (most accurate corresponds to measured unit weights and least accurate corresponds to assumption of 150 pcf).

While the above analysis of *SEE* serves as an objective way to evaluate the relative fit of equations, it does not lend itself to developing a full understanding of the prediction model fits and flaws. For this purpose, the five calibrated prediction equations (for assumed unit weight of 150 pcf) and the experimental data of the stiffness-strength data set (excluding crushed granite) are shown in Figure 6-16.

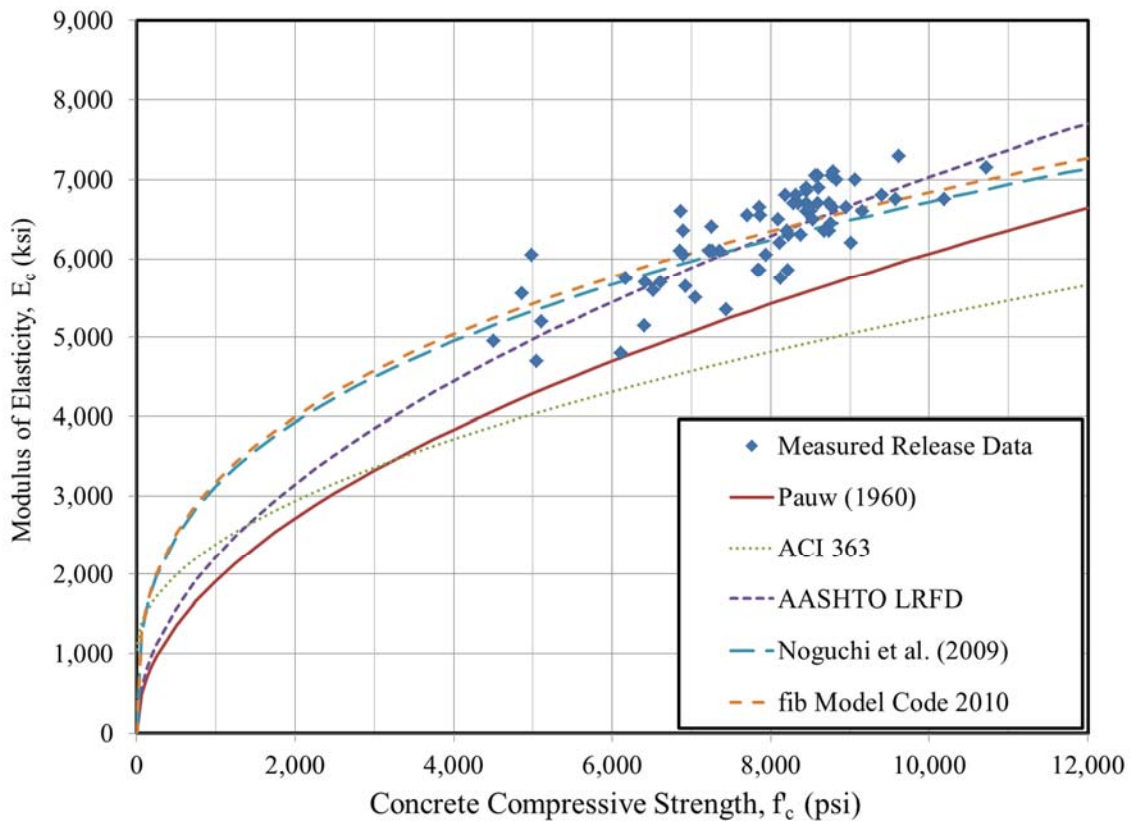


Figure 6-16: Relative Fit of Calibrated Modulus Prediction Equations for Prestress Release Data for Dolomitic Limestones with Assumed Unit Weight of 150 pcf

It can be seen that the recommendation of ACI 363 tends to most significantly under-predict stiffness at the time of prestress release, followed next by the prediction equation of Pauw (1960). The three calibrated equations appear relatively similar through the strength range of experimental data in this project.

6.4.2.5 Preliminary Recommendations for Designers

As a result of the analysis detailed in Section 6.4.2.5 of this report, the following preliminary recommendation is made for designers of precast, prestressed concrete members within the study region:

- The AASHTO LRFD Bridge Design Specifications (AASHTO 2014) prediction equation, with the assumptions and calibrations noted below, is most appropriate for design predictions of the elastic modulus of precast, prestressed concrete at the time of prestress release.

$$E_c = 33,000 \cdot K_1 \cdot w^{1.5} \sqrt{f'_c}$$

where

E_c = static elastic modulus of concrete (ksi);

K_1 = correction factor for source of aggregate;

= 1.16 for dolomitic limestone;

w = unit weight of concrete (kcf);

= assumed equation to 0.150 kcf for design purposes; and

f'_c = concrete compressive strength (ksi).

The K_1 factor referenced above is appropriate for dolomitic limestone most typical of Alabama geologic formations. At the conclusion of this study, only two precast, prestressed producers (Plants A and C) remained active within the study region and both used dolomitic limestone coarse aggregates.

6.4.3 Concrete Stiffness at 28 Days

Accurate prediction of E_c at the time of 28 days after production is not as critical to designers of precast, prestressed elements as the prediction of elastic modulus at prestress release. As previously discussed in Chapter 2, deflections are typically computed for the time of prestress release and modified thereafter by a time-dependent multiplier. Nonetheless, for the purposes of determining appropriate time-dependent multipliers and for completeness of this report, an analysis identical to that of Section 6.4.2 was completed for predicting concrete stiffness at the time of 28 days after production. The analytical procedure (shown in Figure 6-12) was again used in the analysis of this section.

6.4.3.1 Calibration of AASHTO LRFD Equation

Calibration of the AASHTO LRFD Equation for each aggregate type was completed in similar fashion to that discussed in Section 6.4.2.1. The results of the linear regression performed on the compiled data set are shown in Figure 6-17.

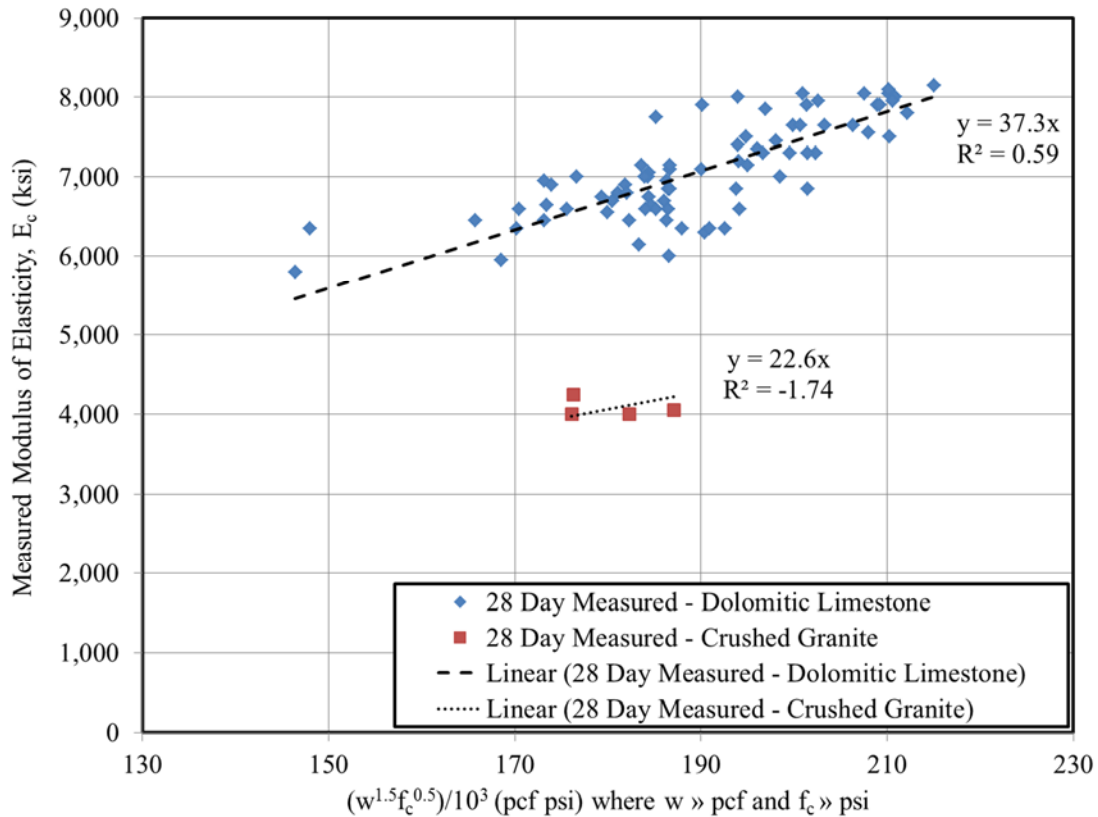


Figure 6-17: Calibration of AASHTO LRFD Equation for 28 Days

The regression coefficients noted in Figure 6-17, when divided by 33.0, yield K_1 factors of 1.13 and 0.68 for dolomitic limestone and crushed granite, respectively. Each of these values is less than the corresponding K_1 factors computed from the release data set (1.16 and 0.72 respectively). A potential reason for this disparity between K_1 values at different times of measurement is discussed in Section 6.4.4.

6.4.3.2 Calibration of *fib* Model Code 2010 Equation

In similar fashion, the *fib* Model Code 2010 prediction equation was calibrated for each aggregate type as shown in Figure 6-18. The values of α_E resulting from the calibration to the stiffness-strength data set

are 1.18 and 0.69, respectively (as compared to those values computed for prestress release of 1.15 and 0.69, respectively).

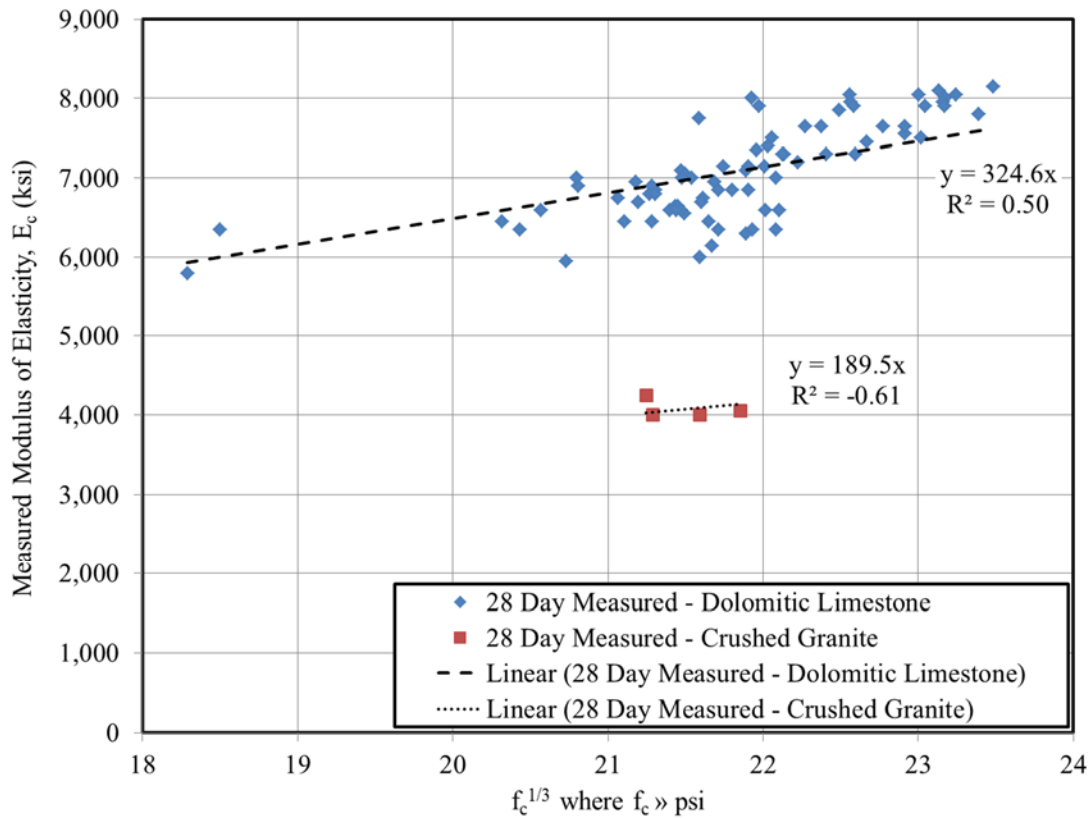


Figure 6-18: Calibration of *fib* Model Code 2010 for 28 Days

6.4.3.3 Calibration of Noguchi et al. (2009) Equation

Finally, the Noguchi et al. (2009) prediction equation is calibrated in a similar manner as previously. The factor k_2 is again taken as 1.0, while the k_1 factor is calibrated to the stiffness-strength data set as shown in Figure 6-19. Again, by dividing the slope of the regression line for each aggregate type by the leading coefficient of Equation 6-8, k_1 for the dolomitic limestone and crushed granite were determined as 1.35 and 0.82, respectively. In this case, the k_1 factor for dolomitic limestone at the time of 28 days exceeds the k_1 for release (previously computed as 1.32), while the k_1 for crushed granite again remains consistent between measurement ages.

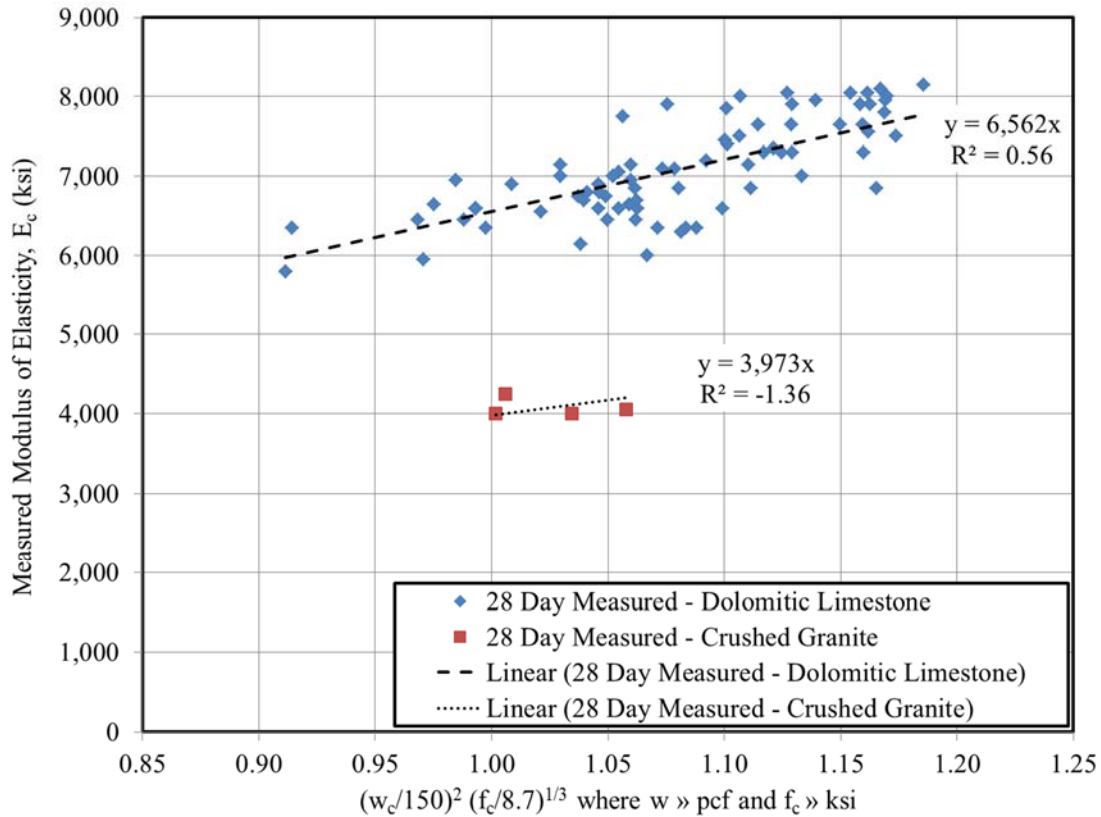


Figure 6-19: Calibration of Noguchi et al. (2009) for 28 Days

6.4.3.4 Comparison of Available Prediction Equations

The final form of each of the five candidate prediction equations included in this study, as calibrated for use at the time of 28 days, is summarized in Table 6-10. This section briefly compares the accuracy of these calibrated prediction equations with the stiffness-strength data set for the varying assumptions of unit weight, w , previously noted. The standard error of the estimate (SEE) for each combination of prediction model, aggregate type, and unit weight assumption is shown in Table 6-11. In general, for all calibrated models, the magnitude of the SEE is less than 10 percent of E_c . The AASHTO LRFD equation yields the most accurate prediction of E_c for the dolomitic limestone subgroup for all varying assumptions of unit weight. In addition, increasingly more refined estimates of the unit weight yield increasing more accurate predictions of modulus—with the most accurate predictions observed for measured unit weight.

Table 6-10: Candidate Modulus Prediction Equations Calibrated for 28 Days

Source	Prediction Equation	Nomenclature
Pauw (1960) / ACI 318-14 / ACI 209	$E_c = 33w^{1.5}\sqrt{f'_c}$	E_c = static elastic modulus of concrete (psi) w = equilibrium unit weight of concrete (pcf) f'_c = concrete compressive strength (psi)
AASHTO LRFD (2014)	$E_c = 33,000 \cdot K_1 \cdot w^{1.5}\sqrt{f'_c}$	E_c = static elastic modulus of concrete (ksi) K_1 = correction factor for source of aggregate = 1.13 for dolomitic limestone = 0.68 for crushed granite w = unit weight of concrete (pcf) f'_c = concrete compressive strength (ksi)
ACI 363 Method	$E_c = (40,000\sqrt{f'_c} + 10^6)(w_c/145)^{1.5}$	E_c = static elastic modulus of concrete (psi) w_c = unit weight of concrete (pcf) f'_c = concrete compressive strength (psi)
fib Model Code 2010	$E_c = 276,000 \cdot \alpha_E \cdot \sqrt[3]{f'_c}$	E_c = static elastic modulus of concrete (psi) α_E = aggregate correction factor = 1.18 for dolomitic limestone = 0.69 for crushed granite f'_c = concrete compressive strength (psi)
Noguchi et al. (2009)	$E_c = k_1 \cdot k_2 \cdot 4,860 \cdot \left(\frac{w_c}{150}\right)^2 \sqrt[3]{\frac{f'_c}{8.7}}$	E_c = static elastic modulus of concrete (ksi) k_1 = correction factor for aggregate stiffness = 1.35 for dolomitic limestone = 0.82 for crushed granite k_2 = correction factor for supplementary cementing materials = 1.0 w_c = unit weight (pcf) f'_c = concrete compressive strength (ksi)

Table 6-11: Standard Error of the Estimate, *SEE*, for Calibrated Modulus Prediction Equations at 28 Days

Prediction Model	Dolomitic Limestone			Crushed Granite		
	<i>SEE</i> Using Assumed $w = 150$ pcf (ksi)	<i>SEE</i> Using Measured w (ksi)	<i>SEE</i> Using w Predicted from f_c (Al-Omaishi 2009) (ksi)	<i>SEE</i> assuming $w = 150$ pcf (ksi)	<i>SEE</i> Using Measured w (ksi)	<i>SEE</i> Using w Predicted from f_c (Al-Omaishi 2009) (ksi)
Pauw (1960) / ACI 318-14 / ACI 209	975	895	939	1,975	1,892	1,974
AASHTO LRFD (2014)	399	379	392	152	172	163
ACI 363	1,786	1,713	1,751	1,182	1,110	1,180
<i>fib</i> Model Code 2010	423	423	423	132	132	132
Noguchi et al. (2009)	439	394	394	159	159	170

With regards to the crushed granite group, the *fib* Model Code 2010 equation, which does not include a term for unit weight, is the most accurate of all considered prediction models. For the assumed unit weight of 150 pcf, the AASHTO LRFD equation yields the second most accurate predictions for E_c . However, for the AASHTO LRFD equation, the most accurate estimate of unit weight yields the least accurate prediction of modulus. This counterintuitive trend suggests that the crushed granite data set may not be robust enough (n=4) to generate meaningful conclusions.

The five candidate modulus prediction equations, calibrated for dolomitic limestone at 28 days, are shown in Figure 6-20 for an assumed unit weight of 150 pcf. In agreement with the results of Table 6-11, the ACI 363 method is the least accurate method, while the equation proposed by Pauw (1960) is the next most accurate. Of the three calibrated equations (AASHTO LRFD, Noguchi et al. (2009) and *fib* Model Code 2010), the shape of the AASHTO LRFD equation appears to fit the experimental data much more closely than the other two expressions. Looking closely at Figure 6-20, it can be seen that the Noguchi et al. (2009) and *fib* Model Code 2010 equations tend to underestimate experimental results for concrete compressive strengths exceeding approximately 11,000 psi, while overestimating experimental results for strengths less than 9,000 psi. The underestimation of results for higher compressive strengths when using the Noguchi et al. (2009) model is unexpected, as Noguchi et al. (2009) calibrated this model with using a compiled data set including compressive strengths exceeding 20.0 ksi.

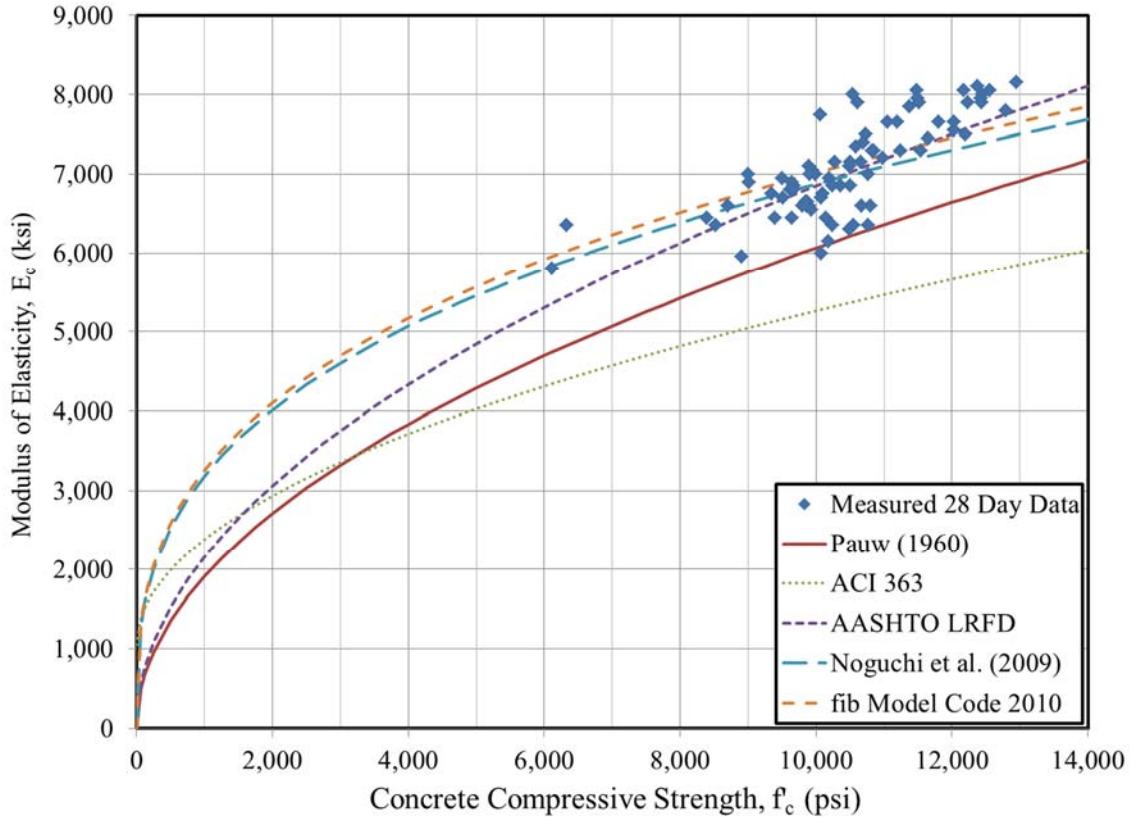


Figure 6-20: Relative Fit of Calibrated Modulus Prediction Equations for 28-Day Data for Dolomitic Limestones with Assumed Unit Weight of 150 pcf

6.4.3.5 Preliminary Recommendations for Designers

Based on the analysis of Section 6.4.3 with regards to evaluating the accuracy of the five calibrated prediction equations for predicting elastic stiffness at 28 days, the following preliminary recommendation is made for designers of precast, prestressed concrete members within the study region:

- The AASHTO LRFD Bridge Design Specifications (AASHTO 2014) prediction equation, with the assumptions and calibrations noted below, is most appropriate for design predictions of the elastic modulus of precast, prestressed concrete at the time of 28 days after production.

$$E_c = 33,000 \cdot K_1 \cdot w^{1.5} \sqrt{f'_c}$$

where

E_c = static elastic modulus of concrete (ksi);

K_1 = correction factor for source of aggregate;

= 1.13 for dolomitic limestone;

w = unit weight of concrete (kcf);

= assumed equation to 0.150 kcf for design purposes; and

f'_c = concrete compressive strength (ksi).

The K_1 factor referenced above is appropriate for dolomitic limestone most typical of Alabama geologic formations for the reasons outlined in previous preliminary recommendations for prestress release outlined in Section 6.4.2.5.

6.4.4 Time-Dependence of Aggregate Stiffness Effect

A phenomenon observed both in the experimental work of this report and the previous work of Keske (2014) and Hofrichter (2014) is the seemingly time-dependent nature of the aggregate stiffness effect on the modulus of elasticity of concrete. Keske (2014) reported that computed aggregate stiffness factors, K_1 , for the time of prestress release consistently were consistently greater than the K_1 computed for the time of 28 days. This trend is also evident in the earlier analysis work of Hofrichter (2014) and the work of this report. Despite the frequency of this phenomenon in regional research work, this trend has not been referenced previously in published literature. This section provides a hypothesized reason for this difference.

The analysis detailed in Section 6.4.1 of this report affirmed that there existed a statistically significant difference between K_1 factors computed at the time of prestress release and at 28 days after concrete production for dolomitic limestones. In an attempt to propose a reason for this disparity, key variables (or factors affecting key variables) correlated to E_c were investigated as potential causes.

First, it was noted that the unit weight intended for use in the equation by Pauw (1960) was the equilibrium or air-dry unit weight of concrete. It was hypothesized that perhaps, concrete specimens tested at the time of prestress release contained more free water (than companion specimens tested at 28 days) and thus, may exhibit a higher unit weight. Because Pauw's expression intended the air-dry unit weight as an input, it would be appropriate to reduce the fresh unit weight to a lesser value. Failure to do so may result in over-predictions of the E_c , therefore causing higher K_1 values. While perhaps logically sound, this approach is highly unlikely due to the negligible change in unit weight of normal-weight

concrete for varying exposure conditions (Neville 2013). Although not likely not the cause of the disparity observed in this research effort, it is interesting to note that for the computation of elastic modulus for lightweight aggregate concrete, the distinction between using the fresh unit weight or air-dry unit weight (up to a 9 pcf difference) may significantly affect the accuracy of predictions.

Another possible reason for the disparity that was explored was the varying moisture conditions of cylinders at the time of testing. Previously, French and O'Neill (2012) noted a disproportionality between the early-age concrete strength and stiffness as part of their on-site material testing effort at a precast, prestressed producer as shown in their published plots reproduced in Figure 6-21.

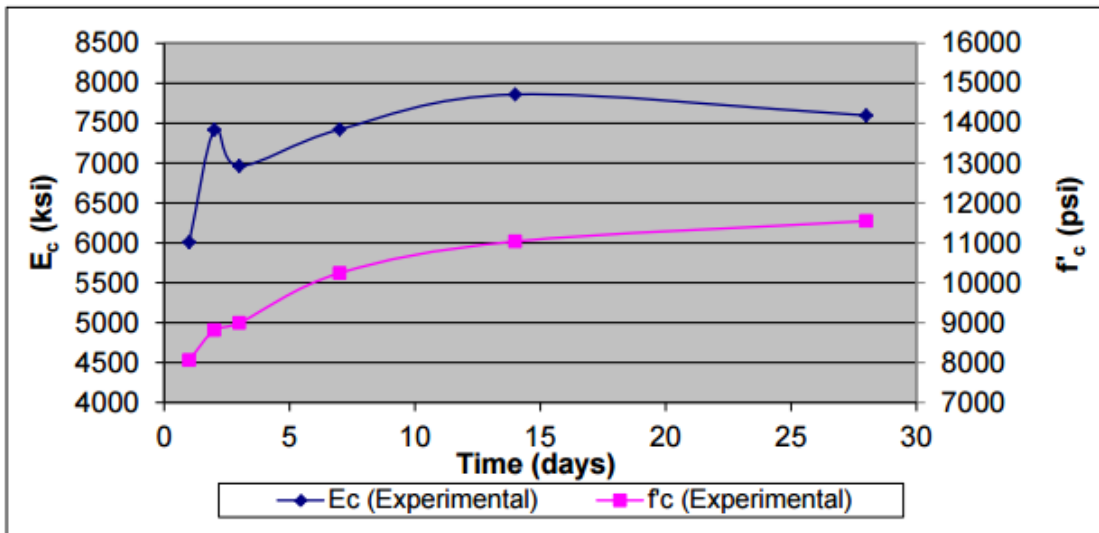
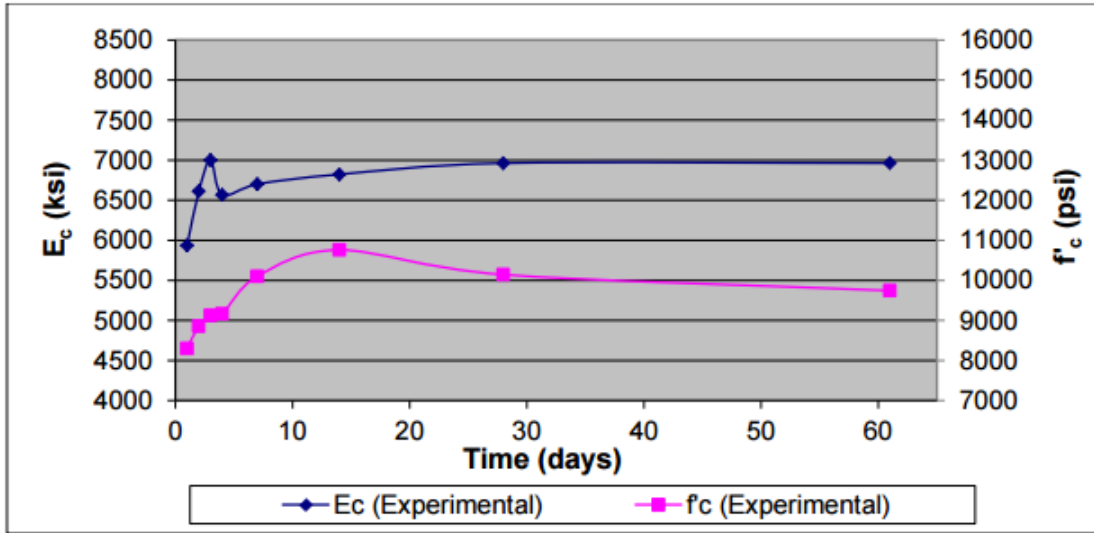


Figure 6-21: Early-Age Disproportionality of Concrete Compressive Strength and Elastic Modulus at Two Producers (French and O'Neill 2012)

French and O'Neill (2012) suggested that the cause of the early-age disproportionality may be due to an increased amount of water inside cylinders at early ages and proposed a separate multiplier of 1.15, not to be confused with K_1 , to account for the difference in E_c observed between the time of prestress release and 28 days. However, due to the relatively consistent curing procedures used in the experimental work of this report, it is not possible to extensively evaluate the hypothesis of French and O'Neill (2012) for the experimental data compiled as part of this effort. However, it is interesting to note that the statistical analysis of Section 6.4.1 did detect a difference in 28-day K_1 factors that is attributable

to either 1) varying curing procedures (e.g. varying temperature or moisture exposures) or 2) the inclusion of SCC in the data set, although definitive assignment of the observed variation is not possible.

After considering the hypothesis of French and O'Neill (2012) and noting that the phenomenon of varying K_1 factors has only been noted in precast, prestressed concrete, an alternative hypothesis capable of explaining the observed disparity of K_1 factors was developed and is presented here. Qualitatively reflecting on the field and laboratory efforts of this study, it was noted that the temperature of cylinders at the time of testing varied greatly throughout the study. While release cylinders tested in the field were typically tested approximately 2 hours after the completion of steam-curing (due largely to on-site coordination issues), cylinders tested at the AU Structural Research Lab were tested within minutes of the completion of simulated steam curing. In fact, specimens tested at the AU laboratory were typically hot to the touch and sometimes even uncomfortable to handle at the time of testing. A statistical analysis of the experimental data set was completed to explore if the K_1 factors at release for the laboratory portion of this work tended to be significantly different than those obtained from in-plant testing. It was confirmed that there was strong statistical evidence ($p=0.01$, t-Test) at significance level $\alpha = 0.05$ that the mean K_1 value determined from laboratory testing exceeded that of the field data.

While not conclusive by any means, the above discussion affirms the plausibility that the temperature at the time of specimen testing may have an effect on the resulting K_1 value. A preliminary literature review on the effect of elevated testing temperature on the compressive strength and E_c of concrete cylinders highlighted several relevant factors. Freskakis, Burrow, and Debbas (1979) concluded

- a. There is a well-documented reduction in the compressive strength of concrete when exposed to elevated temperatures and, particularly when tested at elevated temperatures;
- b. There is a well-documented reduction in the E_c of concrete when exposed to elevated temperatures and, particularly when tested at elevated temperatures;
- c. The decrease in modulus of elasticity due to elevated temperature exposure is more pronounced than the decrease in compressive strength, but varies with mixture proportions;

- d. Specimens heated and then allowed to cool before testing show more strength loss than those tested hot; and
- e. Small specimens usually incur greater strength losses than larger specimens.

Design relationships suggested by Freskakis et al. (1979) suggest that for a change in temperature from ambient to approximately 150°F at the time of testing, approximately a 2–12 percent decrease in the compressive strength is expected. Similarly, a corresponding reduction in the elastic modulus of between 0–20 percent is expected. For design purposes, the *Code Requirement for Determining the Fire Resistance of Concrete and Masonry Construction Assemblies* (ACI 2014) affirms the expected reduction in compressive strength as proposed by Freskakis et al. (1979), but offers no comment on the corresponding reduction in stiffness. The design relationships of the *fib Model Code 2010* assume that the percent loss in compressive strength is the same as the percent loss of E_c , approximately 18 percent for the temperature range typical of accelerated cured precast, prestressed concrete (fib 2010).

The majority of the literature referenced above documents the observed reductions in compressive strength and E_c for hardened concrete exposed to increasing temperatures (either sustained through the time of testing, called “hot testing” or tested after cooling, called “residual testing”). The situation in steam curing of precast, prestressed elements is somewhat the opposite. The temperature change of interest for hardened precast, prestressed concrete begins at the elevated temperatures present at the conclusion of accelerated curing and ends after cooling to ambient temperature. If similar trends hold for this temperature shift typical of precast, prestressed concrete as those noted in the preceding paragraph for hardened concrete, the following possible hypotheses (or more likely, a combination thereof) are proposed to explain the observed differences in stiffness at the time of prestress release and 28 days:

- The initial reduction in stiffness and strength (as observed by French and O’Neill [2012]) may correspond to the cooling of the concrete from the initial accelerated curing temperatures. Specimens tested at higher temperature will tend to show a smaller reduction in concrete strength than those tested when cold. This may explain the “dip” in the observed strength and stiffness, which then is eclipsed by the continually developing time-dependent hardened properties, and

- The relationship between strength loss and stiffness loss for a given temperature change is a critical factor influencing the K_1 factor for a given concrete. Consider the simple assumption contained in the *fib* Model Code that claims the percent change for a given temperature range of strength and stiffness is equal. For a set of cylinders tested for strength and E_c when cold yields the following results: $f_c = 5,000$ psi and $E_c = 4,000$ ksi. Using Equation 6-5 for an assumed unit weight of 0.150 kcf, K_1 is computed as 0.93. Now, if the corresponding cylinders were simultaneously was heated to 150°F and tested again, suppose they exhibit a uniform 10 percent reduction in both strength and stiffness: $f_c = 4,500$ psi and $E_c = 3,600$ ksi, respectively. Again, using Equation 6-5 to compute K_1 , a value of 0.89 is obtained. This simple example affirms the viability of this hypothesis.

It is clear that future research is justified to further examine the effect of cylinder temperature at the time of testing to determine its effect on concrete compressive strength and elastic modulus. This future work will likely be of significant interest to the precast, prestressed concrete industry. Despite identifying a potential cause and mechanism for the observed time-dependent nature of the aggregate stiffness effect, it is not possible at this time to propose a method for combining the stiffness-strength data sets to yield a single K_1 factor for each aggregate type. Accordingly, the recommendations section of this chapter presents two K_1 values for each aggregate type, one for use at prestress release and one at 28 days.

6.4.5 Reduced Stiffness of Crushed Granite Concrete Laboratory Mixtures

The most unexpected result of this study was the comparatively low stiffness exhibited by the crushed granite aggregate mixtures used in the laboratory portion of this research effort. The aggregate in question, currently maintained on ALDOT approved source lists, was previously used by a producer of ALDOT bridge girders (prior to the producer closing in 2013), and, therefore, was selected as a viable aggregate choice for use by a future producer forecasted to begin girder production operations in the same general vicinity of the closed producer. Typically, crushed granites from this region are regarded as excellent aggregates exhibiting relatively high absorption values when compared to other local

aggregates (0.7 percent compared to 0.3 for dolomitic limestone). A study by Haranki (2009) studied the effect of aggregate type on the stiffness of concretes used by the Florida Department of Transportation (FDOT), recommending a K_1 factor of approximately 1.05 for concretes made with similar w/cm and crushed granite aggregate. The K_1 factor proposed by Haranki (2009) greatly exceeds the K_1 factors computed as a result of the experimental effort detailed in this report (0.68–0.72.) Although the use of the crushed granite was not a major portion of this study, the comparatively-low stiffness of the crushed granite concrete mixture, GG-III, was briefly investigated to identify a possible reason for this disparity.

Prior to their use in this research project, it was confirmed that all three coarse aggregates and the single source of fine aggregate met the gradation requirements outlined in the *ALDOT Standard Specification for Highway Construction* (ALDOT 2012). For reference, a random sampling of the crushed granite used in the GG-III mixture is shown in Figure 6-22



Figure 6-22: Crushed Granite (#67) Aggregate Sample

The particles shown on the left side (white with black striping) and center (white with brown coloring throughout) of Figure 6-22 represent typical granite samples that are dense sound particles and comprise approximately 85 percent (by weight) of the #67 aggregate. Conversely, the particles on the right (black, flakey, and shiny) show samples comprising approximately 15 percent by weight of the #67 crushed

granite aggregate. Correspondence with the aggregate supplier confirmed that this dark material is biotite mica schist—a naturally occurring formation found within veins of granite. By inspection, these mica-rich aggregates are relatively soft and unsound particles, easily broken when squeezed between one's fingers. The *ALDOT Standard Specification for Highway Construction* (ALDOT 2012) mandates that all candidate aggregates suspected of containing local deleterious materials (defined in the specification explicitly as shale, mica, marcasite, etc.) be examined by the state laboratory and not exceed two percent of the overall weight (mass) of aggregate for structural concrete applications. In this case, the crushed granite sample obtained and used for the GG-III mixtures in this project is suspected of exceeding this requirement—containing up to 15 percent (by weight) of mica schist. A study by Aitcin and Mehta (1990) observed the presence of unsound aggregate particles in a crushed granite sample in similar amounts result in less than expected concrete compressive strengths and stiffnesses. Aitcin and Mehta (1990) hypothesized that the inherently weak granite particles caused a weak transition zone, prone to debonding and premature failure. Inspection of the compressive failure of a GG-III specimen included in the work of this report, as shown in Figure 6-23, suggests similar behavior with cracking most often protruding from the vicinity of the soft mica schist aggregate particles.

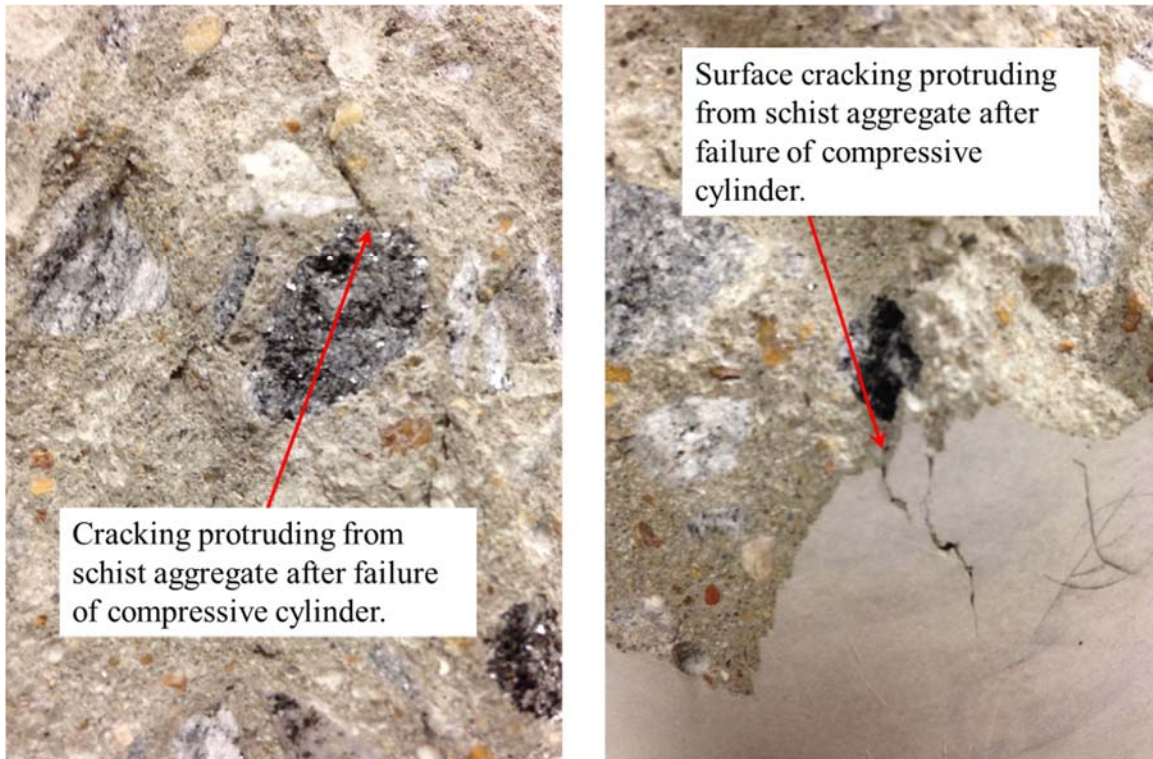


Figure 6-23: Cracking in the Vicinity of Schist Aggregate Particles at Failure

In retrospect, the sample of crushed granite obtained for use in this project is suspected of not meeting the deleterious substance limits of the *ALDOT Standard Specification for Highway Construction* (ALDOT 2012). Approval by the state lab of this aggregate for use in precast, prestressed concrete elements, if tested specifically for suspected high amounts of deleterious substances, would be questionable and likely at the discretion of ALDOT. Accordingly, the major recommendation with regards to the use of regional crushed granite aggregates in precast, prestressed concrete is to ensure that the deleterious substance limits of existing ALDOT specifications (ALDOT 2012) are enforced. That being said, the recommendations for predicting elastic modulus of the crushed granite mixtures contained in the earlier analysis in this chapter are not recommended for implementation by regional designers of precast, prestressed concrete elements due to these results possibly not representing those that may be obtained from sound crushed granite aggregate samples.

6.5 Summary and Conclusions

6.5.1 Summary

The main objective of this chapter was to establish the most appropriate design relationships for use by engineers to accurately characterize the E_c of concrete as a function of compressive strength and other relevant variables likely to be known during the preliminary design phase. By ensuring accurate predictions of concrete stiffness are made at the time of design, the most accurate estimations of short- and long-term deflections can be computed for precast, prestressed concrete members. In this study, a laboratory and field experimental material testing program was relied on to generate a stiffness-strength data set for regional precast, prestressed concretes. Next, a statistical analysis was performed to identify significant variables and groupings for further analysis. For the ages of prestress release and 28 days, four candidate elastic modulus prediction equations were calibrated to the experimental data set and then compared and contrasted using the standard error of the estimate, *SEE*. Finally, design recommendations were offered and various hypotheses presented as potential explanations of unexpected observed behavior.

6.5.2 Conclusions and Recommendations

Key conclusions of the work presented in this chapter include the following:

- No statistical difference in elastic modulus was detectable among the three laboratory mixtures containing varying supplementary cementing materials (SCMs) in typical percent replacements used in Alabama;
- The AASHTO LRFD Bridge Design Specifications (AASHTO 2014) prediction equation, with the assumptions and calibrations noted below, is most appropriate for design predictions of the elastic modulus of precast, prestressed concrete.

$$E_c = 33,000 \cdot K_1 \cdot w^{1.5} \sqrt{f'_c}$$

where

E_c = static elastic modulus of concrete (ksi);

K_1 = correction factor for source of aggregate;

= 1.16 for dolomitic limestone at release;

= 1.13 for dolomitic limestone at 28 days;

w = unit weight of concrete (kcf);

= assumed equation to 0.150 kcf for design purposes; and

f'_c = concrete compressive strength (ksi).

The K_1 factors referenced above are appropriate for dolomitic limestone typical of Alabama geologic formations. At the conclusion of this study, only two precast, prestressed producers (Plants A and C) remained active within the study region and both used dolomitic limestone coarse aggregates. For convenience in design computations not completed in software programs (i.e. manual or approximate computations), the above K_1 factors can be approximated as

$K_1 = 1.15$;

- The use of a regional crushed granite aggregate acquired from an ALDOT-approved source resulted in concretes with less than expected E_c values (K_1 values between 0.68–0.72). However, the acceptability of the crushed granite aggregate (specifically with regards to the permitted percentage of deleterious substances) is questionable;
- It is important that the requirements of the *ALDOT Standard Specification for Highway Construction* (ALDOT 2012) with regards to the permissible levels of deleterious substances are enforced, as failure to do so may result in concretes with stiffnesses significantly less than expected; and
- The effect of the testing temperature of the cylinders at the time of prestress release is a potential source of variability observed in K_1 factors at different ages. More study is needed in this area.

References

- AASHTO. 2014. *AASHTO LRFD Bridge Design Specifications*. 7th ed. Washington, DC: American Association of State Highway and Transportation Officials.
- AASHTO. 2012. *AASHTO LRFD Bridge Design Specifications*. 6th ed. Washington, DC: American Association of State Highway and Transportation Officials.
- Abrams, D.A. 1927. Water-Cement Ratio as Basis of Concrete Quality. *ACI Journal Proceedings* 23 (2): 452-457.
- ACI Committee 211. 2008. Guide for Selecting Proportions for High-Strength Concrete Using Portland Cement and Other Cementitious Materials (ACI 211.4R-08). Farmington Hills, MI: American Concrete Institute.
- ACI Committee 301. 2010. Specifications for Structural Concrete (ACI 301-10). Farmington Hills, MI: American Concrete Institute.
- ACI Committee 363. 2010. Report on High-Strength Concrete (ACI 363R-11). Farmington Hills, MI: American Concrete Institute.
- ACI Committee 209. 2005. Factors Affecting Shrinkage and Creep of Hardened Concrete (ACI 209.1R). Farmington Hills, MI: American Concrete Institute.
- ACI Committee 209. 2008. Guide for Modeling and Calculating Shrinkage and Creep of Concrete (ACI 209.2R-08). Farmington Hills, MI: American Concrete Institute.
- ACI Committee 209. 2008. Prediction of Creep, Shrinkage, and Temperature Effects in Concrete Structures (ACI 209R-92/08). Farmington Hills, MI: American Concrete Institute.
- ACI Committee 214. 2011. Guide to Evaluation of Strength Test Results of Concrete (ACI 214R-11). Farmington Hills, MI: American Concrete Institute.
- ACI Committee 216. 2014. Code Requirement for Determining the Fire Resistance of Concrete and Masonry Construction Assemblies (ACI 216.1-14). Farmington Hill, MI: American Concrete Institute.
- ACI Committee 318. 2014. Building Code Requirements for Structural Concrete (ACI 318-14). Farmington Hills, MI: American Concrete Institute.
- ACI Committee 318. 1971. Building Code Requirements for Reinforced Concrete (ACI-318-71). Detroit, MI: American Concrete Institute.
- ACI Committee 435. 1997. Report on Temperature-Induced Deflections of Reinforced Concrete Members (ACI 435.7R-85). Farmington Hills, MI: American Concrete Institute.

- ACI. 2013. ACI Concrete Terminology (ACI CT-13). Farmington Hills, MI: American Concrete Institute.
- ACI Committee 318. 2011. Building Code Requirements for Structural Concrete (ACI 318-11). Farmington Hills, MI: American Concrete Institute.
- ACI Committee 435. 2003. Control of Deflection in Concrete Structures (ACI 435R), Farmington Hills, MI: American Concrete Institute.
- ACI Committee 435/Subcommittee 5. 1963. Deflections of Prestressed Concrete Members. *Journal of the American Concrete Institute* 60 (12): 1697-1728.
- Adam, I., and M. M. R. Taha. 2011. Identifying the Significance of Factors Affecting Creep of Concrete: A Probabilistic Analysis of RILEM database. *International Journal of Concrete Structures and Materials* 05 (2): 97-111.
- Aitcin, P.C., and P.K. Mehta. 1990. Effect of Coarse-Aggregate Characteristics on Mechanical Properties of High-Strength Concrete. *ACI Materials Journal* 82 (2): 103-107.
- ALDOT. 2014. Structural Design Manual. Montgomery, AL: Alabama Department of Transportation.
- ALDOT. 2014. Bridge Plans Detailing Manual. Montgomery, AL: Alabama Department of Transportation.
- ALDOT. 2009. Method of Controlling Concrete Operations for Structural Portland Cement Concrete (Procedure 170). Montgomery, AL: Alabama Department of Transportation.
- ALDOT. 2015. Production and Inspection of Precast Non-Prestressed and Prestressed Concrete (Specification ALDOT-367-89). Montgomery, AL: Alabama Department of Transportation.
- ALDOT. 2012. Standard Specifications for Highway Construction. Montgomery, AL: Alabama Department of Transportation.
- Alexander, M.G., and T.I. Milne. 1995. Influence of Cement Blend and Aggregate Type on Stress-Strain Behavior and Elastic Modulus of Concrete. *ACI Materials Journal* 92 (3): 227-235.
- Al-Omaishi, N, M.K. Tadros, and S.J. Seguirant. 2009. Elasticity, Modulus, Shrinkage, and Creep of High-Strength Concrete as Adopted by AASHTO. *PCI Journal* 54 (3):44-63.
- Al-Omaishi, N. 2001. *Prestress Losses in High Strength Pretensioned Concrete Girders*. PhD Dissertation, University of Nebraska – Lincoln.
- Aly, T. and Sanjayan, J.P. 2008. Factors Contributing to Early Age Shrinkage Cracking of Slag Concretes Subjected to 7-days Moist Curing. *Materials and Structures Journal*: 41(4):633-624.
- ASTM C1074. 2011. Standard Practice for Estimating Concrete Strength by the Maturity Method. *ASTM International*. West Conshohocken, PA.
- ASTM C192. 2014. Standard Practice for Making and Curing Concrete Test Specimens in the Laboratory. *ASTM International*. West Conshohocken, PA.
- ASTM C31. 2009. Standard Practice for Making and Curing Concrete Test Specimens in the Field. *ASTM International*. West Conshohocken, PA.

- ASTM C157. 2008. Standard Test Method for Length Change of Hardened Hydraulic-Cement Mortar and Concrete. *ASTM International*. West Conshohocken, PA.
- ASTM C512. 2002. Standard Test Method for Creep of Concrete in Compression. *ASTM International*. West Conshohocken, PA.
- ASTM C39. 2010. Standard Test Method for Compressive Strength of Cylindrical Concrete Specimens. *ASTM International*. West Conshohocken, PA.
- ASTM C469. 2010. Standard Test Method for Static Modulus of Elasticity and Poisson's Ratio of Concrete in Compression. *ASTM International*. West Conshohocken, PA.
- Barr, P.J., and F. Angomas. 2010. Differences between Calculated and Measured Long-Term Deflections in a Prestressed Concrete Girder Bridge. *ASCE J. Perform. Constr. Facil*, 24 (6), 603-609.
- Barr, P.J., J.F. Stanton, and M.O. Eberhard. 2005. Effects of Temperature Variations on Precast, Prestressed Concrete Bridge Girders." *ASCE Journal of Bridge Engineering*, 10 (2): 186-194.
- Baughn, J. 2014. Searchable National Bridge Inventory Data. <http://www.uglybridges.com> (accessed February 2, 2015).
- Bazant, Z.P., and L. Panula. 1980. Creep and Shrinkage for Analyzing Prestressed Concrete Structures." *PCI Journal* 25 (3): 68-117.
- Bentley Systems, Inc. 2012. *LEAP CONSPAN User Manual*. Exton, PA.
- Boehm, K. 2008. *Structural Performance of Self-Consolidating Concrete*. MS Thesis, Auburn, AL: Auburn University.
- Boehm, K.M., R.W. Barnes, and A.K. Schindler. 2010. *Performance of Self-Consolidating Concrete in Prestressed Girders*. Final Project Report, Auburn University Highway Research Center.
- Boresi, Arthur P., and Richard J. Schmidt. 2003. *Advanced Mechanics of Materials*. Hoboken, NJ: John Wiley and Sons, Inc.
- Branson, D.E. 1977. *Deformations of Concrete Structures*. New York, NY: McGraw-Hill Book Co.
- Branson, D.E., and A.M. Ozell. 1961. Camber in Prestressed Concrete Beams. *Journal of the American Concrete Institute* 57 (12): 1549-1574.
- Brooks, J.J. 1999. How Admixtures Affect Shrinkage and Creep. *Concrete International*, 21 (4): 35-38.
- Brown, K.M. 1998. *Camber Growth Prediction in Precast Prestressed Concrete Bridge Girders*. PhD Dissertation, University of Idaho, Ann Arbor, MI.
- Buettner, D.R., and J.R. Libby. 1979. Camber Requirements for Pretensioned Members. *Concrete International* 1 (2): 66-72.
- Carino, N.J., and R.C. Tank. 1992. Maturity Functions for Concrete Made with Various Cements and Admixtures. *ACI Materials Journal* 89 (2): 188-196.

- Carrasquillo, R.L., A.H. Nilson, and F.O. Slate. 1981. Properties of High Strength Concrete Subject to Short-Term Loads. *ACI Journal* 78(3): 171-177.
- Chern, J., and Y. Chan. 1989. Deformations of Concretes Made with Blast-Furnace Slag Cement and Ordinary Portland Cement. *ACI Materials Journal* 86 (4): 372-382.
- Collins, M.P., and D. Mitchell. 1991. *Prestressed Concrete Structures*. Englewood Cliffs, NJ: Prentice Hall.
- Cook, J.E. 1989. 10,000 psi Concrete. *Concrete International* 11 (10): 67-75.
- Cook, J.E. 1982. Research and Application of High-Strength Concrete Using Class C Fly Ash. *Concrete International* 4 (7): 72-80.
- Cook, R.A., and D. Bloomquist. 2005. *Field Verification of Camber Estimates for Prestressed Concrete Bridge Girders*. Final Project Report, University of Florida, Tallahassee, FL: Florida Department of Transportation.
- Davis, R.E., and H.E. Davis. 1931. Flow of Concrete Under the Action of Sustained Loads. *ACI Journal Proceedings* 27 (3):837-901.
- Davison, B. 2014. *Prediction of Time-Dependent Stresses and Deflections in Prestressed, Concrete Girders: From Start of Fabrication to End of Service Life*. MS Thesis, Seattle Washington: University of Washington.
- Donza, H., O. Cabrera, and E.F. Irassar. 2002. High-strength Concrete with Different Fine Aggregates. *Cement and Concrete Research* (Pergamon) 32: 1755-1761.
- Dunham, E.L. 2011. *Transfer Length in Bulb-Tee Girders Constructed with Self-Consolidating Concrete*. MS Thesis, Auburn, AL: Auburn University.
- Ellis, M.A. 2012. *Time-Dependent Deformations of Concrete for Precast/Prestressed Bridge Components*. MS Thesis, Auburn, AL: Auburn University.
- Fawzy, F. and K.E. Hanna. 2011. Precast, Prestressed Girder Camber Variability. *PCI Journal* 56 (1): 135-154.
- fib. *Model Code 2010*. Design Code, Lausanne, Switzerland: International Federation for Structural Concrete, 2010.
- French, C.E., and C. O'Neill. 2012. *Validation of Prestressed Concrete I-Beam Deflection and Camber Estimates*. Final Report, University of Minnesota, St. Paul, MN: Minnesota Department of Transportation.
- Freskakis, G.N., R.C. Burrow, and E.B. Debbas. 1979. Strength Properties of Concrete at Elevated Temperatures. *Proceedings of ASCE National Convention Civil Engineering Nuclear Power*. Boston, Massachusetts: American Society of Civil Engineers.
- Ghosh, R.S., and J. Timusk. 1981. Creep of Fly Ash Concrete. *ACI Journal* 78 (5): 351-357.
- Haranki, B. 2009. *Strength, Modulus of Elasticity, Creep, and Shrinkage of Concrete Used in Florida*. MS Thesis, Gainesville, FL: University of Florida.

- He, W. 2013. *Creep and Shrinkage of High Performance Concrete and Prediction of the Long-term Camber of Prestressed Bridge Girders*. MS Thesis, Ames, Iowa: Iowa State University.
- Hibbeler, R. C. 2011. *Mechanics of Materials*. Upper Saddle River, NJ: Pearson Prentice Hall.
- Hibbeler, R.C. 2006. *Structural Analysis*. Upper Saddle River, NJ: Pearson Prentice Hall.
- Hinkle, S.D. 2006. *Investigation of Time-Dependent Deflection in Long Span, High Strength, Prestressed Concrete Bridge Beams*. MS Thesis, Blacksburg, VA: Virginia Polytechnic Institute and State University.
- Hofrichter, A. 2014. *Compressive Strength and Modulus of Elasticity Relationships for Alabama Prestressed Concrete Bridge Girders*. MS Thesis, Auburn, AL: Auburn University.
- Holland, R.C. 2005. *Silica Fume User's Manual*. Lovettsville, VA: Silica Fume Association.
- Holt, R. 1996. *Implementation Program on High Performance Concrete Guidelines for Instrumentation of Bridges*. Research Report, Washington, DC: Federal Highway Administration.
- Hubler, M.H., Wendner, R., Bazant, Z.P. 2015. Comprehensive Database for Concrete Creep and Shrinkage: Analysis and Recommendations for Testing and Recording. *American Concrete Institute Materials Journal* 112 (4): 547-558.
- Huo, X.S., N. Al-Omaishi, and M.K. Tadros. 2001. Creep, Shrinkage, and Modulus of Elasticity of High Performance Concrete. *ACI Materials Journal* 98 (6): 440-449.
- Imbsen, R.A., D.E. Vandershaf, R.A. Schamber, and R.V. Nutt 1985. *Thermal Effects in Concrete Bridge Superstructures* (NCHRP Report 276). Washington, DC: Transportation Research Board.
- Isbiliroglu, L. 2014. *Predicting Time-Dependent Deformations in Prestressed Concrete Girders*. MS Thesis, Auburn, AL: Auburn University.
- Jayaseelan, H., and B.W. Russell. 2007. *Prestress Losses and the Estimation of Long-Term Deflections and Camber for Prestressed Concrete Bridges*. Final Report, Stillwater, OK: Oklahoma State University.
- Johnson, Brandon Ray. 2012. *Time-Dependent Deformation in Precast, Prestressed Bridge Girders*. MS Thesis, Auburn, AL: Auburn University.
- Kavanaugh, B.P. 2008. Creep Behavior of Self-Consolidating Concrete. MS Thesis, Auburn, AL: Auburn University.
- Kelly, D.J., T.E. Bradberry, and J.E. Breen. 1987. *Time Dependent Deflections of Pretensioned Beams* (Research Report 381-1). The University of Texas at Austin, Austin, TX: Center for Transportation Research.
- Keske, S.D. 2014. *Use of Self-Consolidating Concrete in Precast, Prestressed Girders*. PhD Dissertation, Auburn, AL: Auburn University.
- Khatri, B.P., and V. Sirivivatnanon. 1995. Effect of Different Supplementary Cementitious Materials on Mechanical Properties of High Performance Concrete. *Cement and Concrete Research* (Elsevier Science Ltd.) 25 (1): 209-220.

- Lane, R.O., and J.F. Best. 1982. Properties and Use of Fly Ash in Portland Cement Concrete. *Concrete International* 4 (7): 81-92.
- Lee, J.H. 2010. *Experimental and Analytical Investigations of the Thermal Behavior of Prestressed Concrete Bridge Girders Including Imperfections*. PhD Dissertation, Atlanta, GA: Georgia Institute of Technology.
- Levy, K. 2007. *Bond Behavior of Prestressed Reinforcement in Beams Constructed with Self-Consolidating Concrete*. MS Thesis, Auburn, AL: Auburn University.
- Levy, K., Barnes, R.W., Schindler, A.K. 2010. *Time-Dependent Deformations of Pretensioned, Self-Consolidating Concrete*. Proceedings of the 3rd fib International Congress, May 29–June 2, 2010: Washington, DC.
- Limeria, J., M. Etxeberria, and D. Molina. 2011. Mechanical and Durability Properties of Concrete Made with Dredged Marine Sand. *Journal of Construction and Building Products* (Elsevier) 25: 4165-4174.
- Liu, Yanjan, and Mang Tia. 2012. Creep Property of Concretes with Different Types of Coarse Aggregates. *Journal of Applied Mechanics and Materials* (Trans Tech Publications) 174-177: 308-313.
- Magura, D.D., M.A. Sozen, and C.P. Seiss. 1964. A Study of Stress Relaxation in Prestressing Reinforcement. *PCI Journal* 9 (2): 13-57.
- Mahmood, O.I. 2013. *Camber Control in Simply Supported Prestressed Concrete Bridge Girders*. MS Thesis, Lexington, KY: University of Kentucky.
- Mante, D.M. 2016. *Improving Camber Predictions for Precast, Prestressed Concrete Bridge Girders*. PhD Dissertation, Auburn AL: Auburn University.
- Martin, L.D. 1977. A Rational Method for Estimating Camber and Deflection of Precast Prestressed Members. *PCI Journal* 22 (1):100-108.
- Mehta, P.K., and P.J.M. Monteiro. 2014. *Concrete Microstructure, Properties, and Materials*. 4th ed. McGraw-Hill Education.
- Muller, H.S., I. Anders, R. Breiner, and M. Vogel. 2013. Concrete: Treatment of types and properties in fib Model Code 2010. *Journal of Structural Concrete* (Ernst and Sohn) 4: 320-334.
- Naaman, A.E. 2004. *Prestressed Concrete Analysis and Design: Fundamentals*. 2nd ed. Ann Arbor, MI: Techno Press 3000.
- Nawy, E.G. 2010. *Prestressed Concrete - A Fundamental Approach*. Upper Saddle River, NJ: Pearson Education, Inc.
- Nervig, J. 2014. *Improving Predictions of Instantaneous Camber for Prestressed Concrete Bridge Girders* (Paper 13817). MS Thesis. Iowa State University.
- Neville, A.M. 2013. *Properties of Concrete*. New Delhi, India: Dorling Kindersley.

- Noguchi, T., F Tomosawa, K.M. Nemati, B.M. Chiaia, and A.P. Fantill. 2009. A Practical Equation for Elastic Modulus of Concrete. *ACI Structural Journal* 106 (5): 690-696.
- Omar, W., T. Pui Lai, L. Poh Huat, and R. Omar. 2008. Improved Prediction of Pre-Camber of Post-Tensioned Prestressed I-Beam. *Journal of the Institution of Engineers* 69 (1):32-37.
- Pauw, Adrian. 1960. Static Modulus of Elasticity of Concrete as Affected by Density. *Journal of the American Concrete Institute* 57 (2): 679-688.
- Philleo, R.E. 1981. Increasing the Usefulness of ACI 214: Use of Standard Deviation and a Technique for Small Sample Sizes. *Concrete International* 3 (9): 71-74.
- PCI Committee on Bridges. 2012. Camber FAST Team. Chicago, IL: Precast Prestressed Concrete Institute.
- PCI. 2011. *Precast Prestressed Concrete Bridge Design Manual* 3rd ed. Chicago, IL: Precast/Prestressed Concrete Institute.
- Rizkalla, S., P. Zia, and T Storm. 2011. *Predicting Camber, Deflection, and Prestress Losses in Prestressed Concrete Members*. Final Project Report, Raleigh, NC: North Carolina State University.
- Roller, J.J., H.G. Russell, R.N. Bruce, and B. Hasset. 2003. Effect of Curing Temperature on High Strength Concrete Bridge Girders. *PCI Journal* 48 (2): 72-79.
- Rosa, M.A., J. F. Stanton, and M.O. Eberhard. 2007. *Improving Predictions for Camber In Precast, Prestressed Concrete Bridge Girders*. Research Report, University of Washington, Seattle, WA: Washington State Transportation Center (TRAC).
- Schindler, A.K, M.L. Hughes, R.W. Barnes, and B.E. Byard. 2010. *Evaluation of Cracking of the US 331 Bridge Deck*. ALDOT Project Report 930-645. Auburn University, Auburn AL: Highway Research Center.
- Schrantz, C.E. 2012. *Development of a User-Guided Program for Predicting Time-Dependent Deformations in Prestressed Bridge Girders*. MS Thesis, Auburn, AL: Auburn University.
- Schuster, R.L. 1957. *A Review of Research on Deleterious Substances in Concrete Aggregates*. Joint Highway Research Project, Lafayette, Indiana: Purdue University.
- Shi-Cong, K., and P. Chi-Sun. 2009. Properties of Concrete Prepared with Crushed Fine Stone, Furnace Bottom Ash, and Fine Recycled Aggregate as Fine Aggregate. *Journal of Construction and Building Materials* (Elsevier) 23:2877-2886.
- Stallings, J.M., and S. Eskildsen. 2001. *Camber and Prestress Losses in High Performance Concrete Bridge Girders*. Final Research Report: Project 930-373, Auburn, AL: Auburn University Highway Research Center.
- Stallings, J.M., R.W Barnes, and S. Eskildsen. 2003. Camber and Prestress Losses in Alabama HPC Bridge Girders. *PCI Journal* 48 (5): 2-16.
- Storm, T.K., S.H. Rizkalla, and P.Z. Zia. 2013. Effects of Production Practices on Camber of Prestressed Concrete Bridge Girders. *PCI Journal* 58 (1): 96-111.

- Svirsky, A. National Bridges. 2015. www.nationalbridges.com (accessed February 2, 2015).
- Tadros, M.K., N. Al-Omaishi, S.J Seguirant, and J.G. Gallt. 2003. *Prestress Losses in Pretensioned High-Strength Concrete Bridge Girders* (NCHRP Report 496), Washington, DC: National Cooperative Highway Research Program, Project 18-07.
- Tadros, M.K., A. Ghali, and A.W. Meyer. 1985. Prestressed Loss and Deflection of Precast Concrete Members. *PCI Journal* 30 (1): 114-141.
- Tadros, M.K., F. Fawzy, and K.E. Hanna. 2011. Precast, Prestressed Girder Camber Variability. *PCI Journal* 56 (1): 135-154.
- Thoman, W.H., and W. Raeder. 1934. Ultimate Strength and Modulus of Elasticity of High-Strength Portland Cement Concrete. *Journal of the American Concrete Institute* 30 (1).
- Tia, M., Y Liu, and D. Brown. 2005. *Modulus of Elasticity, Creep, and Shrinkage of Concrete*. Final Project Report, University of Florida, Tallahassee, FL: Florida Department of Transportation.
- Troxell, G.E., J.M. Raphael, and R.E. Davis. 1958. Long-Term Creep and Shrinkage Tests of Plain and Reinforced Concrete. *Proceedings of ASTM Annual Meeting 1958*: 1101-1120.
- Vardeman, S.B. and Jobe, J.M. 2001. *Basic Engineering Data Collection and Analysis*. Pacific Grove, CA: Duxbury Thompson Learning.
- Wu, K., B. Chen, W. Yao, and D. Zhang. 2001. Effect of Coarse Aggregate Type on Mechanical Properties of High-Performance Concrete. *Journal of Cement and Concrete Research* (Pergamon) 31: 1421-1425.
- Wyffels, T.A., C.E. French, and C.K. Shield. 2000. *Effects of Pre-Release Cracks in High-Strength Prestressed Concrete*. Final Project Report, University of Minnesota, St. Paul, MN: Minnesota Department of Transportation Office of Research Administration.